

Electronic Thesis and Dissertation Repository

8-10-2012 12:00 AM

A Sensorized Instrument for Minimally Invasive Surgery for the Measurement of Forces during Training and Surgery: Development and Applications

Ana Luisa Trejos
The University of Western Ontario

Supervisor
Dr. Rajni Patel
The University of Western Ontario

Graduate Program in Electrical and Computer Engineering
A thesis submitted in partial fulfillment of the requirements for the degree in Doctor of Philosophy
© Ana Luisa Trejos 2012

Follow this and additional works at: <https://ir.lib.uwo.ca/etd>



Part of the [Biomedical Devices and Instrumentation Commons](#)

Recommended Citation

Trejos, Ana Luisa, "A Sensorized Instrument for Minimally Invasive Surgery for the Measurement of Forces during Training and Surgery: Development and Applications" (2012). *Electronic Thesis and Dissertation Repository*. 837.

<https://ir.lib.uwo.ca/etd/837>

This Dissertation/Thesis is brought to you for free and open access by Scholarship@Western. It has been accepted for inclusion in Electronic Thesis and Dissertation Repository by an authorized administrator of Scholarship@Western. For more information, please contact wlsadmin@uwo.ca.

A SENSORIZED INSTRUMENT FOR MINIMALLY INVASIVE SURGERY FOR
THE MEASUREMENT OF FORCES DURING TRAINING AND SURGERY:
DEVELOPMENT AND APPLICATIONS

(Spine Title: Development of a Sensorized Instrument for Minimally Invasive Surgery)

(Thesis Format: Monograph)

by

Ana Luisa Trejos

Faculty of Engineering

Department of Electrical and Computer Engineering

Submitted in partial fulfillment
of the requirements for the degree of
Doctor of Philosophy

School of Graduate and Postdoctoral Studies

The University of Western Ontario

London, Ontario, Canada

© Ana Luisa Trejos, 2012

THE UNIVERSITY OF WESTERN ONTARIO
School of Graduate and Postdoctoral Studies

CERTIFICATE OF EXAMINATION

Supervisor

Examining Board:

Dr. Rajni Patel

Dr. Ken McIsaac

Supervisory Committee

Dr. Roy Eagleson

Dr. Richard Malthaner

Dr. Alp Sener

Dr. Christopher Schlachta

Dr. Anthony Hodgson

The thesis by
Ana Luisa Trejos
entitled

A Sensorized Instrument for Minimally Invasive Surgery for the Measurement of Forces during
Training and Surgery: Development and Applications

is accepted in partial fulfillment of the
requirements for the degree of
Doctor of Philosophy

Date: _____

Chair of the Thesis Examination Board

Abstract

The reduced access conditions present in Minimally Invasive Surgery (MIS) affect the feel of interaction forces between the instruments and the tissue being treated. This loss of haptic information compromises the safety of the procedure and must be overcome through training.

Haptics in MIS is the subject of extensive research, focused on establishing force feedback mechanisms and developing appropriate sensors. This latter task is complicated by the need to place the sensors as close as possible to the instrument tip, as the measurement of forces outside of the patient's body does not represent the true tool-tissue interaction. Many force sensors have been proposed, but none are yet available for surgery.

The objectives of this thesis were to develop a set of instruments capable of measuring tool-tissue force information in MIS, and to evaluate the usefulness of force information during surgery and for training and skills assessment. To address these objectives, a set of laparoscopic instruments was developed that can measure instrument position and tool-tissue interaction forces in multiple degrees of freedom. Different design iterations and the work performed towards the development of a sterilizable instrument are presented.

Several experiments were performed using these instruments to establish the usefulness of force information in surgery and training. The results showed that the combination of force and position information can be used in the development of realistic tissue models or haptic interfaces specifically designed for MIS. This information is also valuable in order to create tactile maps to assist in the identification of areas of different stiffness. The real-time measurement of forces allows visual force feedback to be presented to the surgeon.

When applied to training scenarios, the results show that experience level correlates better with force-based metrics than those currently used in training simulators. The proposed metrics can be automatically computed, are completely objective, and measure important aspects of performance.

The primary contribution of this thesis is the design and development of highly versatile instruments capable of measuring force and position during surgery. A second contribution establishes the importance and usefulness of force data during skills assessment, training and surgery.

Keywords: Force sensing, mechatronic device design, mechanical design, minimally invasive surgery, medical mechatronics, surgical training, performance metrics

Dedicated to:
Roberto and Mercedes,
without whom, I would not be me.

Acknowledgements

I consider myself blessed to have had so much support from so many different people during the past four years. The person that deserves the most credit for my success is my supervisor and mentor, Dr. Rajni Patel. His support, guidance and encouragement have allowed me to achieve many different goals in my life and I would not have even started this journey if it had not been for him. He was able to provide me with the perfect balance of freedom and direction, while allowing me to pursue my interests and build on my strengths. I could not have asked for a better supervisor.

There have been many different granting agencies that have supported my research in one way or another. Financial support for my work was provided by the Natural Sciences and Engineering Research Council (NSERC) of Canada, through the Alexander Graham Bell Canada Graduate Scholarship. My involvement in the Collaborative Research and Training Experience (CREATE) program grant (# 371322-2009) in Computer-Assisted Medical Interventions allowed me to be involved in several courses, workshops and seminars related to important research fields. The development of the instruments was funded in part by the Western Innovation Fund and the Natural Sciences and Engineering Research Council (NSERC) of Canada under the Idea to Innovation grant I2IPJ/363985-07. Additional support was provided through Dr. Patel's and Dr. Naish's Discovery grants RGPIN-1345 (R.V. Patel), CRDPJ349675-06 (R.V. Patel) and 312383 (M.D. Naish). Laboratory equipment was provided by infrastructure grants from the Canada Foundation for Innovation awarded to the London Health Sciences Centre (Canadian Surgical Technologies & Advanced Robotics (CSTAR)) and to The University of Western Ontario (R.V. Patel). I would like to acknowledge the support from Quanser Inc. that provided the strain gauge amplifiers and the Q8 data acquisition cards and software.

This work would not have been possible without help from many different surgeons who pro-

vided insight from the medical point of view. In particular, Dr. Christopher Schlachta and Dr. Richard Malthaner were incredibly supportive and dedicated a considerable amount of their time to making this project a success. Dr. Bob Kiaii, Dr. Marie-Eve LeBel, Dr. Maria Currie and Dr. Shiva Jayaraman are also acknowledged. Similarly, support from other faculty members who in one way or another assisted with my work is gratefully acknowledged: Dr. Terry Peters, Dr. Sayra Cristancho, and Dr. Yves Bureau.

I would like to acknowledge all of the CSTAR staff for their continued technical and administrative assistance, especially David Browning, Karen Siroen, Tammy Mills, Karen Pilkey, Teresa Burns, and Dorace Ramage. The assistance of Amber Parsons and Sheri Van Lingen during the *in vivo* trials is greatly appreciated. Similarly, the support from the staff in Electrical and Computer Engineering is acknowledged, in particular Sandra Vilovski, Jacquie Taylor, Melissa Harris and Chris Marriott.

Incredible support was received from many students and research assistants at CSTAR. Special thanks go out to Abelardo Escoto, who not only assisted with various parts of this project including the development of the calibration jig for the second prototype and machining parts in the micromachining centre, but was always willing and able to help out with different tasks and always provided support and encouragement. Similarly, Christopher Ward was instrumental to the success of the project by providing his expertise in many different areas, including his knowledge on the development of silicone models.

I would like to acknowledge Dr. Mahdi Tavakoli. This project resulted from initial work done by Dr. Tavakoli on a test bed for investigating haptics in MIS.

I would like to thank everyone at University Machine Services, especially Kevin Barker and Dan Sweiger for their feedback on the machining of the instrumented laparoscopic tools. Also, Gerry Dafoe from the Boundary Layer Wind Tunnel Laboratory for his technical support with strain gauge attachment.

On the software development side, Andrew Lyle spent a couple of years developing, tuning and changing the SIMIS software. He showed extreme patience and dedication through the many iterations that we went through and he deserves special recognition for this. Also, Martin Pytel developed the software for capturing the microBIRD data and calibrating the position sensors.

The following summer students and volunteers are recognized for their help with the project in one way or another: Carolina Subirós, Aleksandar Mihaylov, Carlie Scalesse, Andrea Kwong,

Dustin Hughes, Andrew Johnston, Fraser LeBer and Matt Dawson.

A special acknowledgement goes out to Bernardo Trejos and Marielena Moncada, who helped me to make important decisions in this process and supported me every step of the way. I also want to thank my parents, Roberto Trejos and Mercedes Murillo, and the rest of my family in Costa Rica for always providing me with a supportive environment and allowing me to grow in a financially and emotionally stable home, which was the product of hard work and dedication. If it were not for the encouragement and love that I received from them, my life would be quite different. Special thanks go to Olga Marta Murillo and Ofelia Murillo for their amazing support. In London, I have had amazing support from my parents-in-law, Sharon and David Naish, who have stepped in many times to help me in countless ways. This process would have been a lot more difficult if it had not been for them. I would like to thank Dr. Kelly Rau and Jodi DiGiuseppe for keeping me healthy, especially during the past two years.

Finally, I want to express my most sincere gratitude towards my husband, Michael Naish and my kids, Thomas and Isabel. It is difficult to find the words to properly acknowledge them for everything that they have given me these past few years. They have been a source of constant support, reminding me of what is important in life and keeping me centred. Michael has been my rock allowing me to grow emotionally and academically thorough this process. Thomas and Isabel have given me hope and motivation to continue the journey, while forcing me to stop often to smell the roses along the way. Thank you for being patient and understanding. I love you all so much.

Contents

Certificate of Examination	ii
Abstract	iii
Acknowledgements	vi
Table of Contents	ix
List of Figures	xvi
List of Tables	xx
Nomenclature and Acronyms	xxii
1 Introduction	1
1.1 Motivation	2
1.2 General Problem Statement	3
1.3 Research Objectives	4
1.4 Scope	4
1.5 Overview of the Thesis	5
2 Literature Review	7
2.1 Introduction	7
2.2 Force Sensing in Clinical Applications	8
2.2.1 The Need for Force Sensing	8
2.2.2 Where to Sense?	11

2.2.3	What to Sense?	14
2.3	Force Sensing	15
2.3.1	Technologies	15
2.3.2	Requirements of Force Sensors in Medicine	18
2.3.3	Calibration	20
2.3.4	Interface Requirements	20
2.4	Force Sensing Technologies and New Developments	22
2.4.1	Commercially Available Force Sensors	22
2.4.2	Novel Force Sensors in Clinical Applications	24
2.5	Discussion	24
3	First-Generation SIMIS Instruments	28
3.1	Introduction	28
3.2	Design Specifications	28
3.3	Presentation of the Mechanical Design	29
3.4	Force Sensing	31
3.4.1	Actuation Force	31
3.4.2	Bending Forces	32
3.4.3	Axial Force and Torsion	32
3.5	Instrument Prototype	35
3.6	Additional Hardware and Software Interface	36
3.7	Calibration	39
3.8	Performance Assessment	41
3.8.1	Accuracy, Repeatability and Hysteresis	41
3.8.2	Gravity Compensation	42
3.8.3	Signal Drift and Noise	42
3.8.4	Coupling	43
3.9	Validation of Force Calibration	43
3.9.1	Actuation Force	43
3.9.2	Moments, Torsion and Axial Force	44
3.10	Discussion	45

3.11	Limitations of the First Prototype	46
4	Second-Generation SIMIS Instruments	48
4.1	Introduction	48
4.2	Lessons Learned and Design Solutions	48
4.2.1	Limitation 1: Poor axial and torsional signals	48
4.2.2	Limitation 2: Coupling between the actuation force and the bending mo- ments in one direction	50
4.2.3	Limitation 3: The step on the outer shaft creates difficulties when suturing	51
4.2.4	Limitation 4: Needle driver tips breaking	51
4.2.5	Limitation 5: Long change-over time between the two models	52
4.2.6	Limitation 6: Difficult wiring of the cables	53
4.2.7	Limitation 7: Instrument too short	54
4.2.8	Limitation 8: Cumbersome setup, difficult to move and easy to damage . .	54
4.3	Calibration	55
4.4	Performance Assessment	56
4.4.1	Force Calibration Assessment	56
4.4.2	Multi-tip Calibration Assessment	57
4.4.2.1	Methods	57
4.4.2.2	Results	59
4.4.3	Long Term Calibration Assessment	59
4.5	Further Complications and Modifications	60
4.6	Discussion	62
5	Sterilizable Prototype	66
5.1	Introduction	66
5.2	Reprocessing of Medical Devices	67
5.3	Selection of Adequate Cables and Connectors	68
5.3.1	Cables	68
5.3.2	Connectors	69
5.4	Selection of Materials for Strain Gauge Installation	70
5.4.1	Experimental Methods	70

5.4.1.1	Strain Gauge Installation	72
5.4.1.2	Performance Evaluation	73
5.4.2	Results	74
5.4.2.1	Original Performance	75
5.4.2.2	Performance After Autoclaving	75
5.4.2.3	Summary	76
5.4.3	Additional Evaluation of Best Results	77
5.5	Assembly	78
5.6	Concluding Remarks	78
6	Applications to Surgery	81
6.1	Introduction	81
6.2	Applications to Tissue Characterization	82
6.2.1	Experimental Evaluation	83
6.2.2	Methods	83
6.2.3	Data Analysis	84
6.2.3.1	Filtering	86
6.2.4	Results	87
6.2.5	Discussion and Development Guidelines	89
6.3	Applications to the Development of Haptic Interfaces	90
6.3.1	Experiments	92
6.3.2	Methods	93
6.3.3	Data Analysis	93
6.3.4	Results	94
6.3.5	Discussion and Applications	94
6.4	Applications to Sensory Substitution	96
6.4.1	Experiments	97
6.4.2	Methods	98
6.4.2.1	Preliminary Trials	99
6.4.2.2	Insights from the Preliminary Tests	101
6.4.2.3	Main Trials	102

6.4.3	Data Analysis	103
6.4.4	Results and Discussion	104
6.4.4.1	Time	105
6.4.4.2	Task 1: Palpation	105
6.4.4.3	Task 2: Cutting	108
6.4.4.4	Task 3: Tumour Removal	109
6.4.4.5	Task 4: Suturing	109
6.4.4.6	Task 5: Knot tying	110
6.4.5	Final Remarks	111
6.5	Conclusions	112
7	Applications to Surgical Training	113
7.1	Introduction	113
7.1.1	Motivation	113
7.1.2	Knowledge Acquisition	115
7.1.3	Aspects that Affect Performance	116
7.1.4	Validated Assessment Methods	117
7.1.4.1	GOALS	118
7.1.4.2	FLS / MISTELS	118
7.1.4.3	ICSAD	118
7.2	Simulator-based Training	119
7.2.1	Physical Simulators	120
7.2.2	Virtual Reality Simulators	120
7.2.3	Hybrid Simulators	121
7.2.4	Robotic Surgery Simulators	121
7.2.5	Other Aspects of Simulator Training	122
7.3	Performance Measures	122
7.3.1	Temporal	123
7.3.2	Outcome Measures	123
7.3.3	Motion-based Measures	124
7.3.3.1	Speed	125

7.3.3.2	Acceleration	125
7.3.3.3	Jerk	126
7.3.3.4	Nonlinear Measures	127
7.3.4	Force-based Measures	128
7.3.5	Other Measures	130
7.3.6	Data Processing	130
7.4	Development of New Performance Metrics	131
7.4.1	Methods	132
7.4.2	Data Analysis	132
7.4.2.1	Position-based Measures	133
7.4.2.2	Force-based Measures	134
7.4.2.3	Combined Measures	135
7.4.3	Results	137
7.4.3.1	Time	137
7.4.3.2	Position	138
7.4.3.3	Force	139
7.4.3.4	Combined Measures	142
7.5	Discussion	143
7.6	Conclusions	149
8	Conclusions and Future Work	150
8.1	Contributions	151
8.2	Future Work	153
	References	157
	Appendices	176
A	Software Development	176
A.1	Software Design	176
A.2	Strain Gauge Processing	182
A.2.1	Type I Quarter Bridge	182
A.2.2	Type II Half Bridge	182

A.2.3 Type III Full Bridge 183

A.3 Generic Software Architecture 183

B Permissions and Approvals 185

Curriculum Vitae 191

List of Figures

- 2.1 Information flow in a conventional minimally invasive procedure. 9
- 2.2 Information flow in a robotics-assisted minimally invasive procedure using a master–
slave system. 9
- 2.3 Forces acting on minimally invasive instruments. 12
- 2.4 Examples of strain gauges used in instruments to measure forces during natural
orifice procedures and during laparoscopic procedures. 16
- 2.5 Signal processing flow. 21
- 2.6 Examples of haptic interfaces for MIST applications. 21
- 2.7 ATI Nano-17 force sensor. 22

- 3.1 Instrument design with needle driver handle and tip and with traditional handle
and gripper attachment. 30
- 3.2 Detail of the instrument design showing the o-ring location for attachment of the
outer shaft. 30
- 3.3 Coordinate frame associated with the instrument. 31
- 3.4 Type III full Wheatstone bridge and the corresponding placement of gauges on the
inner shaft. 32
- 3.5 Type II half Wheatstone bridge and placement of the gauges measuring bending
moment 33
- 3.6 Type I quarter Wheatstone bridge and placement of the two-element rosettes mea-
suring torsion and axial forces. 33
- 3.7 Examples of interchangeable tips and handles that can be attached to the instrument. 35
- 3.8 Placement of gauges on the middle and inner shafts 36

3.9	Cable wiring to allow the inner shaft to slide inside the middle shaft in order to accommodate the different tips.	36
3.10	Experimental setup.	37
3.11	Customized software interface including real-time plots and the calibration interface.	38
3.12	Instrument placement for calibration for x and y moments, axial, and torsion.	40
3.13	Signal drift observed in the five measured directions.	43
3.14	Sample image of the instrument compressing a spring for calibration validation.	44
3.15	Comparison of the measured forces by a force sensor and by the strain gauges on the sensorized instrument.	45
4.1	Instrument close-up showing axial concentration element inside the housing.	49
4.2	Stress concentration diagrams as forces increase from 0 to 20 N in the axial direction.	50
4.3	Inner shaft showing the decoupling feature.	51
4.4	New instrument housing.	52
4.5	Inner housing details.	52
4.6	Comparison of tip design.	53
4.7	Quick connect mechanism.	53
4.8	Outer view of opening for cables and inner view of space available for cables.	54
4.9	Modifications to the electronic connections of the instruments.	55
4.10	Calibration jig showing the instrument mounted for calibrating moments and for calibrating grasping forces.	56
4.11	Different tips used in the calibration evaluation.	58
4.12	Broken weld lines on middle shaft.	61
4.13	New axial element on middle shaft.	61
4.14	CAD model of the new middle shaft for construction in the micromachining centre.	62
4.15	Mounting of axial element on micromachining centre.	63
4.16	Completed middle shaft: close up of axial sensing element.	63
5.1	Multi-stranded medical grade cables from Cooner Wire.	69
5.2	Sample sterilizable connector and receptacle from Fischer.	70
5.3	Stainless steel bars with gauges attached.	72
5.4	Experimental jig with stainless steel bar in cantilever.	73

5.5	Strain gauge installation process: gauges clamped for curing and instruments in oven.	78
5.6	Gauges installed and cables soldered: on inner shaft and on middle shaft.	79
6.1	Experimental setup used during the tissue characterization tests: tissue phantom with an embedded tumour and tissue inside training box held by plastic frame. . .	84
6.2	Data flow diagram for tissue characterization data processing.	85
6.3	Overlaid filtered and unfiltered position data with a second order <code>filtfilt</code> filter and a fourth order Butterworth filter.	86
6.4	Power spectrum of the position data for a novice subject.	87
6.5	Tactile map obtained from a systematic palpation across the entire surface, showing the stiffness factors obtained at each (x, y) coordinate in N/mm^2	88
6.6	Image of instrument location during identified peak.	88
6.7	Tactile map obtained from a localized palpation around suspected site, showing the stiffness factors obtained at each (x, y) coordinate in N/mm^2	89
6.8	Data flow diagram of tissue characterization procedure.	91
6.9	Instruments in use during the <i>in vivo</i> trials.	95
6.10	Steps in a complex procedure composed of 5 tasks.	100
6.11	Cause and effect diagram for the preliminary trials.	100
6.12	Average task completion time for all five tasks according to the feedback provided.	105
6.13	Average mean forces with and without force feedback during the palpation task. .	108
6.14	Average mean forces with and without force feedback during the suturing task. . .	110
7.1	Task completion time for the 5 tasks according to the level of experience.	138
7.2	Normalized jerk as a function of experience level for all 5 tasks.	140
7.3	Sample graphs of force-based metrics.	140
7.4	Comparison of the best possible Spearman's Rho correlations between the six levels of experience and several different metrics.	143
7.5	Sample graphs of force and position derivatives.	146
A.1	Graphical user interface for the SIMIS software.	177
A.2	Force graph included in the SIMIS GUI.	178
A.3	Position graph included in the SIMIS GUI.	178

A.4 Window within the SIMIS GUI to input calibration constants and adjustment parameters. 180

A.5 Calibration interface included in the SIMIS GUI. 181

A.6 Video with force overlay included in the SIMIS GUI. 181

A.7 Generic graphical user interface for displaying, recording and calibrating strain gauges. 184

A.8 Window within the generic GUI to select an input channel and assign a bridge type. 184

List of Tables

- 2.1 Experimental evaluations to assess the need for force feedback in MIST. 10
- 2.2 Locations for force sensing. 13
- 2.3 Force sensing technologies. 16
- 2.4 Summary of small commercially available force sensors. 23
- 2.5 Summary of force sensing instruments. 25

- 3.1 Details of the strain gauges used for force sensing. 35
- 3.2 Summary of the strain gauge calibration assessment. 42
- 3.3 Effect of gravity compensation on the bending moments: maximum error measured
when moving in free space. 42
- 3.4 Maximum deviation from a theoretical zero value caused by coupling. 44

- 4.1 Summary of the strain gauge calibration assessment of the second-generation pro-
totype. 57
- 4.2 Maximum deviation from a theoretical zero value caused by coupling. 57
- 4.3 The lengths of the tips used for calibration assessment. 58
- 4.4 Correction factors for torsion and grasp measurements. Calibration was completed
with Tip C. 59
- 4.5 Strain gauge calibration assessment between tips of different lengths. Results show
the RMS errors. 60
- 4.6 Comparison of calibration slopes on different days. 60
- 4.7 Performance assessment of axial measurements with the new sensing element. . . . 62

- 5.1 Relevant information of the adhesives and coatings tested. 71

5.2	Working strain gauges for each combination of adhesive and coating, and their position on the bar.	75
5.3	Sample results of the preliminary evaluation.	76
5.4	Overall performance of the best performing gauges in each combination, as calculated by adding the errors of accuracy, hysteresis, noise and drift.	76
5.5	Summary of results showing average performance for all gauges in each combination.	77
5.6	Results of the additional evaluation with adhesives 2 and 3.	77
6.1	Location of the four corners of the frame.	85
6.2	Results of the <i>in vivo</i> trials showing the range of motion used in each direction. . .	95
6.3	Results of the <i>in vivo</i> trials showing the range of forces applied in each direction. .	95
6.4	Plus and minus table for the 2^3 design and the interpretation of each test.	101
6.5	Effect of force feedback on the grasping force for the five tasks.	106
6.6	Effect of force feedback on the Cartesian forces for the five tasks.	107
7.1	Detailed experience levels.	132
7.2	Task completion time results in seconds for all 5 tasks.	138
7.3	Spearman's Rho correlations between the six levels of experience and each position-based measure evaluated.	139
7.4	Comparison of the force-based metrics between novices and experts for each task. .	141
7.5	Spearman's Rho correlations between the six levels of experience and each force-based measure evaluated.	142
7.6	Scaling factors resulting from the optimization of FP Metric 1.	144
7.7	Scaling factors resulting from the optimization of FP Metric 2.	145

Nomenclature and Acronyms

Acronyms

ABS	Acrylonitrile Butadiene Styrene
ANOVA	ANalysis Of VAriance
API	Application Programming Interface
AR	Augmented Reality
AWG	American Wire Gauge
CSTAR	Canadian Surgical Technologies and Advanced Robotics
DOF	Degree Of Freedom
EMTS	ElectroMagnetic Tracking System
FF	Force Feedback
FLS	Fundamentals of Laparoscopic Surgery
FP	Force-Position
GFF	Graphical Force Feedback
GOALS	Global Operative Assessment of Laparoscopic Skills
GRS	Global Rating Scale
GUI	Graphical User Interface
HFR	High Force Ratio
HGR	High Grasping force Ratio
HMM	Hidden Markov Model
IAV	Integral of the Acceleration Vector
ICSAD	Imperial College Surgical Assessment Device

ISO	International Organization for Standardization
ITER	In-Training Evaluation Report
LVDT	Linear Variable Differential Transformer
LyE	Lyapunov Exponent
MAPR	Movement Arrest Period Ratio
MIS	Minimally Invasive Surgery
MIST	Minimally Invasive Surgery and Therapy
MISTELS	McGill Inanimate System for Training and Evaluation in Laparoscopic Surgery
MMC	Micromachining Centre
MRI	Magnetic Resonance Imaging
OD	Outer Diameter
OR	Operating Room
OSATS	Objective Structured Assessment of Technical Skill
PC	Personal Computer
PCA	Principal Component Analysis
PCI	Peripheral Component Interconnect
PGY	Post-Graduate Year
PVDF	PolyVinylidene Fluoride
PZT	Lead Zirconate Titanate
RITA	Record of In-Training Assessment
RMS	Root Mean Squared
SG	Strain Gauges
SIMIS	Sensorized Instrument-based Minimally Invasive Surgery
SPSS	Statistical Package for the Social Sciences
VFF	Visual Force Feedback
VR	Virtual Reality

Variables

A	Cross-sectional area
A_m	Amplitude
C	Jerk metric
d	Penetration depth
D	Duration
E_a	Strain caused by axial forces
E_i	Strain caused by grasping forces
E_t	Strain caused by torsional forces
E_x	Strain caused by x forces
E_y	Strain caused by y forces
F	Force
F_{iqr}	Interquartile range of the Force
F_{metric}	Force metric
GF	Gauge Factor
I	Moment of Inertia
J	Polar moment of inertia
k	Stiffness factor
M	Moment
P	Path length
P_{ij}	Parameter that minimizes the coupling between the i and j directions
r	Radius of the shaft
R_L	Lead resistance
R_G	Nominal gauge resistance
S_{aa}	Slope of the axial force
S_{ii}	Slope of the grasping force
S_{tt}	Slope of the torsional force
S_{xx}	Slope of the x force

S_{yy}	Slope of the y force
T	Torque
V	Volts
V_{EX}	Excitation voltage
V_r	Voltage ratio
ΔV	Change in voltage
z	Total performance metric
z_i	Individual performance metric
α	Scaling coefficient
λ	Scaling factor
θ	Rotation angle
ν	transverse sensitivity ratio of the strain gauge
σ	Standard deviation
σ_a	Axial stress
σ_m	Bending stress
τ	Shearing stress
ε	Strain

Units

cm	centimetres
g	Gram
GB	GigaByte
Hz	Hertz
mm	millimetres
Pa	Pascals
s	Seconds
N	Newtons

Chapter 1

Introduction

Minimally Invasive Surgery and Therapy (MIST) have altered the effect that surgical and therapeutic procedures have on patients by significantly reducing collateral damage. In these procedures, instruments enter the patient's body through small incisions, or through the patient's natural orifices, in order to perform surgery or deliver therapy. This has led to improved outcomes, reduced recovery time, reduced length of hospital stay, improved cosmesis, and reduced morbidity rates [1].

Technological advances for MIST have significantly progressed in the past 20 years (see [2]); however, certain limitations still exist. The most limiting factor of MIST, and one that has been the subject of significant research, is that the reduced access conditions affect the feel of interaction forces between the instruments and the tissue being treated. The use of master–slave robotic systems for MIST, e.g., the da Vinci[®] Surgical System (Intuitive Surgical, Inc.), significantly improves instrument dexterity, accuracy and control [3]; however, the indirect nature of the system interface causes clinicians to lose all ability to feel realistic interaction forces between surgical or therapeutic instruments and tissue.

This loss of tactile and kinesthetic information leads to several limitations [3–6]:

- It is no longer possible to manually palpate tissue to locate certain structures or assess tissue characteristics.
- Excessive forces can be applied, leading to increased trauma and damage to healthy tissue.
- Insufficient forces might be applied when grasping tissue or sutures leading to slippage, loss of control, and loose intracorporeal knots.

Since tactile and force information is no longer available, clinicians must compensate by using visual cues to estimate the amount of force being applied [4]. This requires a completely different set of perceptual and motor skills, for which extensive training is required [6].

Although some procedures are successfully performed in a minimally invasive manner without accurate force feedback or without any force information, the loss of haptic information limits the widespread application of MIST to all fields [7]. Procedures in which dexterous fine movements need to be performed require accurate control of both the forces applied and instrument positions [8]. In an effort to overcome these limitations, extensive training requirements are often mandated.

1.1 Motivation

Many research studies have focused on evaluating the need for haptic feedback when performing different tasks. Other studies have looked at the development of methods that provide force information to the user through sensory substitution or haptic interfaces, while still others have aimed to develop sensors that are able to measure kinesthetic or tactile information during surgery. The latter task is complicated by the need to place the sensors as close as possible to the instrument tip, as the measurement of forces from outside of the patient's body is affected by interaction forces between the instruments and the trocar at the incision point, torques from the abdominal walls or nearby organs, internal instrument friction and mechanical advantage. This significantly constrains the size and sterilization requirements of the sensors that may be used. Many force sensors and sensing methods have been proposed, but none are currently available for accurate measurement of the tool-tissue interaction forces during surgery. Several research studies have focused on determining whether force sensing is really necessary, and if so, which degrees of freedom (DOFs) are most important and which tasks would benefit more from the availability of force information.

In spite of these research efforts, there is still no consensus as to whether surgical procedures or surgical training can be improved with the availability of haptic information. An in-depth study that analyzes the need for haptic information in different applications has not yet been performed. It is necessary to determine the types of procedures that would most benefit from force feedback, the number of DOFs in which forces need to be sensed for different procedures, the required resolution and accuracy with which forces need to be measured, and the effect that a lack of force reflection has on experts and trainees (i.e., which limitations can be overcome by training).

The search for answers to these questions is complicated by the fact that there are currently no surgical instruments that are capable of measuring tool–tissue interaction forces. The availability of such instruments would allow the design of experiments that might be able to address some of the unknowns, with the ultimate goal of guiding the development of new instruments and devices.

Sensorizing instruments is not an easy or inexpensive solution, so the need for force information has to be properly justified before committing to the addition of sensors to surgical instruments and/or training systems. Knowledge of which tasks can be safely and effectively performed without force feedback will simplify the development of tools and instruments for those procedures. Proper justification could also be provided for the development of more complex instruments for those procedures that do benefit from force information. The availability of sensorized instruments also has an application to the development of simulators for training and skills assessment. The force profiles obtained from real-tissue experiments could be used to develop virtual-reality based simulators with increased levels of fidelity and realism for tasks that truly require force feedback. Procedures that can be safely performed without force feedback, or those for which the addition of force feedback does not improve the performance of novice trainees, can be taught using lower fidelity simulators that focus on the development of the required skills.

1.2 General Problem Statement

In an ideal world, a surgeon would perform a surgical procedure by accessing the surgical site with excellent visualization and direct contact with the tissue being treated, while the patient benefits from a procedure with no side-effects and minimal invasiveness. Unfortunately, the reduced access conditions required to minimize the invasiveness to the patient’s body affect the haptic feel of the tool–tissue interaction. Due to the quick adoption of minimally invasive procedures into the standard of care, there are many unknowns about the need for haptic feedback that remain unanswered.

Nevertheless, in order to provide the best patient care, surgeons will have to continue to deal with these limited conditions. Although it is unknown to what extent the lack of haptic information impacts the effectiveness of the procedure, many researchers have shown that there are clear limitations that arise from this lack of information [9,10].

To address these issues, there is a need to develop instruments and devices that are capable

of providing haptic information. Once these instruments become available, experiments can be designed to establish the importance of force information and find answers concerning the importance of haptic feedback. These instruments would also make an important contribution to the development of instruments for surgical applications that are capable of measuring interaction forces with tissue.

This work proposes to develop a set of sensorized instruments capable of measuring force information in all degrees of freedom available during minimally invasive surgery (MIS) with the best resolution possible, to perform a series of experiments to validate their feasibility and to establish the importance of force information during minimally invasive surgery and training.

1.3 Research Objectives

The main goal of this thesis is to advance our understanding of the importance of force information during minimally invasive surgery and training. To achieve this objective, the work has focused on the following objectives:

- To design, build and test a set of instruments capable of measuring tool–tissue force information in all degrees of freedom available during MIS and integrate it with a software platform capable of allowing the visualization, calibration and recording of the measured data.
- To investigate solutions for the development of sterilizable sensorized elements, and to incorporate them into the development of a sterilizable version of the sensorized instruments.
- To investigate the usefulness of force information in surgical applications.
- To investigate the usefulness of force information for training and skills assessment.

1.4 Scope

Haptics is composed of three main categories: kinesthetic feel, tactile feel and proprioception [11–13]. Kinesthetic information or force feedback refers to the ability to sense position, forces and movement using muscle receptors, tendons and joints. Tactile feel deals with the sensation of vibration, shapes and textures relying on mechanoreceptors in the skin. Proprioception deals with the perception of the position and movement of body segments, and it is rarely taken into account

when developing haptic interfaces for virtual environments. Its consideration is important when fully representing haptic interaction between the hands and the objects in contact. A few studies have concluded that to achieve proper haptic feedback, tactile and force sensing feedback must be present [8, 14].

Ongoing projects at Canadian Surgical Technologies and Advanced Robotics (CSTAR) have investigated the importance of tactile information [15,16] in surgical and therapeutical applications. In contrast, the work presented in this thesis is focused specifically on investigating the importance and value of kinesthetic information. Furthermore, the emphasis of this work has been on the development of sensorized instruments and in showing their value and potential. Answers to the questions stated above require extensive experimentation and the experiments presented herein are intended as a starting point in the investigation of the effect that the lack of haptic information has during MIST.

1.5 Overview of the Thesis

The structure of the rest of the thesis is as follows:

- Chapter 2** Literature Review: Summarizes the state of the art in force sensing techniques for medical interventions.
- Chapter 3** SIMIS Instruments: Outlines the design and development of the first prototype of the force sensing instruments, its limitations and preliminary evaluation.
- Chapter 4** Modified SIMIS Instruments: Presents how the limitations of the original prototype were addressed through three subsequent iterations of the prototype design, as well as the evaluation of their performance and the lessons learned.
- Chapter 5** Sterilizable SIMIS Instruments: Presents the work done towards the development of a sterilizable version of the instruments. This includes the evaluations performed to identify the optimal combination of adhesives and coatings for installing strain gauges on the instruments such that they are able to withstand an autoclave cycle. The identification of cables and connectors, as well as how the instrument can be cleaned and sterilized after use are also part of this work.

-
- Chapter 6** Applications to Surgery: Explains how the instruments can be used for force sensing in surgery and the development of a set of experiments aimed at determining the usefulness of force information when performing a surgical task. This chapter includes insights into how the instruments could be used for tissue characterization, and to collect data to inform the development of haptic interfaces for surgery and simulation.
- Chapter 7** Applications to Surgical Training: Describes how the instruments can be used for skills assessment and training and the development of performance metrics based on force information.
- Chapter 8** Concluding Remarks: Highlights the contributions of this thesis and proposes suggestions for future work.
- Appendix I** Software Development: Describes the development of the SIMIS software interface.
- Appendix II** Permissions and Approvals: Presents approval letters for copyrighted material, as well as proof of ethics approval for the trials that involved human subjects.

Chapter 2

Literature Review

2.1 Introduction

This chapter presents a summary of the state of the art in force sensing techniques for medical interventions in order to identify existing limitations and future directions. Although a significant amount of work has also been directed towards tactile sensors and haptic interfaces, the focus of this chapter is on force sensors and sensing techniques. An extensive literature search was performed during the period of January to July 2009 using Google Scholar and a combination of the following keywords: force, sensor, sensing, haptics, minimally invasive, surgery and therapy. The resulting initial list of papers and the references therein were reviewed giving priority to papers published in the previous 15 years. A total of 126 papers were included in the compiled database. This literature review resulted in the work presented in [9]. This initial review has been complemented with an additional literature search performed in June 2012.

Based on the relevant information found in these papers, the remainder of this chapter is organized as follows: Section 2.2 outlines the need for force sensing and the environmental characteristics that affect force sensing in clinical applications. Section 2.3 describes the technologies that can be used to measure force, as well as their most critical requirements when used in clinical applications. Section 2.4 describes the technological developments to date that are commercially available and those that are still at a developmental stage. Finally, in Section 2.5, the current state of the art is summarized with an outline of future directions.

2.2 Force Sensing in Clinical Applications

The desire to measure forces in MIST arises from the limitations imposed by minimally invasive access conditions, which affect the forces that a clinician can feel with respect to tool–tissue interactions. However, the need to measure these forces is not always obvious and becomes a balance between cost, equipment complexity and actual benefit.

2.2.1 The Need for Force Sensing

In traditional minimally invasive surgery or therapy, a clinician holds an instrument that enters the patient’s body through a small incision in which a trocar is placed. The trocar, abdominal wall and other nearby tissues exert forces on the instrument that, together with the leverage effect, cause the forces felt at the hand–tool interface to poorly represent the forces arising from the tip–tissue interaction. Figures 2.1 and 2.2 show the conditions found in minimally invasive procedures and robotic master–slave procedures and illustrate how force sensing comes into play. Measurements from tool–tissue force sensors enable the force information to be provided to the clinician in the form of graphic, auditory, vibratory, or other types of interfaces. In the case of a master–slave system, the information can also be used to directly provide force feedback through a haptic interface.

Since the systems represented in Figures 2.1 and 2.2 become more complex and costly with the introduction of force sensing capabilities, the need for force sensing must be fully justified. Force sensing information can be useful for robot control, to provide instrument–body interaction information to reduce damage and ensure effective manipulation of the tissue, to magnify interaction forces for enhanced sensation, or to identify tissue characteristics. This could lead to increased safety and reduced intraoperative time, and could allow less experienced surgeons to perform more intricate procedures with less practice.

Many procedures, however, are being performed successfully in a minimally invasive manner; therefore, the question arises as to whether force sensing is necessary and, if so, which procedures would benefit most from the availability of force information. Those procedures that receive no benefit from force sensing can then be performed with simpler and more cost-effective tools, while those procedures that do benefit from force information can be performed with increased safety and efficiency.

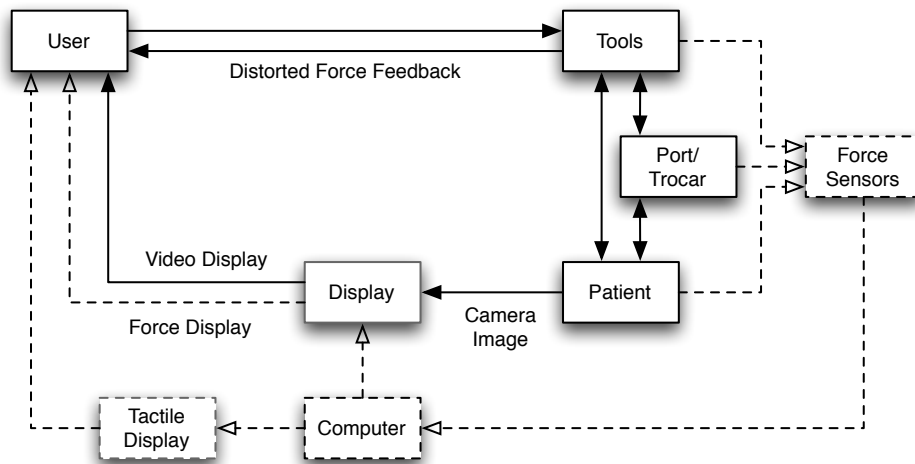


Figure 2.1: Information flow in a conventional minimally invasive procedure. The dashed lines represent the information that becomes available through force sensing.

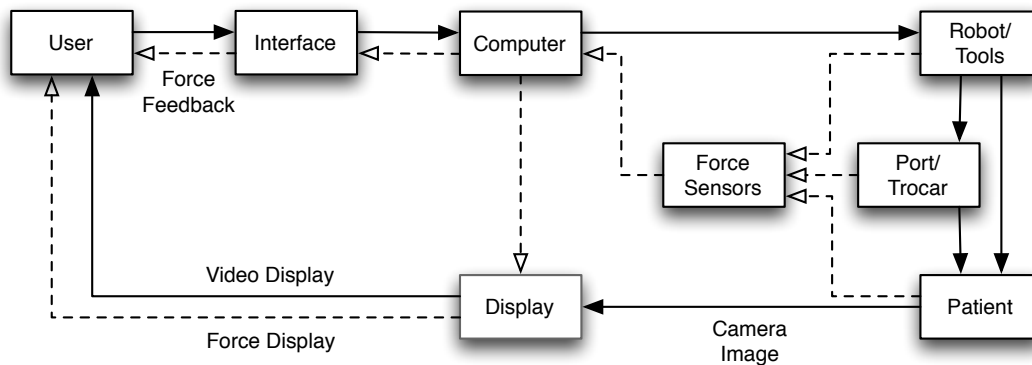


Figure 2.2: Information flow in a robotics-assisted minimally invasive procedure using a master-slave system. The dashed lines represent the information that becomes available through force sensing.

A number of studies have been performed to determine the need for haptic feedback (see Table 2.1 for a summary). These studies show that the benefit of force feedback is very much task, user and system dependent. Although most results indicate that there is a need for haptic feedback in MIS, the number of subjects is limited in each study, and there is still no consensus as to when force sensing is necessary or beneficial [5].

Situations in which direct haptic feedback has been shown to make a difference include: (i) microsurgery, where the ability to scale forces to perceivable levels can significantly benefit per-

Table 2.1: Experimental evaluations to assess the need for force feedback in MIST.

Ref.	Equipment	Compared	Task	Results	Subjects
[17]	Tension measuring device and the da Vinci system	VFF compared to no feedback	Knot tying	Haptic feedback allows surgeons to be more precise, more consistent and to apply greater tensions to sutures without breaking.	5 expert surgeons
[18]	2 master, 2 slave system with robotic arms and da Vinci tools. 2 DOF force sensing	FF 0%, 100% and 200%	Suture breakage arteriosclerosis detection and knot tying	FF improved all measures. Lower forces applied when knot tying, better approximation of the suture break force without breaking, and lower force applied while palpating. Also shows less fatigue.	25 surgeons at different experience levels
[3]	AESOP arms with sensorized instruments and a PHANToM controller	Robotic surgery with and without FF (scaled 22, 32, 45, 64%)	Dissection	The use of a robotic system with force feedback reduced the number of unintended injuries. High force scaling caused more injuries.	25 expert MIS surgeons
[19]	Surgical Assistant Workstation and da Vinci robot	VFF, FF or both	Palpation	A combination of haptic and graphical feedback reduced the number of errors compared to either one alone or no feedback.	7 surgeons: experts and novices
[20]	Tension measuring device and the da Vinci system	Robotic vs. conventional MIS and VFF	Knot tying	Concludes that user performance using the robot is worse than manual, but force feedback did not always improve the outcome.	6 surgeons: residents and attending
[21]	Customized master-slave system with 1 DOF feedback	Manual vs. grasper vs. FF grasper	Stiffness palpation	FF grasper significantly reduced the number of errors, but the hand is still better.	10 subjects: surgeons and non-surgeons
[22]	Customized master-slave system with 1 DOF feedback	FF, VFF+GFF or both	Suturing	The complement of visual feedback methods has the potential to reduce the applied forces when performing tasks.	8 non-surgeons
[23]	Customized master-slave system with 1 DOF	VFF, FF, GFF or FF+GFF	Palpation	Rate of success was highest with graphical feedback.	6 non-surgeons
[24]	Customized cutting instrument on a master-slave system	VFF, FF or both	Cutting	The combination of visual and force feedback was better than either individually.	20 subjects: surgeons and non-surgeons
[25]	2-Phantom setup with ATI mini	FF 0%, 75% and 150%	Blunt dissection	FF reduced RMS force by 30 to 60% and peak force by a factor of 2-6. Also reduced errors.	8 non-surgeons
[26]	2-master, 2-slave robotic system with 7 DOF feedback	VFF, FF or none	Knot tightening	VFF increased consistency of applied forces, FF increased control.	7 subjects: experts and novices

FF: Force Feedback

VFF: Visual Force Feedback: video display of the task site

GFF: Graphical Force Feedback: graphical display of the forces being applied

formance [25, 27, 28]; (ii) knot tying, where haptic feedback increases precision and consistency to ensure the knots are tight while preventing suture breakage [17, 29, 30]; (iii) palpation, where force sensing allows for the evaluation of tissue compliance, stiffness and viscosity [31, 32] to identify abnormal tissue and the location of anatomical features [6]; (iv) robotic applications, where a robot is controlled through force control to prevent tissue damage and compensate for organ motion [33] and in general master–slave systems, where force reflection helps position the tools and reduce applied forces [32]; and (v) in needle-based procedures, where knowledge of the insertion forces can improve needle placement [34]. Review papers assessing the need for haptic feedback include [5, 35].

Other benefits of force sensing related to clinical applications include: the measurement of applied forces for the development of new instruments and devices [36, 37]; determination of the magnitude of forces that result in damage to different kinds of tissue, allowing for the development of smart instruments or robots that can limit the amount of force applied to tissue [38]; tissue modelling [7, 21, 39]; and using force profiles as an aid to skills assessment and training [40, 41].

2.2.2 Where to Sense?

A first question that might arise when the need for force sensing is identified is where to sense the forces. To answer this question, it is necessary to consider the configuration of medical instruments and the forces that act on these instruments. Since there are many different points of contact with the environment, placement of the sensors must be carefully optimized [14]. A very detailed description of the forces acting on laparoscopic instruments is presented in [11]. These include: friction at the trocar, resistance of the abdominal wall, scaling and mirroring of the tip forces, internal friction within the instrument and inefficiency of the mechanism itself. The forces acting on the instrument along the access channel also need to be considered in catheter-based procedures and those that access the surgical site through natural orifices.

Figure 2.3 presents a diagram of the forces that may act on a surgical or therapeutic instrument when inserted in a minimally invasive manner. Forces at the handle are what the user feels in hand-held procedures or what the robot applies in master–slave systems. All instruments are affected by the internal structure of the instrument and by internal instrument friction. Furthermore, it has been shown that commercially available dissectors for minimally invasive surgery (MIS) have low mechanical efficiencies (between 8 and 42% [42]) that cause the forces at the handle and at

the tips of the instruments to be significantly different and nonlinearly related [43, 44]. At the port location, the forces acting on the instrument are a combination of the friction caused by the trocar and the moments generated by the abdominal wall when tilting the instrument [45, 46]. Other forces could be generated by nearby organs acting on the instrument shaft. These latter forces are significant in procedures that use flexible instruments, such as natural orifice procedures, single-port access procedures or catheter-based therapies.

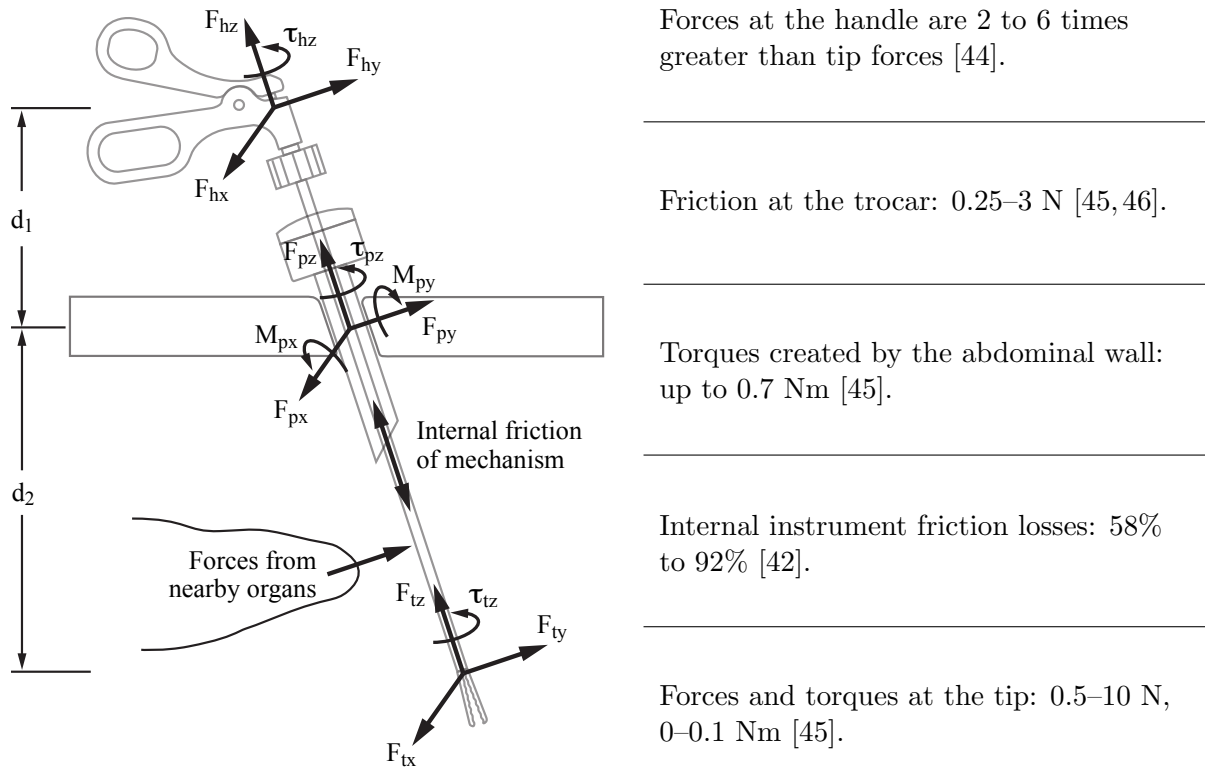


Figure 2.3: Forces acting on minimally invasive instruments.

Table 2.2 presents a summary of the different places where forces can be sensed [4]. Depending on the need for force sensing, it might be necessary to measure the hand–tool interaction forces, (for example, to determine the forces required to insert needles, for the development of training simulators or to determine the requirements of surgical robotic systems), or the forces applied by a robotic system on the tool (for example, for force feedback control [47]). Measuring the tool–tissue interaction forces at the trocar or through the access channel might be desirable if the purpose is to

Table 2.2: Locations for force sensing.

Location	Advantages	Limitations	Examples
On or near actuation mechanism	Some of the information is readily available, no need for sterilization or miniaturization of additional sensing elements.	Affected by friction, mechanism play, backlash, gravity, and inertia within the instrument. Sensing is taking place far away from where the forces are being applied. Indirect force measurement can overestimate the grasping forces [50].	[50–52]
On shaft outside entry port	No constraint with respect to size. Does not necessarily need to be sterilizable. The information is useful for the design of robotic devices or when calculating the amount of force the hand needs to apply.	Measurements are affected by forces at the trocar so they are not a good estimate of tool–tissue interaction forces.	[41, 53]
On the access channels	Can measure interaction forces between the instrument and the tissue surrounding the instrument as it enters the body in order to minimize tissue damage.	Entering the body requires the sensing elements to be sterilizable and to work in warm and humid environments. The size of the elements is limited to the size of the access channels.	[54–56]
On shaft inside the body	Capable of measuring kinesthetic forces acting at the tip of the instrument.	Must be sterilizable and must work in warm and wet environments. The size of the elements is also limited to the size of the port. Affected by mechanism friction distal to the sensor placement.	[48]
On tool tip	Capable of measuring kinesthetic and tactile forces acting at the tip of the instrument. Not affected by mechanism friction.	Must be sterilizable and must work in warm and wet environments. Severe space limitations, as the size of the elements is limited to the tool tip.	[50]

minimize damage to the abdominal wall when twisting the instrument to reach difficult areas, or to minimize damage when inserting flexible instruments through vessels or through natural orifices. In most applications, the goal is to obtain the tip–tissue interaction forces in order to assess tissue trauma or provide feedback during surgery.

The measurement of forces is simplified by placing the sensors outside of the body, since size and sterilization constraints are not involved. However, using this information to estimate forces acting at the instrument tip is inaccurate. The effect of friction at the trocar, abdominal wall forces, and the leverage effect make it such that tool–tissue interaction forces can only be accurately sensed by placing the sensors as close as possible to the instrument tip [48, 49]. The forces at the tip are sometimes so delicate that other forces acting on the instruments can easily mask them [35].

Owing to the difficulties inherent in placing sensors inside the body, researchers have been trying to address the discrepancy between handle and tip forces. The design of a mechanically efficient instrument for sensing grip forces at the handle is presented in [57]. This instrument uses rolling mechanisms to create an instrument that is 96% efficient. The results of their experiments

show a significant improvement in the ability to detect grip forces based on handle forces (stiffness of tissue and arterial pulse). To address the frictional forces introduced at the trocar, it was shown in [46] that friction within a trocar could be significantly reduced with a proper design of the sealing mechanism or by using lubricants. Finally, [58] developed a model for friction compensation, in their case using the da Vinci instruments. They show that a “friction compensator with multiple single-state elastic friction models” is reasonably effective at cancelling the Coulomb friction of the joints of the slave manipulator in unidirectional motion. These solutions, however, do not deal with the effect of the abdominal wall on the instrument, or the scaling that occurs due to the fulcrum location on the instrument.

Sensing for needle-based procedures presents unique challenges. It has been shown that knowing the forces that act on the needle during insertion can lead to improved placement precision [34]. Due to the small size of the needles, placement of sensors anywhere within the needle shaft is extremely difficult and most systems measure the forces outside of the body [59]; however, novel sensor designs have been capable of estimating needle tip force and sidewall friction in 7 DOFs [60, 61].

2.2.3 What to Sense?

Another consideration when dealing with force sensing in MIST is to identify which forces need to be measured. Full representation of the instrument interaction can only be achieved by simultaneously measuring three orthogonal forces, three orthogonal moments, and the actuation force (grip or cut depending on the instrument). For telemanipulators to be completely transparent, sensing and display of all 7 DOFs of haptic information are needed [14], in addition to tactile information [62]. Furthermore, asymmetry between the number of DOFs in force sensing and the number of DOFs in a haptic device can affect stability in bilateral teleoperation.

For some applications and tasks, however, sensing forces in some of the degrees of freedom might be sufficient to achieve the desired results. Identification of which degrees of freedom need to be sensed for particular tasks still remains an open area of research. Considerations include the differences arising from the use of different instruments and instrument configurations, the task being performed, the level of expertise of the subjects, and the type of procedure.

Some limited studies have tried to identify the benefit of measuring forces in different directions. The asymmetry in bilateral haptics-enabled teleoperation was assessed in [63], where it is shown

that feeding back forces in just two degrees of freedom for certain tasks is a significant improvement over no force feedback, while adding the axial direction does not make a significant difference in terms of applied forces. Another study, presented in [62], concludes that grip forces and Cartesian forces are decoupled; in other words, providing feedback in translational forces does not help with grip force control and vice versa.

2.3 Force Sensing

After assessing the need to sense forces and the characteristics of the environment that affect force sensing in clinical applications, consideration must be given to determine which type of sensor can best meet the design constraints. This section outlines existing technologies for force sensing and how these different technologies can be applied to achieve sensing in multiple degrees of freedom.

2.3.1 Technologies

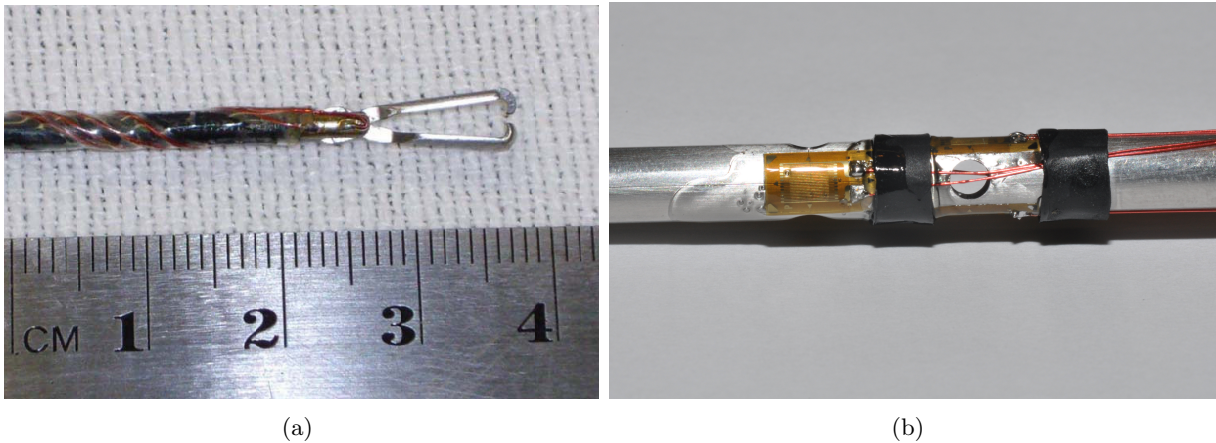
The most commonly used technologies for sensing forces are strain gauges, piezoelectric sensors, capacitive-based sensors, and optical sensors. These technologies and other more novel methods are summarized in Table 2.3 and discussed below.

Strain gauges: The most common technology employed for force sensing uses thin metal foils applied to the surface of an instrument to measure the deformation caused by the applied force. These foils, when attached to a thin plastic backing material and oriented in a particular arrangement, are called strain gauges [64]. Strain gauges have been successfully used in instruments for medical applications [23, 36, 65, 66] (more details on these instruments are provided in Section 2.4.2). Figure 2.4 shows examples of strain gauges applied to MIST instruments.

To achieve multi-axis measurements using strain gauges, special structural elements are commonly used on which strain gauges are placed at different locations to allow the different forces and moments to be measured. A review of force sensing structures found in the literature is presented in [67]. The Stewart Platform [68], the Maltese Cross [69], and Junyich's configuration [70, 71] and their variations are the most commonly used structures. Other novel structures for multi-axis sensing are presented in [67, 72–74]. The selection of one of these structures for force sensing purposes depends on the desired balance between signal noise levels, measurement isotropy, signal coupling, the number of sensing elements and the size of the structure.

Table 2.3: Force sensing technologies.

Technology	Advantages	Limitations
Strain gauges	Small size and can be sealed in a waterproof environment. Multi-axis measurement is easily achieved.	Sensitive to electromagnetic noise and temperature changes leading to drift and hysteresis. Tradeoff between the sensitivity of the measurement and the stiffness of the structure [4].
Optical sensors	Forces can be measured in as many as 6 DOFs [75]. They can be used inside Magnetic Resonance Imaging (MRI) scanners [76]. Also, they can detect changes with high sensitivity and reproducibility with no hysteresis [75].	Limitations include sensitivity to noise, and that optical fibres cannot typically achieve small bending radii [4].
Measurement of actuator input	The system is no longer limited by the sensor bandwidth (which can make a control or feedback system unstable), and it is not necessary to incur the cost of force sensors [77]. Does not rely on force sensors, which often do not operate properly when exposed to high temperatures and humidity [78].	Very sensitive to uncertainties [78]; if the system cannot be properly modelled (due to high joint friction, for example), the estimation error can be significant.
Capacitive-based sensing	Limited hysteresis, better stability and increased sensitivity compared to strain gauges [4, 79].	Require more complex signal processing and are more expensive than other methods [4, 79].
Resonance-based sensing	High signal to noise ratio and digital processing is possible.	Affected by nonlinearities and hysteresis [79].
Piezoelectric sensing	Since these materials generate their own voltage, no additional power supply is needed [4]. They have high bandwidth, high output force, compact size and high power density [79].	Very temperature dependent and subject to charge leakages [4]). This results in a drifting signal when static forces are applied, thus making them suitable for the measurement of dynamic loads only.

Figure 2.4: Examples of strain gauges used in instruments to measure forces during natural orifice procedures [37] (*left*) and during laparoscopic procedures [80] (*right*).

Optical sensors: Another technology often used for sensing force is based on measuring the change in intensity or phase of a light signal as it passes through a flexible structure. When forces are applied to the structure, the way in which the structure flexes creates a change in the intensity of the light or causes the phase of the light signal to vary proportionally, making it possible to estimate the amount of force or pressure being applied. The design of 6-DOF optical force sensors is presented in [75,76], while the development of optical force sensors for MIST is discussed in [81,82].

Measurement of actuator input: When actuators are used to drive the joints of a manipulator, the input to the motor (for example, the current drawn by electrical motors or the variation in the pneumatic pressure in pneumatic actuators), can be directly related to the amount of force or torque generated. Since these signals are affected by internal joint friction and actuator nonlinearities [4], knowledge of the mechanism kinematics and friction dynamics is critical for force and torque measurements to be accurate. Measurement of actuator input is mostly used in master–slave (teleoperation) systems for force or torque control or for haptic feedback.

In order to use the input to the actuators as a means of estimating applied forces, an observer-based control system is commonly used. For this purpose, a model of the system needs to be developed and the uncertainties of the model compensated for or measured. Observer-based sensing compares the difference between the output of the nominal model and the actual system output. If the uncertainties are known, the disturbance observer can estimate the amount of force generated at the output based on the actuator input [83]. To measure uncertainties, [84] uses neural networks to estimate friction, inertia, and gravity, while [78] uses a modified extended Kalman filter to compensate for the modelling error, sensing bias and measurement noise. A Nicosia state observer is utilized in [85] together with a general bilateral control law that ensures matching of the forces at the master and the slave. Examples of these types of controllers are presented in [77,78,83,84], while only the latter has actually been used in MIST.

Capacitive-based sensing: This type of sensing is commonly used to measure tactile information. It depends on the use of a membrane, which when deflected, causes the distance between two electrodes separated by a dielectric material to change. Examples of instruments based on this concept include [86,87].

Resonance-based sensing: This type of sensing is also membrane based. A change of force and pressure can be detected by measuring the change in the resonant frequency of the membrane.

Piezoelectric sensing: In piezoelectric materials, a change in mechanical stress results in

a voltage change across the material [79]. The most commonly used piezomaterials for sensing and actuation purposes include a piezoceramic called Lead Zirconate Titanate (PZT) and a piezopolymer called Polyvinylidene Fluoride (PVDF) (see [88] for more details on these and other piezomaterials).

Other technologies: It is possible to find in the literature other technologies for measuring forces that still have not been used in MIST applications. *Deflection sensors* are one of these technologies, which are based on the ability to measure the deflection of a component with known material properties to estimate the amount of force being applied on it. The key for these sensors to be effective is to be able to properly measure displacement. Displacement sensors include potentiometers, Linear Variable Differential Transformers (LVDTs), and encoders [89]. A 3-DOF force sensor based on measuring beam deflection using LVDTs is presented in [90].

Some force sensors utilize *piezomagnetic* materials, in which a change in the stress applied can be detected as a change of permeability in the presence of a magnetic field [79]. In [91], a 6-DOF force sensor has been designed using *ultrasound* transducers. The sensor measures the amount of time it takes for an ultrasound pulse to travel from the emitter to the sensor. As forces are applied to the object, an elastomer layer deforms, changing the distance that the ultrasound pulse needs to travel. A series of transducers are placed in a particular pattern to measure multi-axial forces and torques. The authors claim that these sensors are highly accurate, robust and inexpensive compared to other modalities.

2.3.2 Requirements of Force Sensors in Medicine

In order to select the appropriate technology for clinical applications, it is necessary to consider the particular requirements that force sensors must meet when used in minimally invasive medical instruments. The most critical requirements are as follows:

Range and Resolution: Force sensors need to be properly designed to measure the range of forces commonly found in MIST, with sufficient resolution to obtain meaningful information. Ultimately, the force sensors must be able to sense the forces that are commonly applied during clinical procedures. The range can be determined based on the maximum and minimum forces expected. In order to reduce the effect of quantization error, the sensor resolution should be one order of magnitude less than the force difference that needs to be resolved [92]. In [81], it is stated that for common MIST procedures, a force range of ± 10 N with a resolution of 0.2 N is desired.

In [82], it is determined that a force range of ± 2.5 N with a 0.01 N resolution was optimal for needle driving tasks. Similarly, [92] showed that a 0 to 2 N range with 0.01 N resolution was required for lung tumour localization using kinesthetic feedback.

Size and weight: Applications of force sensors in MIST are also limited by constraints on the size and weight of the sensors. Regardless of location, sensors must be lightweight [93], as they need to be maneuvered with the instrument without significantly increasing its inertia. For sensors placed inside of the body, they must be smaller than the size of the trocar being used [81,93]. In most cases, this limits the diameter of the sensor to 10 mm, while the length can be up to several centimetres.

Biocompatibility: When force sensors need to enter the patient's body, they must be made from biocompatible materials. Any system that treats, augments or replaces any tissue or organ needs to be made from biocompatible materials [94]. The requirements for the selection of the materials to be used for force sensors are not as stringent as for devices that are implanted within a body, nonetheless, the effect that the material has on the body, as well as the effect that the body has on the material, must still be considered [95]. Appropriate materials must be nontoxic, must not produce an immune response in the body and must not react with the body in any way. Biocompatible materials include certain polymers, ceramics, carbons and metals. See [94] for a detailed description of these materials and the international standards that they must meet.

Sterilizability: All sensors that enter the patient's body must be able to withstand a sterilization procedure. Sterilization of medical instruments refers to "the use of a physical or chemical procedure to destroy all microbial life, including those microorganisms that exist on inanimate objects" [96]. Sterilization is necessary to prevent infections caused by fungi, bacteria, and viruses [4]. The most common sterilization methods include steam (autoclave), ethylene oxide, and gamma and electron beam irradiation [97]. The procedure for sterilization and disinfection is specific to each application and must be developed according to the infection risk of the medical device being used.

In hospitals, the most widely available method is the autoclave: steam sterilization reaching 105–135 °C at high pressure for at least 15 minutes. It is difficult to design electronic components that can withstand these conditions. In order to meet sterilizability requirements, sensors must be able to withstand at least one sterilization method.

Sealed: In order to work in environments that are wet and warm, sensors must be waterproof

and sealed [81]. Small crevices and cracks within the sensors must be avoided, as biomatter and/or fluids may infiltrate into them. If this is not possible, a proper cleaning and sterilization procedure must be developed to remove the contaminants without causing damage to sensing elements or associated electronics.

Sensitivity: For force sensors to be effective, design considerations must include the required accuracy, bandwidth, hysteresis, creeping [98], sensitivity to noise, and sensitivity to temperature and humidity variations.

Other requirements: Ideal sensors should be inexpensive [14], especially if they are to be integrated into disposable or limited use devices. A modular design is also desirable [55], allowing sensors to be integrated into different instruments for multiple applications.

2.3.3 Calibration

Once an appropriate technology has been selected to meet the design constraints presented above, design engineers must consider how the data from the sensing modality selected will be used in order to obtain meaningful information. To achieve this, it is necessary to establish a relationship between the signals being measured and the actual forces or torques being applied. For this purpose, a calibration procedure needs to be performed.

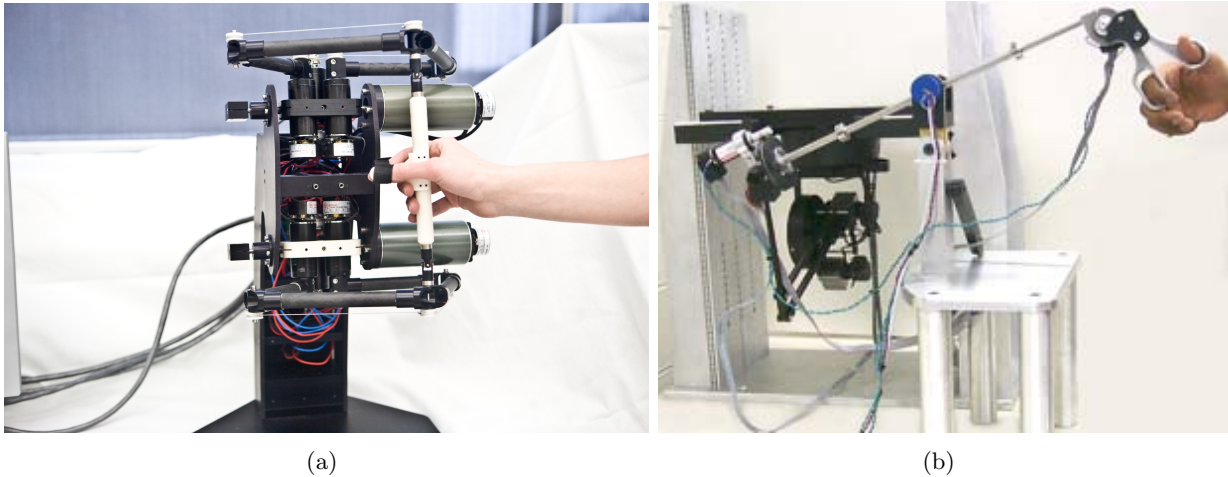
In most cases, the calibration procedure consists of applying known forces throughout the operating range of the sensor and measuring the resulting change in the output signal. A calibration equation or matrix can then be developed and used to estimate sensor accuracy, reproducibility and hysteresis. Examples of calibration methods for different types of sensors are presented in [66, 75, 99].

2.3.4 Interface Requirements

Once the force sensing information is acquired, it must be transferred back to the user in a manner that is useful and effective. Most of the time the signals produced by the technologies presented above are very small with some degree of noise. Thus, to be useful, these signals must often be filtered and amplified prior to use (see Figure 2.5 [64]). The signals must then be digitized for acquisition by a computer, where subsequent processing and/or recording may be performed [100]. There are many different ways of processing this information in order to present it to the user through haptic interfaces or other graphical force representations.



Figure 2.5: Signal processing flow.

Figure 2.6: Examples of haptic interfaces for MIST applications: reference [111] (*left*) and reference [103] (*right*).

Haptic interfaces refer to input devices that incorporate actuators that may be used to move or to prevent motion in certain directions [101]. This creates the impression that forces are acting on the device as the user manipulates the handle. 3-DOF devices, which provide “single point interaction,” have been shown to produce a significant improvement in performance over no force feedback; however, the limitations of the 3-DOF interface impair the ability to determine shape, stiffness, size and other characteristics [102]. Feedback provided in all 6-DOF might be better, especially when combined with tactile information. Examples of haptic interfaces designed for MIST include a system for surgery and therapy [103] (see Figure 2.6), haptic forceps for microsurgery [104], a force reflection scheme for a master system using actuated and sensorized forceps [32], and a haptic interface device that provides kinesthetic feedback as well as tactile information via an array of pins [105,106]. Examples of master–slave systems with force feedback include [49,85,101,107–111].

An alternative to haptic interfaces is to use sensory substitution to relay force information. The data can be presented to the user in the form of graphical or auditory signals. The benefits of sensory substitution, apart from avoiding the cost of haptic interfaces, include the ability to

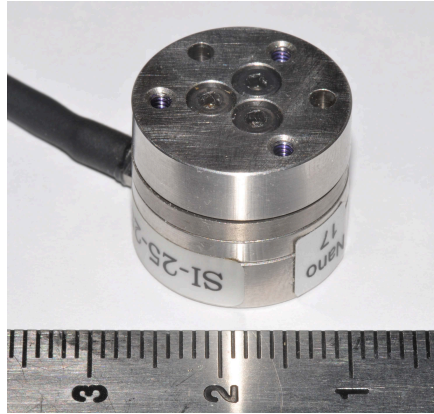


Figure 2.7: ATI Nano-17 force sensor.

increase haptic resolution and magnify forces while not conveying force information to the user that could result in misleading or erroneous conclusions. However, there is a fundamental difference between direct force feedback and various types of sensory substitution in that when the senses are substituted, cognitive attention is required to respond [112]. This means that people can respond to direct force feedback more quickly than to sensory substitution. Studies that focused on determining how sensory substitution compares to haptic feedback have been presented in Section 2.2.

2.4 Force Sensing Technologies and New Developments

Using the technologies presented above, a significant amount of research has been done in order to develop adequate force sensors for different applications. Several force sensors are available commercially but most are still at an experimental stage. The most significant contributions to the field, with details on the technologies used, are presented in the following sections.

2.4.1 Commercially Available Force Sensors

A list of commercially available force sensors and their main characteristics is presented in Table 2.4. This table shows that there are no force sensors available that can sense forces in multiple DOFs and that are small enough to fit through minimally invasive surgical ports. The closest commercial sensor is the Nano-17 (ATI, Industrial Automation), which measures forces in 6 DOF, is 17 mm in diameter and can be sterilized with ethylene oxide or formaldehyde, see Figure 2.7.

Table 2.4: Summary of small commercially available force sensors.

Company	Website	Smallest size (mm)	DOF		Sterilization	Technology
Vishay	www.vishay.com	5.8 × 3.0 × 0.02	1	A	No	SG
Futek	www.futek.com	30.5 × 6.4 × 0.0762	1	A	No	SG
Sensy	www.sensy.com	40 OD × 11	1	C	No	SG
PCB Piezotronics	www.pcb.com	16.5 OD × 7.9	1	C	No	SG
HBM	www.hbm.com	17 OD × 6	1	A/T	No	SG
Sherborne	www.sherbornesensors.com	17 OD × 53	1	A	No	SG
Gefran	www.gefran.com	31.75 OD × 17	1	C	No	SG
Flintec	www.flintec.com	150 × 40 × 25	1	A	No	SG
Haehne	www.haehne.de	40 OD × 60 or 55 OD × 24	1	C	No	SG
TME	www.tme-france.com	24 OD × 21	1	A	No	SG
Dytran Instruments	www.dytran.com	19 OD × 45	1	A	No	Piezo electric crystals
Statek	www.statek.com	tine width is 7.1 thickness 7–8	1	A	No	Quartz crystal resonators
Kistler	www.kistler.com	7 OD × 3 or 6.3 OD × 43.3	1	A/T	No	Piezo electric quartz
Interlink Electronics	www.interlinkelectronics.com	5 × 5 × 0.2	1	C	No	Customized resistors
SensorTechnics	www.sensortechnics.com	9 × 4 × 3	1	A	No	Piezo resistors
Honeywell	sensing.honeywell.com	17.15 OD or 3.25 × 5.6 × 11.7	1	A	Fully sealed, sterilizable with isopropyl alcohol	Piezo resistors
Femto Tools	www.femtotools.com	36.4 × 15.9 × 5.3	1	A	Sterilization of the silicon tip of the instrument	Capacitive sensors
Strain Measurement Devices	www.smdsensors.com	66.04 × 6.35 × 0.46	1	C	Autoclave, radiation or diluted bleach	Thin film SG
MicroStrain	www.microstrain.com	5 × 1.4 × 1.8	1	A	Alcohol, radiation or gas sterilization	SG
Omega	www.omega.com	9.6 OD × 3	1	C	Alcohol sterilization of stainless steel products	SG
Tekscan Inc.	www.tekscan.com Flexiforce sensors	0.208 × 51 × 14	1	C	Gamma radiation; some autoclaveable	Piezo resistors
Bokam Aura/Supra	www.bokam.com	36.3 × 24 × 18	3	F	No	SG
BL Autotec	www.bo-autotec.co.jp	18 OD × 32.78 25 OD × 22	6	M, F	No	SG
ATI	www.ati-ia.com	17 OD × 14.5	6	M, F	Ethylene oxide, formaldehyde	Silicon SG

OD: outer diameter

C: compression, unidirectional

A: axial, tension and compression

T: torque

F: three orthogonal forces, x , y and z

M: three orthogonal moments about the three main axes

SG: Strain gauges.

2.4.2 Novel Force Sensors in Clinical Applications

A summary of force sensing technologies that have been proposed in the literature is presented in Table 2.5. Of note is a novel method of force sensing proposed in [113], which uses noninvasive biofeedback sensors incorporated into standard surgical tools to quantify oxygen levels in tissue. Tissue oxygen levels can be directly related to the magnitude of the force exerted on them, and the information can be used to warn the clinician if oxygen levels drop below acceptable levels. Also, the system presented in [48, 114] is able to sense forces in all DOFs available in surgery. The distal end of the instrument is sterilizable in an autoclave. The electronics are packaged in a thermally stable material and covered with a synthetic resin for insulation [114]. Information from these types of instruments can be combined with tactile information for full haptic feedback.

A review of tactile sensors for industrial applications can be found in [98]. The development of a compliant tactile microsensor for a multi-fingered hand is presented in [115]. Similarly, [2] presents the design of a robot for arterial pulse palpation that utilizes a sensorized finger based on custom capacitance-based technology and strain gauges on the finger joints. Finally, the tactile sensing and feedback system presented in [105] uses a tactile sensor developed by [87] and a tactile array based on a series of pins to provide feedback. However, some researchers have determined that tactile sensing is not particularly beneficial [12]. A study presented in [15] identified that tactile information alone cannot be fully interpreted unless paired with force information.

2.5 Discussion

The sections above have presented a thorough review of what has been accomplished in the field of force sensing in general and more specifically for clinical applications. In summary, the science of force sensing has come very far through the introduction of novel technologies and configurations that allow sensing to be performed in small spaces and in multiple directions. Many researchers are actively engaged in developing methods to restore the force information that is currently impaired or missing from the tools, instruments, and systems used for MIST.

Many studies have focused on determining if force sensing is really necessary, and if so, which degrees of freedom are most important and for which tasks. Force sensing information has been shown to be useful in situations where the applied forces are extremely small and cannot be detected by the human hand, when tissue characteristics need to be determined through palpation, and

Table 2.5: Summary of force sensing instruments.

Reference	DOF	Sensing What?	Sensing Method	Purpose	Type	Actuation Method	Size	Accuracy
Grip forces only								
[7, 31]	1	Grip forces and angle	Strain gauges on ring and optical sensor	Characterization of tissue properties	Grasper	Hand	Too large for MIS	No details provided
[21, 39, 108] FREG	1	Grip forces	Actuator motor currents	Tissue characterization by palpation	Babcock grasper	Hand	5 mm shaft diameter	No details provided
[38, 93] The MEG adapted from FREG	1	Grip forces	Strain gauges	Identification of forces that are damaging to different tissues	Babcock grasper	Motor on handle	5 mm shaft diameter	No details provided
[116, 117]	1	Grip forces	Strain gauges	Microsurgery	Gripper	Piezoelectric motor	$17 \times 7.5 \times 0.4$ mm 4 different prototypes; some are for MIS	Good linearity in the range 0-22 mN
[113]	1	Grip forces	Tissue oxygenation level	Measurement of grip forces in surgery	Gripper	Hand or robot		No details provided
[118]	1	Grip forces	Strain gauges	Large organ manipulation	Grasper	Motor driven	10 mm shaft diameter	Maximum 0.7 N for 10 N range
[119]	1	Grip forces	Piezoelectric sensor	Microsurgery	Tweezers	PZT actuator	$69 \times 14 \times 13$ mm	Maximum 0.086 N for 0.8 N range
Forces measured at the trocar								
[55]	2	Bending moments in x and y	Sleeve that goes over the instrument with two strain gauge bridges	Measurement of forces in MIS	Any MIS instrument can be used	Hand	For 5 mm shaft diameter	Max 7.22% error
[33, 56]	3	Trocar forces	ATI Nano 43 F/T sensor	Sensing of forces during MIS	Any MIS instrument can be used	Motor driven	Depends on instrument inserted	No better than that of the ATI sensor
Forces measured at the handle								
[53]	6	Forces and torques at the handle	ATI mini F/T sensor	Modelling of surgical gestures	Grasper	Hand	No details provided	No better than that of the ATI sensor
[40, 41] BlueDragon	7	Forces, torques and grip at the handle	ATI mini F/T sensor, force sensor on tool handle to measure grip (no details), pots on mechanism to measure position	Training in laparoscopic surgery	Grasper/cutter	Hand	Large manipulator holding a laparoscopic tool	No better than that of the ATI sensor
[120-122]	7	Forces, torques and grip at the handle	ATI mini F/T sensor and a Futek load cell (FR-1010) on the handle	Training in laparoscopic surgery	Atraumatic or Babcock grasper, curved dissector	Hand	10 mm after the force sensor	No better than that of the ATI and Futek sensors

Reference	DOF	Sensing What?	Sensing Method	Purpose	Type	Actuation Method	Size	Accuracy
Forces measured at the handle and trocar								
[123–125]	3	Forces	Strain gauges	Measurement of forces in master–slave MIS	Forceps	Robotic actuation	10 mm	0.1 N
[36]	4	Forces and grip	Strain gauges	Design, simulation and understanding of tissue trauma	Forceps	Hand	Fits through 5.5 mm port	0.05 V for grip and 0.1 V for port forces for a 1 N range.
Forces measured at the tip								
[126–128]	2	Parallel forces	Micromachined components and capacitive detection	Measurement of forces in laparoscopic surgery	Forceps	Robotic	5 mm	No information; range 0 to 1.7 N
[129]	3	Tangential and normal forces	Piezo resistors	Cutting during fetal surgery	Cutter	N/A	7.4 mm in diameter	0.02 N for a 1 N range
[66]	3	Forces at the tip	Strain gauges	Amplification of forces in microsurgery	Generic tip	Hand	12.5 mm in diameter	0.013 N in a ± 0.5 N range
[130]	3	Forces at the tip	Optical sensors	Force sensing in robotic surgery	Sensor only	Hand or robot	10 mm in diameter (hollow)	0.1 N in x and y , 0.5 N in z for a 10 N range
[131]	3	Forces at the tip	Optical sensors	Minimally invasive tumour localization	Palpation tip	Robot	10 mm in diameter	0.15 N for a 3 N range
[132]	3	Forces at the tip	Strain gauges	Force sensing in robotic surgery	Sensor only	Hand or robot	3.4 mm in diameter	0.005 N for a 2 N range
[82]	3	Forces at the tip	Optical fibers within a customized structure	Measurement of forces in robotic surgery	Needle driver	Hand or robot, as needed	5 mm	2.5 N range axially, 1.7 N range radially; 0.04 N resolution
[65] Evolved from [24, 52]	3	x, y forces and grip	Strain gauges for x and y ; resistive sensor on gripper	Teleoperation with haptic feedback	Graspers and scissors	Motor driven	~ 12 mm diameter	Resolution 0.1 N (no details provided)
[50, 133]	3	x, y forces at the tip and grip	Piezoelectric sensors for x and y ; thin film sensor for grip	Identification of tissue abnormalities through palpation	Grasper	Robotic	About the size of a quarter	0.125 N in grip; others are not specified
[22, 23, 49, 109]	5	Forces at the tip, grip and torsion	Strain gauges; load cell for grip	Master–slave teleoperation with haptic feedback	All types of graspers, scissors	Hand	< 10 mm	No details provided
[134]	6	Forces and moments	Strain gauges	Measurement of forces in laparoscopic surgery	Forceps	Hand	> 10 mm	No details provided
[84]	4	Forces and grip	Pressure from pneumatic actuators	Measurement of forces in robotic surgery	Gripper	Pneumatic actuators	10 mm	0.1 N at the tip
[48, 114]	7	Grip, forces and torques	Strain gauges and uniaxial force sensor	Teleoperation with haptic feedback	Grasper	Motor driven	10 mm diameter	0.05 N in x and y and 0.25 N in z

in robot control. Particular tasks like knot tying and tissue manipulation could benefit from the availability of force information to ensure that sufficient forces are applied to avoid slippage but that no damaging forces are exerted on the tissue. It has been suggested that knowing the mechanism by which force feedback improves performance can help in the design of proper interfaces and to identify those tasks in which force feedback is needed [112].

The availability of quality force information requires the development of properly designed force sensors. The requirements of force sensors depend significantly on what information needs to be collected, which determines where the sensors need to be located on the instrument. For most applications, the goal is to place the sensors as close as possible to the point at which the instruments interact with the tissue—this significantly constrains the size and sterilization requirements of the sensors. Commercially available sensors can be used in customized configurations to sense forces in multiple degrees of freedom and within the patient’s body. However, none of the sensors available commercially can sense forces in 6 DOFs (let alone 7 DOFs), in a package small enough to enter the patient’s body in a minimally invasive manner.

Researchers aiming to circumvent the constraints imposed by MIST have come up with some ingenious solutions. The development of a mechanically efficient instrument to reduce internal friction is a great solution to the inability to sense gripping forces directly. Master–slave systems that compensate for instrument friction in dexterous instruments are aiming to achieve a similar goal, with benefits that could extend to multiple degrees of freedom.

The force sensor presented in [48,114] is the closest design to an ideal force sensor for detecting tool–tissue interaction forces in MIST. The commercial availability of this sensor would aid in the development of systems capable of providing force feedback in 6 DOFs and can be integrated with other sensors to provide 7 DOFs. Once the force information is available, determining the best way of processing and displaying the information is another active area of research. The development of haptic interfaces ensures that the forces are presented to the user in an intuitive manner. Alternatively, sensory substitution allows the force information to be merged with other sensing and imaging modalities and could prove to be more beneficial for certain tasks.

Filling in the gaps in the current state of the art is the focus of this work. The first step was to develop instruments capable of sensing forces and torques in all 5 DOFs available in laparoscopic MIS. The following chapter presents the design of the first prototype of the sensorized instruments.

Chapter 3

First-Generation SIMIS Instruments

3.1 Introduction

As presented in the previous chapter, a significant amount of work has been done to address the issue of degraded haptics in MIS. However, there is still a need for an independent force sensing system that can be used in any surgical or training scenario (laparoscopic trainer, animal labs or real surgery) for the purpose of measuring kinesthetic forces applied at the instrument–tissue interface. To address this need, the Sensorized Instrument-based Minimally Invasive Surgery (SIMIS) system was developed. This chapter describes the design, development and assessment of the first prototype. This chapter is based on reference [80].

3.2 Design Specifications

The goal of this work was to design and develop a highly versatile system that can be used in real surgical procedures and that provides force and position information through novel design features. Such an instrument offers several benefits to practitioners of MIS: force information can warn of excessive forces being applied on delicate tissue or insufficient forces applied when grasping or cutting; force data can aid in characterizing tissue stiffness and identifying diseased areas such as tumours or calcifications; force and position information can be used to provide warnings about the application of damaging forces while the instruments are out of the field of view; force and position trajectories recorded when performing standardized tasks can be used for training and skills assessment; instrument position data can be used to provide warnings when entering high

risk areas; or available force and position data could be merged with preoperative or intraoperative images to provide additional guidance to the surgeon. The specifications for the instrument were then outlined as follows:

1. The instrument must fit through a standard minimally invasive surgery port (maximum outer shaft diameter is 10 mm).
2. It must be capable of measuring forces and torques acting in all 5 DOFs available during laparoscopic MIS. These include the 3D forces acting at the tip, the torque about the instrument axis and the gripping or cutting force, depending on the instrument.
3. It must allow measurement of instrument tip position and orientation in 6 DOFs.
4. The overall appearance and weight must be similar to traditional hand-held laparoscopic instruments. This requirement is critical for the development of proper techniques when used in training. If the instrument is restricted at the entry point, or heavy cables are pulling down on the handle, the normal movement of the instrument will be compromised, and surgical skills might not be developed properly.
5. In order to increase versatility and reduce overall cost, it must allow attachment of interchangeable tips and handles according to the different tasks that must be performed.
6. The software interface must allow the force and position data to be recorded while trainees perform a series of standardized tasks.

3.3 Presentation of the Mechanical Design

A first prototype of the sensorized laparoscopic instrument has been designed to noninvasively measure the interaction of the instrument with tissue in the form of forces or torques acting in all five DOFs available during MIS. The instrument is composed of three concentric shafts. An inner shaft (2.50 mm in diameter) controls the opening and closing of the tip and is directly connected to the handle. A middle shaft (4.76 mm in diameter) provides rigidity to the instrument and connects the static components of the handle and the tip. An outer shaft (9.53 mm in diameter) “floats” over the middle shaft, providing a sealed environment for the sensing elements and protecting them from moisture and wear. Figure 3.1 shows the overall design of the instrument in two different

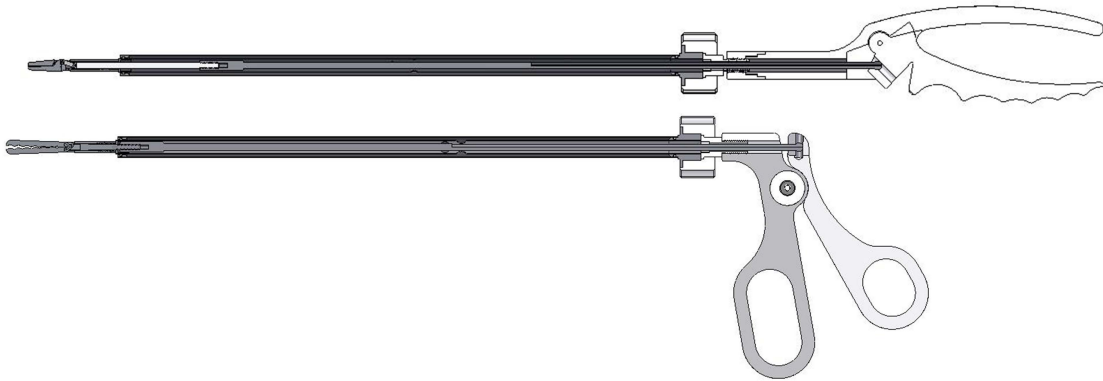


Figure 3.1: Instrument design with needle driver handle and tip (*top*) and with traditional handle and gripper attachment (*bottom*).

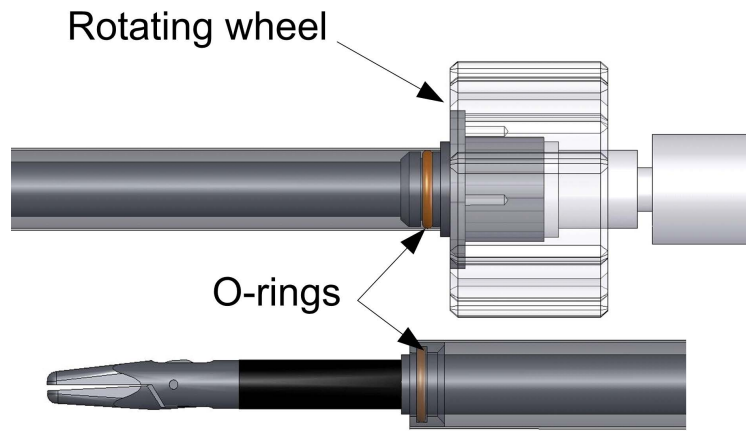


Figure 3.2: Detail of the instrument design showing the o-ring location for attachment of the outer shaft. The rotating wheel shown in the top image allows the user to rotate the distal end of the instrument in order to reorient the tip with respect to the handle.

configurations: a typical scissor-like handle with a gripper attachment (41.8 cm long) and a needle driver handle and tip (49.1 cm long). The outer shaft is held by two o-rings as shown in Figure 3.2. These o-rings seal the inside of the instrument from moisture and ensure that the outer shaft is held firmly in place. For ease of use, a rotating wheel allows the user to reorient the tip with respect to the handle to optimize ergonomic conditions. The instrument has been designed in a cost-effective and versatile manner with the addition of interchangeable tips and handles. The sensors are all attached to the middle and inner sections of the instrument. This way, the same sensorized elements can be used to perform the wide variety of tasks encountered during endoscopic surgical procedures by attaching different tips and handles.



Figure 3.3: Coordinate frame associated with the instrument.

3.4 Force Sensing

A survey of suitable force sensors was performed prior to the design of the instruments, as presented in Section 2.4.1. It was found that none of the commercially available force sensors were adequate for measuring forces at the tip of laparoscopic instruments due to their large size. Previous experience with strain gauges [49] demonstrated that they would be appropriate for measuring the deformation of the instrument shaft in order to determine the associated forces at the tip. A large number of resources, including books and websites, provide information and guidelines on gauge selection and placement in order to measure strain in different directions.

The specific placement and configuration of the gauges was selected based on a finite element model analysis to determine the areas of increased stress concentration, as detailed in the following sections. For reference, Figure 3.3 shows how the coordinate frames have been assigned to the instrument.

3.4.1 Actuation Force

Actuation of the instrument tip is achieved by sliding the inner shaft of the instrument as the handle is opened and closed. The applied force when gripping or cutting is therefore directly related to the axial forces acting on this inner shaft. Preliminary calculations showed that the maximum expected forces produced very little strain on the initial design of the inner shaft, thereby requiring the ability to sense extremely small changes in resistance. In order to increase

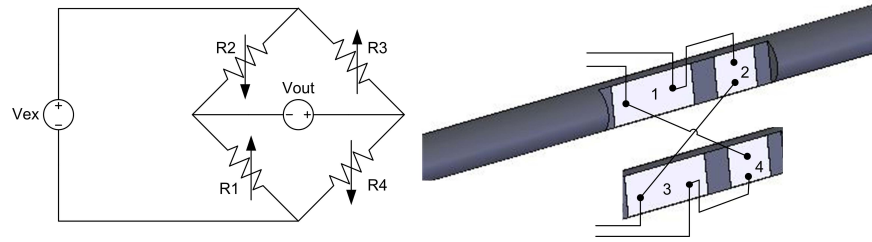


Figure 3.4: Type III full Wheatstone bridge (*left*) and the corresponding placement of gauges on the inner shaft (*right*).

the axial strain, the cross-sectional area of the shaft was locally reduced by machining a 1 mm thick flat section, 12.7 mm long, about 70 mm from the tip. This not only provided a better surface for gauge placement, but also increased the axial strain by 140%. Furthermore, in order to maximize the signal in the axial direction, a type III full Wheatstone bridge was used (see Section A.2). This typical configuration for measuring axial forces is characterized by the use of four active strain gauge elements. Two are mounted in the direction of the axial strain on opposite sides of the shaft. The other two are mounted perpendicular to the first two gauges. When the four strain gauges are connected in a type III configuration, the axial forces are maximized while rejecting bending strain, compensating for the effects of changes in temperature, and compensating for lead resistance. The details of the gauge placement and their connections are shown in Figure 3.4.

3.4.2 Bending Forces

The forces acting at the tip of the instrument in the x and y directions produce bending moments that are proportional to the distance from the tip to where the strain is being measured. In order to measure these moments, linear strain gauges were used. Two sets of two gauges were mounted on opposite sides of the shaft in a half bridge type II configuration (Section A.2), as shown in Figure 3.5. This configuration rejects axial strain and measures only bending strain while compensating for the effects of changes in temperature. Also shown in Figure 3.5 is the von Mises maximum distortion strain energy distribution caused by a 3 N force acting at the tip of the instrument.

3.4.3 Axial Force and Torsion

Preliminary analysis indicated that the strain caused by forces acting in the x and y directions was several orders of magnitude higher than the strain caused by forces acting in the z direction or

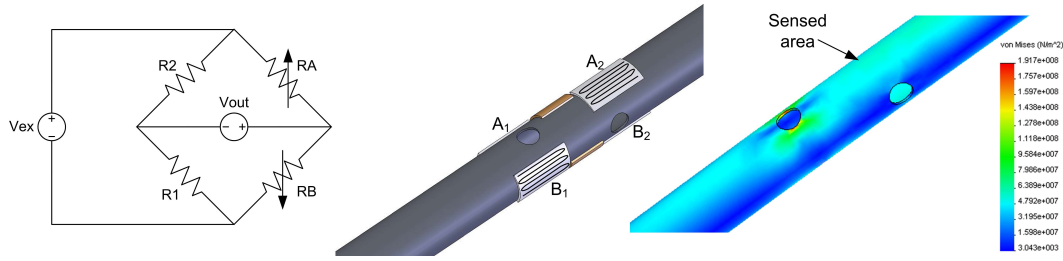


Figure 3.5: Type II half Wheatstone bridge (*left*); placement of the gauges measuring bending moment (gauges labeled A1 and B1 are wired together, while A2 and B2 are wired as the other half bridge (*centre*) and stress concentration caused by a 3 N force acting at the tip of the instrument (*right*).

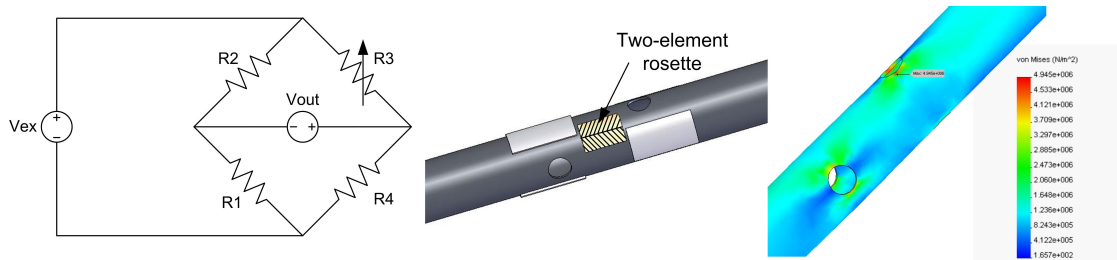


Figure 3.6: Type I quarter Wheatstone bridge (*left*); placement of the two-element rosettes measuring torsion and axial forces (each element is wired independently to a quarter bridge (*centre*) and stress concentration caused by a compression force of 5 N in the axial direction (*right*).

by torques about the z -axis. Thus, two 2.5 mm holes were drilled through the shaft in orthogonal directions to locally increase the strain caused by axial forces and torsion.

Isolation of these two forces required the placement of two two-element rosette strain gauges on opposite sides of the shaft (see Figure 3.6). Each rosette contains two gauges placed at 90 degrees with respect to each other, at a 45 degree angle from the centre axis of the gauge. The rosette elements were wired independently in a type I quarter bridge configuration, also called a 3-wire connection. Figure 3.6 also shows the von Mises maximum distortion strain energy distribution caused by a 5 N compression force acting in the z direction.

Connecting each of the four elements separately allows both the axial and the torsional forces to be isolated. There are three main sources of stress acting on the material below the gauges:

1. Shearing stress caused by torsional forces: $\tau = T \cdot r / J$, where T is the torque acting about the z -axis, r is the radius of the shaft, and J is the polar moment of inertia of the cross section of the shaft;

2. Axial stress: $\sigma_a = F/A$, where F is the axial force and A is the cross sectional area of the shaft; and
3. Bending stress: $\sigma_m = M \cdot r/I$, where M is the maximum moment acting about an axis perpendicular to the gauge plane and I is the moment of inertia of the cross section of the shaft.

Assuming symmetry, the rosettes located on the opposite sides of the shaft are subject to the same shear stress. However, due to the orientation of the sensing elements on each rosette, the shear stress is equal in magnitude, but opposite in sign, on each element of the same rosette. If the rosettes are located with their central axis perfectly aligned with the axis of the shaft, the axial force produces the same stress on all four elements. The bending moment, on the other hand, produces stresses on the top and bottom rosettes that are equal in magnitude but opposite in sign. These differences in how the stresses affect the four elements of the rosettes allow the desired force or torque to be isolated by adding or subtracting the appropriate signals. Therefore, if the four elements are labeled using numbers 1 to 4, with 1 and 2 being on the same side, and 3 and 4 being on the opposite side, the stresses acting on these elements are:

$$\sigma_1 = -\tau + (\sigma_a + \sigma_m) \cdot \cos(45^\circ), \quad (3.1)$$

$$\sigma_2 = \tau + (\sigma_a + \sigma_m) \cdot \cos(45^\circ), \quad (3.2)$$

$$\sigma_3 = -\tau + (\sigma_a - \sigma_m) \cdot \cos(45^\circ), \quad (3.3)$$

$$\sigma_4 = \tau + (\sigma_a - \sigma_m) \cdot \cos(45^\circ). \quad (3.4)$$

It is straightforward to prove that adding all four stress signals ($\sigma_1 + \sigma_2 + \sigma_3 + \sigma_4$) allows the stress caused by the axial forces to be isolated, while adding 1 and 3 and subtracting 2 and 4 ($\sigma_1 - \sigma_2 + \sigma_3 - \sigma_4$) isolates the stress caused by the torsional forces.

Table 3.1 provides the details of the strain gauges selected to measure the different forces acting on the instrument. These gauges were selected based on the analysis presented above and the specifications and recommendations of the manufacturer.

Once the system is set up to measure strain on the instrument shaft, it is possible to determine the magnitude of the forces and torques acting in all 5 DOFs available during MIS. A calibration

Table 3.1: Details of the strain gauges used for force sensing.

Location	Gauge Number (Vishay Micro-Measurements)	Gauge Factor	Resistance (Ω)
Inner—axial strain	EA-06-031DE-350	2.12	$350 \pm 0.2\%$
Inner—Poisson only	MA-06-060PB-350	2.095	$350 \pm 0.2\%$
Middle—bending moments	J2A-06-S033P-350	2.10	$350 \pm 0.3\%$
Middle—two-element rosettes	EA-13-062TV-350	2.055	$350 \pm 0.2\%$

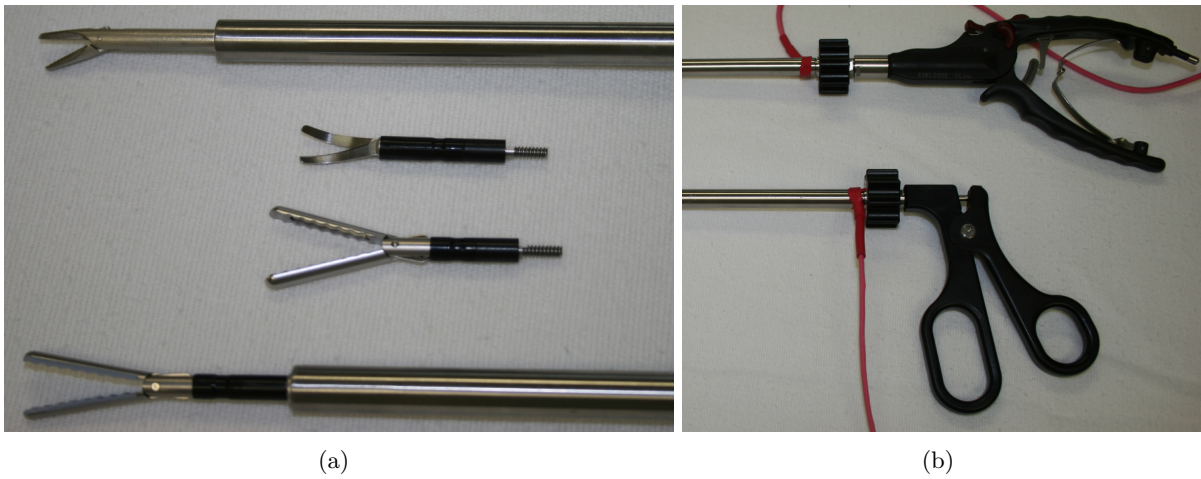


Figure 3.7: Examples of interchangeable tips (a) and handles (b) that can be attached to the instrument.

procedure can be followed to establish an accurate correlation between the signal being measured and the actual forces acting at the tip of the instrument, see Section 3.7.

3.5 Instrument Prototype

Two identical prototypes of the instruments were constructed from 316 stainless steel. The scissor handles were constructed of ABS plastic. The needle driver handles used were obtained from commercially available laparoscopic needle drivers (models 8393.941 and 8393.0005, R. Wolf, Inc.). The instrument tips include the Raptor Grasper tip (ML-3291-E), the Endocut Scissor tip (ML-3141E) and the Super-Atrau Raptor Grasper (ML-3632, Microline Pentax, Inc.). The needle driver tips were designed and constructed of stainless steel. Figure 3.7 shows the tips and handles that can be attached to the same sensorized shafts. Figure 3.8 shows the strain gauges mounted on the inner and middle shafts.

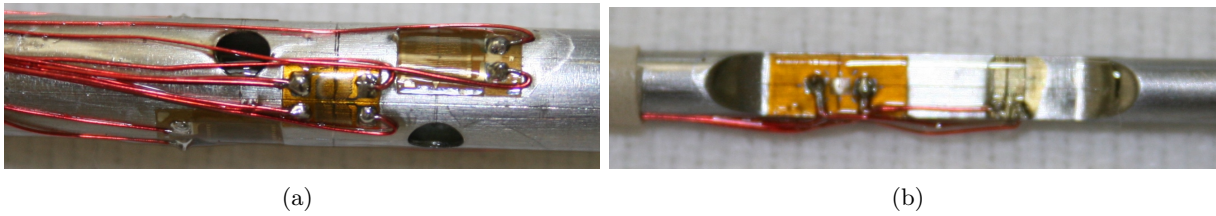


Figure 3.8: Placement of gauges on the middle (a) and inner shafts (b).

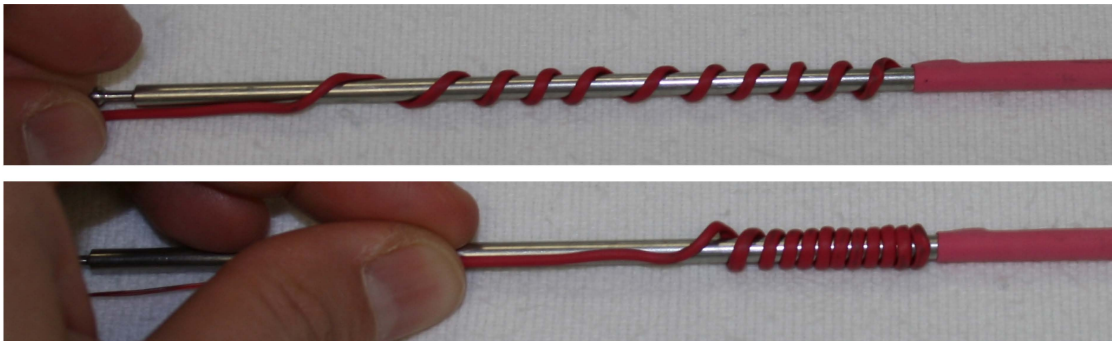


Figure 3.9: Cable wiring to allow the inner shaft to slide inside the middle shaft in order to accommodate the different tips.

Due to the configuration of the different handles, the inner shaft needs to slide with respect to the middle shaft when the handles are replaced, while still maintaining the ability to open and close the gripper without the cables getting tangled. Figure 3.9 shows how the cables have been wired to allow the inner shaft to slide inside the middle shaft and accommodate the different tips and handles. The inner shaft can slide with respect to the middle shaft without causing the cable to get tangled or pinched.

3.6 Additional Hardware and Software Interface

The equipment used to capture force and position information in real time is shown in Figure 3.10. It includes three major components: a personal computer (PC), the position sensing system, and the force sensing elements.

The microBIRD™ Electromagnetic Tracking System (EMTS) is used for position sensing. This system connects directly to the PC through a PCI card, through which the signals from the two electromagnetic sensors are captured.

The strain gauges attached to each instrument are connected to seven Quanser strain gauge

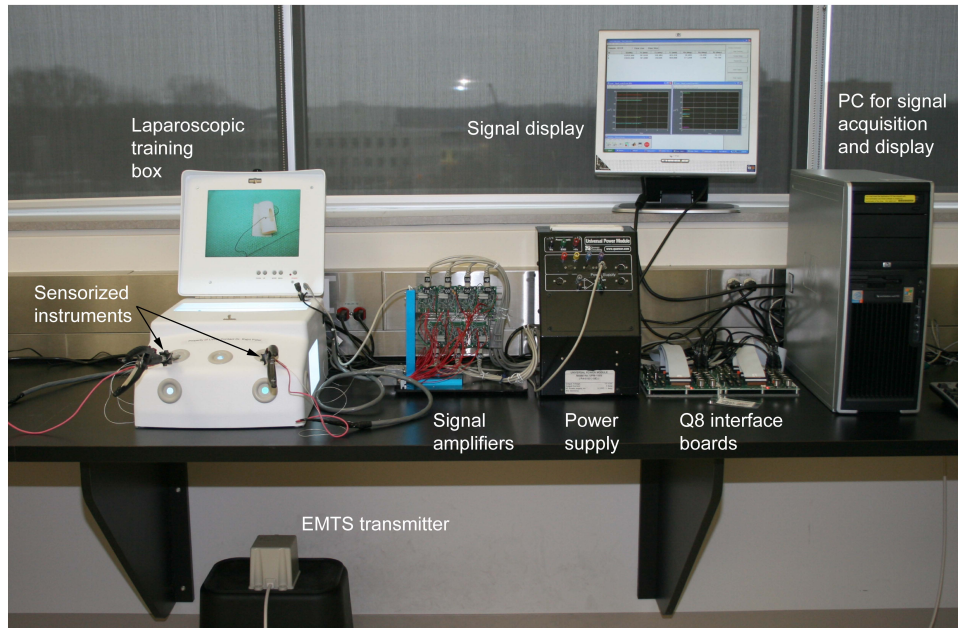
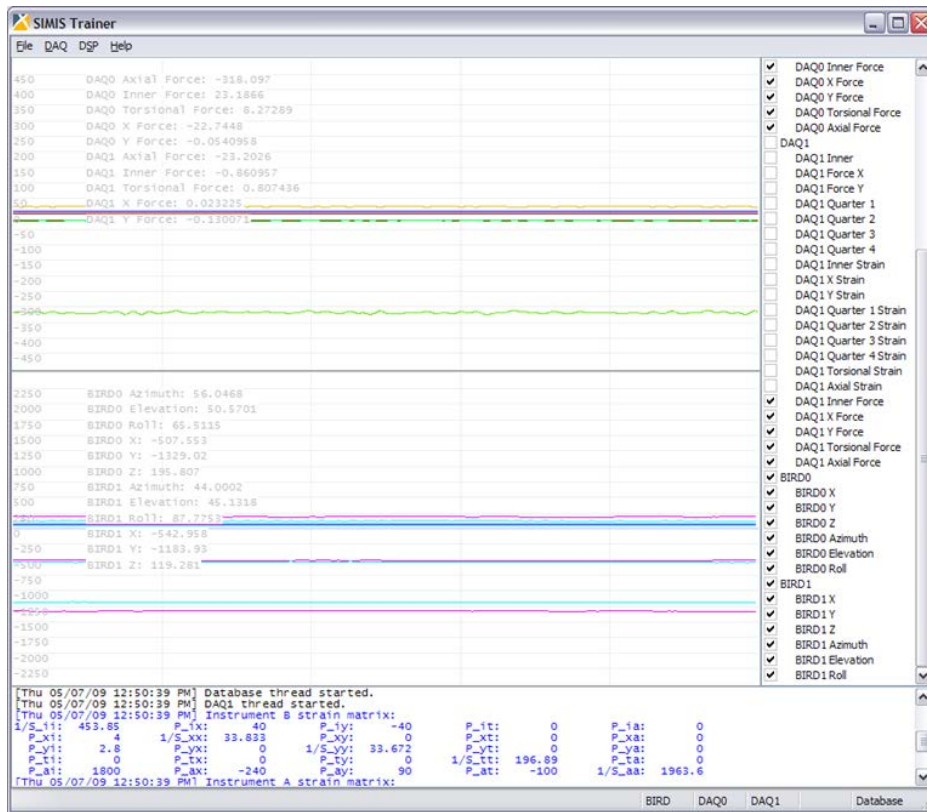


Figure 3.10: Experimental setup.

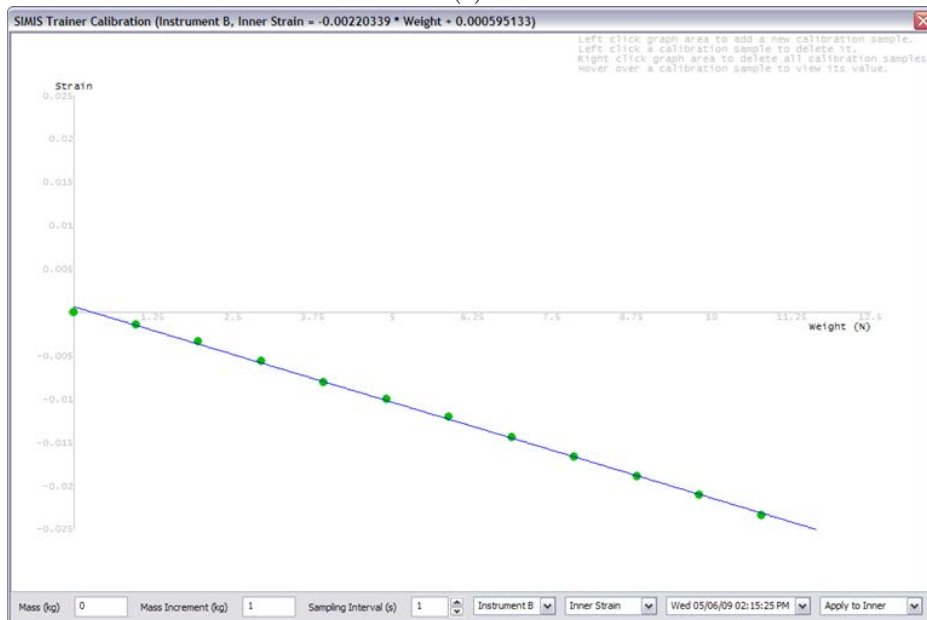
amplifiers that are powered by a Quanser Universal Power Module (model UPM-1503). The gain from these amplifiers ranges between 40 and 2000 depending on the potentiometer setting. Two Quanser Q8 Hardware-in-the-Loop boards (one for each instrument) are responsible for capturing the signals from the amplifiers.

The personal computer used is an HP xw4100 workstation with an Intel 2.8 GHz Pentium 4 HT Processor, 1 GB RAM, and running Windows XP. Customized software running on this computer serves to capture, process and record the information from the electromagnetic sensors and the strain gauges. The computer also facilitates the acquisition of video streams from an RS-170A compatible endoscope or camera connected to an installed Matrox Meteor II PCI frame grabber.

A customized software interface (see Figure 3.11(a)) was developed in C++ by a research engineer. The graphical user interface (GUI) presents real-time plots that display the force and position data as indicated by the user. On another window, an interface facilitates force calibration (see Figure 3.11(b)). All of the data displayed and computed by the software, as well as the video, can be recorded into a database for offline processing and analysis. See Appendix A for more details on the software.



(a)



(b)

Figure 3.11: Customized software interface including real-time plots (a) and the calibration interface (b).

3.7 Calibration

In order to determine the relationship between the voltage changes measured by the strain gauges and the actual forces and torques being applied at the instrument tip, a calibration procedure was performed using the setup shown in Figure 3.12. The instrument was placed in different positions and orientations in order to apply forces in each of the individual axes during calibration. To calibrate the inner shaft, which measures actuation forces, weights were applied to the moving gripper while the instrument shaft was supported along its entire length. Preloading of the gripper was necessary to remove any play within the actuation system. The x and y moments were calibrated by applying forces at the tip while the instrument was cantilevered, supported at the rotating wheel (Figure 3.12(a)).

A special tip was designed to allow the application of pure torque and pure axial forces to the instrument (see Figures 3.12(b) and 3.12(c)). During the torque calibration, the instrument shaft was fully supported. When calibrating the z axis, the instrument was mounted on a gimbal that ensured that the forces were applied axially (Figure 3.12(d)). In each case, the forces and torques were calibrated by measuring the voltage increase when weights were applied in 100 g increments from 0 to 1000 g. The calibrated values obtained are as follows: $S_{ii} = -.0022$, corresponding to the slope of the actuation force; $S_{xx} = -.0295$, corresponding to the slope of the x forces; $S_{yy} = -.0297$, corresponding to the slope of the y forces; $S_{tt} = -.0051$, corresponding to the slope of the torsional forces; and $S_{aa} = -.00051$, corresponding to the slope of the axial forces.

In an ideal situation, the strain gauges would be completely decoupled from each other and would only sense forces applied in the direction they were designed to measure. This, unfortunately, is not the case in practice and so a method for decoupling the different signals was developed. It was observed that the forces applied in the x and y directions were decoupled from the torsional forces and from the axial forces. The only coupling present was caused by the grip. The coupling factor in this case was determined by trial and error, adjusting it until actuation of the gripper produced no observable force in the x and y directions.

To decouple the actuation force from the other signals, data were recorded for about 1 minute, during which time forces were applied in all directions except for actuating the gripper. The data were then run through an optimization process using the `fminimax` function in MATLAB. The goal of the optimization was to find the optimal parameters (P_{ix} , P_{iy} , P_{it} and P_{ia}) that minimized



Figure 3.12: Instrument placement for calibration for: x and y moments (a), axial (b); and torsion (c). (d) Shows a close up of the gimbal designed for the application of axial forces. Note that in these pictures, the stainless steel outer shaft was replaced by an ABS plastic shaft. Photo credit: Meg Woodhouse.

the maximum value of the following expression:

$$(1/S_{ii}) \cdot E_i + P_{ix} \cdot E_x + P_{iy} \cdot E_y + P_{it} \cdot E_t + P_{ia} \cdot E_a, \quad (3.5)$$

where E_i is the strain measured by the gauges on the inner shaft, E_x and E_y are the strains caused by bending moments in the x and y directions respectively, E_t is the strain caused by torsional forces and E_a is the strain caused by the axial force in the z direction. Considering that when this data were recorded, no actuation forces were being applied, evaluation of this expression should in theory be zero. Finding the parameters that minimize the maximum value of the equation would then represent the best way to compensate for the coupling of the signals.

The same process was repeated for each of the axial and torsional forces using these expressions:

$$P_{ti} \cdot E_i + P_{tx} \cdot E_x + P_{ty} \cdot E_y + (1/S_{tt}) \cdot E_t + P_{ta} \cdot E_a, \quad (3.6)$$

$$P_{ai} \cdot E_i + P_{ax} \cdot E_x + P_{ay} \cdot E_y + P_{at} \cdot E_t + (1/S_{aa}) \cdot E_a. \quad (3.7)$$

3.8 Performance Assessment

Assessment of the strain gauge calibration process was performed as detailed in the following sections:

3.8.1 Accuracy, Repeatability and Hysteresis

To assess the accuracy and repeatability of each signal, the instrument was placed in the same setup used during calibration. Weights were applied to each of the axes in 100 g increments from 0 to 600 g. This process was repeated 3 times. The accuracy was calculated as the RMS of the differences between the measured signal and the theoretical force applied by the weights. The total error percentage was also calculated. Repeatability is presented as the maximum standard deviation (σ) observed during all of the trials. To assess hysteresis, weights were applied to each of the axes from 0 to 600 g and then back to 0 g in 100 g steps. The values at each weight were then compared and the RMS error was computed. The results are summarized in Table 3.2.

Table 3.2: Summary of the strain gauge calibration assessment.

Direction	Typical range	Noise/drift (10 min)	RMS error	Max error (%)	Repeatability (max σ)	Hysteresis
Actuation	0 to 50 N	0.05/0.26 N	0.35 N	22*	0.78 N	0.352 N
x axis	± 5 N	0.0041/0.02 N	0.07 N	2.3	0.032 N	0.016 N
y axis	± 5 N	0.0034/0.026 N	0.03 N	1.12	0.031	0.019 N
Torsion	± 80 N·mm	1.2/3.3 N·mm	1.5 N·mm	2.34	2.7 N·mm	3.65 N·mm
Axial	± 25 N	1.12/6.5323 N	**	**	**	**

* A very high error was obtained for low grip values. For grip forces higher than 3 N, the maximum error was less than 4.5%.

** For these factors, the influence of noise, signal drift and coupling was too great to allow proper measurement.

3.8.2 Gravity Compensation

Gravity has a small effect on the forces in the x and y directions. Ideally, the effect of gravity can be eliminated by using compensation terms that drive the measured forces to zero under no-load conditions. To determine the value of the compensation terms, the instrument was rotated in free space while recording the raw force and position data. An optimization script was then generated using the MATLAB function `fminsearch` to determine the term that minimized the error caused by gravity as a function of the rotation and elevation angles. The compensation term was then incorporated into the calibration equations. The maximum error obtained when rotating the instrument in free space with and without gravity compensation is shown in Table 3.3.

Table 3.3: Effect of gravity compensation on the bending moments: maximum error measured when moving in free space.

Direction	No gravity compensation (N)	With gravity compensation (N)	Reduction of error (%)
x	0.007284	0.003021	58.5
y	0.007244	0.002557	64.7

3.8.3 Signal Drift and Noise

To measure the amount of signal noise and drift, the instrument was placed within the workspace without any forces applied at the tip. Data were recorded for 10 seconds to measure signal noise and for 10 minutes to measure total drift. The results of this analysis are presented in Table 3.2. Figure 3.13 shows a representative graph of the drift observed in the 5 signals. As shown, the drift present in the axial signal dominates the other signals.

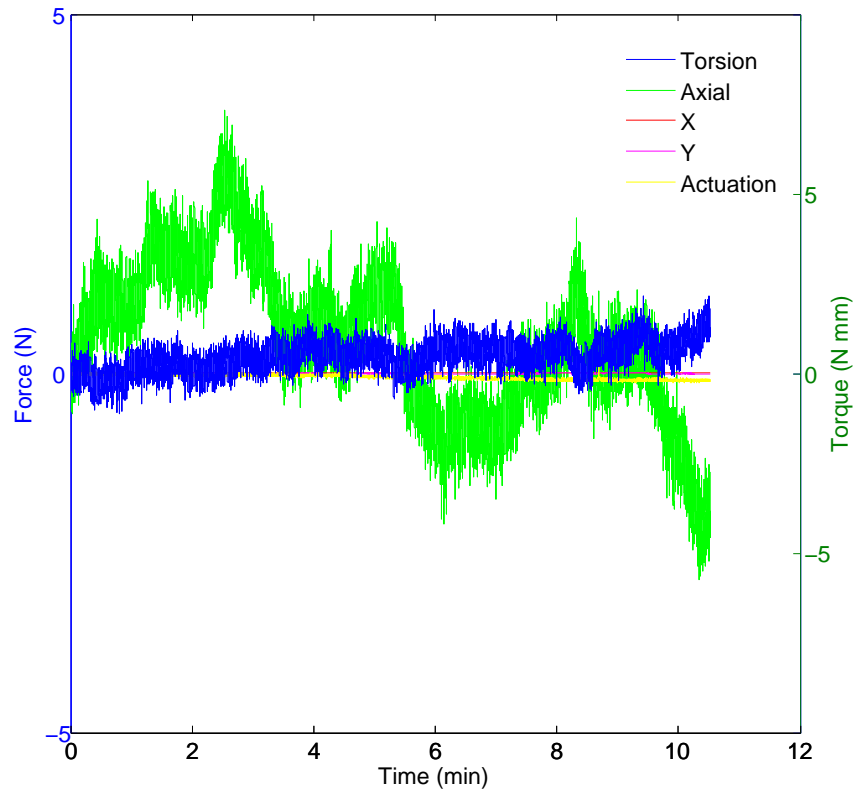


Figure 3.13: Signal drift observed in the five measured directions.

3.8.4 Coupling

To assess the coupling of the signals, the effect on all of the signals of applying forces in each individual direction was measured. The maximum deviation from theoretical zero values was recorded. The results are presented in Table 3.4.

3.9 Validation of Force Calibration

Since the calibration of the instrument and the assessment were performed using the same setup, alternate methods were used to validate the instrument. Different methods were used to validate the actuation forces and the forces acting in the other directions, as presented below.

3.9.1 Actuation Force

To validate the calibration of the actuation force, the calibrated instrument was compared to the estimated forces applied when compressing a small spring. To measure the compression of

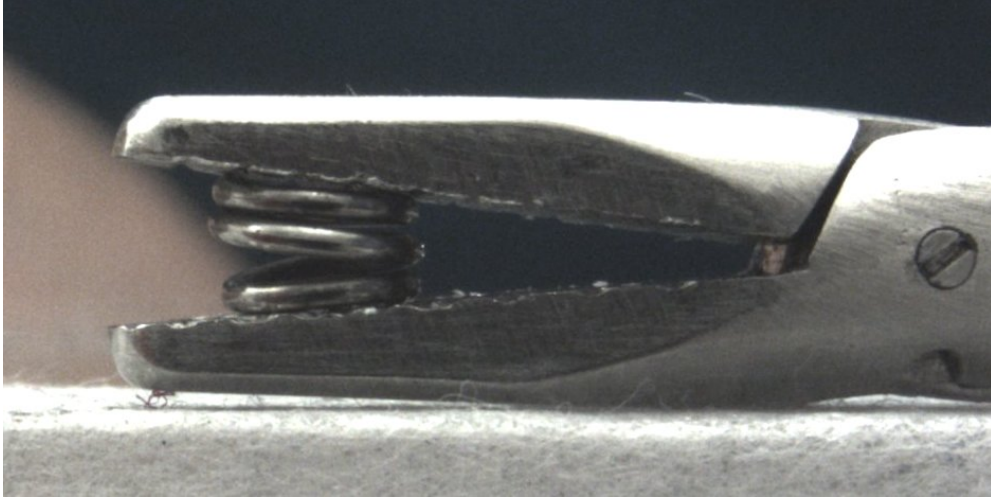


Figure 3.14: Sample image of the instrument compressing a spring for calibration validation.

Table 3.4: Maximum deviation from a theoretical zero value caused by coupling.

	Effect on the actuation force (N)	Effect on the x forces (N)	Effect on the y forces (N)	Effect on torsional forces (N·mm)	Effect on axial forces (N)
Caused by actuation	Range: 0–66	0.45	0.14	10.6	23.9
Caused by x - y forces	2.5	Range: ± 6	Range: ± 6	11.8	69
Caused by torsional forces	0.26	0.27	0.54	Range -120–80	11.9
Caused by axial forces	0.42	0.79	0.29	19.4	Range: -25–25

the spring, images were acquired using a Flea2 digital camera (Point Grey Research, model FL2 14S3C) with a varifocal lens (Computar, model T4Z2813CS, 2.8–12 mm, f/1.3, CS Mount) and the PGR FlyCapture software. Measurements of the spring length were performed using *ImageJ* software (US National Institutes of Health) [135]. An initial assessment of the spring was performed by applying known weights to determine the spring constant. After the spring constant was determined, the instrument was used to compress the spring by different amounts, as shown in Figure 3.14. The results show an RMS error of 0.31 N.

3.9.2 Moments, Torsion and Axial Force

To validate the calibration of the other forces, the forces measured by the sensorized instrument were compared to those measured by a Nano-17 6-DOF force sensor (ATI Industrial Automation). A customized attachment was designed to ensure that the forces applied by the instrument were aligned with those applied to the force sensor. Comparisons were made between the x - y force

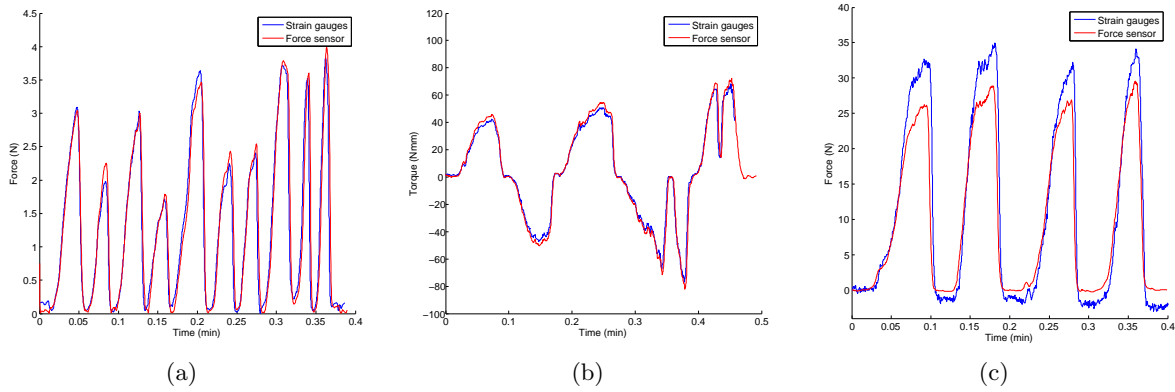


Figure 3.15: Comparison of the measured forces by a force sensor and by the strain gauges on the sensorized instrument: x , y force vector (a), torsion (b), and axial forces (c).

vector applied to the instrument and the x - y force vector measured by the force sensor, between the torque applied to the instrument and to the force sensor in the z direction, and between the axial forces applied to the instrument and to the force sensor about the z axis. The results of these comparisons are shown in Figure 3.15 and correspond to a total RMS error of 0.26 N for the moments, 3.8 N·mm for torsion and 4.3 N for the axial forces. A correlation factor between the two sets of data was computed using the Pearson product moment correlation. The results show R^2 values of 0.9750 for the moments, 0.9971 for torsion and 0.9639 for the axial forces.

3.10 Discussion

A sensorized laparoscopic instrument was designed and two prototypes were constructed. The novelty and benefits of these instruments over existing technologies can be summarized as follows:

1. The instruments measure the forces and torques acting in all 5 DOFs available during MIS. The forces being measured are those acting on the tip of the instrument and not on the handle or at the port location. Furthermore, electromagnetic sensors attached to the instruments provide position feedback in 6 DOFs. Other instruments found in the literature provide forces at the handle of the instrument or only provide force measurements in three axes or directly on the gripper.
2. Despite containing force and position sensors, the instrument is similar in shape, size and weight to traditional laparoscopic instruments. A small, lightweight and flexible cable is at-

tached to the shaft such that no limiting forces exist and the instrument motion is unaffected. This allows surgical skills to be properly developed and assessed. Although the BlueDragon system [40] also measures forces and position, a large manipulator is attached to the tool, which may affect the proper development of skills when used for laparoscopic training.

3. Replaceable tips and handles make the instruments more affordable since all of the sensing elements are on the shaft and different tasks can be performed by converting them into the appropriate instruments. Despite increasing the complexity of the instruments by adding sensors, the versatility of the instruments is maintained.
4. The instruments can be used in any training environment, e.g., in simulators, animal labs or real surgery. Since the sensors are attached directly to the instruments and are not part of a training box, the benefit of using them for skills assessment and training can be transferred to any training environment for laparoscopic surgery.

The results of the actuation force calibration show a maximum RMS error of 0.35 N with good repeatability and low hysteresis. The coupling effect of the other signals on the gripper force is a maximum 2.5 N. Optimal results are obtained from the calibration assessment of the forces in the x and y directions, which shows 0.07 N RMS error, excellent repeatability and very low hysteresis. Furthermore, the maximum effect of coupling with the other signals is less than 0.8 N.

The torque calibration assessment shows a maximum RMS error of 1.5 N·mm with low errors caused by hysteresis and repeatability. Unfortunately, the effect of coupling on torsion is significant (up to 19 N·mm, while the typical range of torques applied during the performance of standardized tasks is ± 80 N·mm). That said, there is excellent correlation between the torque measurement from the instrument and that measured by a commercially available force/torque sensor. The validation of the calibration using the spring and the ATI force sensor shows strong correlations between the values measured by the instrument and the theoretical results.

3.11 Limitations of the First Prototype

The large amount of drift and noise present in the axial signal are caused by the way the quarter bridges are combined. Since all four signals are added, the noise present in all of the signals also gets added and cannot be cancelled out. While trying to assess the calibration of the axial signal,

it was not possible to zero the signal for long enough to perform a proper comparison between the signals. It should be emphasized that the amount of drift, noise, and coupling present in the axial forces is very high, making the data obtained unreliable. As such, the data acquired from these gauges cannot be taken as a true measure of the forces. However, when the axial forces measured by the instrument were compared to those of a force sensor, it was observed that the signal obtained follows the true signal and can be a good indication of the general trend of the forces being applied axially on the instrument. Furthermore, for the present application, the main purpose of the instrument is to be able to compare the forces between different users, in which case, a comparison of trends can still be performed.

Some experiments were successfully performed at CSTAR using these instruments [136, 137]; however, the need for an improved design was recognized, as presented in the following chapter.

Chapter 4

Second-Generation SIMIS Instruments

4.1 Introduction

The first generation of the SIMIS instruments had some novel aspects and effectively sensed forces in some directions; however, the instruments suffered from a few limitations. This chapter outlines how the limitations present in the first prototype were addressed by the second-generation prototype.

4.2 Lessons Learned and Design Solutions

The limitations with the first prototype and the solutions integrated into the design of the new prototype were as follows:

4.2.1 Limitation 1: Poor axial and torsional signals

Having separate gauges connected in a quarter-bridge configuration with the intention of separating the axial and torsional signals should have worked in theory. In practice, however, the signals are affected by noise that does not cancel out when adding and subtracting the signals. This caused the axial signal to have significant drift and both the axial and the torsional signals to be significantly coupled with the other signals, to the point that they did not provide reliable information during

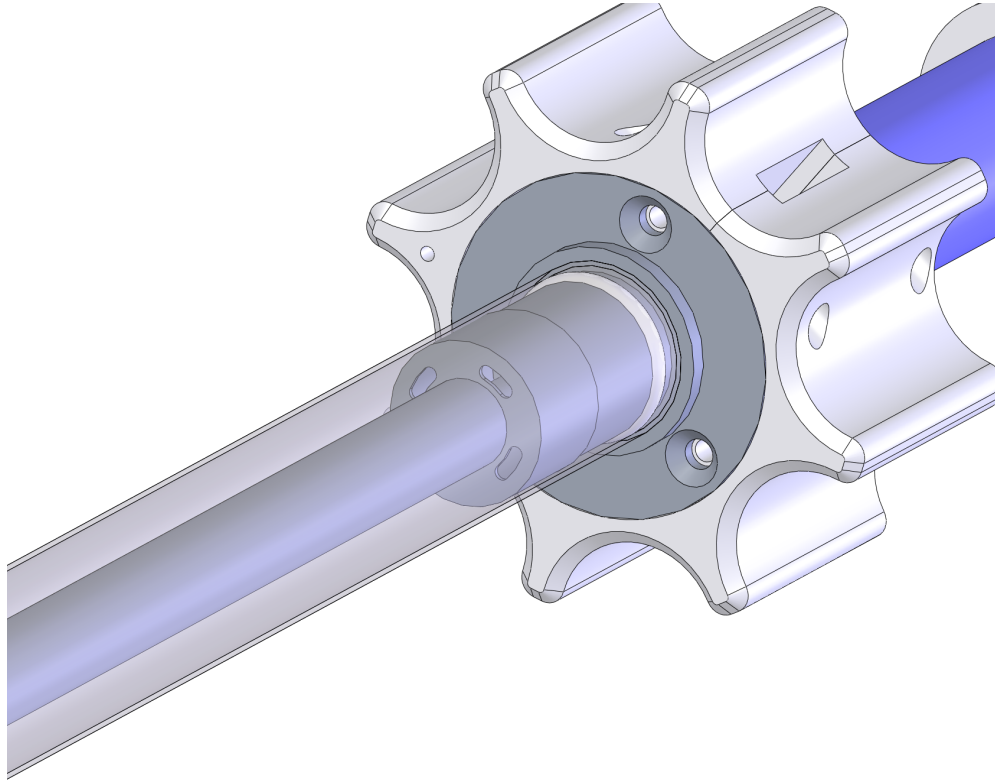


Figure 4.1: Instrument close-up showing axial concentration element inside the housing.

calibration or during sensing.

Design solution: Individual strain gauges were used for each signal in two separate full bridge configurations. Measurement of the torsional forces acting about the instrument shaft required two sets of two-element rosettes connected in a full torsion bridge configuration, see Section A.2. Each rosette contains two gauges placed at 90° with respect to each other at a 45° angle from the centre of the gauge.

A structural element was developed to maximize and decouple the signal used to measure axial forces. This involved a specialized element with a thin wall section perpendicular to the instrument axis, with four small slots. Figure 4.1 shows the structural element, while Figure 4.2 shows how it deforms when axial forces are applied. Strain gauges placed between the slots measure this deformation while cancelling other forces. Two dummy gauges placed on the main shaft allow the gauges to be connected in a type III full bridge configuration to maximize the signal, reduce noise and compensate for variations in temperature, see Section A.2.

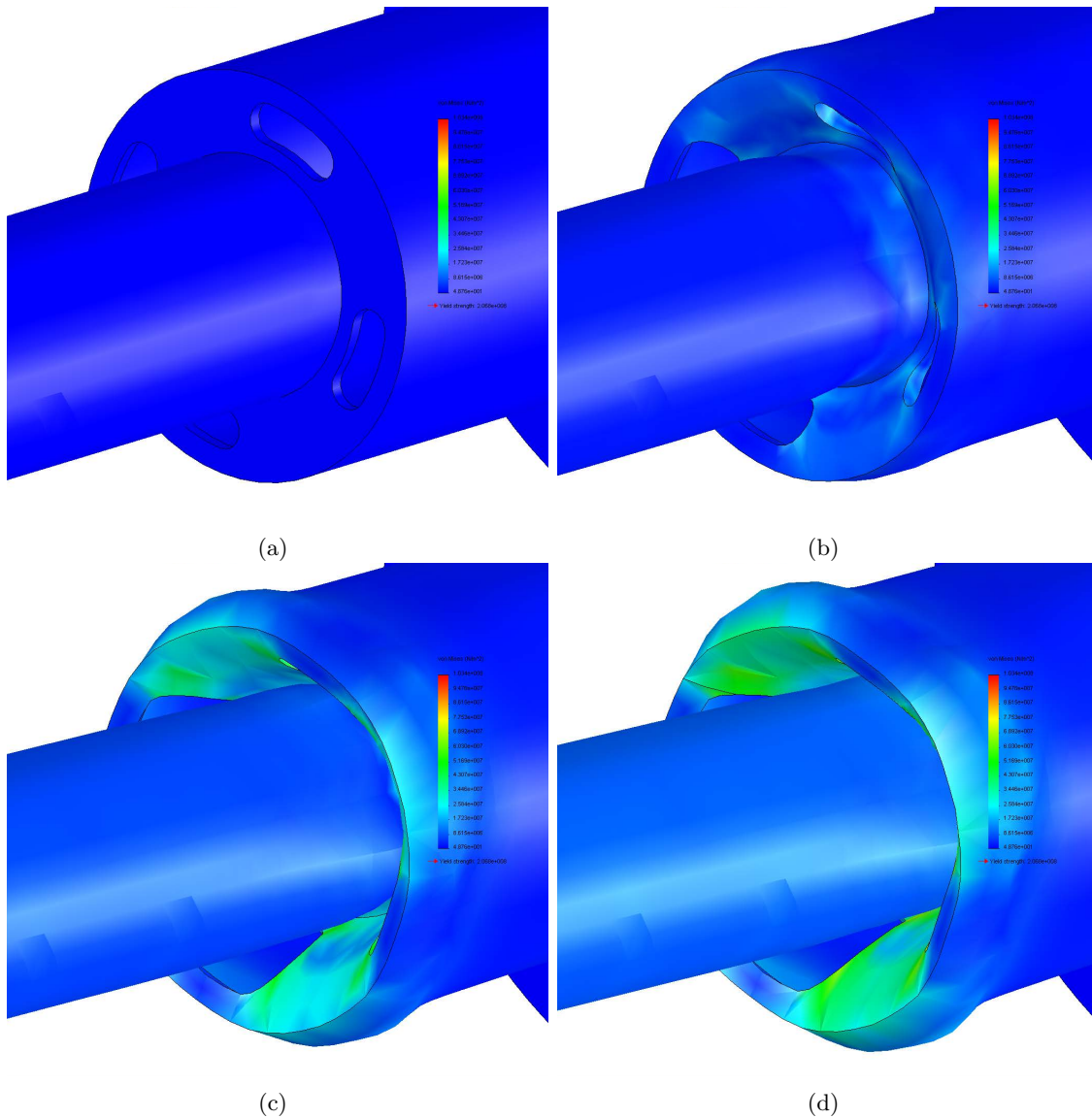


Figure 4.2: Stress concentration diagrams as forces increase from 0 to 20 N in the axial direction.

4.2.2 Limitation 2: Coupling between the actuation force and the bending moments in one direction

In order to increase the deformation and for ease of strain gauge installation, a flat section, 1-mm thick, was machined on the shaft. Due to this narrowing of the inner shaft, it tends to bend more when forces are applied perpendicular to this flat surface, compared to when forces are applied in a parallel direction. This created an undesired coupling between the actuation signal and the bending moments in one direction only.

Design solution: To alleviate this coupling, a joint on the inner shaft was added with its axis parallel to the surface of the flat in order to mechanically isolate the anterior and posterior parts of the inner shaft. When bending moments act on the instrument, the joint relieves the stresses on the inner shaft minimizing the coupling between the signals. See Figure 4.3.

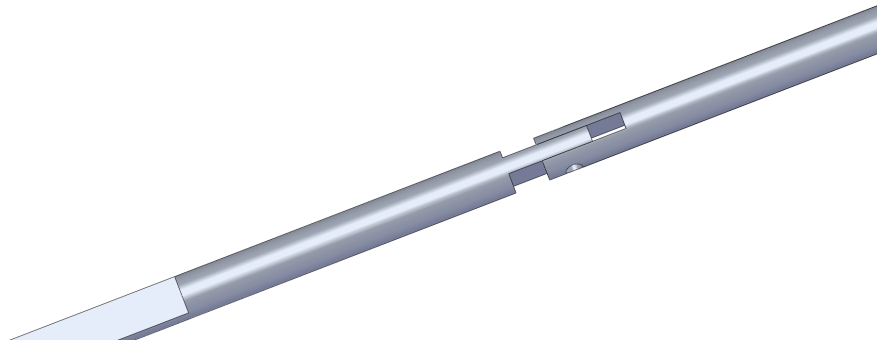


Figure 4.3: Inner shaft showing the decoupling feature.

4.2.3 Limitation 3: The step on the outer shaft creates difficulties when suturing

The presence of the step between the instrument shaft and the tip caused the thread to sometimes become stuck during suturing, limited the visualization of the tip in certain orientations and reduced the amount of surface available for wrapping the suture during knot tying.

Design solution: To avoid these complications, the shaft was smoothed out by gradually reducing the diameter further up the shaft. This design still provided enough room for the wires and the gauges, see Figures 4.4 and 4.5.

4.2.4 Limitation 4: Needle driver tips breaking

The thin walls of the link that forms part of the needle driver tip mechanism broke a few times as the actual gripping forces applied during suturing were significantly higher than those expected (it was common for subjects to apply 60 N of force when grasping the needle as opposed to the expected 20 N).

Design solution: The tip was designed with slightly thicker walls on the link, Figure 4.6. Also the material was changed from stainless steel 316 (yield strength of 138 MPa) to a Grade 5 titanium

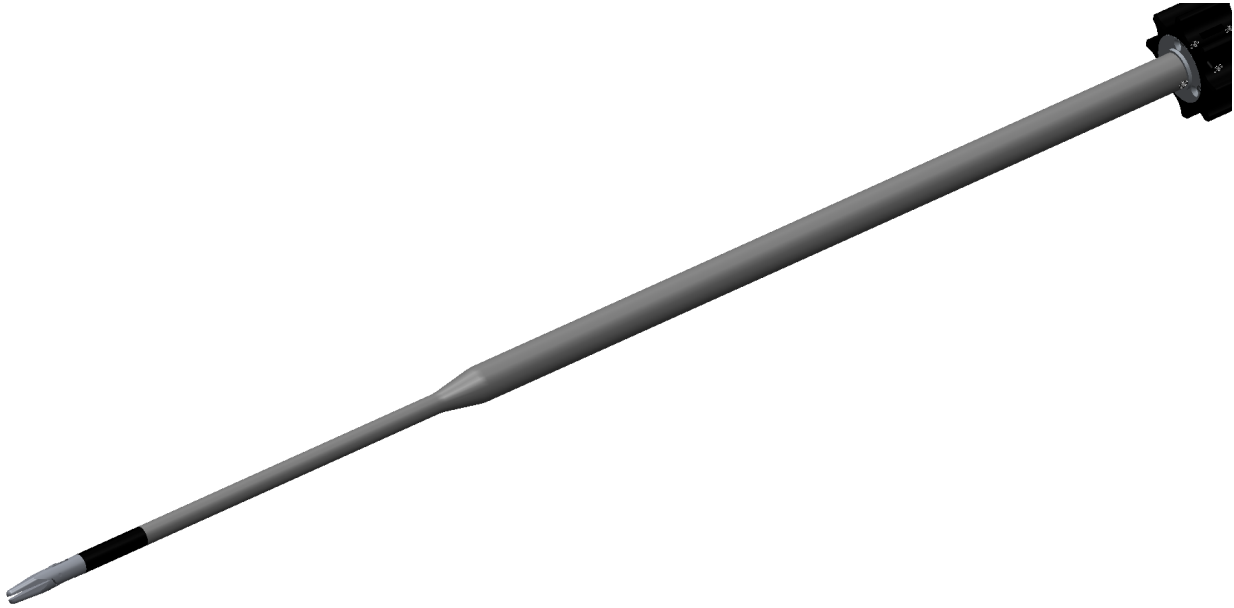


Figure 4.4: New instrument housing.

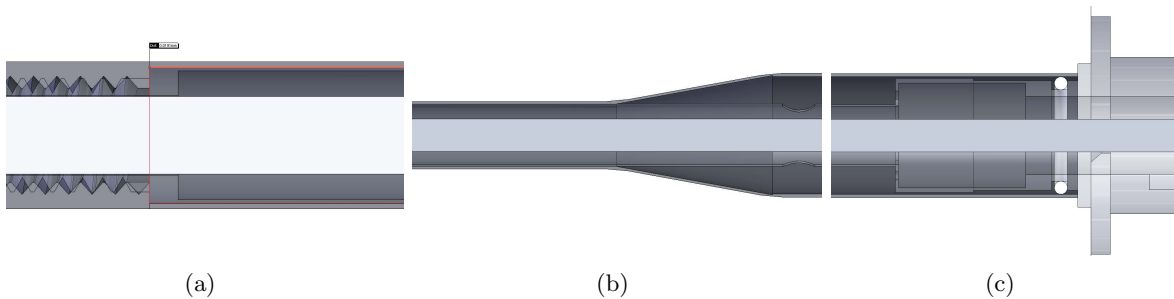


Figure 4.5: Inner housing details: close-up of interface at the distal end (a), close-up of the reduced diameter (b), and close-up of interface at the proximal end (c).

alloy (called Ti 6Al-4V because of the addition of Aluminum and Vanadium alloying elements) with a yield strength of 827 MPa.

4.2.5 Limitation 5: Long change-over time between the two models

In order to change over from the needle driver handle to the scissor handle, a screw needed to be removed from the scissor handles prior to taking them apart. The linking components then needed to be screwed in and out, which caused the wires to tangle and increased the risk of breaking.

Design solution: To solve this problem, a quick connect mechanism was added between the handles and the shaft, see Figure 4.7. Furthermore, the design of the scissor handles was changed

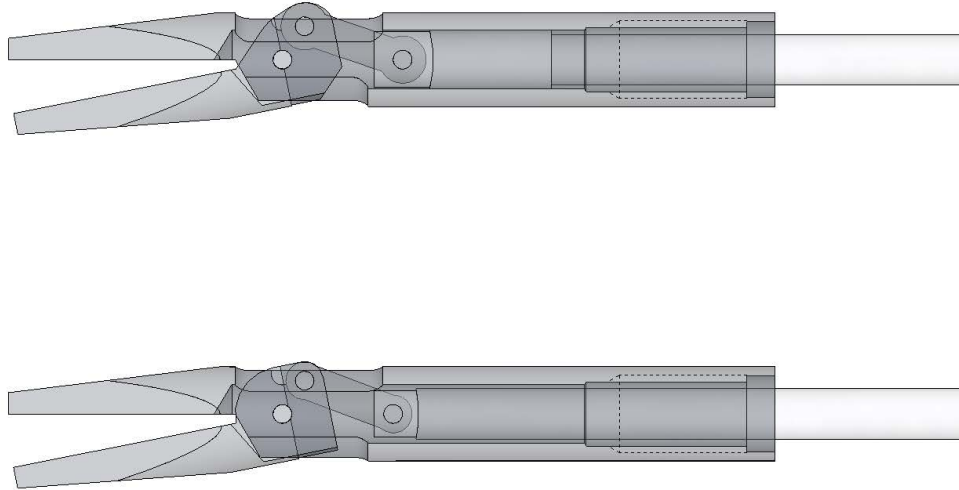


Figure 4.6: Comparison of tip design: new (*top*) and old (*bottom*).

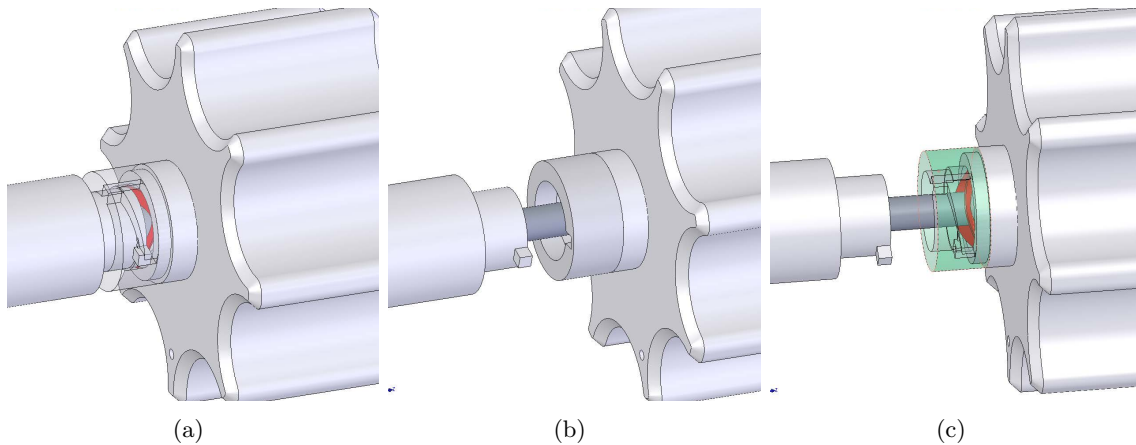


Figure 4.7: Quick connect mechanism: in closed position (*a*), in open position (*b*), and in open position showing the inner spring (*c*).

so that they could be attached to the instrument without disassembling them.

4.2.6 Limitation 6: Difficult wiring of the cables

The thin nature of the wires and the fact that they need to be routed around moving components, caused them to break easily through rubbing or due to tangling. Wire repair is very time consuming and affects the noise present in the signals.

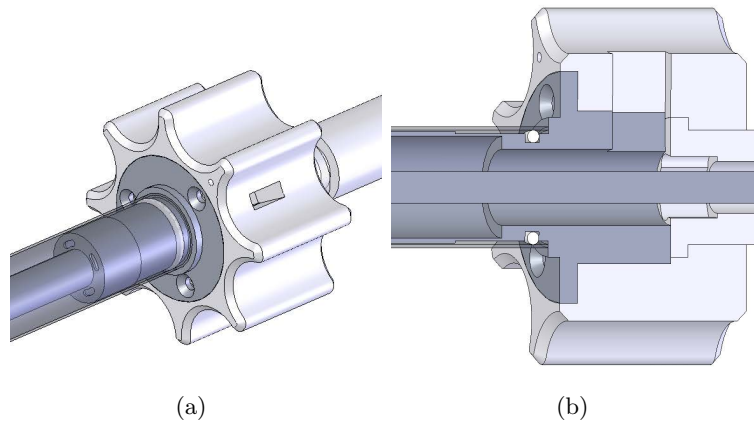


Figure 4.8: Outer view of opening for cables (a) and inner view of space available for cables (b).

Design solution: Routing of the cables was completely planned out in the new design and enough room was provided so that these could be protected as they came out through the rotating wheel, see Figure 4.8.

4.2.7 Limitation 7: Instrument too short

Due to the position of the rotating wheel with respect to the tip of the instrument, it was determined that the section of the instruments that could enter the patient's body was in fact too short.

Design solution: The length of the instrument after the rotating wheel was increased by 6.3 cm (to 31.8 cm, as measured from the rotating wheel to the tip base, up from 25.5 cm).

4.2.8 Limitation 8: Cumbersome setup, difficult to move and easy to damage

The initial version of the electronics included the 7 strain gauge amplifiers mounted on a vertical plate, completely exposed. The cables would then run up to the breakout boards for the data acquisition cards (Q8 DAQ, Quanser, Inc.) outside of the computer, which would then have another cable going into cards located inside of the computer case.

Design solution: The strain gauge amplifiers were connected directly to the data acquisition cards inside of the computer case and were mounted in a plastic enclosure to which the instruments connect directly. Figure 4.9 shows the old and the new components.

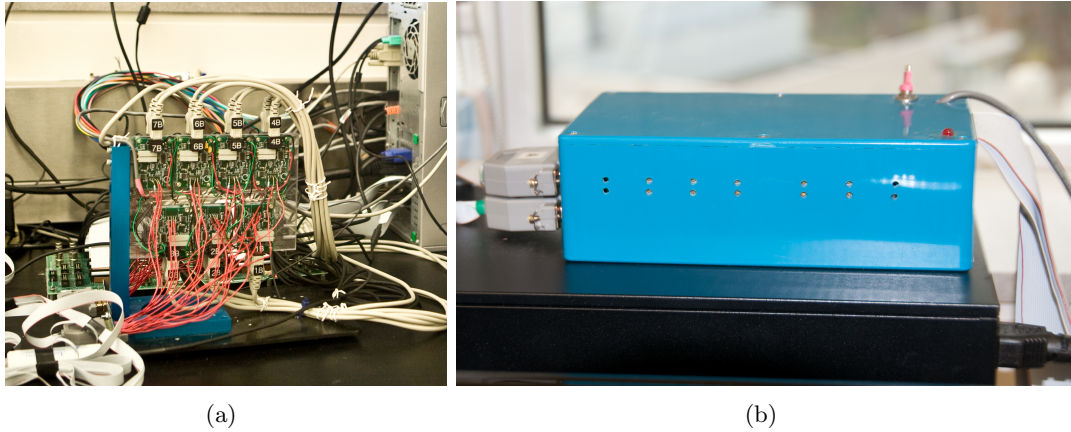


Figure 4.9: Modifications to the electronic connections of the instruments: old design (a) and new, more compact design (b).

4.3 Calibration

As with the previous prototype, in order to obtain reliable measurements from the sensors, the system must first be calibrated. Force calibration is required to establish the relationship between the measured voltages and the forces acting on the instruments. The calibration jig, shown in Figure 4.10, was designed by a research assistant, considering the lessons learned from the calibration jig used with the first prototype. This jig still allows weights to be placed in each of the directions being calibrated, but simplifies control of the position of the instrument when calibrating the x and y directions. Through a rotating wheel attached to the jig, it is possible to fine tune the position of the instrument to ensure that it is properly aligned prior to calibration. As with the first prototype, the x and y moments were calibrated by applying weights at the tip while the instrument was held in a cantilever configuration. For the torsional moments, the instrument was supported at three points along the shaft length and weights were applied to the tip of the open gripper. The axial forces were calibrated by holding the instrument in a perfectly vertical position and hanging weights from a string attached to the tip.

To calibrate the inner forces, a small force/torque sensor was used (Nano-17, ATI Industrial Automation). A component was designed so that as the grasper was closed, the grasping forces would create a torque on the sensor that could be directly related to the grasping force. To ensure consistency, the instrument was mounted on the calibration jig and levelled with the force sensor. Several values were recorded from the sensor and the instrument as the grasping force was gradually increased using the ratcheting mechanism on the instrument handle.

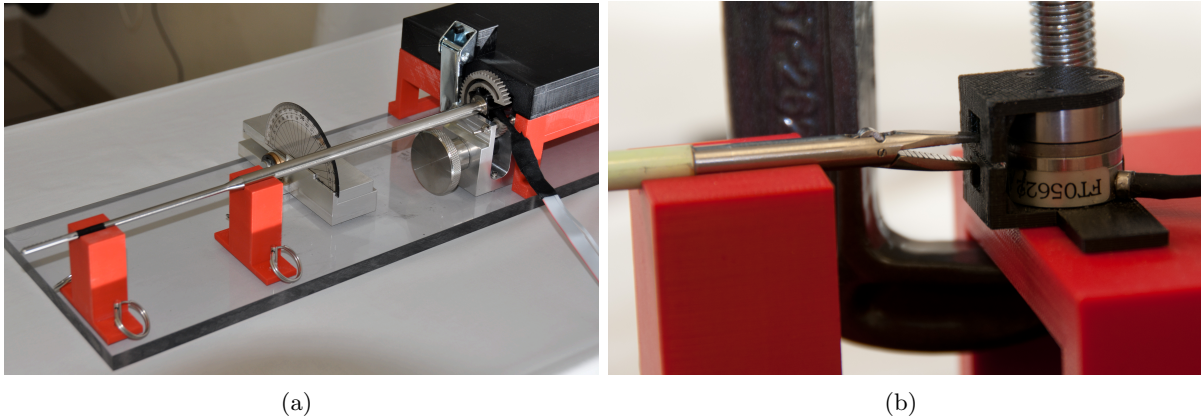


Figure 4.10: Calibration jig showing the instrument mounted for calibrating moments (a) and for calibrating grasping forces (b).

4.4 Performance Assessment

4.4.1 Force Calibration Assessment

A series of experiments were conducted to evaluate the performance of the force sensors when forces were applied at the tip of the instrument, as follows:

1. Accuracy: To assess the accuracy of each signal, the instrument was placed in the calibration test bench while weights were applied from 0 to 500 g in 100 g increments in each direction. This process was repeated 3 times. The accuracy was calculated as the root mean squares (RMS) of the differences between the measured forces and the theoretical forces.
2. Repeatability: With the same data obtained for accuracy, repeatability was determined by calculating the maximum standard deviation observed during all of the trials.
3. Hysteresis: To assess the effect of hysteresis, weights were applied in each direction from 0 to 500 g and back to 0 in 100 g increments. The values at each weight level were then compared and the RMS error was calculated.
4. Signal drift and noise: Data were recorded for 10 seconds to measure signal noise and for 10 minutes to measure drift.
5. Coupling: the effect that each force has on the other forces was measured as the maximum deviation in all other signals when applying a force of 5 N in each direction.

Table 4.1: Summary of the strain gauge calibration assessment of the second-generation prototype.

Direction	Typical range	Noise/drift (10 min)	RMS error	Repeatability (max σ)	Hysteresis
Actuation	0 to 50 N	0.013 / 0.058 N	0.36 N	0.18 N	0.28 N
x axis	± 5 N	0.015 / 0.057 N	0.10 N	0.04 N	0.10 N
y axis	± 5 N	0.021 / 0.054 N	0.07 N	0.06 N	0.21 N
Torsion	± 80 N·mm	0.04 / 0.27 N·mm	0.7 N·mm	1.2 N·mm	1.0 N·mm
Axial	± 25 N	0.039 / 0.030 N	0.16 N	0.13 N	0.14 N

Table 4.2: Maximum deviation from a theoretical zero value caused by coupling.

Effect on:	actuation force (N)	x forces (N)	y forces (N)	torsional forces (N·mm)	axial forces (N)
Caused by actuation	Range: 0–66	0.07	0.06	0.12	0.50
Caused by x - y forces	0.21	0.06 (y) Range: ± 6	0.14 (x) Range: ± 6	0.57	0.04
Caused by torsional forces	0.03	0.03	0.30	Range -120–80	0.65
Caused by axial forces	0.1	0.05	0.05	0.11	Range: -25–25

The evaluation results are presented in Tables 4.1 and 4.2.

4.4.2 Multi-tip Calibration Assessment

A series of experiments were performed to determine the effect of changing the instrument tips on the force calibration. The purpose of these experiments was to determine if the instruments needed to be re-calibrated when a new tip was attached to the instrument or if it was possible to find a calibration factor for each tip. Parts of this evaluation were performed by a volunteer.

4.4.2.1 Methods

Using the calibration jig shown in Figure 4.10, the evaluation was performed by calibrating the instrument with one tip attached and then assessing accuracy after changing to other tips. To ensure consistency between the different tips, the x and y moments were calibrated by applying weights 2 mm from the tip of the closed gripper. The torsional moments were calibrated by applying weights 2 mm from the tip of the open gripper. The axial forces were calibrated by setting the laparoscopic instrument in a vertical position on the calibration jig and by applying weights to a string that was tied to the open gripper. The grasping forces were calibrated by

placing the instrument in the calibration jig while grasping the element attached to the ATI force sensor.

To determine whether calibration was necessary each time a new tip was used, four tips of differing lengths were tested (Figure 4.11). The lengths of the tips were measured from the joint where the grasper pivots, to the distal end of the grasper, and labelled by decreasing length from A to D (Table 4.3). All tips were able to open up to 60 degrees.

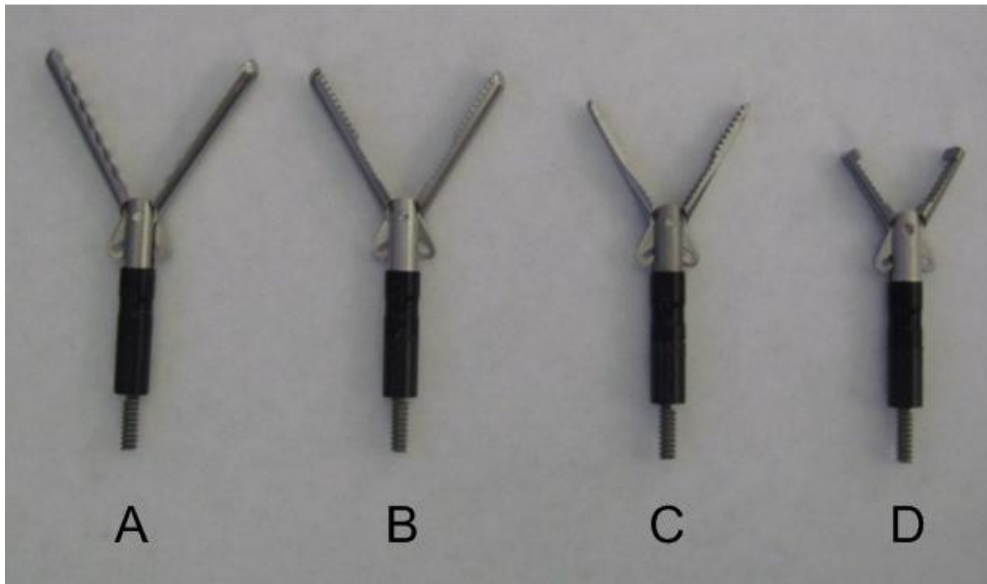


Figure 4.11: Different tips used in the calibration evaluation.

Table 4.3: The lengths of the tips used for calibration assessment.

Tip	Length (cm)	Perpendicular length (cm)
A	2.8	1.4
B	2.5	1.25
C	2.0	1.0
D	1.4	0.7

First, Tip C was calibrated using the software and following the standard procedure (this tip was selected as the baseline due to its intermediate length). Then, using the calibrated slope of Tip C, the accuracy of the force readings was measured for all four tips, applying weights in 100 g increments from 0 to 500 g and then back to zero. The grasping force was calibrated by progressively increasing the grasping force and then correlating the forces measured by the force

sensor and the forces measured by the instrument. As it is significantly more difficult to apply forces up to a certain predetermined value, it was not possible to increase forces by equal amounts as with the other directions. Instead, the forces were increased by closing the grasper a small amount each time.

4.4.2.2 Results

A first examination of the results showed that changing the instrument tip only had an effect on the torsional measurements and the grasping forces, as these are functions of the length and mechanism of the grasper. In the case of the torsional forces, the difference should be proportional to the perpendicular distance from where the weights are applied to the instrument shaft. In the case of the grasping forces, the difference would be affected by the length of the grasper itself and the mechanism within each tip, including friction. It was then decided to evaluate whether the incorporation of a conversion factor for each tip would eliminate these effects.

The conversion factors were determined by computing a relative slope between the actual force values and the measured force values for each direction. If any values were significantly far away from the trend line, they were removed from the slope calculation. This was done to eliminate the effect of outliers and reduce the errors due to improper measurements. The resulting corrected slopes are shown in Table 4.4. Upon incorporating the corrected slopes, the calibration performed using only one tip was found to be applicable to other tips of different lengths (see Table 4.5).

Table 4.4: Correction factors for torsion and grasp measurements. Calibration was completed with Tip C.

Tip	Conversion factor for Torsion	Conversion factor for Grasp
A	1.2	1.2
B	1.5	1.12
D	0.95	0.86

4.4.3 Long Term Calibration Assessment

To determine whether calibration was necessary each time the system was reset, Tip C was recalibrated for each force dimension on three different days between 5 to 7 days apart. Each day, the newly calibrated slope of the same tip was applied to determine the accuracy of the force reading

Table 4.5: Strain gauge calibration assessment between tips of different lengths. Results show the RMS errors.

	Tip A	Tip B	Tip C	Tip D
<i>x</i> axis (N)	0.043	0.045	0.0019	0.0004
<i>y</i> axis (N)	0.061	0.010	0.010	0.016
Axial (N)	0.133	0.087	0.034	0.340
Torsion (N·mm)*	0.96	0.33	0.25	0.11
Grasp (N)*	0.034	0.032	0.071	0.046

* Corrected.

Table 4.6: Comparison of calibration slopes on different days.

Week	1	2	3	% Difference
<i>x</i> axis	0.0079	0.0089	0.0098	15.82
<i>y</i> axis	0.0069	0.0079	0.0085	21.73
Torsion	-0.0034	-0.0042	-0.0043	20.86
Axial	-0.00081	-0.00070	-0.00082	20.40

at 100 g increments from 0 g to 500 g and back to zero. There was found to be a significant percent difference in calibration slopes each day the tip was calibrated about a week apart (Table 4.6).

4.5 Further Complications and Modifications

After completion of the prototype described above and the completion of the calibration assessment, one of the middle shafts broke off at the axial element, see Figure 4.12. This was an unexpected problem caused by the manufacturing process. The construction of this axial element required a thin wall to be laser welded to the large shaft at the base of the instrument and to the thin instrument shaft at 90° angles. This element proved to be difficult to manufacture and the instruments needed to be sent to a company that specialized in laser welds for fabrication. Initially, the sensing element performed very well and survived some very stringent testing on our part. However, ultimately the welds failed at forces much lower than the design specifications.

Upon examination of the failed components, it was noted that the laser weld lines were very superficial. Instead of melting together the entire two contacting surfaces, only a very thin weld line was observed, which was not apparent prior to the failure. The laser welding company would not take responsibility for the poor manufacturing job; therefore, a solution that did not involve



Figure 4.12: Broken weld lines on middle shaft.

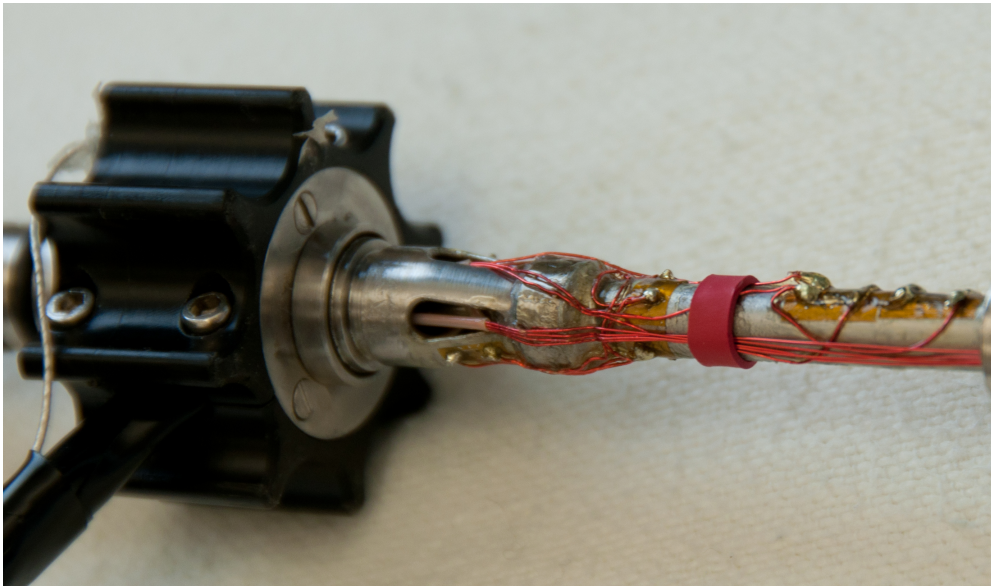


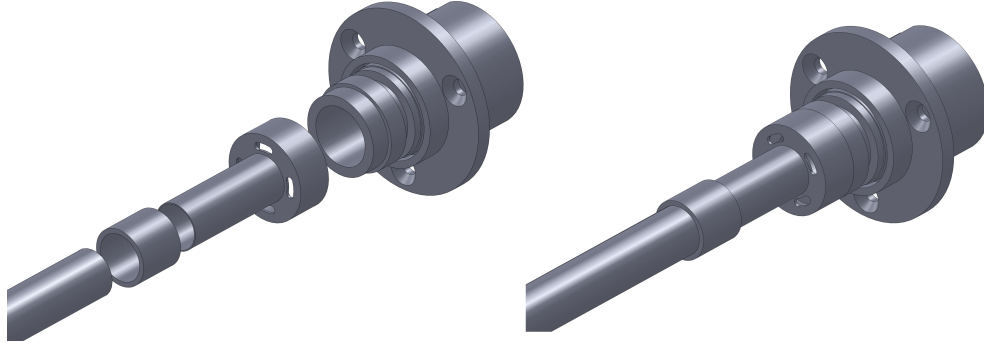
Figure 4.13: New axial element on middle shaft.

laser welding was sought.

A new axial element was developed, see Figure 4.13, to increase the strength of the instrument. Unfortunately, this resulted in a reduction of the sensitivity of the axial measurement with very high signal noise, see Table 4.7 and the bottom row of Table 4.1.

Table 4.7: Performance assessment of axial measurements with the new sensing element.

Noise (10 s)	Drift (10 min)	RMS error	Repeatability (max σ)	Hysteresis
3.41 N	4.67 N	0.58 N	0.68 N	0.78 N

Figure 4.14: CAD model of the new middle shaft for construction in the micromachining centre: exploded view (*left*) and assembled view.

With the acquisition of a 5-axis micromachining centre (MMC) in the Fall of 2011, a new middle shaft was designed, see Figure 4.14. This middle shaft contains an axial element with the same dimensions as the original middle shaft presented in Section 4.2.1. In order to strengthen the design, the weld lines were moved away from the axial element, thereby allowing the contact area where the welds are located to be significantly increased.

In order to manufacture the axial element, some extra steps were taken to accommodate the thin wall thicknesses. Once the inside holes were drilled to size, a brass dowel pin was placed inside the narrowest hole as shown in Figure 4.15. The dowel allowed the outside features to be machined, protected the thin walls from accidentally collapsing and allowed the piece to be mounted on the base in order to drill the stress concentration slots. After the machining of the element was complete, the dowel was removed and the element was welded to the base and the shaft of the instruments, as shown in Figure 4.16.

4.6 Discussion

The redesigned prototype was able to significantly improve performance when compared to the first prototype. The accuracy was measured to be between 0.07 and 0.36 N, repeatability was between 0.04 and 0.18 N, and hysteresis was between 0.1 and 0.28. All of these measures are



Figure 4.15: Mounting of axial element on MMC: axial element with brass dowel (*top left*), element mounted on MMC during drilling of small slots (*bottom*), and element mounted on MMC after machining (*top right*).



Figure 4.16: Completed middle shaft: close up of axial sensing element.

considered to be excellent compared to other existing technologies (see Table 2.4), allowing the developed instruments to effectively measure forces in all DOFs present in MIS. The force calibration assessment was performed within the range of 0 to 5 N. This is considered to be a typical range of forces applied by MIS instruments, except for the grip forces, where the average of the forces when driving needles could be 4 to 5 times higher.

The decoupling design element incorporated into the inner shaft was able to significantly reduce the effect of coupling caused by the x and y moments from 2.5 N in the previous prototype to 0.21 N in the new prototype. Coupling between the axial and the actuation force was inevitable with the current design, since the closing of the handle creates tension on the inner shaft, leading to compression of the middle shaft. To completely eliminate the coupling of these signals, future work will focus on devising a method to measure the actuation forces right at the tip of the instrument, which could be further enhanced by incorporating tactile sensors into the gripper.

It should be noted that the level of resolution required in actual surgical procedures remains unknown. Depending on the procedure and the task being performed, the required force resolution might be quite different. However, having instruments capable of accurately sensing forces might allow further research in order to determine the level of resolution required for different procedures.

This section presented an improved calibration process based on the results presented in the previous chapter. However, it is recognized that many improvements to the calibration procedure could be made in order to increase accuracy and reduce the amount of time it takes to complete the process. With the current design, it is difficult to mount the instrument on the adjusting wheel and to ensure that forces are being applied only in the direction of interest. Also, axial force calibration was found to be the most difficult to perform consistently because the string tends to swing. Similarly, inaccuracies were found when the axial force calibration was started with no weight because the string was not taut. Alternatives to the axial calibration procedure that do not utilize a string may have to be considered. Furthermore, it was found that calibration should be done prior to each procedure. This means that a simple, straight-forward calibration procedure with clear guidelines will need to be developed if the instruments are used commercially. Ideally, this would involve placing the instrument into a calibration jig while an automated system performs the entire calibration procedure. This should be considered future work.

As this prototype allows several different tips and handles to be used, it was also important to evaluate the effect on calibration of changing the tips. From the experimental evaluation, it

was found that recalibration does not need to be done when changing tips on the laparoscopic instrument, as long as a calibration factor is incorporated into the calculation of the torsional and grasping forces. It was expected that the moments would also be affected when using different tips, as the overall distance to the tip was different. No significant differences were found in the measurements, and this could be because the difference is masked by the measurement accuracy of the instruments themselves and/or by inaccuracies of the calibration assessment. If more accurate calibration methods are developed, or if the accuracy of the instruments is improved, it might be necessary to include a conversion factor for the x and y forces as well. Axial standard deviation was found to be the largest out of the four force directions measured, which could be explained by the inaccuracies of the calibration assessment itself.

A formal evaluation of the impact of changing the handles was not performed. As the change of handles requires a translation of the inner shaft within the instrument, which affects the wrapping of the wires within the instrument, the grasping signal changes significantly and using the same calibration values for the two models is not appropriate. There is also a change in the overall structure of the mechanism within the instrument as the needle driver tip is longer to accommodate the different handle configuration. It is recommended that the instrument is recalibrated if the handles are changed in order to avoid errors in the measurements.

The key to accurate axial force sensing was the design of the axial sensing element. Having a specialized element allowed the bending moments, torsion and axial forces to be completely decoupled. Unfortunately, the manufacturing of the original element was deficient and it was not able to withstand the forces applied to the instrument. This resulted in a significant delay in the experiments and increased cost due to the required reattachment of the gauges. The new design is much more robust, but also resulted in reduced sensitivity. Going forward, a micromachining system allows this element to be manufactured in a more robust manner with the features of the original axial element for maximum sensitivity.

It is recommended to investigate the ways in which the instruments and the calibration process can be further improved. The versatility and low cost of the software means that these types of smart surgical tools could have significant impact on how future laparoscopic procedures are carried out. The system has the potential to assist during minimally invasive procedures and in MIS training, allowing characterization and localization of tissues, as well as facilitating guidance around anatomical features for the surgeon.

Chapter 5

Sterilizable Prototype

5.1 Introduction

The previous chapters presented the design of the sensorized laparoscopic instruments that form the basis of the SIMIS system. The prototypes were built using metal and plastic capable of withstanding any sterilization procedure. However, the following characteristics of the design prevent them from surviving a complete procedure of cleaning and sterilization:

1. The instruments were not fully sealed to prevent moisture or debris from entering the inside of the instrument.
2. The cables and wires used on the instruments were not selected to withstand the cleaning and sterilization process.
3. The adhesives and coatings used to attach the strain gauges were not selected to withstand an autoclave environment.

This chapter outlines the work that was done to develop a sterilizable prototype of the SIMIS instruments. It also provides guidelines for cleaning and outlines the future work. In order to understand the design requirements and constraints, it is first important to understand the rules and regulations surrounding the use of reusable medical devices, as outlined in the following section.

5.2 Reprocessing of Medical Devices

All medical devices that are not disposable need to follow certain procedures to ensure that it is safe to use them in clinical applications [138]. Safe reprocessing of medical devices has two objectives: to eliminate all disease-causing microorganisms and to protect the devices from damage caused by foreign materials.

Tools and devices that come in contact with patients during surgical and therapeutic procedures need to go through the following steps: disassembly, cleaning, sterilization, drying, reassembly, and functional testing. It is up to the manufacturer of the equipment to outline how to disassemble, clean, and reprocess the equipment and devices. They can provide a list of recommended detergents, exposure times, method of sterilization and how many times each device can be reprocessed. However, they also must provide evidence that the cleaning and sterilization process is effective and has been validated.

For a critical device, which is one that enters the sterile tissues of the body, the following two steps must be completed:

Clean This process involves physically removing all debris from the devices. It involves washing with soap and water, and using detergents and enzymatic cleaners.

Sterilize This process involves the elimination of all microorganisms that could cause disease. Although different methods of sterilization exist, steam sterilization in an autoclave is the preferred method. A typical autoclave cycle requires exposing the instrument to 121° Celsius, at 207 kPa and 100% humidity for 30 minutes.

Some design features can prevent the successful disinfection and sterilization of medical devices by making the cleaning and sterilization process more difficult. These features include long and narrow lumens and channels, rough or porous surfaces, hinges, cracks, joints and crevices. A successful sterilizable device must not only avoid these features, but all materials and any electronics must be able to withstand the sterilization cycle. The selection of proper materials for a sterilizable prototype is presented in the following sections.

5.3 Selection of Adequate Cables and Connectors

Extensive searches were performed to identify companies that make cables and connectors that are adequate for the design of these instruments. The following sections outline the requirements and final result of these searches.

5.3.1 Cables

Cables are required to wire the strain gauges within the instruments. A total of 20 individual wires (four wires for each of the five bridges) need to come out of the instrument and be properly routed and protected so that they don't break or tangle. The specifications of the cables for the sterilizable instruments were determined as follows:

- Made from medical grade materials
- Multi-conductor with at least 4 coated conductors
- Covered with a protective outer sheath with a maximum outer diameter of 1 mm for every 4 conductors
- Very flexible to allow it to wrap around the inner shaft
- Able to withstand temperatures of over 121° Celsius

The cables that were found to meet the requirements were from Cooner Wire [139]. These are teflon coated, multi-stranded bare copper conductors, with a gold plated copper braided shield, Figure 5.1. The selected model (CZ-1223-4) has 4 conductors (size AWG 38) with a nominal outer diameter of 0.82 mm. The cables are rated to 200° Celsius.

The limitation still present with this wire is that in order to ensure that the cable is flexible enough to be routed around the inner shaft, a braided shield needs to be selected. This shield does not have a smooth surface and can cause debris to accumulate, making cleaning more difficult. To avoid this problem, it will be necessary to coat the cable once it has been routed through the instrument.



Figure 5.1: Multi-stranded medical grade cables from Cooner Wire.

5.3.2 Connectors

In addition to the cables, a properly sealed connector is required so that the instrument can be unplugged from the electronics and placed in an autoclave for sterilization. The specifications for the connectors were the following:

- Fully sealed to moisture
- Must withstand 121° Celsius
- Provide a minimum of 18 pins (4 for each of the three full bridges and at least 3 for the two half bridges), 20 pins would be ideal in order to ensure equal lead resistances in all of the bridge arms
- Accommodate miniature cables (AWG 32 or smaller)

The connector that was found to be adequate for this application is from the Fischer Core Series [140] (part number 1031A019-130 for the connector and K1031A019-130 for the corresponding receptacle). A connector with the same body but with a different number of pins is shown in Figure 5.2. These are high performance connectors, hermetically sealed for use underwater, in high-pressure conditions and corrosion resistant. They are rated to up to 200° Celsius. The model selected is a 19-pin connector that fits cables in the AWG range of 28–32.

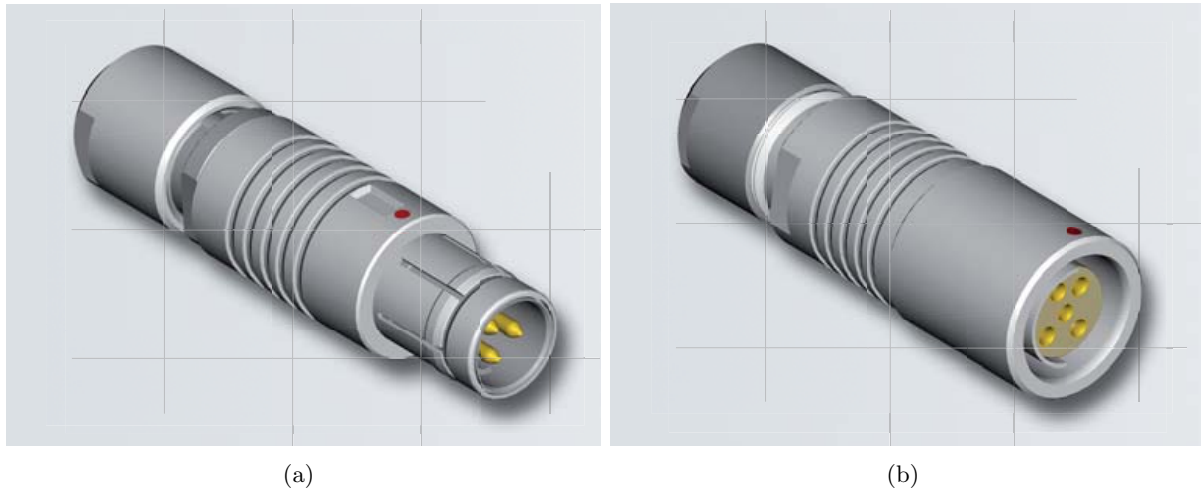


Figure 5.2: Sample sterilizable connector and receptacle from Fischer.

5.4 Selection of Materials for Strain Gauge Installation

The most significant limitation with the previous SIMIS prototype, regarding the sterilizability of the instruments, was that the sensorized elements would not be able to withstand an autoclave cycle. An experimental evaluation was performed to determine the best combination of strain gauge adhesives and coatings to allow for sterilization of the SIMIS instruments.

An exhaustive search was performed to identify adhesives and coatings that could withstand temperatures higher than 121° Celsius and that would not be weakened by exposure to high humidity. Furthermore, the materials should not contain toxic chemicals. The materials that were found suitable are detailed in Table 5.1.

This table shows that two of the adhesives and two of the coatings are compliant with the International Organization for Standardization (ISO) 10993 series [141]. This series regulates the biocompatibility of medical devices and is considered a critical condition that must be met for new devices to be approved for clinical trials. The following section presents the details of the evaluation that was performed to assess the best combination of adhesive and coating.

5.4.1 Experimental Methods

The purpose of this experiment was to identify if there is one particular combination of adhesive and coating that will allow the strain gauges to withstand more sterilization cycles while maintaining excellent sensing performance. The evaluation was designed as a full factorial test with two factors

Table 5.1: Relevant information of the adhesives and coatings tested.

Number	Name	Manufacturer	Distributor	Specifications
Adhesives				
1.	M-Bond 610	Vishay	Intertechnology	Operating temperature between -269° and 175° C. Formulated for bonding strain gauges. Curing requires a three-step process at different temperatures in an oven. Contains toxic substances in the liquid state but is no longer toxic once cured.
2.	Loctite M-3981	Henkel	Acklands Grainger	ISO 10993 certified—further strengthens in an autoclave environment. Designed for medical applications. Must be cured in an oven.
3.	SILASTIC Medical Adhesive Silicone, Type A	Dow Corning	Dow Corning	Operating temperature of up to 150° C. Designed specifically for medical applications. ISO 10993 certified.
Coatings				
4.	M-Coat C	Vishay	Intertechnology	Reasonable moisture protection, operating temperature -60° to 260° C. Contains toxic substances in the liquid state but is no longer toxic once cured.
5.	Loctite M-31CL	Henkel	Acklands Grainger	ISO 10993 certified, 150° C operating temperature. Not recommended for products that will see more than 3 sterilization cycles.
6.	Loctite M-11FL	Henkel	Acklands Grainger	-60° to 250° C operating temperature, ISO 10993 Certified. Not recommended for products that will see more than 3 sterilization cycles. Must be cured in an oven.

(adhesive and coating) at three levels each (3^2 design) for a total of 9 different combinations. To ensure sufficient power and to account for the learning curve in strain gauge installation, the experiment was designed with 11 replicates.

Stainless steel bars of the same material as the instruments (Stainless Steel 316) were used to perform the assessment. It was decided that to ensure consistency, all 9 combinations of strain gauges would be installed on the same stainless steel bar. All 9 strain gauge combinations were placed on each bar in a random order, see Figure 5.3.

To evaluate the performance of the gauges, the bars were held in cantilever, while weights of increasing size were used as a load. To ensure consistency, the bars were built with a series of equally spaced holes that allowed them to be mounted on a calibration jig in such a way that the distance between the mounting point and the strain gauge was the same for each gauge, see Figure 5.4. Similarly, holes on the other side of the bar allowed the weights to be applied at the same distance from each strain gauge. An undergraduate summer student designed the bars and the mounting base, built the actual components, and installed the strain gauges, as described below.

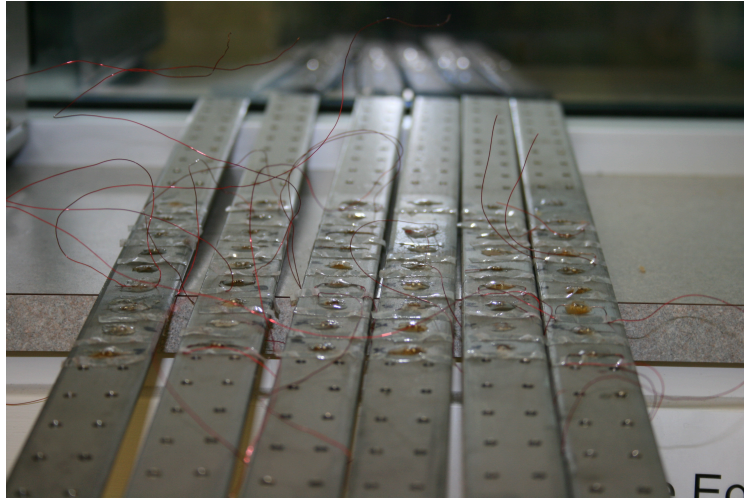


Figure 5.3: Stainless steel bars with gauges attached.

5.4.1.1 Strain Gauge Installation

All three coatings and adhesives were combined in each of the 11 stainless steel bars, for a total of 9 strain gauges per bar. The laying of the gauges was done in blocks based on the adhesive. Gauges requiring M-Bond 610 were placed first, as curing this adhesive required a complex procedure in an oven. The gauges attached with the Loctite adhesive were done second, also cured in an oven, followed by the gauges using the Silastic adhesive. The installation guidelines for each adhesive and coating were followed to ensure consistent results. Several gauges fastened with the Silastic product had to be refastened. The soldering and coating of the gauges was done from bar to bar in a continuous fashion.

For this performance evaluation, the strain gauges were directly connected to an amplifier in a type I quarter bridge configuration. To read the information from the strain gauges, a Quanser strain gauge amplifier was mounted on a board and wired such that reading the information from the different gauges could be done through a quick change over that only required clamping the two cables with screws. The other components included a dual output power supply (Agilent Technologies, model E3620A) and a data acquisition card (Keithley Instruments, model KPCI-3108). A customized software program developed at CSTAR (see Section A.3) was used to read the data from the gauges, filter the signals, perform the calibration and record the resulting force data.

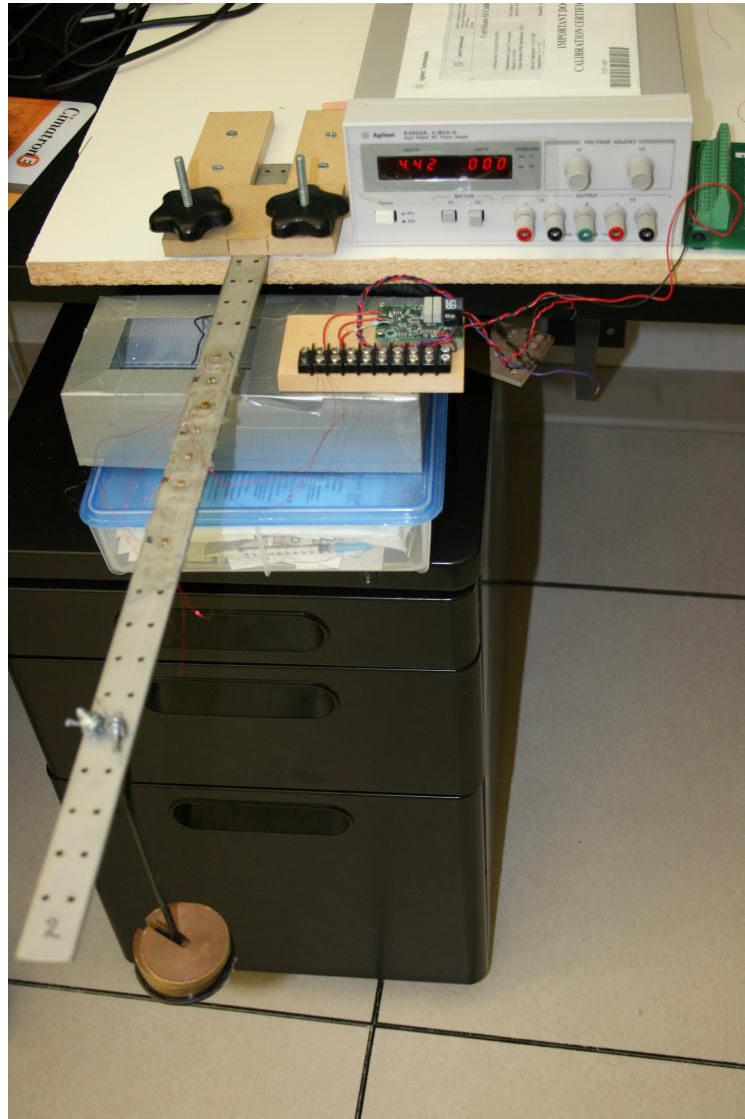


Figure 5.4: Experimental jig with stainless steel bar in cantilever.

5.4.1.2 Performance Evaluation

To evaluate the performance of the installed gauges and their resistance to autoclaving, the following procedure was followed:

1. Each bar was mounted in cantilever as described above. In order to maintain the distances from the mounting point to the gauge and from the gauge to the weight location constant, the bar needed to be repositioned for each gauge.
2. Each gauge was then calibrated through the application of weights from 0 to 1 kg in 100 g

increments. The slope of the relationship between the voltage and the forces applied was then recorded as a measure of sensitivity. All calibrations were originally performed at a standard voltage of 5.26 V, but in some cases after autoclaving, some of the gauges required a higher voltage to register a signal.

3. Data were recorded for 10 s when no forces were being applied to evaluate noise and drift.
4. Data were then recorded while applying weights at 0 g, 500 g, 1000 g, 500 g and 0 g again.
5. Finally, the performance was assessed by computing the following measures:
 - (a) Accuracy was measured by comparing the measured values to the theoretical values.
 - (b) Hysteresis was assessed by comparing the values at 0 g and at 500 g when increasing and decreasing the applied load.
 - (c) Noise was measured by comparing the maximum and minimum values of the data when no forces were being applied.
 - (d) Drift was computed by comparing the average of the first 500 samples and the average of the last 500 samples when no forces were being applied.
 - (e) A final performance measure was computed by adding the above error measures. The lower the value, the better the performance exhibited by the gauges.

Once the calibration and assessment was completed for all 99 gauges, the bars were placed in an autoclave (Getinge Castle 500LS series steam sterilizer) for a complete standard cycle. After the bars were dry and had returned to their normal environmental temperature, the calibration and assessment procedure was repeated. The autoclave/assessment cycle was performed a total of five times.

5.4.2 Results

A preliminary evaluation was performed to assess the performance of the 99 original strain gauges after installation. The results of the assessment are presented below.

5.4.2.1 Original Performance

Only 51 of the 99 strain gauges provided a valid force measure after installation, as presented in Table 5.2. The results of the preliminary evaluation are presented in Table 5.3. As the gauges within each combination had similar performance, one combination was selected as representative of the whole set.

In summary, there were 22 working gauges with adhesive 1, 14 working gauges with adhesive 2, and 16 working gauges with adhesive 3. Similarly, there were 12 working gauges with coating 4, 24 working gauges with coating 5, and 16 working gauges with coating 6.

It is apparent from these values which adhesives and coatings made the installation process more difficult. A steeper learning curve might be involved in the application of some of these substances. The starting performance of the gauges adhered with adhesive 3 is much poorer than the performance of the other gauges.

5.4.2.2 Performance After Autoclaving

Sample results of the performance of the gauges following the autoclave cycles is presented in Table 5.4. For simplicity, only the best performing gauge was presented. A summary of the overall results for all of the gauges is presented in Table 5.5. It is clear from this table that coating 6 was the only one able to protect the gauges well enough for any gauge to survive all 5 cycles.

Table 5.2: Working strain gauges for each combination of adhesive and coating, and their position on the bar.

Combination	Working gauges	Position on the bar
1/4	3	1,3,7
1/5	10	9,9,6,4,7,5,2,4,6,7
1/6	9	9,4,3,8,6,1,5,1,8
2/4	4	4,6,1,2
2/5	8	3,5,2,7,1,9,6,4
2/6	2	1,6
3/4	5	3,6,2,9,3
3/5	6	7,4,1,5,1,7
3/6	5	8,5,9,3,9

Table 5.3: Sample results of the preliminary evaluation (all values in N).

Combination	Slope	RMS error	Repeatability	RMS Hysteresis	Noise	Drift	Total performance
1/4	-122.48	0.03	0.04	0.05	0.17	0.02	0.31
1/5	-121.10	0.06	0.07	0.04	0.23	0.03	0.43
1/6	-122.63	0.04	0.04	0.12	0.15	0.00	0.35
2/4	-124.13	0.08	0.05	0.20	0.19	0.02	0.54
2/5	-121.78	0.13	0.09	0.21	0.21	0.07	0.71
2/6	-121.79	0.05	0.05	0.04	0.18	0.03	0.35
3/4	-713.62	1.64	0.44	1.48	0.93	0.09	4.58
3/5	-206.48	0.25	0.08	0.17	0.34	0.04	0.88
3/6	-709.01	2.32	0.87	1.43	1.31	0.45	6.38

Table 5.4: Overall performance (in N) of the best performing gauges in each combination, as calculated by adding the errors of accuracy, hysteresis, noise and drift.

Bar	Pos.	Combination	Original	Cycle 1	Cycle 2	Cycle 3	Cycle 4	Cycle 5
7	7	1/4	0.319	1.474	-	-	-	-
1	4	2/4	0.420	0.319	0.422	1.618	-	-
10	9	3/4	3.28	-	-	-	-	-
8	2	1/5	0.356	0.724	1.307	-	-	-
2	3	2/5	0.182	0.434	0.621	1.300	-	-
4	1	3/5	0.888	29.40	9.051	-	-	-
7	6	1/6	0.348	0.334	0.544	0.459	0.380	0.406
3	6	2/6	0.602	0.680	0.764	0.808	1.365	0.992
2	5	3/6	4.627	5.508	10.34	7.494	8.185	8.712

5.4.2.3 Summary

The results presented above show that the only gauges that survived all 5 cycles were those installed with coating 6. Although adhesive 1 had one gauge that survived all 5 cycles with this coating, it was the only one out of 9 that survived any autoclaving. Almost all of the gauges properly installed with adhesives 2 and 3 and coating 6 survived all 5 cycles. It might be possible that the low number of working gauges with the 2/6 combination and the poor gauge performance with the 3/6 combination was caused by inexperience in the installation process. It was therefore decided to examine these two combinations further, as described in the following section.

Table 5.5: Summary of results showing average performance for all gauges in each combination and overall comments on ability to survive the autoclave cycles.

Combination	Average performance (N)	Autoclave survival
1/4	1.28 ± 1.26	Poor results, only one gauge survived one cycle
2/4	3.85 ± 7.14	2 out of 5 survived after 1st cycle, only one survived cycles 2 and 3
3/4	4.57 ± 1.26	No gauges survived cycle 1
1/5	0.57 ± 0.40	Out of 10 gauges, none survived more than 2 cycles
2/5	0.57 ± 0.30	Out of 8 gauges, none survived more than 3 cycles
3/5	8.10 ± 9.24	Out of 6 gauges, none survived more than 2 cycles. Poor performance
1/6	0.38 ± 0.11	Only one gauge out of 9 survived cycle 1 and continued to work until the end
2/6	0.77 ± 0.38	Difficult to apply, only 2 were working from the start. The ones that did survive had excellent performance and survived 3 cycles or more.
3/6	7.46 ± 4.50	Almost all survived but original performance was very poor. Initial performance might improve with a better installation process.

Table 5.6: Results of the additional evaluation with adhesives 2 and 3.

Combination	Average performance (N)	Autoclave survival
2/6	0.26 ± 0.14	Survived all 5 cycles
2/6	0.23 ± 0.11	Survived all 5 cycles
3/6	1.11 ± 0.96	Survived all 5 cycles
3/6	1.35 ± 0.62	Survived only 3 cycles

5.4.3 Additional Evaluation of Best Results

Based on the results obtained from the first evaluation, a total of 4 additional gauges were installed with coating 6, two with adhesive 2 and two with adhesive 3 in order to perform one last comparison and tune the installation process. The installation process was modified slightly to ensure an even distribution of the adhesive over the entire gauge. All four gauges worked properly from the start. The results of the performance evaluation after autoclaving are shown in Table 5.6. These results clearly show that Loctite M-3981 (adhesive 2) had much better performance and all gauges survived more cycles.



Figure 5.5: Strain gauge installation process: gauges clamped for curing (a) and instruments in oven (b).

5.5 Assembly

Based on the results from the previous section, a sterilizable prototype is under construction. The strain gauges were installed using Loctite M-3981 and coated using Loctite M-11FL. As this adhesive required curing in an oven, the gauges were placed and then clamped with a teflon layer to prevent the clamps from sticking, while ensuring an even distribution of the adhesive, see Figure 5.5(a). The parts were then cured in an oven, as shown in Figure 5.5(b).

For the inner shaft, 4 gauges were laid in a full bridge configuration as shown in Figure 5.6(a), two inline with the shaft, and two in a transverse position (Poison). The middle shaft contained 4 different bridges: two half bridges to measure the forces acting perpendicular to the shaft, one full bridge to measure torsion and one full bridge to measure axial forces. The tiny gauges required to measure the axial forces were difficult to install. To simplify the process, a teflon disk was constructed and attached to the instrument using a cable tie to increase the surface area, as shown in Figure 5.6(b). The teflon disk was kept in place to prevent any damage to the solder pads prior to assembly.

5.6 Concluding Remarks

The remainder of the instrument is under construction. The connectors required to complete the assembly have been ordered but have not arrived. A final build of the prototype with a full performance evaluation is expected to be completed over the next few months.

Additional work is required in order to determine the best way to seal and clean the instrument.

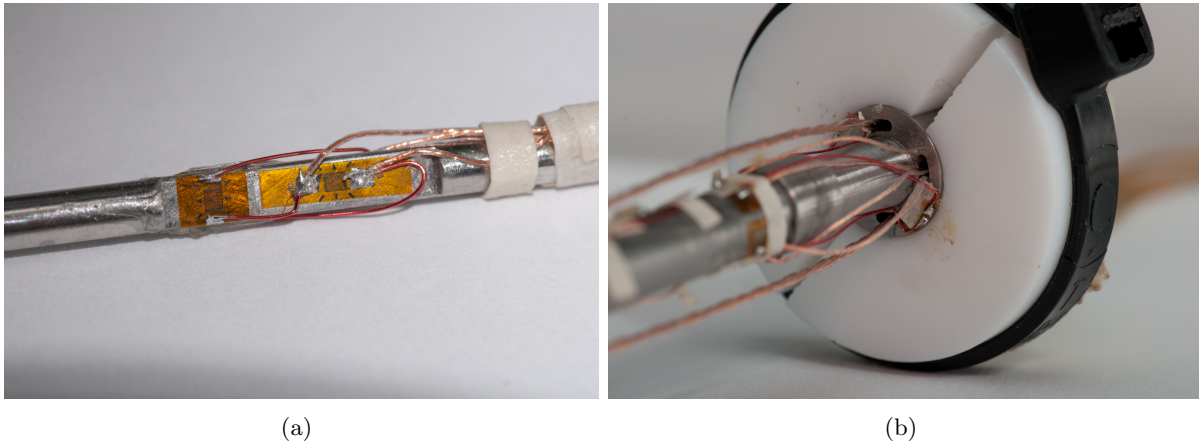


Figure 5.6: Gauges installed and cables soldered: on inner shaft (a) and on middle shaft (b).

The long narrow lumen of the instrument cannot be fully sealed to foreign substances due to the use of interchangeable tips and due to the nature of the actuation mechanism of the instruments. Methods for flushing the inside of this type of devices have been implemented in the past for medical devices and a similar procedure is expected to be acceptable for this instrument as well. However, there are also mating surfaces between components that need to be sealed in order to ensure that debris does not enter these areas, as it would not be possible to properly flush them without full disassembly—a process that would expose sensitive parts of the instruments and should be avoided. Research into proper sealing materials is necessary.

Finally, the cleaning and disinfecting procedure required for medical devices will have to be properly outlined. Experiments need to be performed to find detergents and enzymatic cleaners that do not react with the sealing materials or with the adhesives and coatings selected above. This will also involve determining the required exposure times and validating that the instruments are fully disinfected prior to reassembly and sterilization.

An adequate method for calibrating the instruments once sterilized will also need to be outlined. It is not feasible to have the instruments calibrated using the current techniques if they have been sterilized for surgical use. Recommendations for better calibration systems are presented in Chapter 8.

The process of approval of a medical device is not an easy task. There are significant considerations that need to be in place, which make this process lengthy and time-consuming. This chapter has presented a thorough experimental evaluation aimed at selecting adequate materials that will allow the instruments to survive an autoclave sterilization procedure. The results show

that the Loctite M-3981 adhesive in combination with the Loctite M-11FL coating provide the proper protection of the stain gauges to survive five sterilization cycles with excellent performance. A sterilizable prototype based on the results is under construction.

Chapter 6

Applications to Surgery

6.1 Introduction

The previous chapters have dealt with the design, development and construction of the SIMIS instruments, as well as an evaluation of their sensing ability. This chapter focuses on evaluating the feasibility of using the SIMIS system to assist real surgical applications or to optimize the development of instruments specifically designed for MIS, based on data collected during real surgical procedures.

As was described in Chapter 2, it has been recognized that the availability of force information could have an impact during minimally invasive surgery, as the sense of touch is affected by the limited access conditions present in this type of surgery. The following are three applications in which force information has been recognized as being useful:

- Tissue characterization and the localization of areas of different stiffness as possible sources of disease
- Measurement of applied forces and instrument motion during surgery in order to inform the development of devices specifically designed for MIS
- Providing force feedback during surgery in order to prevent the application of excessive forces to tissue, or insufficient forces

The following sections outline the three experimental evaluations that were performed to assess the usefulness and feasibility of the SIMIS system in these surgical applications.

6.2 Applications to Tissue Characterization

The need to characterize tissue has been recognized as important in the identification of areas of increased or decreased stiffness, which can indicate the presence of pathological abnormalities, such as cancerous tumours or calcifications. In open surgical procedures, this is usually done by directly palpating tissue. In MIS, however, the ability to directly interact with tissue is hampered by the small incisions required to minimize invasiveness.

Researchers have been working on defining mathematical models that can characterize the stress–strain relationship of artificial and real tissue. Although most researchers simplify this model as a linear relationship, it has been found that due to the nonhomogeneous nature of tissue, both in location and direction, human tissue exhibits nonlinear properties [142, 143].

Noninvasive techniques, such as magnetic resonance imaging (MRI) or ultrasonography are often used to characterize tissue, but can only determine models in the linear range [142]. The Mooney-Rivlin strain energy function and the Ogden and Arruda-Boyce strain function are often used to model nonlinear behaviour, with no consensus over which one is better [142]. In [143], after an evaluation of seven different models, the Hunt-Crossley equation was found to reduce the simulated error compared to artificial phantom tissue. This model is represented by the following equation:

$$F = kd^n + \lambda d^n \dot{d}, \quad (6.1)$$

where F is the sensed force, k is the stiffness factor, λ is a scaling factor, d is the penetration depth and \dot{d} is the speed during penetration. In [142], the value for n was found to be between 1.3 and 2 depending on the tissue. Based on this equation, and assuming that the instruments are moved in very slow motion so that \dot{d} is negligible, the stiffness factor may be computed by the following equation:

$$k = F/d^n. \quad (6.2)$$

Recent work at CSTAR has shown the benefit of using tactile sensors to identify areas of increased stiffness [15, 16] with promising results. The feasibility of using kinesthetic feedback for the same purposes has also been demonstrated [92]. In this section, the goal is to take advantage

of the fact that the SIMIS instruments are able to measure the applied forces and instrument tip position in order to establish a method of using kinesthetic data for tissue characterization.

6.2.1 Experimental Evaluation

A preliminary experiment was conducted to evaluate the feasibility of using a combination of the force and position data obtained using the SIMIS instruments in order to identify the location of areas of increased stiffness in a laparoscopic training box. The purpose of the experiment was to evaluate whether the force and position data collected using the SIMIS instruments during a palpation task could be combined in such a way that a tactile map could be generated to provide information about the stiffness of the underlying tissue. The hypothesis was that it is possible to find a way to combine the available information such that the location of a mimicked tumour can be identified. The following sections describe how the experiments were conducted and the results that were obtained.

6.2.2 Methods

To perform the experiments, an experimental setup was made out of foam and silicone of different compositions. A 1-cm cylinder made of silicone rubber (Sorta-Clear 18, Sculpture Supply Canada, Shore hardness 18A¹) was embedded within a tissue phantom (from the Chamberlain Group [146]) in order to mimic soft tissue with an embedded tumour. A replaceable top skin surface made of soft rubber (EcoFlex, Sculpture Supply Canada, Shore hardness OO-30) was used to visually hide the lump, see Figure 6.1(a). A plastic frame was designed and built out of acrylonitrile butadiene styrene (ABS) plastic and was used to attach the model to the laparoscopic box and hold it in place, see Figure 6.1(b). The location of the centre of the tumour was later measured to be [-122, -367] in the coordinate system of the instruments (see Section 6.2.3).

As the penetration depth needed to be calculated, it was necessary to determine the location of the plane of the top of the plastic frame with respect to the origin of the coordinate frame of the EMTS used to track the SIMIS instrument motion. Therefore, prior to the start of the experiments, position data were collected while the tip of one of the SIMIS instruments was placed

¹The Shore hardness scale is the preferred method for measuring the hardness of elastic materials [144]. It measures the resistance to indentation, hence a higher number indicates a stiffer material. There are 12 different scales depending on the hardness of the material. The A scale is used for soft materials such as rubber, leather and felt. The OO scale refers to very soft materials such as gels and foam [145].

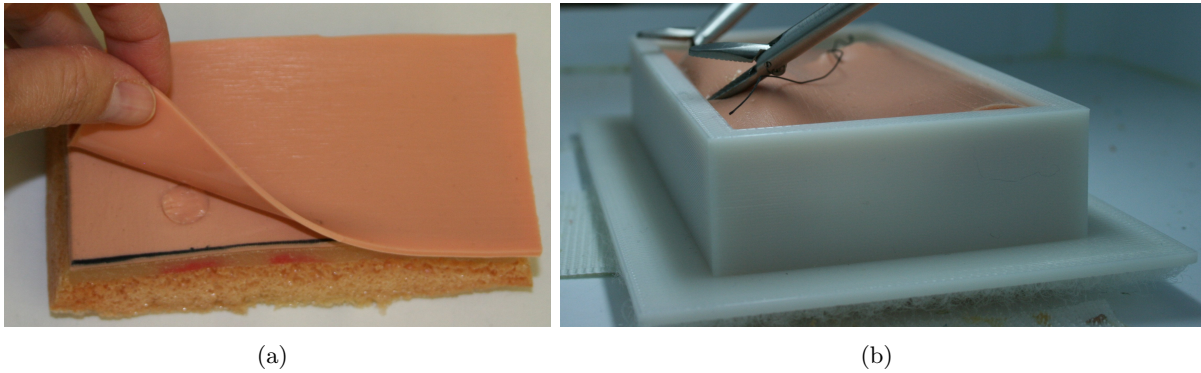


Figure 6.1: Experimental setup used during the tissue characterization tests: tissue phantom with an embedded tumour (a) and tissue inside training box held by plastic frame (b).

at each corner of the frame.

An evaluation was then performed by a subject who was blinded to the actual location of the tumour. One of the SIMIS instruments was used to systematically palpate the tissue throughout the entire surface. During this palpation task, it was possible to visually identify a suspected tumour location based on the deformation of the tissue in the surrounding area (this might not always be the case during real surgery). A second evaluation was performed using the same instrument to palpate randomly around the suspected lump location. During both of these palpation trials, the following important variables were recorded: applied Cartesian forces, instrument position in 3 DOFs, and videos of the trials.

6.2.3 Data Analysis

Once the data were collected and recorded, the files were processed using MATLAB to determine the location of the four corners of the plastic frame in the coordinate frame of the EMTS. The video was analyzed to extract four time ranges corresponding to two seconds of data collected at each corner. The mean value of the measured locations (of the x , y and z coordinates) during each of these time frames was defined as the location of each corner.

The locations of the four corners of the reference frame are presented in Table 6.1. Based on these values, the three coordinate points used to identify the frame plane were: $[-166.6, -335.6, -377.3]$, $[-166.6, -390.1, -391.2]$, and $[-53.5, -390.1, -391.2]$, calculated as the average of the two similar values at each corner.

A MATLAB script was written to process the data from the two palpation trials. The data

Table 6.1: Location of the four corners of the frame.

x	y	z
-164.9167	-333.6564	-383.2384
-168.1946	-388.5077	-392.2571
-54.8700	-391.6660	-390.1576
-52.1919	-337.4846	-371.3062

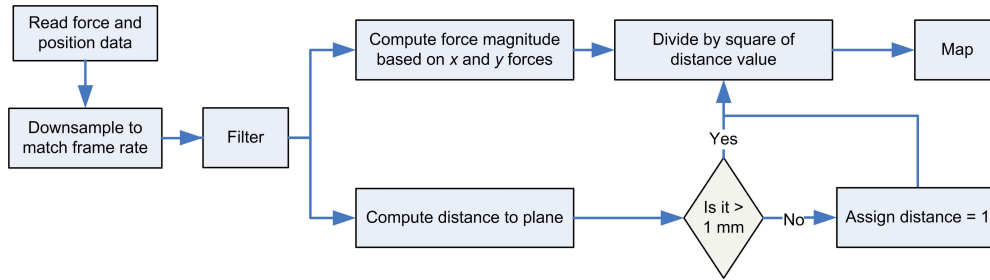


Figure 6.2: Data flow diagram for tissue characterization data processing.

flow followed by this script is outlined in Figure 6.2. The data collected was first downsampled by averaging the values in each window, so that both the force and position data would have the same number of data points and so that each data point corresponded to one frame in the video. The data were then filtered (see Section 6.2.3.1) at a low-pass frequency rate of 128 Hz to eliminate high-frequency noise. The magnitude of the force was computed from the force components measured in the x and y directions (the axial force was not used due to the limitations mentioned in Chapter 4). The position data were processed to compute the perpendicular distance from each point to the plane of the plastic frame².

As a measure of stiffness, the simple nonlinear measure shown in Equation 6.2 was implemented with $n = 2$. It was found in [148] that sensors are able to detect lumps at average indentation depths of 1.75 to 2.75 mm. For this reason, and to avoid high stiffness values erroneously created by near-zero penetration depths, the minimum penetration depth that was considered was set to 1 mm. The stiffness equation used was then the following:

²To determine the perpendicular distance to the plane of the frame, the coordinates of three points on the frame were used to compute the normal to the plane as the cross product of the vectors between those points. Then the function for the plane was defined as the dot product of a symbolic vector $[x, y, z]$ and the normal to the plane. To compute the perpendicular distance from a point P , the coordinates of point P were substituted into the plane function and divided by the norm of the normal vector [147].

$$k = \begin{cases} F/d^2 & d \geq 1, \\ 0 & d < 1. \end{cases} \quad (6.3)$$

6.2.3.1 Filtering

In order to determine which filter to use, a survey of the published literature was conducted to find typical filters used for processing human motion data. A fourth-order low-pass Butterworth filter is used in [149] with a cutoff frequency of 25 Hz, and low-pass filters are also used in [150] and [151] with cutoff frequencies of 15 Hz and 3 Hz, respectively. In earlier work at CSTAR, a specialized filter defined in MATLAB as the `filtfilt` function [92] was used. This function filters data in the forward direction and then re-filters the output in the reverse direction so that phase distortion is eliminated, as shown in Figure 6.3. This also doubles the order to the filter, so a second-order Butterworth filter is equivalent to a fourth-order filter without the `filtfilt` function.

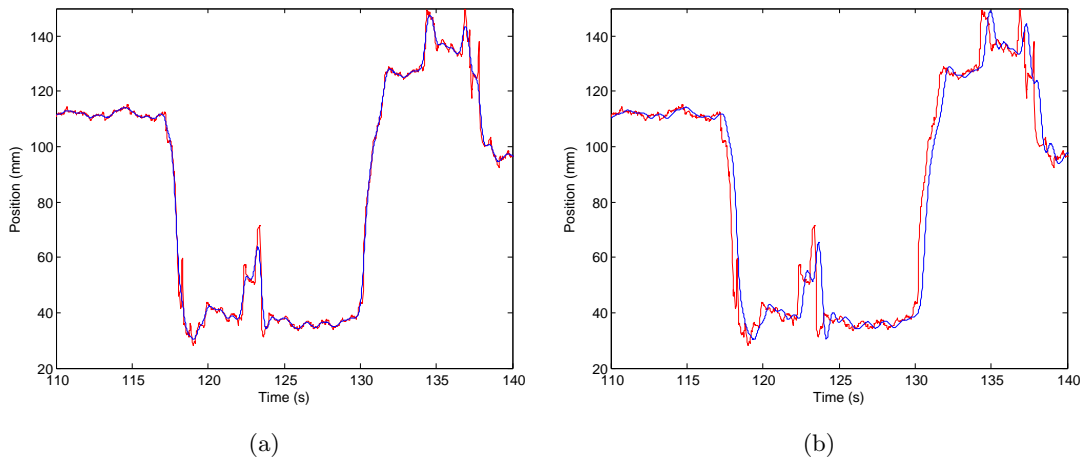


Figure 6.3: Overlaid filtered (*blue*) and unfiltered (*red*) position data with a second order `filtfilt` filter (*left*) and a fourth-order Butterworth filter (*right*).

It was then decided for these experiments to implement a second-order Butterworth filter with the `filtfilt` function (A similar filter is used in [152] with a cutoff frequency of 10 Hz). The raw data were used to create power spectrum maps to determine the ideal cutoff frequencies, see, for example, Figure 6.4. A cutoff frequency of 1.25 Hz was determined to be adequate for both the position and force data in its raw form, in order to eliminate high frequency noise without losing important details of the data profile. As the data was downsampled during the tissue

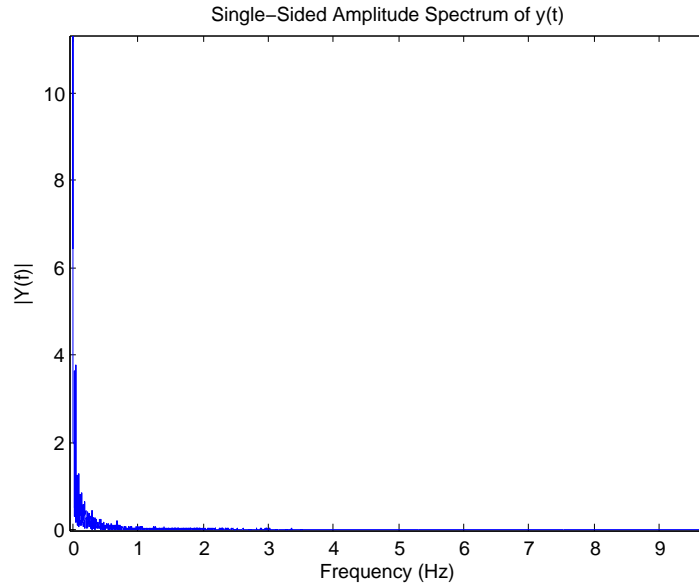


Figure 6.4: Power spectrum of the position data for a novice subject.

characterization trials, a cutoff frequency of 128 Hz was used to avoid excessive smoothing of the data.

6.2.4 Results

The results of the initial palpation are shown in Figure 6.5. In this figure, the stiffness factor is shown as a dot that varies in size and colour. For small stiffness factors, a small blue dot is used. As the factor increases, so does the size of the dot. A large stiffness factor is represented by a large dark red dot. The maximum applied force during this palpation task was 7 N.

It was noted from this figure that the peak in the localization map was at $[-138.2, -361.2]$, which is significantly far away from the actual location of the tumour (centred at $[-122, -367]$). The video was then analyzed to identify the cause of the error in the localization. The position of the instrument at the moment the palpation measure peaks is presented in Figure 6.6. It was noticed from the video that although the tip of the instrument was located at the top left of the tumour, the shaft of the instrument was in fact in contact with the tumour; hence, the palpation measure showed a peak. Considering the data recorded during a more focused palpation procedure in the vicinity of the suspected location of the tumour, Figure 6.7, the palpation peaks at $[-121.9, -363.8]$, which is within the actual location of the tumour. The maximum applied force during the

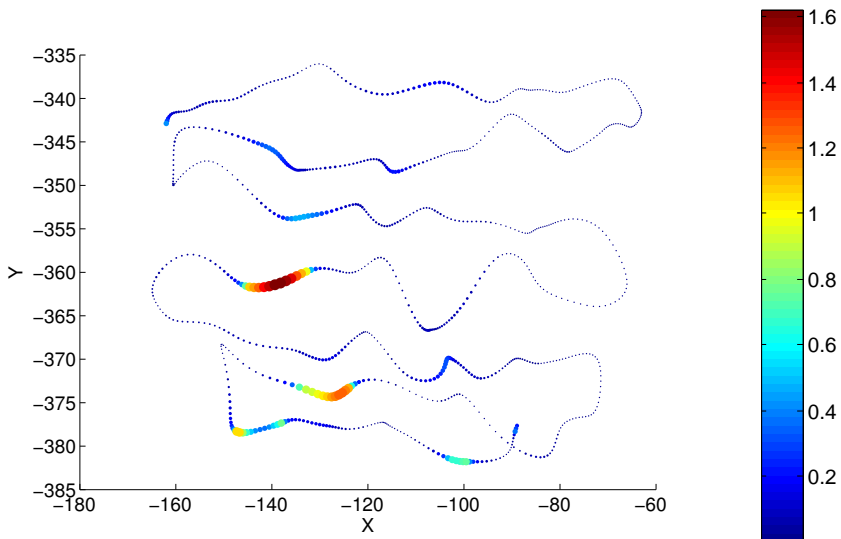


Figure 6.5: Tactile map obtained from a systematic palpation across the entire surface, showing the stiffness factors obtained at each (x, y) coordinate in N/mm^2 .



Figure 6.6: Image of instrument location during identified peak.

second palpation task was 13.2 N, resulting in larger dots as compared to Figure 6.5.

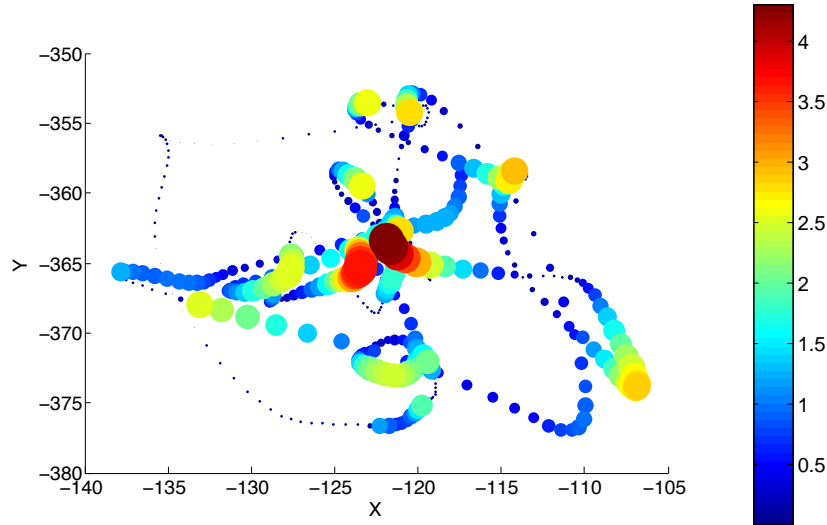


Figure 6.7: Tactile map obtained from a localized palpation around suspected site, showing the stiffness factors obtained at each (x, y) coordinate in N/mm^2 .

6.2.5 Discussion and Development Guidelines

This experiment shows a very simple evaluation of the potential that the SIMIS system has to localize areas of increased stiffness. The purpose was to demonstrate the feasibility of using the SIMIS instruments to identify the location of an area of increased stiffness.

The results show that it is possible to identify the location of a lump, but for increased accuracy in localization, care must be taken in how the instrument contacts the tissue and sufficient force must be applied. A very simple way of determining stiffness was implemented in these preliminary tests. There are many possible ways to improve the performance by using more elaborate algorithms. Some considerations and development guidelines are as follows:

- The calculation of the penetration depth could be automated by determining when contact with the tissue begins (i.e., what is the position of the instrument when the forces exceed a certain minimum threshold). From that point on, the relationship between the position and the force measured can be used directly to characterize tissue stiffness. A tissue characterization model can then be implemented as shown in Figure 6.8.
- In real surgical settings, the surface of the tissue may not be horizontal as in these experiments. Instead, the incline of the surface changes from one location to another. The forces applied in the three Cartesian directions could be combined to determine the direction

in which the forces are being applied in order to calculate the penetration depth in that direction. This would require the force sensing accuracy to be similar in all three directions.

- Some of the advantages of using the SIMIS instruments for tissue characterization arise from the fact that they can measure force in different directions. This permits directional force measurements not present in most tactile sensing systems, which only measure pressures normal to the surface. An interesting area of research would be to investigate the use of the sliding instrument motion for tumour localization. This approach might be able to provide a measure that better corresponds to how a surgeon's hand palpates during open surgery.
- Proper tissue characterization also has an effect on the development of simulators (both physical and virtual reality simulators, see Chapter 7). Using materials of incorrect properties during training can lead to the development of poor habits and other adverse effects [142]. Research has shown that *in vitro* tissue characteristics differ significantly from those found in *in vivo* situations [142]. Being able to measure forces during real surgical procedures can provide information to inform the development of better tissue models.
- If future modifications are made to the instrument to allow the opening angle of the grasper to be measured, then the grasping data could also be used to characterize tissue in a similar manner.

In these experiments, due to the orientation of the instrument with respect to the tissue, the axial forces were not as important when estimating the contact force with the tissue, as the forces acting perpendicular to the shaft dominate. However, in other applications, the axial force could be important. Another limitation of this study is that only one tissue phantom was palpated, as this was meant to be a proof of concept evaluation. Future work should focus on a properly designed experiment with sufficient power, using several different tissues and performed by various subjects.

6.3 Applications to the Development of Haptic Interfaces

The availability of data collected from real surgical procedures can lead to the development of better tissue models for training and planning. Another application in which this information

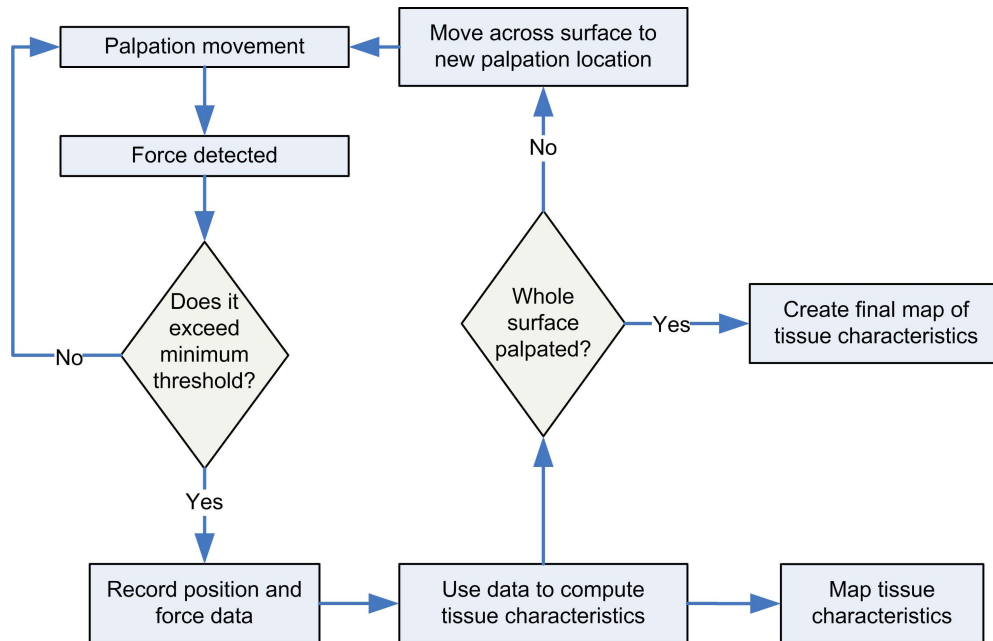


Figure 6.8: Data flow diagram of tissue characterization procedure.

would be valuable is in the development of devices that are optimally designed for use in MIS. For example, Chapter 2 presented the concept of a haptic interface as a device that applies resistance in certain directions so that the user feels as though they are in contact with the tissue. A haptic interface can then be used to control a surgical robot or as an interface to a surgical simulator. Although haptic interfaces are commonly used in applications outside of the medical field with great success, their success in controlling a surgical robot or as an interface to a surgical simulator has been limited. Some of the reasons for this limited success are as follows:

1. Providing haptic feedback depends on the ability to accurately sense information during surgery, or on the realism of the simulated tissue in simulators. The feedback provided can only be as good as the sensors used or the accuracy of the model. Current surgical systems are not able to accurately measure interaction forces during surgery, thereby limiting the applications of haptic interfaces. Current simulators do not have realistic models in part due to insufficient information about real tool–tissue interactions.
2. The effectiveness of haptic interfaces is also limited by the ability to ensure transparency in the control system. This requires the position data to be transferred from the interface to the robotic system or the simulator, and the force data to be transferred back in a smooth

and accurate manner with no time delay. Other work at CSTAR has focused on addressing these difficulties, see for example [153–156].

3. If the goal is to ensure transparency, feedback in all 7 DOFs must be provided. There are very few haptic interfaces currently in the market that can provide 7 DOF of force feedback. Some examples are Sigma.7 and Omega.7 (Force Dimension, Nyon, Switzerland), and the Freedom 7S (MPB Technologies, Montreal, QC, Canada). Also, a customized interface was adapted at CSTAR from Quanser’s Haptic Wand [111]. However, these interfaces do not match the motion and force ranges required for surgical applications thereby limiting their application to surgery.
4. Current haptic interfaces do not provide realistic feedback due to limitations of the actuation systems employed for the interface. The range of forces and stiffnesses required are not well defined for surgical applications, making the development of haptic devices specific to MIS difficult.

To assist in this research area, the objective of this section is to investigate the use of the SIMIS instruments to inform the development of haptic interfaces, by collecting force interaction data and motion information from real surgical settings. To achieve this objective, it was first necessary to determine if the instruments could be successfully used in *in vivo* settings to properly measure force and position information.

6.3.1 Experiments

An experiment was performed to meet these objectives. The hypotheses were as follows:

1. The SIMIS instruments are able to provide information on the tool–tissue interaction forces, as well as the motion of the instrument tips during *in vivo* surgical procedures.
2. Data collected during *in vivo* surgical procedures can be used to obtain information about the typical range of motion and forces applied in the individual directions, in order to inform the selection or development of haptic interfaces for MIS.

6.3.2 Methods

The experiment was performed in an *in vivo* porcine model (only one animal was used). Ethics approval was obtained from the University Council for Animal Care at Western prior to the date of the procedure. To perform this experiment, the SIMIS system was brought to the animal lab at the completion of another test.

The field generator that forms part of the electromagnetic tracking system was mounted on a plexiglass board and clamped to the surgical table near the head of the animal, away from the metal railings. The computer and amplifiers were placed on a cart near the surgical table. In order to prevent liquids from entering the inside of the instruments, plastic drapes were used to cover the rotating wheels and the cable openings.

The SIMIS instruments were calibrated prior to the start of the procedure. An experienced thoracic surgeon and a novice surgeon performed the tests. Using standard laparoscopic instruments, the expert surgeon created an incision in the stomach wall of the animal and inserted an artificial tumour (like the ones used in the previous experiments) and then, using the SIMIS instruments, proceeded to palpate the stomach with the objective of identifying the location of the tumour. It was not possible to identify the location of the tumour, as the tumour was not held in place at a specific location, but was free to move inside the stomach; however, data were collected regarding the force and position of the instruments during a palpation task.

In the second stage of the experiments, both the expert and the novice surgeons passed one suture and tied one intracorporeal knot each (consisting of a double knot followed by two single knots). The position and force applied during these two tasks was recorded as well as the video from the endoscopic camera.

6.3.3 Data Analysis

To analyze the data, a MATLAB script was developed to read and filter the data according to the method outlined in Section 6.2.3.1. The data were then processed to extract the mean, maximum and minimum values of the forces applied in each of the 5 directions, as well as the minimum and maximum values of the motion data in each of the 6 directions. This was performed for all of the tasks and for both the novice and the expert surgeons.

A first look at the data revealed a direct coupling between the axial and the grasping forces.

Therefore, a decoupling procedure was followed to subtract the scaled grasping data from the axial data. As the quantity of data was small, the scaling factor was determined empirically through direct observation of the force graphs.

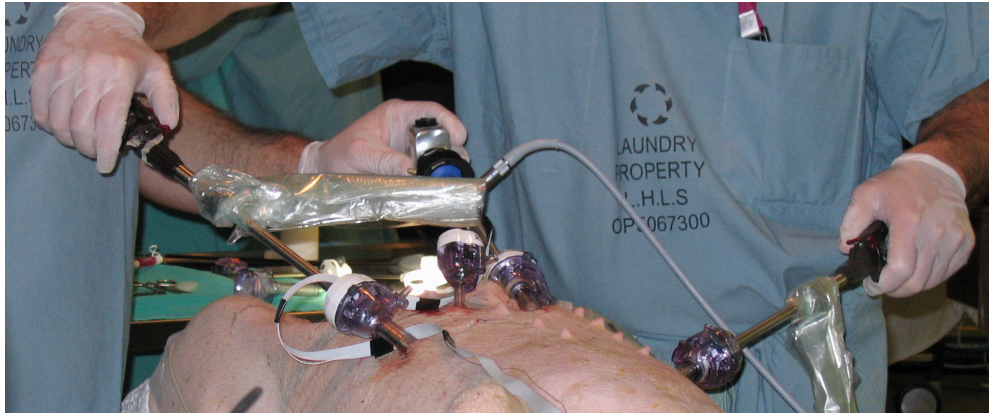
6.3.4 Results

The instruments were successfully used to measure force and position in a porcine *in vivo* model, as shown in Figure 6.9. The instruments were able to measure position and force information and the SIMIS system effectively recorded the data and video of the procedures. The results obtained from the data analysis are shown in Tables 6.2 and 6.3.

The values shown in Table 6.3 correspond to maximum Cartesian forces of 13.3 N for the right hand and 8.2 N for the left hand. Other studies that measure tool–tissue manipulation forces in an *in vivo* setting have not been found in the literature. Many studies have measured applied forces for the purpose of tissue characterization, but these do not represent typical tissue manipulation forces during minimally invasive applications. Others have measured forces outside of the patient’s body; for example, [152] shows that the Cartesian forces during laparoscopic cholecystectomy were around 18 N. The forces presented in [157] include maximum Cartesian forces of 16.1 N during suturing and 4.4 N during knot tying in a flexible plastic gel phantom using the da Vinci system. The forces during cutting of *ex vivo* pig liver were found to be less than 4.5 N in [158]. Our previous studies measuring manipulation forces in a porcine model during a natural orifice appendectomy showed tissue manipulation forces as high as 15.8 N. The values presented herein represent the first complete measurement of typical tool–tissue manipulation forces in all of the degrees of freedom available during MIS.

6.3.5 Discussion and Applications

The SIMIS system was successfully used in an *in vivo* setting. The required computer and other electronics were able to sit close enough to the surgical table without interfering with the space required by the surgeons while still allowing the instruments to properly reach the surgical site. After the procedure was completed, the tips were cleaned following the standard methods of cleaning and disinfection used in the laboratory setting. The rest of the instruments and the cables were wiped clean using disinfecting cloths.

Figure 6.9: Instruments in use during the *in vivo* trials.Table 6.2: Results of the *in vivo* trials showing the range of motion used in each direction.

Direction	Measure	Value (mm)	Direction	Measure	Value (degrees)
x	minimum	-172.3	Azimuth	LH / RH min	-160 / 124
x	maximum	129.2	Azimuth	LH / RH max	-118 / 187
x	range	301.5	Azimuth	max range	63
y	minimum	-129.2	Elevation	minimum	-42
y	maximum	151.2	Elevation	maximum	23
y	range	280.4	Elevation	range	65
z	minimum	-139.2	Roll	minimum	-119
z	maximum	203.2	Roll	maximum	107
z	range	342.4	Roll	range	226

Table 6.3: Results of the *in vivo* trials showing the range of forces applied in each direction.

	Actuation (N)	x (N)	y (N)	z (N)	Torsion (N·mm)
Left hand					
Maximum	51.9	3.2	2.1	1.5	1.3
Minimum	0	-1.7	-3.5	-1.8	-2.0
Range	51.9	4.9	5.6	3.3	3.3
Right hand					
Maximum	68.6	3.3	6.7	4.0	54.6
Minimum	0	-2.9	-1.3	-4.6	-37.6
Range	68.6	6.2	8.0	8.6	92.2

Care must be taken when placing the field generator near the surgical site. It is important for it to be close enough to the instruments so that the sensors are always within the tracking field, but not so close that there is interference from the surgical table. Using a carbon fibre table would solve this problem. Also, if the sensors move below the top of the field generator, it leads to noise in the position tracking data. The generator needs to be placed sufficiently low to ensure that this does not occur.

A limitation of this study is that the axial forces were obviously coupled with the grasping forces. Some decoupling measures were implemented but the results still showed some coupling between the signals. However, the resulting range of forces in the axial direction is similar to that of the other directions. Although full decoupling of the signals is impossible due to the design of the instruments, the use of the third version of the SIMIS instruments shown in Section 4.5 with more accurate axial sensing and reduced noise should be able to partially address these problems in future experiments.

This experiment has provided an example of an application of the SIMIS system. Tests could be performed to inform the development or selection of haptic interfaces for specific tasks or specific environments. The use of the sterilizable SIMIS instruments in human procedures could inform the development of haptic interfaces that are optimized for use in surgery. These experiments have provided a proof of concept for the use of the SIMIS system to collect data during real procedures.

6.4 Applications to Sensory Substitution

A potential benefit of measuring tool–tissue interaction forces during MIS is to address the problems caused by the distorted haptic feel that result from the reduced access conditions. Although master–slave robotic systems allow the use of haptic devices that can provide haptic feedback directly to the hands of the user, in a laparoscopic setting the force information needs to be provided in an indirect manner, as the surgeon is directly manipulating the surgical instruments. The SIMIS customized software is able to apply an image overlay to the endoscopic image in order to provide force information in a visual manner. This opens up an interesting area of research in sensory substitution and human factors with respect to surgeons' ability to use visually displayed data in some form or another to minimize tissue damage or to ensure that suture knots are tight.

The effect of providing visual force feedback in master–slave surgical robotic systems has been

investigated by various groups, see Table 2.1. In [30] and [159], force information is overlaid onto the surgical view in the form of force bars that change in size and colour as the force magnitude increases. In both of these studies, very few significant differences were found in the amount of force applied with visual force feedback compared to when no feedback was provided. To investigate whether overlaying the force information directly on the instrument shafts would cause the surgeons to pay more attention to the applied forces, a specialized overlay program was presented in [19]. The results were not much better when only visual feedback was provided, as opposed to when direct haptic feedback was also available.

In all of these trials, the only information provided was the Cartesian forces acting perpendicular to the instrument shaft, and no more than 10 subjects performed the procedure, limiting the power of the evaluations. To the best of our knowledge, the effect of providing visual force feedback in conventional laparoscopic applications and the effect of providing information in different degrees of freedom have not been explored.

The overall objective of this experimental evaluation was to determine when force feedback is necessary in minimally invasive procedures and what type of force feedback should be provided. Furthermore, it would be of benefit to determine whether everyone benefits in the same manner, or if the level of expertise has an effect on the perceived benefit.

6.4.1 Experiments

A series of experiments were performed to achieve the objectives stated above. Considering the difficulties that other researchers have had in finding significant differences in the applied forces when visual feedback was provided, it was important to properly design the experiments considering all of the possible factors that could influence the outcomes and the levels of these factors. The following factors were originally identified:

1. **Variability between subjects:** The level of expertise among subjects ranges from novice to expert and could be formally divided in up to 6 intermediate levels depending on their year of training. This first set of experiments focused on a comparison between novices (those that have never before received training in MIS) and expert surgeons. Nuisance factors related to the subjects include differences in their personalities, interest in the project, and mood. These factors were not formally addressed in the design and their effect was minimized

through randomization.

2. **Amount of feedback:** Using the SIMIS system, feedback can be provided in up to 5 DOFs. If too much information is provided, however, it might be difficult to interpret its meaning. For simplicity of interpreting the information provided, these 5 DOFs were divided into three sets: force feedback (i.e., the magnitude of the forces in x , y and z), rotational force feedback or torsion, and actuation force feedback (i.e., grip or cut depending on the task).
3. **Type of force feedback:** Force feedback can be provided in several different manners. Since in this MIS setup the subjects are directly manipulating the instruments, the force information can only be provided in a visual or an auditory manner. Most surgeons consider auditory force feedback to be disruptive in a surgical environment and as such it was not implemented in these experiments; however, the optimal presentation of auditory force feedback during MIS could be the subject of future work.
4. **Effect of training:** Training prior to each task is considered important to familiarize the user with the experimental setup, the instruments and the tasks. Training can be provided in different amounts and using different methods. The effect of training should be minimized by ensuring consistency in the training that the subjects receive prior to commencing the task.
5. **Tasks:** A critical step in the design of these experiments was to identify which tasks could benefit the most from having force feedback. There are many simple tasks that can easily be performed in a minimally invasive manner without force feedback. These tasks are not ideal for assessing the importance of force information, as they have already been shown to be possible without force feedback. More critical are tasks that have a high degree of complexity. The selection of the task was critical as discussed in the following section.

6.4.2 Methods

It was desired to develop a complex procedure that required both technical and cognitive skills to complete, and that was composed of those tasks that have been shown to require some form of force information: palpating tissue to localize a lesion or tumour, intracorporeal suturing and knot tying, and cutting near a critical anatomical feature.

To perform this procedure the setup presented in Section 6.2.2 was used with different tissue samples. The location of the tumours was varied randomly and the subjects were blinded to the location of the tumour. This setup allowed participants to perform a complex procedure, composed of 5 tasks, as follows:

Task 1 Palpation: The SIMIS instruments were used to palpate the tissue in order to locate the tumour. This task was usually completed when they could visually identify the object (Figure 6.10(a)).

Task 2 Cutting: The instrument in the dominant hand was replaced by a set of standard laparoscopic scissors, which were used to cut the thin skin covering the tumour (Figure 6.10(b)).

Task 3 Tissue Handling: The SIMIS instruments were again used to remove the tumour (Figure 6.10(c)).

Task 4 Suturing: The instruments were used to drive a needle through the tissue, as shown in Figure 6.10(d).

Task 5 Knot tying: An intracorporeal surgeon's knot was tied, composed of one double knot and two single knots (Figures 6.10(e) and 6.10(f)).

Information about the applied forces was displayed directly on the video screen that was observed by the participants. This information was displayed as bars that increase in size and change colour as the force increases (from green, to yellow, to orange, to red). The point at which the bar changes to red was set to 10 N or 30 N·mm, in order to prevent tissue damage [38].

6.4.2.1 Preliminary Trials

A first set of tests were performed considering the cause and effect diagram outlined in Figure 6.11, with experience level as a between-subjects factor and the types of feedback as within-subjects factors. This first set of tests was performed to determine which factors or high-order interactions were completely irrelevant to the outcome and to establish a measure of error. The measure of error allows the standard deviation in the measurements to be established, allowing the sample size of future experiments to be determined. The preliminary trials also served to iron out any issues with the methods prior to enlisting a large number of subjects.

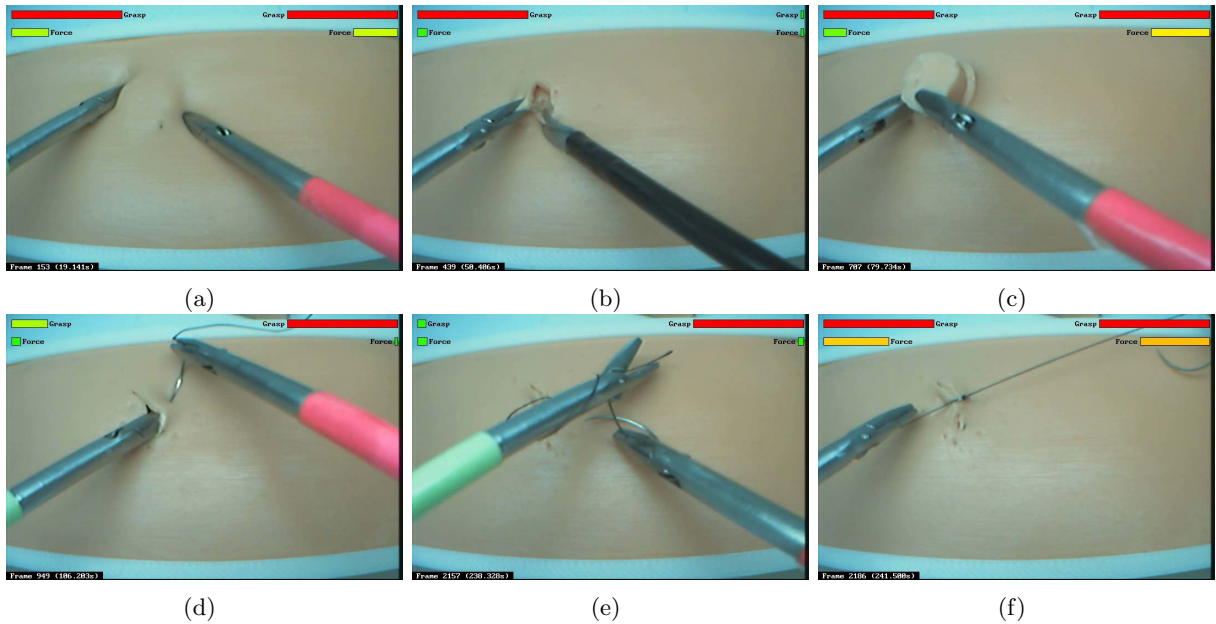


Figure 6.10: Steps in a complex procedure composed of 5 tasks: palpate tissue to identify tumour location (a), cut top surface to expose the tumour (b), remove tumour (c), pass a suture (d) and tie and tighten an intracorporeal surgeon's knot (e,f).

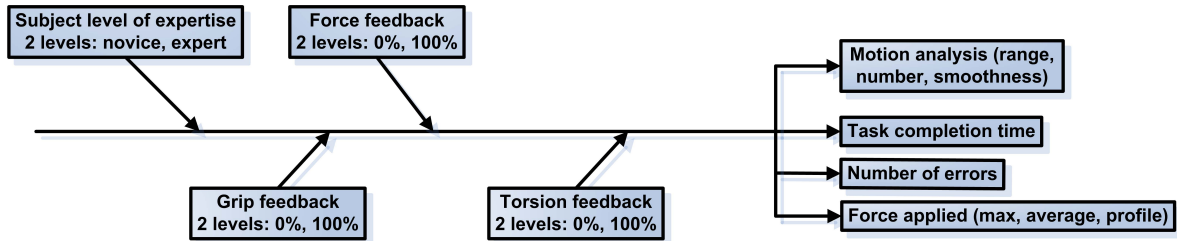


Figure 6.11: Cause and effect diagram for the preliminary trials.

The design of these experiments follows a typical 2^3 design (three factors at two levels each), assessed with 8 tests per replicate, as shown in Table 6.4. A full factorial test was performed (implementing all possible combinations), permitting the assessment of low- and high-level interactions. Performing at least two replicates allows the measurement error to be computed, hence a total of four replicates were performed with two expert surgeons and two novices. Similar to previous experiments, the following variables were recorded during the trials: task time, applied forces (3 DOFs), torque, grasp force, instrument position in 6 DOFs and videos of the trials.

The outcomes from the procedures that were measured and analyzed during the preliminary trials were as follows:

Table 6.4: Plus and minus table for the 2^3 design and the interpretation of each test.

Run	Force	Grip	Torsion	Description
1	-	-	-	No force feedback
2	+	-	-	Only Cartesian force feedback
3	-	+	-	Only grasping feedback
4	+	+	-	Cartesian force and grasping feedback
5	-	-	+	Only torsional feedback
6	+	-	+	Cartesian force and torsional feedback
7	-	+	+	Grasping and torsional feedback
8	+	+	+	All force feedback

Task completion time The time required to perform each of the five tasks was extracted from the videos.

Number of errors The videos were analyzed to determine the total number of errors performed in each trial. Errors noted included: incorrectly identifying the lump location, improperly cutting the incision (too small), dropping the needle, incorrectly placing the sutures, loose knots, breaking the needle off of the suture, and tearing the tissue.

Applied forces The mean forces applied in the Cartesian directions, the grasping forces and the torsion about the instrument axis for each of the five tasks were calculated from the recorded data.

Instrument motion Instrument tip motion was processed to extract the total motion range and volume.

6.4.2.2 Insights from the Preliminary Tests

The results show a series of interesting insights and guidelines for the next round of experiments. First of all, the number of errors seemed to be linked only to experience level, the run number for each subject, and the task that was being performed. Similarly, task completion time and the task volume were mostly affected by the level of expertise of the user. It is understandable that force feedback would not have an effect on the volume, as the motion range can be considered unrelated to the amount of force applied during a task. Task completion time might still be affected if cognitive loading increases or decreases significantly with visual force feedback.

The results also show that the Cartesian forces applied on both instruments were the most sensitive to the type of force feedback provided, regardless of the task. Grasp and torsional forces were only significantly different in the last three tasks, leading to the conclusion that, for the palpation and the cutting tasks, only the Cartesian forces applied may need to be analyzed.

It was also noted that in cases where two or more forms of feedback were provided, performance was better if only one form of feedback was given. In other words, performance was improved if only one form of feedback was provided and decreased if no force feedback or too much information was given. This indicates that there might be a mental overload when more than one force graph is being displayed on the screen and users might have ignored the feedback provided in these situations. It is interesting to note that torsional feedback did not have an effect on the torsional forces applied.

A complex task consisting of all 5 steps was a good way of measuring the effect of force feedback. Tasks 3 and 4 were the most sensitive to the type of feedback provided.

When analyzing the data, it was noticed that it was difficult to find a correlation between the time frame on the video and the force and motion data. The sampling rate of the video turned out to be variable and it was difficult in some cases to match up the data appropriately. It was then decided to modify the software to record the sample time directly on the screen.

Based on these preliminary results, the main trials outlined in the following section were determined. Using DesignExpert (version 8.0.7.1, StatEase, Inc. Minneapolis, MN) and based on the data, it was determined that a total of 30 subjects had to complete the next round of experiments with 15 subjects at each experience level. To minimize the mental overload caused by too much information provided to the users, it was decided to provide only Cartesian force and grasping feedback, as Torsional feedback did not seem to have an effect on the torsional forces during any of the tasks. Furthermore, torsional forces really only come into play during the suturing task, and can be considered bothersome during the other tasks, causing subjects to ignore them completely.

6.4.2.3 Main Trials

Considering the results of the first set of tests, the main trials were then performed. After watching a video describing the procedure that needed to be performed, 30 subjects performed the trials. Subjects with no surgical experience practiced tying an extracorporeal knot using standard instruments prior to starting the experiments. All of the subjects were also allowed to practice

manipulating the instruments until they felt comfortable with their operation. All of the subjects were right-handed, 7 were female and 23 were male. 13 subjects were considered experts, while 17 subjects were considered novices.

The experiment was designed as a repeated measures study with two factors (force feedback and grasping feedback) at two levels each (2^2 design). Each subject then performed the procedure a total of four times, with varying visual feedback: no feedback, force feedback only, grasping feedback only, and force and grasping feedback together. For each subject, the different forms of feedback were provided in random order. They were told to attempt to remain in the green range (below 4 N) when manipulating tissue, but to go to the red (above 10 N) when grasping the needle to minimize slippage.

The following variables were recorded during the trials: task time, applied forces (3 DOFs), torque, grasp force, and instrument position in 6 DOFs. Videos of the trials were also recorded. Modifications to the software allowed the video to display the frame number, which was then paired to the frame numbers in the force and position data, allowing full synchronization of all data sources.

6.4.3 Data Analysis

The videos of all 120 trials were observed and analyzed as follows: 1) the start and end times of each task were identified and recorded; 2) time frames were recorded for any events that were out of the ordinary, for example: if the needle was dropped and no longer visible, the subject took a break, the instruments needed to be fixed, or the skin lifted off of the setup and needed to be replaced; and 3) the time frames corresponding to actions in between the tasks were also identified. This process was followed in order to reduce variability in the data, as the subjects were all unique in their way of removing the instruments from the setup, or dropping the tumour to the side. There was no dead time in between Tasks 4 and 5.

Once these frame times were recorded, a MATLAB script was run to separate the data into the different tasks, compute the total range of forces applied in each direction, and create individual plots for evaluation. The forces in the x and y directions were combined into one force magnitude (again axial forces were not considered due to the issues noted in in Chapter 4). The plots were then reviewed to identify any discrepancies in the data.

If anomalies were identified, the video was analyzed further to identify the cause of the problem.

Any anomalies in the position and force data were removed through linear interpolation. For example, it was noted that if the instruments crashed against each other, which happened often as the instrument was brought back into place after cutting, it produced a blip in the position data that did not correspond to the instrument motion. In these cases, the data were cleaned by linearly interpolating between the values before and after the blip.

Finally, the data were processed to compute the average and the maximum forces for the Cartesian force vector and for the grasping force. Also, the ratio of high forces to the total task completion time was also computed. This measure was developed to reflect how a person might respond to visual force feedback. When the display bars change from green to yellow to orange to red, the subject would tend to reduce the applied forces and therefore minimize the amount of time higher forces are applied. The thresholds for what was considered to be high forces were set to 8 N the Cartesian forces and 10 N for grasping forces.

The Statistical Package for the Social Sciences (SPSS) version 19 was used to perform statistical analysis of the data. An analysis of variance (ANOVA) test was used to determine if any significant differences exist between the data sets with force and grasping feedback as the within-subjects factors and experience level as a between-subjects factor. The results obtained are presented below.

6.4.4 Results and Discussion

The experiments were successfully performed by all 30 subjects. One additional subject did not complete the trials as it triggered a prior upper-body injury. In one of the 30 cases, the calibration file had been accidentally deleted and, although the data were collected, the visual force feedback provided to the user was useless. This was not noted until the trials were completed, therefore the results presented below correspond to 29 of the 30 subjects.

The instruments were able to successfully measure force and position data during the trials with minimal problems. Some of the problems that occurred with the SIMIS instruments included: errors in force data collection caused by pinching of the cables (this resulted in a complete saturation of the signal), the inner shaft disengaging from the handle, and the instrument tips not closing fully. As soon as these issues were identified during the trials, the experiments were stopped and the problems corrected prior to continuing.

The results of the data analysis are presented in Tables 6.5 and 6.6 as discussed in the following

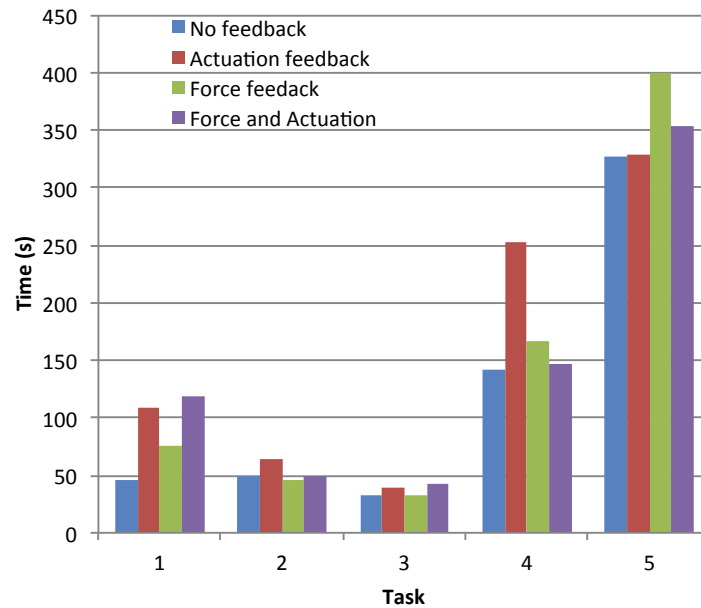


Figure 6.12: Average task completion time for all five tasks according to the feedback provided.

sections. Trends are presented for $p < 0.25$.

6.4.4.1 Time

The effect of feedback on task completion time was only significant during the first of the 5 tasks, see Figure 6.12. It was noted that when actuation feedback was provided, task completion time increased (121.3 s vs. 61.4 s, $p = 0.001$). During the other tasks, visual feedback had no effect on the task completion time.

The fact that task completion time increased during the first task when actuation feedback was provided indicates that the subjects required more time to adjust to the information that was being provided. Grasping was not used during the first task, so it might have been a confusing factor for the subjects as they would see the force bars increase although they might not have been in contact with the tissue. Furthermore, as this was the first task, it is possible that the subjects were adjusting to the information that was provided.

6.4.4.2 Task 1: Palpation

During the palpation task, the availability of force information had no significant effect in any of the measures. Although the grasping force had no effect on the palpation as the tissue itself

Table 6.5: Effect of force feedback on the grasping force for the five tasks.

Variable	Task 1		Task 2		Task 3		Task 4		Task 5	
	Left	Right	Left	Right	Left	Right	Left	Right	Left	Right
Mean (N)	Mean: 4.6 \pm 0.6, no effect from feedback, $p = 0.84$.	Mean: 4.0 \pm 0.6, no effect from feedback, $p = 0.85$.	Mean: 4.0 \pm 0.5, no effect from feedback, $p = 0.52$. Marginal grasp force decrease with force feedback, $p = 0.063$.	Mean: 4.5 \pm 0.9, no effect from feedback, $p = 0.21$. Novices were more gentle with feedback, while experts grasped harder, $p = 0.042$.	Mean: 4.5 \pm 0.5, no effect from feedback, $p = 0.72$.	Mean: 10.2 \pm 0.9, no effect from feedback, $p = 0.21$. Novices were more gentle with feedback, while experts grasped harder, $p = 0.042$.	Mean: 4.3 \pm 0.4, no effect from feedback, $p = 0.40$.	Mean: 19.2 \pm 1.7, no effect from feedback, $p = 0.16$. Tendency to apply less force with feedback (20.1 vs. 18.4).	Mean: 8.8 \pm 1.2, no effect from feedback, $p = 0.79$.	Mean: 11.1 \pm 1.1, no effect from feedback, $p = 0.19$. Tendency to apply less force with feedback (11.8 vs. 10.4).
Maximum (N)	Mean: 14.1 \pm 1.6, no effect from feedback, $p = 0.83$.	Mean: 13.2 \pm 1.8, no effect from feedback, $p = 0.63$.	Mean: 11.9 \pm 1.2, no effect from feedback, $p = 0.21$. Tendency to grasp harder with feedback (10.6 vs. 13.1).	Mean: 40.6 \pm 2.4, no effect from feedback, $p = 0.47$.	Mean: 18.8 \pm 2.2, no effect from feedback, $p = 0.21$. Tendency to grasp harder with feedback (16.4 vs. 21.2).	Mean: 28.3 \pm 2.5, no effect from feedback, $p = 0.64$.	Mean: 49.8 \pm 2.8. Feedback reduced the grasping force, $p = 0.045$ (52.0 vs. 47.6).	Mean: 45.5 \pm 3.2, no effect from feedback, $p = 0.72$.	Mean: 43.2 \pm 2.5. Feedback reduced the grasping force, $p = 0.045$ (44.9 vs. 41.4).	
High Grasping-Force Ratio (HGR) (10 N)	Mean: 0.179 \pm 0.04. No effect from feedback, $p = 0.63$.	Mean: 0.167 \pm 0.03, no effect from feedback, $p = 0.67$.	Mean: 0.161 \pm 0.03, no effect from feedback, $p = 0.57$. The ratio of time that grasping force was high decreased with force feedback, $p = 0.012$ (0.21 vs. 0.11).	Mean: 0.327 \pm 0.02. Feedback reduced the ratio of time forces were higher than 10 N, $p = 0.039$ (0.361 vs. 0.292).	Mean: 0.141 \pm 0.02, no effect from feedback, $p = 0.59$.	Mean: 0.147 \pm 0.02, no effect from feedback, $p = 0.75$.	Mean: 0.575 \pm 0.02, no effect from feedback, $p = 0.94$.	Mean: 0.318 \pm 0.04, no effect from feedback, $p = 0.94$.	Mean: 0.428 \pm 0.03, no effect from feedback, $p = 0.36$.	

Table 6.6: Effect of force feedback on the Cartesian forces for the five tasks.

Variable	Task 1	Task 2	Task 3	Task 4	Task 5	
Mean (N)	<p>Left</p> <p>Mean: 1.90 \pm 0.11, no effect from feedback, $p = 0.50$.</p> <p>Right</p> <p>Mean: 1.91 \pm 0.11, no effect from feedback, $p = 0.49$.</p>	<p>Left</p> <p>Mean: 1.74 \pm 0.13, no effect from feedback, $p = 0.32$.</p> <p>Right</p> <p>Mean: 1.86 \pm 0.09, no effect from feedback, $p = 0.61$.</p>	<p>Left</p> <p>Mean: 2.27 \pm 0.18, no effect from feedback, $p = 0.21$. Tendency to apply more force with feedback (2.09 vs. 2.45).</p> <p>Right</p> <p>Mean: 2.27 \pm 0.18, no effect from feedback, $p = 0.21$. Tendency to apply more force with feedback (2.09 vs. 2.45).</p>	<p>Left</p> <p>Mean: 1.00 \pm 0.07, no effect from feedback, $p = 0.44$.</p> <p>Right</p> <p>Mean: 1.04 \pm 0.08, no effect from feedback, $p = 0.45$.</p>	<p>Left</p> <p>Mean: 1.05 \pm 0.06, no effect from feedback, $p = 0.77$.</p> <p>Right</p> <p>Mean: 1.04 \pm 0.08, no effect from feedback, $p = 0.45$.</p>	<p>Left</p> <p>Mean: 0.73 \pm 0.06, no effect from feedback, $p = 0.34$.</p> <p>Right</p> <p>Mean: 0.73 \pm 0.06, no effect from feedback, $p = 0.34$.</p>
Maximum (N)	<p>Mean: 5.76 \pm 0.26, no effect from feedback, $p = 0.91$.</p>	<p>Mean: 3.68 \pm 0.29, no effect from feedback, $p = 0.38$.</p>	<p>Mean: 4.29 \pm 0.33, no effect from feedback, $p = 0.12$. Tendency to apply more force with feedback (4.01 vs. 4.57).</p>	<p>Mean: 3.08 \pm 0.17, no effect from feedback, $p = 0.37$.</p>	<p>Mean: 4.52 \pm 0.24, no effect from feedback, $p = 0.77$.</p>	<p>Mean: 5.2 \pm 0.23, no effect from feedback, $p = 0.69$.</p>
High Force Ratio (HFR) (8 N)	<p>Mean: 0.029 \pm 0.01, no effect from feedback, $p = 0.29$.</p>	<p>Mean: 0.015 \pm 0.009, no effect from feedback, $p = 0.49$.</p>	<p>Mean: 0.039 \pm 0.015, no effect from feedback, $p = 0.37$. Higher ratio when only one type of feedback was provided, $p = 0.044$.</p>	<p>Mean: 0.002 \pm 0.001, no effect from feedback, $p = 0.20$. Tendency to apply fewer high forces with feedback (.0029 vs. 0.0002).</p>	<p>Mean: 0.001 \pm 0.0003, no effect from feedback, $p = 0.50$.</p>	<p>Mean: 0.002 \pm 0.0005, no effect from feedback, $p = 0.28$. Tendency to apply fewer high forces with feedback (0.006 vs. 0.003). HFR increased with actuation feedback, $p = 0.047$.</p>

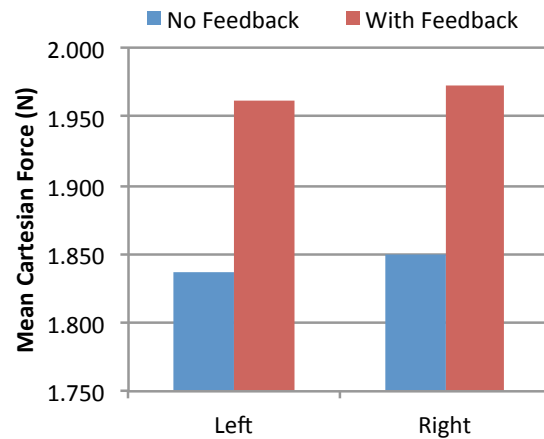


Figure 6.13: Average mean forces with and without force feedback during the palpation task. The difference is not statistically significant, $p = 0.50$.

was not being grasped, both the grasping and the actuation forces were analyzed, as this might provide some insight into how the instruments were held during a palpation task. In many cases, the subjects may have chosen to ignore the grasping force, but having to consciously think about it might have resulted in the increased time presented above.

In all of these trials, the forces applied were quite low, thereby rarely reaching the orange or red ranges (average and maximum Cartesian forces were about 1.9 N and 6.0 N respectively). Looking at the mean forces only, there was a nonsignificant trend to apply greater forces when feedback was provided, see Figure 6.13. All of these forces were still well below the range of forces allowed, so it is speculated that having feedback allowed subjects to know that they were not exceeding high forces and that they would not damage the tissue.

As subjects could not tell how deeply they were palpating, the availability of feedback did not help in tumour localization. To aid in tissue characterization, a map needs to be developed as presented in Section 6.2 to fully take advantage of kinesthetic feedback for lump localization.

6.4.4.3 Task 2: Cutting

During the cutting task, the recorded information was limited to the left hand only, as standard laparoscopic scissors were used on the right hand. Although the SIMIS instruments can be converted to scissors by replacing the handle and the tip, it was decided to use standard instruments to save on instrument conversion time and to prevent damage that could be caused to the cables during the instrument changeovers (240 changeovers would have been required).

During this task, the left instrument was used to grasp the tissue and assist during the cutting process. Force and grasp should both be minimal to prevent tissue damage.

Similar to the previous task, there was an insignificant trend of higher applied forces when feedback was provided. Although Cartesian force feedback did not have an effect on the Cartesian forces applied, it did have an effect on the amount of time that grasping forces exceeded 10 N. The high-force grasping ratio was significantly reduced from 21% to 11% ($p = 0.012$).

Analysis of this task is difficult because not all subjects were grasping the tissue when the high forces occurred. Some subjects used the grasper to push on the tissue only, so interpreting high grasping forces is difficult. A more detailed analysis of the video would be of benefit to recognize the times when tissue was actually being grasped and to determine whether the visual force feedback had an effect during those time frames.

6.4.4.4 Task 3: Tumour Removal

During the tumour removal task, the subjects usually used the left hand to push the skin out of the way, while the right hand grasped the tumour and pulled it out. Some subjects had difficulty grasping the tumour as it would slip out of the instrument jaws. Overall, to succeed in tumour removal, the tumour had to be grasped hard. This is reflected in the increase in grasping forces compared to the first two tasks, with the right hand showing much greater forces than the left hand (mean forces of 10.2 N in right hand vs. 4.5 N in left hand).

The grasping forces tended to be higher with force feedback in the left hand (4.3 vs. 4.6 N, $p = 0.72$), but lower with force feedback on the right hand (11.1 vs. 9.4 N, $p = 0.21$). The only significant difference was in the high grasping force ratio on the right hand, which was reduced from 36% to 29% when feedback was provided, $p = 0.039$. Similar to Tasks 1 and 2, the Cartesian forces applied by both hands were well below the threshold and there was no significant effect caused by the availability of visual force feedback.

6.4.4.5 Task 4: Suturing

During the suturing task, both instruments were involved in properly orienting the needle prior to penetration. Once the needle was in place, the right instrument was predominately used to pass the needle through, with the left instrument assisting again at the end to remove the needle from the other side of the tissue. High grasping forces were required on the right-hand instrument to

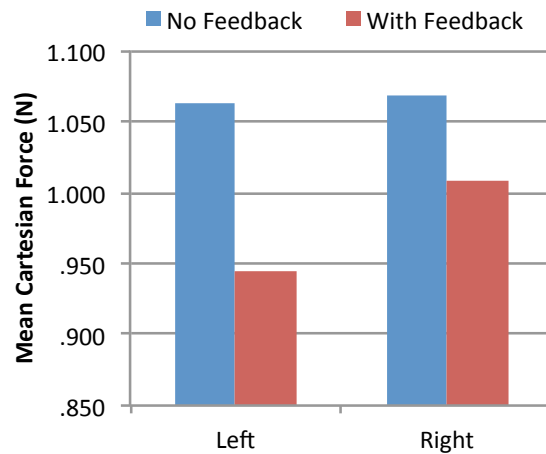


Figure 6.14: Average mean forces with and without force feedback during the suturing task. The difference is not statistically significant, $p = 0.45$.

grab the needle properly when penetrating the tissue. This is reflected again in the much higher grasping forces applied by the right instrument.

The effect of visual force feedback was significant during the suturing task. Subjects tended to apply less grasping force with the right hand when grasping feedback was provided, showing a significant difference in the maximum grasping force applied ($p = 0.045$). This is an interesting observation, as the range of the forces was significantly higher than the point at which the grasping feedback bar turned red. Although the subjects observed no difference when forces were higher than 10 N, there is a significant difference in the data when grasping feedback was provided. One possibility is that when the subjects observed the red bar, it caused them to be more careful overall and apply less force.

Looking at the mean forces only, there was a nonsignificant trend to apply reduced forces when feedback was provided, see Figure 6.14. The ratio of forces higher than 8 N also tended to be less in both instruments when feedback was provided (0.3% vs. 0.02% in the left hand, $p = 0.2$ and 0.6% vs. 0.3% in the right hand, $p = 0.15$).

6.4.4.6 Task 5: Knot tying

The knot-tying task was by far the most difficult to complete for the novice subjects. There was a significant increase in task completion time compared to other tasks. There was also a noticeable level of frustration in the novice subjects that would cause them to pay even less attention to the

visual force information provided.

During this last task, the grasping forces need to be high to ensure that the needle does not slip during tying. Grasping of the needle needs to alternate between the two instruments when tying the different knots. This is reflected in similar maximum forces measured with the two instruments (45.5 vs. 43.2 N). As with Task 4, the availability of grasping feedback reduced the maximum grasping forces on the right hand instrument (from 44.9 to 41.4 N, $p = 0.045$).

The Cartesian forces did not show any significant differences when visual feedback was available. The forces applied were quite low in all cases. The analysis of this task was also complicated by the different motions involved in knot tying. The subjects needed to be gentle to ensure that there was no unnecessary pushing of the tissue, but had to make sure that the three knots were tight. A more thorough analysis of this task, separating the time frames when tightening the knots, would be beneficial. It was expected that the maximum forces would reflect these tightening values, but still no significant effects were observed.

It should be noted that, compared to the other tasks, the mean Cartesian forces and the high-force ratios are much smaller. This was caused by the drastic increase in task completion time and the fact that, while the subject is orienting the needle and the suture, there are few times when the instruments are not in contact with anything except for grasping the suture.

6.4.5 Final Remarks

Section 6.4 presented an evaluation of the usefulness of visual force feedback during conventional laparoscopic surgery. Similar to the results obtained by other researchers evaluating the usefulness of visual feedback during robotics-assisted surgical procedures, there were only a few instances in which visual feedback produced a change in the forces applied by the subjects, regardless of their experience level. It was noted that when the typical forces applied were well below the range of allowable forces, subjects tended to increase the amount of force applied, but as the required force increased, visual force feedback tended to reduce the applied forces, especially for the dominant hand.

It is very possible that subjects did not care to use the visual force information. The fact that there was no change in task time would indicate that the subjects were not interested in using the force feedback consciously (there was no cognitive overload). In fact, some experienced subjects commented on how they did not need the force information and that they were not going to use it.

Other novice subjects were too focused on completing the task to even be able to consider using the visual force information.

It is recommended that when visual force feedback is presented, it should be very specific to the task being completed and very clear guidelines be given to the user. Training in the use of force feedback might also be required. Current training methods do not focus on consciously teaching the proper application of forces. The availability of systems that allow the users to know the amount of force that is being applied opens up new areas of research in training that could lead to better outcomes in the future.

6.5 Conclusions

This chapter showed that there are several applications in which the SIMIS instruments can enhance real surgery settings. The combination of force and position information can be used in the development of realistic tissue models or haptic interfaces specifically designed for MIS. This information is also valuable in order to create tactile maps to assist in the identification of areas of different stiffness. The real-time measurement of forces allows visual force feedback to be presented to the surgeon. For this information to be effective, it needs to be specific to the task being done and surgeons must be trained in the use of force information.

From the experiments performed, interesting conclusions can be drawn regarding the effect that experience level has on performance and the applied forces. The following chapter investigates the usefulness of the SIMIS system in training and skills assessment.

Chapter 7

Applications to Surgical Training

7.1 Introduction

This chapter presents the use of the SIMIS system for skills assessment during training. After a thorough review of the current state of the art in training and skills assessment in MIS, the experiments performed are described, followed by the development of new performance metrics based on force as well as the analysis of the experimental results.

7.1.1 Motivation

Recent analyses of medical errors have indicated that 44,000 to 98,000 people die every year in the USA due to medical errors [160], and that 32,000 deaths were considered to be surgery related in the year 2000 [161]. It has also been found that up to 24,000 deaths occur in Canada every year due to preventable medical errors (34% of those are related to surgical procedures) [162]. Other research shows that most surgical mistakes happen in the operating room and are due to technical issues, the majority of them occurring during routine operations performed by experienced surgeons [163].

Preventable surgical errors may be the product of ineffective or inconsistent training methods and curriculum. When it comes to surgical procedures, trainees must acquire cognitive skills, communication abilities, judgement, and motor skills, including dexterity and technical competence. The standard method of training is for a trainee to follow the instructions of the surgeon directly in the operating room (OR). However, research has shown that the OR is not an adequate place to learn motor skills for several reasons [164–168]: there are ethical concerns (when is it ok to let the

trainee do the work?); there are legal concerns (if there is a mistake, who is to blame?); the presence of new technologies means that there is more to learn and that experts are learning as well; new legislations have come into play (which has significantly reduced the number of hours that residents can work); there are time constraints (the need for increased efficiency and reduced costs means less OR time); and public awareness has become more demanding (which places pressure on surgeons to reduce patient morbidity and complications, and increase patient safety).

With the introduction of laparoscopic surgery, the rise in the number of surgery-related injuries created an awareness for the need to properly measure technical competence [169] and to develop better training methods. Achieving technical competence in MIS procedures is not easy. The learning process is affected by perceptual and motor limitations [149] that create a steep learning curve, for example [167, 170, 171]:

- 2D vision creates a lack of depth perception.
- The reduced field of view leads to spatial disorientation and unintended contact with healthy tissues.
- Degraded motion perception creates disorientation (motion illusions caused by viewing the site through a reduced aperture).
- Passive viewing causes dissociation between action and perception (this occurs when the assistant controls the camera, as the surgeon's movements do not correspond with the received visual information).
- The fulcrum effect produces motion reversal and scaling of forces.
- The lack of haptic feedback limits sensory perception.
- Manipulation using long tools reduces comfort and dexterity.

It has been recognized that it is not sufficient to learn techniques for open surgery, but that specific training for MIS is required [172]. To complicate things further, the number of people 65 years and older continues to grow dramatically in North America, leading to more patients who require less invasive procedures [172] and more complex illnesses that need to be treated [168].

This has led to the introduction of new requirements for training, where all residents need to achieve certain competency levels prior to operating on humans [167]. Thanks to new technologies

that allow us to record activities in the OR, it is now possible to develop metrics and quantitative descriptors that characterize technical performance [173]. However, identifying how best to quantify technical performance is the subject of extensive research and no ideal solution has been found. In order to understand how these metrics have been developed, it is important to consider the learning process, as described below.

7.1.2 Knowledge Acquisition

A large number of researchers have worked for many years to understand better how learning occurs in order to develop better training methods. Training methods must be effective (i.e., meet all of the objectives) and efficient (i.e., reduce the learning curve and the cost) [174].

To understand how motor skills are acquired, Fitts and Posner proposed three stages of motor skill development [168, 175, 176]: the cognitive phase, which is what students do in class: read, watch and listen; the integrative phase, when students start to apply the knowledge with some guidance but with lack of fluidity; and finally the automatous phase, which is when fully independent learning occurs with no supervision or guidance.

As learning occurs by doing, not just through observation [177], the most important variable for skill acquisition is how long the trainee practices for [178]. However, all trainees learn at a different rate, and identifying the level of acquired technical competence in a trainee is important.

Another thing to consider is which environment is the best for knowledge acquisition. There is currently no ideal option [175]:

- From the point of view of skill acquisition, practicing on a real patient in the OR is ideal, although it comes with significant ethical and legal concerns, as discussed above. Assessments in the OR have to consider that patients and situations are all unique.
- Learning on cadavers eliminates the risk to patients, but there is limited availability and the conditions are not the same as in a live patient.
- Animal models are more available than cadavers but their anatomy is different from humans; there is also some risk of transferring diseases to those working with the animals.
- Synthetic models allow good skill comparisons, but it is hard to know how effective the training itself is (i.e., do the acquired skills transfer to real surgery).

- Virtual reality (VR) simulators allow very accurate assessments based on performance patterns. They are more costly and are unable to give proper haptic feedback, which means they lack fidelity. Transferability of the skills acquired in a VR simulator to real surgery is not easy to measure, as the metrics used in the simulators are not always clinically relevant.

7.1.3 Aspects that Affect Performance

Many things can have an impact on training and can make the development and evaluation of new training methods more difficult. For example:

1. Variability between subjects: performance is significantly affected by the subject's attitude towards a task, their self motivation [179] and innate abilities [179,180].
2. Training schedule: the practice schedule for trainees can be fixed, random, or adaptive. Adaptive scheduling has been shown to improve performance more quickly by allowing trainees to progress at their own pace [179]. Adaptive scheduling can consist of adjusting the number of trials, adjusting the difficulty or adjusting both, based on learner performance [178,181].
3. Feedback [161,179,182,183]: Providing feedback to the user when learning a new task has been shown to significantly reduce the learning curve [184]. The frequency, the type of feedback, and how it is delivered need to be considered [179,183]. Some argue that feedback should be focused on performance throughout the task [184], while others think that it should focus on the outcome [183]. Another thing to consider is whether the feedback focuses on what the trainees are doing right or on correcting their mistakes.
4. Mental overload [185,186]: Higher mental workload in the operating room can be one of the reasons why performance in a simulator is better than in the OR [160]. As trainees practice, they develop automaticity, which decreases mental workload and frees up mental capacity for other tasks to be performed effectively [186]. Training should reflect the conditions in the OR to ensure that trainees do not experience overload when transferring to the OR setting.
5. Mental training: Thinking about the steps of a procedure prior to performing it has been shown to improve results when paired with physical practice [164,183,187]. The amount of mental training a subject has done will affect their performance during physical practice.

Nevertheless, efforts to improve training and skills assessment methods have been significant. The following sections describe research efforts that have been proposed to assess motor skill development in surgical applications.

7.1.4 Validated Assessment Methods

In order to assess how a trainee acquires a particular skill, it is important to have a way of testing if learning has occurred and to what degree. Unfortunately, motor skills are not easy to measure [161,175] and there is considerable controversy regarding the best method for assessing motor skills.

For many years, the Record of In-training Assessment (RITA's or ITER's) has been used to assess progress by means of interviews [175]. The standard method of assessing motor skills is through the use of checklists or standard rating scales. Global Rating Scales (GRS) in general have been proposed for use in many areas, for example gynecology [188] and emergency medicine [189]. A more standardized method of laboratory training is called the Objective Structured Assessment of Technical Skill (OSATS), which combines checklists and GRS in order to provide a structured evaluation that attempts to be objective, readily accessible and allows the measurement of a proper learning curve [166,175,188].

The limitations of these performance measures include: being subjective (can result in biased and inconsistent assessments and produce high inter-rater variability) [161,180,190], not providing feedback when learning complex skills [184], not being trainee and procedure specific [189], and requiring extra cost and time due to the need for an evaluator [161].

The following sections present other methods of assessment that have been developed specifically for MIS, and have attempted to address these limitations. In general, in order to assess the effectiveness of proposed training methods, they must meet a series of evaluations, which are aimed at assessing reliability and validity as follows [191]: face validity (subjective—experts assess the contents to determine if it is appropriate), content validity (subjective—experts assess how effective the contents are according to what is being assessed), construct validity (objective—evaluates if it a hypothesis is true), concurrent validity (comparison of two methods, one of which is validated) and predictive validity (can predict who will be able to perform a task better). The proposed MIS skills assessment methods and their level of validity are presented below.

7.1.4.1 GOALS

The Global Operative Assessment of Laparoscopic Skills (GOALS) has been accepted and validated as a training method. It was developed as a way of standardizing the assessment of minimally invasive procedures [165,192]. The assessment is done by a trained expert who watches a video of the trainee performing the task and provides a score on 5 elements: depth perception, bimanual dexterity, efficiency, tissue handling, and autonomy. Although the results are no longer biased, as it is possible to perform a blind assessment, the evaluation is still subjective and requires a significant amount of time on the evaluator's part.

7.1.4.2 FLS / MISTELS

Another validated training method is the McGill Inanimate System for Training and Evaluation in Laparoscopic Surgery (MISTELS) [193], which has been incorporated into the Fundamentals of Laparoscopic Surgery (FLS) curriculum as the manual skills component [194]. It requires trainees to achieve proficiency for 5 basic tasks performed inside a physical simulator environment with inanimate objects. A performance measure is calculated based mostly on the task completion time, together with an evaluation of the final outcome of the task.

Construct validity was shown in [194] using four levels of experience (2nd year, 5th year, laparoscopic fellows, laparoscopic surgeons), while inter-rater reliability was shown in [195]. Concurrent validity with the GOALS system was shown as a randomized control trial in [196]. Some limitations of this type of training are: the evaluation of final outcome is still a subjective measure that requires an expert evaluator; the tasks are very simple and can only assess basic motor skills; and no feedback is provided to the trainee, which can result in the development of poor habits. Furthermore, it has been criticized because beginner trainees that have not reached the automatous phase should not be judged based on task completion time [165].

7.1.4.3 ICSAD

To address some of the limitations of the FLS curriculum, research has focused on the development of metrics that assess performance over the entire task in an automated manner. The Imperial College Surgical Assessment Device (ICSAD) was developed for this purpose. It uses position sensors attached to the hands of the trainee and computes performance based on task completion

time, number of movements and total path length [197]. Construct validity for MIS was shown in [198] using vascular anastomosis as a complex task. This study compares the ICSAD measures to subjective measures: size, angle, spacing between sutures, suture depth, damage to tissue, and leaks. The results showed that improvements in the measures were observable as the trainees gained experience and differences were found between novices and experts.

The ICSAD system was used in [199] to investigate whether there is a correlation between visual-spatial abilities, manual dexterity and surgical ability. Surgical performance was assessed with the ICSAD system and the OSATS method. Visual and manual dexterity were assessed using other validated methods (Mental Rotations Test, Surface Development Test, Gestalt Completion Test, Phase Discrimination Test, and Crawford Small Parts Dexterity Test). Some correlation was found with spatial ability and surgical ability in novices, while some correlations were found between manual dexterity and efficiency of hand motion.

The limitations of the ICSAD system are that it can only evaluate the performance that can be related to motion and time and that large external markers need to be worn by the trainee [200]. However, a significant advantage of ICSAD is that it can be used in any training environment, including in simulators, as presented in the following sections.

7.2 Simulator-based Training

A simulator entails some sort of model that allows a trainee to practice specific tasks related to the surgical procedures that are being learned. Simulator-based training has been proposed as a means of developing surgical skills in MIS, as the type of skills that need to be learned for MIS are easily trained with simulators [167]. The fidelity of the simulator model may vary significantly, as well as the tasks that are performed. Regardless of the complexity of the system, for a simulator to be effective, it needs to be part of a curriculum and follow a competency-based program, as opposed to just providing performance metrics [167]. Research that aims to evaluate the importance of high- versus low-fidelity simulators will be needed to fully exploit the potential of simulators as an educational tool [201].

There are three different types of simulators [176]: training boxes or physical simulators, virtual reality simulators and augmented reality or hybrid simulators. The following sections present the different types of simulators in more detail.

7.2.1 Physical Simulators

Physical simulators are described as real objects that mimic to some extent the conditions present in surgery. For MIS, physical simulators often involve a training box that mimics the patient's body, while the instruments enter through small openings. The MISTELS program described above is performed inside a physical simulator [193]. Other examples include the Simulab™ LapTrainer [170, 202], the LaproTrain™ [203], and the i-Sim [204].

These simulators have the advantage of being low cost, portable, adaptable, and simple [170]. Their low cost means that they are more available to schools [165]. However, the most important advantage over virtual reality simulators is that, because real instruments are used in contact with real objects, realistic haptic feedback is provided to the trainee [205]. The main limitation of physical simulators is that they do not provide a measure of performance other than task completion time. Performance evaluation has to be done using GOALS, ICSAD or the FLS evaluation for the MISTELS tasks. Some researchers indicate that only those simulators that provide an objective measure of performance (other than time) can improve training and provide an adequate measure of skill [176].

7.2.2 Virtual Reality Simulators

VR simulators are those in which a computer program is used to create a model of the surgical environment and the instruments. These types of simulators address the problem of lack of feedback by computing performance metrics based on the movement of the instruments and/or of the trainee's hands and their interactions with the virtual environment [191]. The interface usually allows a specific training schedule to be followed by the trainee and their progress over time can be measured and tracked. However, these simulators are usually costly and they lack realistic haptic feedback.

Although some studies indicate that a large number of injuries result from poor haptic feedback [185], there is no consensus regarding the importance of haptics when performing surgery. Nevertheless, research has shown that haptics in VR training is important [176], especially during early basic skills training [5]. During MIS a distorted sense of haptic sensation is still present, as opposed to the complete loss of haptic feedback that results from robotic surgery; therefore VR trainers without haptics should only be used to learn hand-eye coordination [5].

Significant research has been directed towards the development of VR simulators with haptic feedback. For example, a system developed at the University of Washington to simulate a suturing task uses the SensAble PHANToM[®] haptic interfaces with needle drivers attached to the end-effector [190]. However, VR simulators with some form of haptic feedback are not very realistic [167] and they are very costly [172].

7.2.3 Hybrid Simulators

In some applications, both physical and VR simulators have been shown to be equally effective for the development of basic MIS skills. VR trainers have the advantage of providing objective performance measures, while physical simulators provide accurate haptic feedback; however, neither of them is ideal. Augmented Reality (AR) or hybrid simulators can provide the best of both worlds [167]. They combine real environments with realistic haptic feedback and software programs that are able to enhance the surgical view, track instrument motion, provide performance metrics and track trainee progress. An example of an AR simulator is the ProMIS[™] system, a hybrid simulator in which real instruments can be used, while the system tracks instrument tip motion to provide a measure of performance [206].

7.2.4 Robotic Surgery Simulators

As the skills required for laparoscopic surgery and robotic surgery are different, it is necessary to train and assess the skills in simulators that are appropriately designed for the type of procedure [161]. The dV-Trainer[™] by Mimic Technologies [207] is a VR simulator that was designed for training in the use of the da Vinci surgical system. Ongoing work at CSTAR is currently focused on assessing the transferability of the skills learned on the Mimic system to the da Vinci using a Mastery Learning approach to training. Similarly, [177] presents the use of SimSurgery[®], a 2D virtual reality simulator for the da Vinci with no haptic feedback.

AR simulators that allow the use of any real instrument can also serve as trainers for robotic surgical systems. For example, the da Vinci system was used with the ProMIS system mentioned above in [208]. The results showed construct validity for the use of the ProMIS measures as a means of measuring robotic performance.

7.2.5 Other Aspects of Simulator Training

To determine which type of simulator is more appropriate for a particular task, several different measures are used to assess simulator effectiveness [189]: validity (do the results of the assessment properly measure what is being trained?), reliability (is equal performance measured equally every time?), and sensitivity (is it capable of detecting small changes in the skill level of what is being trained?). Deciding which type of simulator to use or to implement into a curriculum is not a straight-forward decision. There are many simulators that have been developed and evaluated, and they all have their advantages and disadvantages. An excellent summary of simulators and their level of validity is presented in [167].

Some of the recognized disadvantages of simulators include: being too expensive [164, 172], allowing unsupervised training that can lead to the development of bad habits [166], having unknown or mixed results about the transferability to the clinical environment [189], and not showing a reduction in the learning curve [172].

For simulators to be effective, proper motivation needs to be given to the trainees so that they fulfill the training hours required for proficiency [167]. They must also provide feedback while learning, allow trainees to repeat each skill several times, adapt progressively to more difficult tasks, provide individualized learning in a controlled environment, and provide well-defined outcomes [189]. A significant amount of work has focused on measures of performance outcome, as described in the following section.

7.3 Performance Measures

Properly designed performance measures are required in order to determine the level of experience that surgeons and trainees have when performing specific tasks. For performance measures to be effective they need to be standardized and their use fully defined. A standard measure is defined as “a quantifiable level of performance that serves as a boundary between those who perform well enough and those who do not” [189]. However, there is no consensus on how these standards should be developed.

A step in this direction is the work presented in [209], which outlines that performance measures must show “low intra-subject variability, moderately low intra-group variation [grouped by skill level] and significant inter-group variation.” Some researchers have focused too much on developing

objective measures that improve with practice, e.g., [210], and this leads to questions regarding the measures used in simulators as a way of measuring performance [179]. Little work has been done to correlate these types of measures with the actual outcome of the procedure [179,211], and new measures need to be found [149].

Surgical performance requires a “mix of cognitive and technical components” that varies between people [184]. A proper performance measure needs to consider both components, be related to the outcome and describe how the movement is generated [184]. The ideal performance measure is one that can be automatically computed in an objective manner. It should be a single measure that describes the global characteristics and the fine details of a movement [212]. Safe, complete and error-free procedures are more desirable outcomes than efficient ones [179]. However, for new metrics to be adopted, they need to be proven to be better than existing evaluation standards [172].

An interesting way of developing an effective performance measure is presented in [173], where they looked at what is considered important, identified a metric that could characterize it, and then figured out a way to combine the measures into one. Others have also recognized that each parameter alone is not sufficient and that a combination needs to be found [149].

The following sections provide an overview of the performance measures that have been developed in the literature. They are divided into 5 categories: temporal, outcome, motion-based, force-based and nonlinear measures.

7.3.1 Temporal

Task completion time is a common way of assessing trainee performance. Most simulators and evaluation metrics currently in use employ time in one way or another to measure skill. Task completion time has been used for skills assessment in [121, 149, 184, 185, 197, 205, 208, 211, 213, 214] and may provide an indication of trainee skill level when combined with other performance measures. Another way of using time as a measure of performance is to look at the time between subtasks [190] as a measure of hesitation.

7.3.2 Outcome Measures

Outcome or qualitative measures refer to those that assess the final outcome of each task or of the procedure as a whole. These measures don't look at how the procedure was performed but instead are only concerned with the end result. Some examples of this type of measure are the number

of errors [179,185], the number of attempts required to achieve the desired outcome [213], or the quality of the outcome [190].

Other more specific criteria can be defined for specific tasks. For example, [198] outlines the evaluation criteria for a vascular anastomosis, defining a 6-point score composed of a series of questions about size, angle, space between sutures, depth, damage and leak defects. Similarly, [180] has looked at anastomoses leakage and cross sectional area of anastomoses. For suturing in general, other measures consider fluidity of motion, accuracy, placement and tightness of the knot [208].

An analysis and categorization of the typical errors made by trainees during laparoscopic surgery is presented in [181] in an effort to identify common errors and their causes. Outcome errors were identified as being either procedural (e.g., skipped or missed step) or executional (force application or actual performance). It was found that the dominant errors were skipped steps, incorrect sequence and use of excessive force.

Although implementing outcome measures requires less time commitment on the part of the evaluator compared to the measures described in Section 7.1.4, it is still time consuming and subjective. Furthermore, the type of assessment has to be very specific to the task being performed.

7.3.3 Motion-based Measures

Motion-based measures are the most commonly used metrics for objectively measuring performance. It is possible to identify objective parameters that truly characterize the surgeon's movement through the biomechanical analysis of hand or instrument motion [149].

Some of the commonly used motion-based measures include the number of movements [180, 197, 211] and the distance travelled (path length) [149, 150, 179, 205, 208, 211], which is also used for robotic procedures [214]. One way of computing the path length is [173, 205]:

$$P = \int_0^D \sqrt{\left(\frac{dx}{dt}\right)^2 + \left(\frac{dy}{dt}\right)^2 + \left(\frac{dz}{dt}\right)^2} dt, \quad (7.1)$$

where D is the task duration and the variables in the brackets correspond to the first derivative of the motion in the three Cartesian directions x , y and z .

Other less common metrics measure the straightness of the path (i.e., the ratio of the straight line connecting the start and finish points, to the actual path followed) [149], the path deviation (i.e., the maximum perpendicular distance from the actual path to the straight line connecting the

end points) [149], the maximum roll angle [184], and the response orientation, defined as [173,205]:

$$P = \sqrt{\int_0^D \left(\frac{d\theta}{dt} \right)^2 dt}, \quad (7.2)$$

where θ is the rotation angle about the instrument axis. Other measures are proposed in [182,214] to assess performance using a robotic system, and include curvature (which measures straightness of the path), and relative phase (which measures instrument coordination, computed as the difference in the phase angle between the two instruments).

7.3.3.1 Speed

Speed is an important consideration when measuring performance and many measures are based on this metric, which is computed as the first derivative of the motion profile. Some of the measures proposed in the literature include: a normalized speed measure—computed as the mean of the speed divided by the peak speed (this is lower as the intervals between submovements increase) [215], the mean speed [149], the peak speed [149,184], the magnitude of the velocity vector [150,214], 3D instrument tip velocity [209], the number of changes in velocity over time [208], and the number of peaks in speed [215].

Roher, et al. [215] also use the Movement Arrest Period Ratio (MAPR, proposed in [216]) as a measure of how often the speed is zero (measures hesitation) and is defined as the proportion of time that the movement speed exceeds a given percentage of the peak speed (10% was selected).

7.3.3.2 Acceleration

Another measure commonly used is acceleration, computed as the second derivative of the motion profile. Measures based on acceleration include the number of accelerations and decelerations [179], the mean acceleration [149], and the maximum acceleration [149]. Another measure is the integral of the magnitude of the acceleration vector (I_{AV}), which measures the energy expenditure and is defined as [149]:

$$I_{AV} = \int_0^D \sqrt{\left(\frac{d^2x}{dt^2} \right)^2 + \left(\frac{d^2y}{dt^2} \right)^2 + \left(\frac{d^2z}{dt^2} \right)^2} dt. \quad (7.3)$$

7.3.3.3 Jerk

The use of the third derivative of the motion profile, known as jerk, has been used by several researchers as a measure of motor skill, usually applied to assessing the progress of certain diseases like Huntington's disease, Parkinson's disease [151], injuries to the jaw [150] or the effects of having a stroke [215]. The smooth motion characteristic of voluntary movements has minimum jerk [212,215]. Measures based on the minimum jerk can predict the smoothness because it provides a measure of the intention that a person has when moving [212]. A curved path has more jerk than a straight path, even when there is constant velocity, and it increases with high accelerations; therefore, the jerk measure provides a measure of suboptimal coordination [151].

The advantages of using jerk include “analytical tractability, computational manageability, and theoretical simplicity” [215]. Jerk has been shown to discriminate between healthy patients and those with motor dysfunctions and can be used to identify progress when learning [150]. It was proposed as a means of assessing skill development in MIS in [205] and in [152], although in the latter study, no differences were found between novices and experts due to lack of power.

A limitation of the minimum jerk measure is that it is inversely dependent on the second power of task completion time, hence it is not completely independent of task duration. Several different ways of normalizing jerk have been proposed in [217]. As the integral of the jerk squared has units of length²/time⁵, to normalize they suggest multiplying by the duration (D) to the power of five and dividing by the power of the amplitude A_m , as follows:

$$C = \frac{D^5}{A_m^2} \int_{t_1}^{t_2} \ddot{x}(t)^2 dt. \quad (7.4)$$

The results of their evaluation show that the dimensionless measure remains constant as the amplitude of the motion and the duration vary. It is sensitive to increases in the number of peaks, amplitude of the peaks, and periods of arrest, indicating that it provides a real measure of smoothness. Based on this, a three-dimensional jerk measure is presented in [149]:

$$Jerk_{\text{norm}} = \sqrt{\frac{D^5}{2A_m^2} \int_0^D \left(\left(\frac{d^3x}{dt^3} \right)^2 + \left(\frac{d^3y}{dt^3} \right)^2 + \left(\frac{d^3z}{dt^3} \right)^2 \right) dt} \quad (7.5)$$

There still needs to be care when using the jerk measure to assess performance. It is important to note that smoothness will be measured as high if there are large pauses between movements,

which is counterintuitive as a performance measure [215]. Therefore if a novice predominantly uses the dominant hand, the motion profile will show higher jerk than the other hand.

7.3.3.4 Nonlinear Measures

Nonlinear measures have also been proposed as a metric for motor skill. The work presented in [218] shows that human movement is best characterized as a dynamic nonlinear system. The use of linear analysis attributes all of the variation to noise, and in the case of human movement, there are definite patterns that are exhibited that are not noise. Using nonlinear theory, it is possible to gain better insight into the characteristics of human movement. Furthermore, looking at the structure of the variability instead of its amount is a better measure of behaviour, as there seems to be a decrease in variability as people develop a skill, which then increases again when they become experts and they find alternate ways of effectively performing a skill [219].

Nonlinear theory has been applied to the assessment of experience level for intracorporeal suturing, through the evaluation of the Hurst Exponent and phase plane plots [220, 221]. The results show that the swing range and bandwidth of the plots, as well as the chaotic exponent of the motions, decrease as trainees gain experience. Also, the largest Lyapunov Exponent (LyE) was used as a measure of consistency of performance in [222]. The largest LyE is a measure of stability that indicates how quickly successive trajectories diverge in space [218]. Finally, approximate entropy can also be used as a measure of regularity. It usually provides the same result as the LyE, but with higher statistical accuracy [218].

Another nonlinear-type analysis includes Hidden Markov Models (HMMs), which are language models commonly used to analyze speech patterns. They have been used to analyze surgical gestures (for example during knot tying) in order to provide a measure of skill that reflects the performance throughout the task [122, 161]. HMMs provide a means of assessing the statistical similarity of a data set measured for a subject with apparently unknown skill level to expert and novice surgeons [122]. However, HMMs require each step of the procedure to be categorized during analysis. A common approach relies upon manual decomposition of the video, which is just as time consuming as OSATS-type measures. Some automation has been attempted for decomposing surgical gestures automatically from the video but it is very computer intensive.

HMMs have also been used to quantify applied forces and torques during MIS for characterization of surgical skills for training advanced laparoscopic procedures [120]. Markov models were

shown to provide a good objective metric of performance (87.5% accurate). However, a significant limitation of the HMM's is that in order to extend it to new procedures, an expert surgeon must "provide the specifications for building the topology of the HMMs," which cannot be easily done by most surgeons [200].

7.3.4 Force-based Measures

Similar to position data, force data can be analyzed in many ways to extract valuable information. Newly developed instruments and devices that allow force information to be measured during training have initiated the development of performance measures that try to reflect the trainee's ability to be gentle or to apply sufficient force when required. Very little work has been done in the use of force information for skills assessment and training in MIS, limited by the ability to measure force in real surgery.

Applied forces may be an important measure to consider when characterizing trainee skill level, but it is not straightforward to determine what distinguishes an expert from a novice, as ideal applied forces are task-dependent [190]. Some efforts to develop force-based metrics can be found in the literature. The da Vinci application programming interface (API) was used in [214] to provide information on the relative grasping force. This is not a true measure of force, as the information is presented as a percentage of the current drawn by the motors. An experimental setup was used in [223] to evaluate the usefulness of using force information to quantify performance in stroke patients. Some VR simulators have been developed with objective assessment metrics, some of which are based on the maximum forces applied [190] or grasping with excessive pressure [191]. Finally, a study was presented in [152], where a laparoscopic grasper was instrumented with a force/torque sensor and strain gauges on the handle of the instrument to measure the applied forces during real surgical procedures. Unfortunately, apart from only being able to measure the applied forces from outside of the patient's body, this study was underpowered and no significant differences were found in the forces applied by novices and experts.

An interesting study presented in [181] found that it was difficult for trainees to be gentle with tissue, often referred to as "the heavy hands" of the beginner. This study found that 92% of consequential errors that dominated during simulated MIS procedures were skipped steps (procedural error), wrong sequence (procedural error) and use of excessive force (executional error). Force related errors (too much or too little) dominated 58% of consequential errors and 31% of

inconsequential errors.

Some of the force-based measures that have been used and some that are inspired by motion-based measures include the following:

1. **Force Range:** Refers to the difference between the minimum and the maximum forces applied during a task. This measure is important because it encompasses the magnitude of the forces in both directions.
2. **Interquartile Range:** This measure takes into account the 50% of the data that are closest to the median. In other words, it does not consider the data that are in the lowest quartile (the 25% of the data with the lowest values) and in the highest quartile (the 25% of the data with the highest values). Similar to the force range, this measure combines the forces applied in the positive and the negative directions, but by taking only the interquartile range, outliers do not have an effect on the overall measure.
3. **Average Force:** The average or median force is important to identify the mid-point value of the data. The range only makes sense in conjunction with this value. Average forces were used in [184] as a measure of skill.
4. **Maximum Force:** The maximum value of the absolute force applied might also be an important measure. It is affected by outliers, so care must be taken when interpreting the information. This measure was used in [184], but did not show a difference between experience levels.
5. **Integral of the Force:** This value provides a measure of high forces and the amount of time that the forces are high. If a single peak occurs, the integral of the force will not be much higher, but if the forces are high for a long time, the integral will be significantly higher.
6. **Derivatives of the Force:** Refers to the first and second derivative of the force as a measure of consistency in force application. These measures are used in [224] as a way of analyzing muscle behaviour, but have not been used as a measure of surgical performance.
7. **Smoothness of the Applied Forces:** This value refers to the third derivative of the force and the equivalent to the jerk measure. It provides a quantitative measure of how smoothly the forces are applied. The integral of the squared force jerk was used to measure smoothness

when applying forces in [223], where it is stated that it provides a measure of “spontaneous accelerative behaviours in the grip force profile”.

One of the main goals of skills training is to learn to gauge the applied forces better [181], but current simulators do not allow trainees to receive information about the applied forces. Providing visual force feedback during training might allow trainees to develop a more refined sense of touch in order to learn to be gentle with tissue and to apply sufficient force when required, however, they need to be trained to use this information.

7.3.5 Other Measures

Other interesting ways of measuring performance have been proposed in the literature. In [225], researchers used biomechanical data in a simulated environment that tracks the surgeon’s motions. Force, displacement, velocity and work of various muscles in the arms and back are extracted from the simulator to evaluate skill. Physiological behaviour is used in [226] as a means of assessing surgeon performance during laparoscopy. They measure heart rate, respiration, pulse wave and perspiration in addition to the movements of the body. This study presents an evaluation of time and breathing rate using an elastic band with a strain gauge attached. The results show that the expert surgeon had a significantly lower breathing rate compared to all of the novices.

A method for measuring trainee performance, called the MScore, was developed for the dV-Trainer [227]. It is based on a variety of metrics, some of which can only be measured when operating in a simulated environment, e.g., pose efficiency, pose accuracy and proficiency distance. Other metrics include task completion time, total path length, instrument collisions, master workspace range, instruments out of view, and other metrics specific to the tasks being performed. It also includes a measure of force that is based on the current drawn by the motors.

7.3.6 Data Processing

Analysis of these measures is usually done through standard ANOVA tests. Principal Component Analysis (PCA) was used in [209] to identify skill level based on instrument motion with good results. However, in order to compare various measures of performance, they need to be within the same range and ideally unitless. Different ways of normalizing performance data have been proposed in the literature. In [226], the results were all normalized with respect to the expert. A

more elaborate method is presented in [173,205]. This method involves comparing each individual parameter to those obtained from a group of experts, as follows:

$$z_i = \frac{P_i^N - \overline{P_i^E}}{\sigma_i^E}, \quad (7.6)$$

where P_i^N is the value obtained by the trainee for that particular metric and $\overline{P_i^E}$ is the mean of the metric for the expert group. σ_i^E is the standard deviation for the expert group. A total measure is then computed as follows:

$$z = 1 - \frac{\sum_{i=1}^N \alpha_i z_i}{\sum_{i=1}^N \alpha_i z_{\max}} - \alpha_0 z_0, \quad (7.7)$$

where N is the number of parameters, α_i and α_0 are coefficients that may be used to balance the influence of each parameter, and z_0 is the outcome of the task. This equation provides a way of generating a combined performance metric from individual metrics.

7.4 Development of New Performance Metrics

It should be noted from the review presented above, that there is still a very clear need to develop measures of performance that meet the following requirements:

1. Should be automatically computed based on motion or force data.
2. Should be objective measures that do not rely on the user's input for assessment.
3. Should provide a measure of the performance throughout the task, not only the final outcome.
4. Should provide a measure of aspects that are actually important to consider during surgery, such as safety and dexterity.

An experimental evaluation was performed to select or develop new performance metrics that are able to identify different experience levels during MIS and meet the requirements outlined above.

The same data collected during the experiment described in Section 6.4 were used to determine better performance measures for skills assessment. As the experiment was designed as a full

factorial test with experience level as the between-subjects factor, it is possible to analyze the same data to determine which performance measures are able to differentiate between the different experience levels.

The hypothesis is that it is possible to process the force and/or position data in such a way that a high correlation can be found between experience level and the value of the resulting metrics.

7.4.1 Methods

A total 30 subjects performed the complex procedure composed of 5 tasks: palpation, cutting, tumour removal, suturing and knot tying. 13 subjects were considered experts, while 17 subjects were considered novices. A more detailed division of the experience of the subjects was created, as described in Table 7.1, based on background, post-graduate year (PGY) level, and years of practice.

Table 7.1: Detailed experience levels.

Basic	Detailed	Description
Novice $n = 17$	1 ($n = 6$)	No medical background, e.g., Engineers
	2 ($n = 6$)	Medical students
	3 ($n = 5$)	PGY 2-3 and surgeons with no MIS training
Expert $n = 13$	4 ($n = 2$)	PGY 4-5 with training
	5 ($n = 5$)	Fellows with training
	6 ($n = 6$)	Expert surgeons

7.4.2 Data Analysis

The preparation and analysis of the data follows the methods outlined in Section 6.4.3. It was observed that although many of the results did not show significant differences from the within-subjects analysis on the effect of visual force feedback, most measures showed significant differences from the between-subjects effects, i.e., they showed differences between the novices and the experts. However, for the more detailed experience levels shown in Table 7.1, there were not enough subjects per group to have sufficient power to observe between-subjects effects in all cases. It was therefore decided to perform a more thorough analysis by performing a Spearman's Rho correlation between the different metrics and the detailed experience levels.

Considering the existing metrics found in the literature and presented in Section 7.3, different measures could also be computed from the data. This is described in the section below.

7.4.2.1 Position-based Measures

The position-based metrics that were proposed in the literature were computed and compared, as follows:

1. The total volume used by the instruments was computed by calculating the maximum and minimum in each direction and then multiplying the resulting three ranges of motion. This measure was computed in cm^3 .
2. To avoid the effect of outliers in the total volume calculation, the interquartile volume was also computed in cm^3 . The function `iqr` from the MATLAB Statistics Toolbox was used to calculate the interquartile ranges in each direction, which were then multiplied to compute the volume.
3. The tip velocity was computed by calculating the first derivative of the motion profile for x , y and z (using the MATLAB function `diff` with a sampling time of 0.02 s). The three velocity components were then combined into one through the Euclidean norm of each data point. The tip velocity profile was then used to compute the following metrics:
 - (a) The consistency of the speed was calculated as the standard deviation of the velocity profile in mm/s .
 - (b) The number of peaks in the speed was calculated using the MATLAB function `findpeaks` to find the number of local peaks in the velocity profile.
 - (c) The peak speed was calculated as the maximum of the velocity profile in mm/s .
 - (d) The average speed was calculated as the mean of the velocity profile in mm/s .
 - (e) The MAPR was calculated as defined in Section 7.3.3.1 for values that exceeded 25% of the maximum speed.
 - (f) The path length was calculated as the integral of the velocity profile using the MATLAB function `trapz` in mm , as defined in Equation 7.1.

4. The acceleration profile was computed by differentiating the velocity profile in each direction and then combining the components into one using the Euclidean norm. The following metrics were then computed:
 - (a) The consistency of acceleration was calculated as the standard deviation of the acceleration profile in mm/s^2 .
 - (b) The peak acceleration was calculated as the maximum of the acceleration profile in mm/s^2 .
 - (c) The average acceleration was calculated as the mean of the acceleration profile in mm/s^2 .
 - (d) The *IAV* was computed as the integral of the acceleration profile in mm/s^2 , as defined in Equation 7.3.
5. The normalized jerk was calculated by differentiating the acceleration profile in each direction and then combining the components using Equation 7.5.

Of these measures, the interquartile volume, and the standard deviation in the speed and acceleration as a measure of consistency have not been used previously for assessing motor performance. The number of peaks in speed and the MAPR have not been used previously in the assessment of surgical performance.

7.4.2.2 Force-based Measures

The force data were processed as described in Section 6.4.3. The resulting data consisted of a grasping force profile and a Cartesian force profile for each task in each trial. The force-based metrics implemented in the analysis include the following:

1. The average forces in each direction were calculated as the mean of the grasping force profile and of the Cartesian force profile.
2. Similarly, the peak forces in each direction were computed as the maximum of each force profile.
3. The interquartile range was computed using the MATLAB function `iqr` for the grasping and the Cartesian force profiles.

4. The integrals of the grasping and the Cartesian force profiles were calculated using the MATLAB function `trapz` with a sampling time of 0.002 s.
5. The vector of force derivatives was computed using the `diff` function. The derivative measure (dF_{metric}) was then calculated using the following equation:

$$dF_{\text{metric}} = \sqrt{\frac{D}{2 \cdot F_{\text{iqr}}^2} \int_0^D \left(\frac{dF}{dt} \right)^2 dt}, \quad (7.8)$$

where F_{iqr} is the interquartile range of the force profile.

6. Similarly, the vector of the second derivative of the force was computed by differentiating the first derivative, and the second derivative measure (d^2F_{metric}) was computed using the following equation:

$$d^2F_{\text{metric}} = \sqrt{\frac{D^3}{2 \cdot F_{\text{iqr}}^2} \int_0^D \left(\frac{d^2F}{dt^2} \right)^2 dt}. \quad (7.9)$$

7. The third derivative was computed by differentiating the second derivative, and the third derivative measure (d^3F_{metric}) was calculated using the following equation:

$$d^3F_{\text{metric}} = \sqrt{\frac{D^5}{2 \cdot F_{\text{iqr}}^2} \int_0^D \left(\frac{d^3F}{dt^3} \right)^2 dt}. \quad (7.10)$$

Of these measures, only the peak and the mean forces have been used previously for the assessment of surgical performance. The second derivative has been used to assess the smoothness of movement in stroke patients. All of the other measures are considered in this experimental evaluation for the first time for skills assessment in surgery.

7.4.2.3 Combined Measures

It was also decided to implement measures that combined various force- and position-based metrics, to come up with one overall measure of performance, which could then be adapted to be task dependent. The goal of this implementation was to account for various important skills that need to be developed together, in order to ensure that a trainee has acquired the required level of experience. In the work presented in [165], the GOALS score is computed as a combination of

several different measures. Following those same measures and considering what could in fact be measured with the SIMIS system, the following measures were considered to be important:

- **Depth Perception:** As a measure of depth perception, the GOALS score looks at overshooting targets and how quickly the subjects correct for the overshooting. This can be represented as the smoothness in the motion, i.e., as the jerk measure.
- **Bimanual Dexterity:** To compute the bimanual dexterity, it was necessary to develop a measure of how much each hand was being used relative to the other one. The MAPR measure already calculates the percentage of time that the instrument is being used, so a measure of bimanual dexterity was developed by subtracting the MAPR value for the nondominant hand from the MAPR value for the dominant hand.
- **Efficiency:** As a measure of efficiency, the total volume utilized for each task and the number of peaks in speed were considered important. It was decided to not include task completion time as the number of peaks in speed is already correlated with time.
- **Tissue Handling:** This is a measure of how roughly the tissue is handled or if any tissue damage occurs. The force-based measures come into play to assess tissue handling abilities. The measures considered for tissue handling included the integral and the derivative of the grasping and the Cartesian forces for both instruments.

Considering the measures for the left and the right hand, this resulted in a total of 15 measures that needed to be combined. However, it was important to combine them in such a way that not one measure dominated over the others and so that they could be adapted to the task being performed. For example, during the palpation task (Task 1), the volume measure is not relevant as the motion was completely dependent on the location of the tumour in the tissue. For the cutting task (Task 2), bimanual dexterity could not be computed as the right-hand movements were not measured. Also, the value of the jerk measure was higher than 10^6 , while the change in MAPR was lower than 1.

To accommodate these requirements, the data needed to be normalized and each measure multiplied by a scaling factor according to the task being performed.

Two different methods of normalization were implemented for the combined force–position (FP) metrics, as follows:

1. FP Metric 1: A normalization method was developed with the purpose of minimizing the effect of outlier-type data, which tends to dominate when all of the data are normalized to the maximum value. This measure assigned a value of 0.5 to the trimmed mean of the data set, i.e., the mean of the values without the top three maximum and minimum values. Each measure was then capped at 5 to ensure that the outlier data did not dominate.
2. FP Metric 2: The method outlined in [205] was implemented following Equations 7.6 and 7.7. The data from one of the subjects considered to be the most experienced was used as the standard to which the other subjects were compared.

Furthermore, to determine the scaling factors, two different methods were followed:

1. An *ad hoc* definition of the weights was determined based on the requirements of each task.
2. An optimized scaling vector was determined with the goal of maximizing the Spearman's Rho correlation with the experience level. The MATLAB function `fmincon` can be used to find optimal parameters constrained between a lower and an upper bound (set to 0 and 1 respectively). It was used to find the set of scaling values that generated the minimum correlation (maximum negative correlation) between the measure and the experience level for each of the tasks.

The results of these experiments are presented in the following sections.

7.4.3 Results

A first analysis of the results showed that one of the experienced subjects created outlier data during the palpation task (Task 1). This subject had difficulty localizing the tumour in every try, having to make up to 5 incisions in order to find the correct location of the tumour. As this was a statistically significant outlier confirmed using DesignExpert (based on the Externally Studentized Residuals), it was removed from the data for the analysis of Task 1 only.

7.4.3.1 Time

Task completion time results are presented in Figure 7.1 and Table 7.2. Time shows a significant correlation with experience level in all tasks, decreasing as experience increases. The correlations

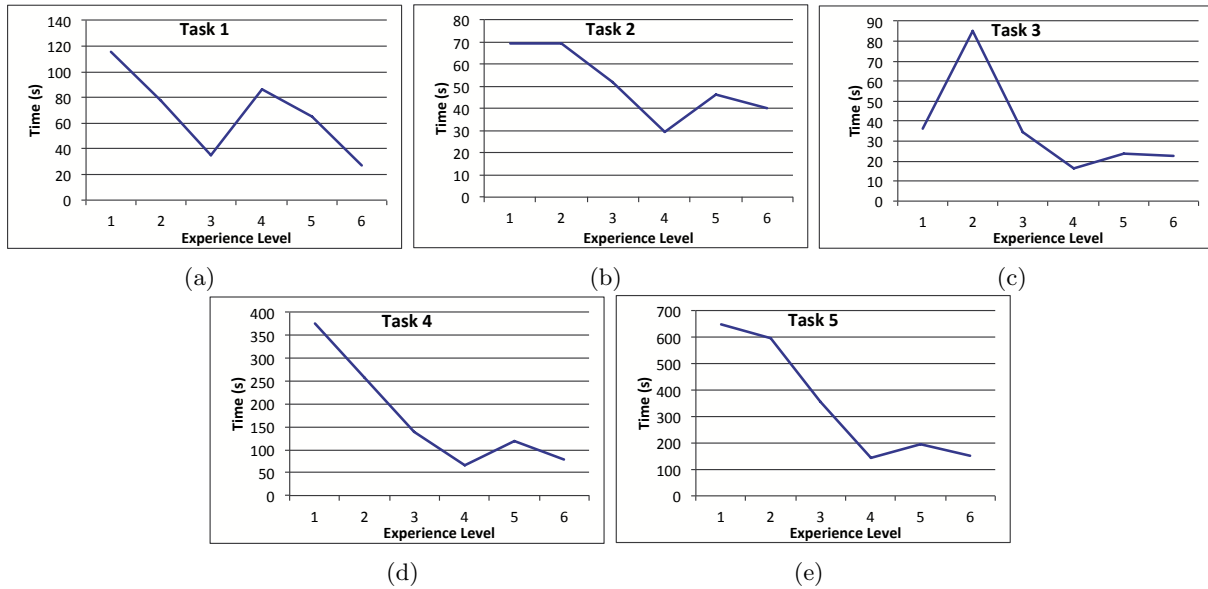


Figure 7.1: Task completion time for the 5 tasks according to the level of experience.

Table 7.2: Task completion time results in seconds for all 5 tasks.

	Task 1: Palpation	Task 2: Cutting	Task 3: Handling	Task 4: Suturing	Task 5: Tying
Mean Time	64.0 ± 11.4	52.6 ± 5.0	37.6 ± 7.2	178.1 ± 24.2	356.1 ± 31.2
Novices	78.4 ± 14.6	64.3 ± 6.6	53.1 ± 9.5	263.8 ± 31.9	545.4 ± 41.1
Experts	49.5 ± 17.4	40.9 ± 7.5	22.1 ± 10.8	92.4 ± 36.5	166.8 ± 47.0
Significance	$p = 0.215$	$p = 0.026$	$p = 0.041$	$p = 0.001$	$p < 0.0001$
Correlation	-0.336, $p = 0.0002$	-0.242, $p = 0.008$	-0.297, $p = 0.001$	-0.437, $p < 0.0001$	-0.769, $p < 0.0001$

are weak for the simpler tasks and become stronger as the task complexity increases. It can be observed from these figures that a consistently decreasing trend cannot be observed for any of the tasks. The suturing and knot-tying tasks (Tasks 4 and 5) show a plateau after experience level 4, which is the point at which students are considered trained in basic MIS tasks.

7.4.3.2 Position

Not all of the position measures showed significant correlations. Table 7.3 shows the correlations that were significant for each of the tasks. It can be observed that the number of peaks in speed and the normalized jerk show significant correlations for all of the tasks. Looking more closely at the speed peaks, it was noted that they were directly coupled with the task completion time, showing the same shaped graphs as time for all of the tasks. Normalized jerk provided a better

Table 7.3: Spearman’s Rho correlations between the six levels of experience and each position-based measure evaluated. Results show left and right hand values for each task when applicable. Bolded correlations are significant with $p < 0.05$ (LH: left hand, RH: right hand).

Measure	Task 1: Palpation (LH, RH)	Task 2: Cutting (LH only)	Task 3: Handling (LH, RH)	Task 4: Suturing (LH, RH)	Task 5: Tying (LH, RH)
Total Volume	-0.182, -0.197	0.020	-0.054, -0.122	-0.331, -0.223	-0.541, -0.528
Speed Consistency	-0.220, -0.202	-0.114	-0.132, -0.116	-0.250, -0.177	-0.465, -0.357
Speed Peaks	-0.338, -0.345	-0.237	-0.330, -0.302	-0.445, -0.434	-0.767, -0.772
Max Velocity	-0.062, -0.058	0.121	0.010, 0.150	-0.206, 0.006	-0.230, 0.024
Mean Velocity	0.175, 0.291	0.117	0.171, 0.260	0.207, 0.546	0.270, 0.562
MAPR	0.151, 0.211	-0.092	0.095, -0.018	0.334, 0.262	0.481, 0.436
Path Length	-0.305, -0.276	-0.154	-0.188, -0.195	-0.348, -0.316	-0.725, -0.680
Acceleration Consistency	-0.235, -0.216	-0.138	-0.148, -0.127	-0.233, -0.173	-0.465, -0.340
Max Acceleration	-0.102, -0.075	0.120	-0.005, 0.104	-0.142, -0.027	-0.196, 0.079
Mean Acceleration	0.096, 0.255	0.204	0.151, 0.253	0.214, 0.555	0.252, 0.525
IAV	-0.319, -0.283	-0.155	-0.199, -0.180	-0.342, -0.316	-0.725, -0.671
Jerk	-0.341, -0.333	-0.243	-0.296, -0.268	-0.409, -0.406	-0.750, -0.736
IQR Volume	-0.0153, -0.065	0.156	0.081, -0.031	-0.319, -0.149	-0.285, -0.269

measure of performance, as shown in Figure 7.2. It can be observed in this graph that in most tasks there is a decrease in the jerk as the experience level increases; however, this decrease also tends to plateau after level 4. Some of the correlations found with the position measures are slightly stronger than the correlations found with task completion time.

7.4.3.3 Force

Looking at the effect of experience level on applied forces as a between-subjects factor, there were no significant differences found in the cutting and tissue handling tasks (Tasks 2 and 3). The results are presented in Table 7.4. Compared to time and position, stronger correlations were observed in some of the force-based measures as shown in Table 7.5. More important, however, is the fact that some of the measures showed consistently decreasing slopes for the palpation task, as well as during suturing and knot tying (Tasks 1, 4 and 5). Some examples of these measures are shown in Figure 7.3.

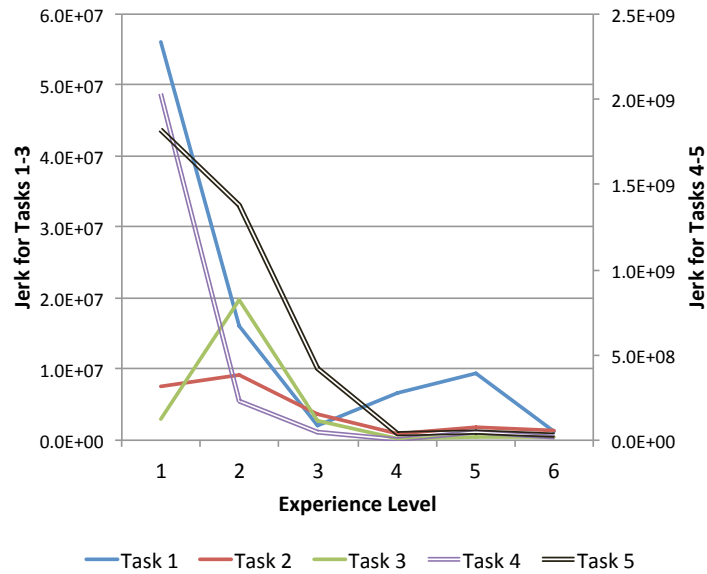


Figure 7.2: Normalized jerk as a function of experience level for all 5 tasks.

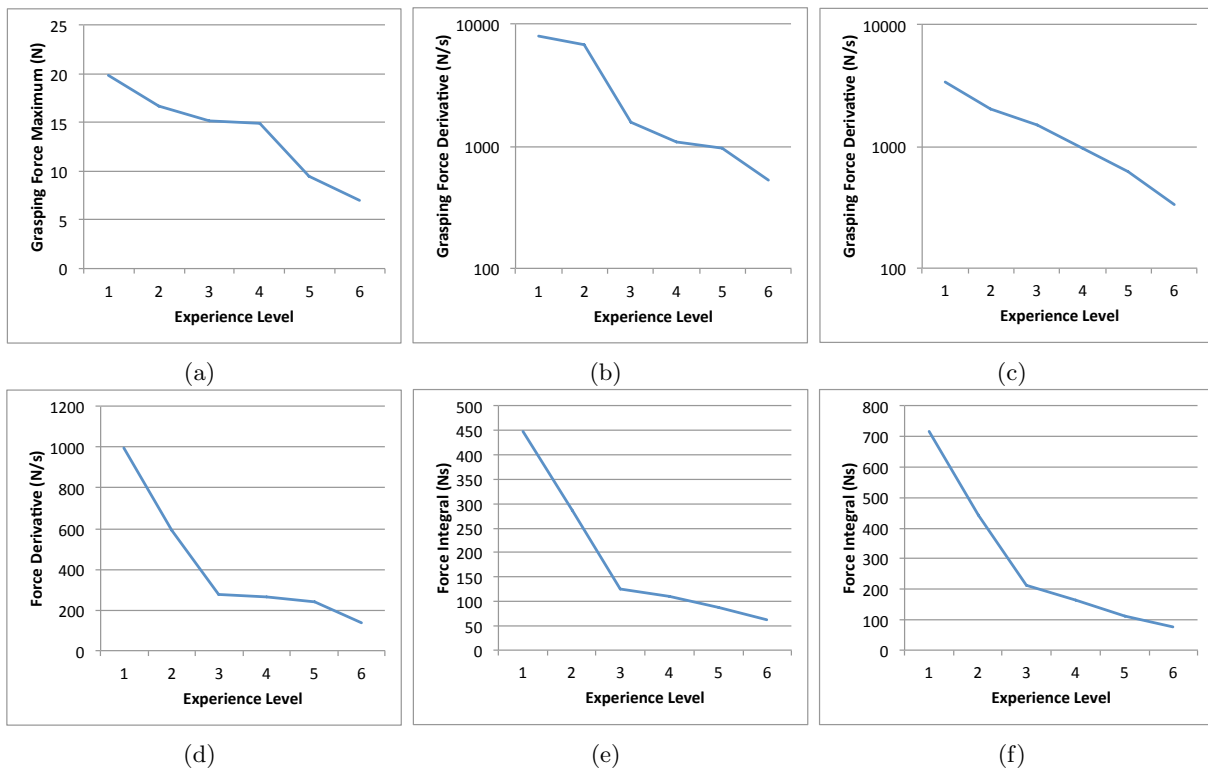


Figure 7.3: Sample graphs of force-based metrics: maximum grasping force for Task 1 (a), derivative of the grasping force for Task 4 (b), derivative of the grasping force for Task 5 (c), derivative of the Cartesian force for Task 4 (d), integral of the Cartesian force for Task 4 (e), and integral of the Cartesian force for Task 5 (f).

Table 7.4: Comparison of the force-based metrics between novices and experts for each task (LH: left hand, RH: right hand).

	Task 1 LH Palpation	Task 1 RH Palpation	Task 2 LH Cutting	Task 3 LH Handling	Task 3 RH Handling	Task 4 LH Suturing	Task 4 RH Suturing	Task 5 LH Tying	Task 5 RH Tying
Grasping Forces									
Mean (N)	6.0 vs. 3.2, $p = 0.02$	4.4 vs. 3.4, $p = 0.42$	4.1 vs. 4.0, $p = 0.91$	4.4 vs. 4.3, $p = 0.91$	10.5 vs. 9.8, $p = 0.68$	5.5 vs. 3.1, $p = 0.004$	22.0 vs. 16.3, $p = 0.10$	10.9 vs. 6.6, $p = 0.07$	12.1 vs. 9.6, $p = 0.27$
Maximum (N)	17.4 vs. 10.5, $p = 0.04$	15.0 vs. 10.7, $p = 0.24$	12.5 vs. 11.4, $p = 0.66$	17.6 vs. 19.0, $p = 0.76$	44.4 vs. 35.8, $p = 0.08$	37.0 vs. 19.8, $p = 0.001$	55.1 vs. 43.8, $p = 0.049$	53.6 vs. 36.5, $p = 0.01$	48.0 vs. 37.1, $p = 0.03$
IQR (N)	5.3 vs. 2.8, $p = 0.02$	3.0 vs. 2.7, $p = 0.65$	2.7 vs. 3.0, $p = 0.72$	3.2 vs. 4.2, $p = 0.36$	16.0 vs. 13.3, $p = 0.43$	5.2 vs. 3.0, $p = 0.04$	30.6 vs. 24.6, $p = 0.22$	13.8 vs. 7.5, $p = 0.03$	16.0 vs. 10.1, $p = 0.08$
Integral (N·s)	501.1 vs. 171.0, $p = 0.07$	562.4 vs. 163.8, $p = 0.20$	309.9 vs. 181.9, $p = 0.21$	301.6 vs. 107.0, $p = 0.08$	422.2 vs. 183.5, $p = 0.02$	1.6E3 vs. 0.3E3, $p = 0.001$	5.5E3 vs. 1.5E3, $p = 0.002$	5.6E3 vs. 1.0E3, $p < 0.001$	6.6E3 vs. 1.6E3, $p = 0.001$
First Derivative (N/s)	111.9 vs. 61, $p = 0.16$	367.3 vs. 100.5, $p = 0.13$	100.8 vs. 90.0, $p = 0.61$	107.4 vs. 92.4, $p = 0.67$	543.6 vs. 123.2, $p = 0.02$	1.3E3 vs. 0.4E3, $p = 0.05$	5.7E3 vs. 0.8E3, $p = 0.02$	2.4E3 vs. 0.5E3, $p = 0.004$	7.9E3 vs. 0.9E3, $p = 0.006$
Second Derivative (N/s ²)	2.1E4 vs. 0.9E4, $p = 0.40$	1.0E5 vs. 0.2E5, $p = 0.38$	8.0E3 vs. 4.6E3, $p = 0.17$	8.8E3 vs. 3.0E3, $p = 0.18$	5.1E4 vs. 0.4E4, $p = 0.08$	5.2E5 vs. 0.8E5, $p = 0.09$	3.7E6 vs. 0.1E6, $p = 0.06$	11.7E5 vs. 0.9E5, $p = 0.003$	4.9E6 vs. 0.2E6, $p = 0.003$
Third Derivative (N/s ³)	6.7E6 vs. 2.3E6, $p = 0.44$	6.0E7 vs. 0.4E7, $p = 0.40$	10.2E5 vs. 3.4E5, $p = 0.08$	11.7E5 vs. 0.16E5, $p = 0.20$	8.1E6 vs. 0.2E6, $p = 0.13$	3.4E8 vs. 0.2E8, $p = 0.12$	4.0E9 vs. 1.8E9, $p = 0.15$	7.2E8 vs. 0.2E8, $p = 0.01$	35.3E8 vs. 0.4E8, $p = 0.001$
Cartesian Forces									
Mean (N)	2.2 vs. 1.7, $p = 0.06$	2.1 vs. 1.8, $p = 0.24$	2.0 vs. 1.5, $p = 0.07$	2.3 vs. 2.2, $p = 0.77$	1.9 vs. 1.8, $p = 0.48$	1.1 vs. 0.9, $p = 0.06$	1.2 vs. 0.9, $p = 0.08$	1.3 vs. 0.3, $p = 0.001$	0.8 vs. 0.6, $p = 0.046$
Maximum (N)	6.4 vs. 5.1, $p = 0.01$	6.7 vs. 5.5, $p = 0.06$	3.8 vs. 3.6, $p = 0.70$	4.5 vs. 4.0, $p = 0.49$	6.6 vs. 6.0, $p = 0.40$	3.6 vs. 2.6, $p = 0.005$	0.2 vs. 0.1, $p = 0.14$	5.3 vs. 3.7, $p = 0.002$	5.9 vs. 4.7, $p = 0.02$
IQR (N)	1.8 vs. 1.5, $p = 0.40$	2.1 vs. 2.0, $p = 0.82$	0.75 vs. 0.74, $p = 0.97$	0.86 vs. 0.89, $p = 0.82$	2.0 vs. 1.8, $p = 0.39$	0.42 vs. 0.42, $p = 0.98$	0.9 vs. 0.7, $p = 0.04$	0.6 vs. 0.3, $p = 0.001$	0.04 vs. 0.3, $p = 0.02$
Integral (N·s)	148.2 vs. 83.9, $p = 0.12$	148.0 vs. 91.6, $p = 0.25$	129.7 vs. 62.6, $p = 0.05$	117.5 vs. 40.9, $p = 0.03$	85.2 vs. 39.9, $p = 0.07$	320.4 vs. 78.7, $p = 0.005$	295.9 vs. 79.2, $p = 0.002$	693.1 vs. 141.3, $p < 0.001$	472.4 vs. 103.3, $p < 0.001$
First Derivative (N/s)	98.8 vs. 45.1, $p = 0.064$	100.2 vs. 39.9, $p = 0.03$	73.4 vs. 39.1, $p = 0.07$	46.3 vs. 21.2, $p = 0.05$	93.8 vs. 49.5, $p = 0.18$	350.0 vs. 70.2, $p = 0.02$	641.8 vs. 197.1, $p = 0.01$	631.2 vs. 157.5, $p < 0.001$	1.6E3 vs. 0.5E3, $p < 0.001$
Second Derivative (N/s ²)	1.5E4 vs. 0.5E4, $p = 0.59$	2.2E4 vs. 0.6E4, $p = 0.16$	7.5E3 vs. 1.7E3, $p = 0.057$	4.8E3 vs. 0.7E3, $p = 0.10$	1.1E4 vs. 0.2E4, $p = 0.19$	2.4E5 vs. 0.1E5, $p = 0.047$	4.5E5 vs. 0.3E5, $p = 0.04$	3.9E5 vs. 0.2E5, $p = 0.001$	10.4E5 vs. 0.9E5, $p < 0.001$
Third Derivative (N/s ³)	4.9E6 vs. 0.8E6, $p = 0.22$	9.7E6 vs. 1.3E6, $p = 0.24$	12.9E5 vs. 1.1E5, $p = 0.13$	8.2E5 vs. 0.3E5, $p = 0.19$	2.3E6 vs. 0.1E6, $p = 0.23$	2.4E8 vs. 0.02E8, $p = 0.06$	5.5E8 vs. 0.8E8, $p = 0.10$	3.2E8 vs. 0.04E8, $p = 0.01$	9.5E8 vs. 0.2E8, $p = 0.002$

Table 7.5: Spearman’s Rho correlations between the six levels of experience and each force-based measure evaluated. Results show left and right hand values for each task when applicable. Bolded correlations are significant with $p < 0.05$ (LH: left hand, RH: right hand).

Measure	Task 1: Palpation (LH, RH)	Task 2: Cutting (LH only)	Task 3: Handling (LH, RH)	Task 4: Suturing (LH, RH)	Task 5: Tying (LH, RH)
Grasp					
Mean	-0.251 , -0.038	0.039	-0.034, -0.112	-0.352 , -0.290	-0.238 , -0.191
Maximum	-0.336 , -0.107	0.024	0.034, -0.322	-0.388 , -0.349	-0.369 , -0.337
IQR	-0.181 , 0.096	0.106	0.029, -0.045	-0.164, -0.234	-0.142, -0.179
Integral	-0.320 , -0.190	-0.082	-0.178, -0.386	-0.520 , -0.523	-0.678 , -0.666
First Derivative	-0.386 , -0.418	-0.053	-0.130, -0.363	-0.393 , -0.524	-0.695 , -0.721
Second Derivative	-0.330 , -0.374	-0.139	-0.193 , -0.384	-0.411 , -0.514	-0.748 , -0.769
Third Derivative	-0.306 , -0.352	-0.179	-0.227 , -0.357	-0.408 , -0.505	-0.763 , -0.782
Cartesian Forces					
Mean	-0.137, -0.142	-0.257	-0.109, -0.054	-0.159, -0.418	-0.406 , -0.397
Maximum	-0.284 , -0.356	-0.080	-0.059, -0.170	-0.304 , -0.439	-0.371 , -0.402
IQR	0.044, 0.025	-0.029	0.011, -0.050	-0.109, -0.278	-0.488 , -0.378
Integral	-0.293 , -0.313	-0.376	-0.311 , -0.339	-0.454 , -0.567	-0.755 , -0.780
First Derivative	-0.355 , -0.381	-0.129	-0.203 , -0.256	-0.459 , -0.437	-0.729 , -0.652
Second Derivative	-0.322 , -0.315	-0.228	-0.260 , -0.290	-0.470 , -0.460	-0.769 , -0.729
Third Derivative	-0.303 , -0.291	-0.247	-0.283 , -0.302	-0.465 , -0.450	-0.776 , -0.748

7.4.3.4 Combined Measures

The two FP metrics were implemented and evaluated. The results of the FP metrics when implemented with the *ad hoc* scaling factors were not much stronger than plain task completion time; therefore, the data presented herein corresponds to the optimized metrics as described in Section 7.4.2.3.

Figure 7.4 shows a comparison between the correlations found with task completion time, peaks in speed, jerk, the integral of the force, and the two optimized FP metrics. Both FP metrics combine the jerk measure, the difference in the MAPR value between the two hands, the total volume, the number of peaks in speed, and the integrals and derivatives of the grasping and Cartesian forces. In both cases, the scaling factors were determined through an optimization strategy that aimed to find the strongest correlations with experience level. FP metric 1 was computed by normalizing each measure with respect to the range of values obtained within each measure.

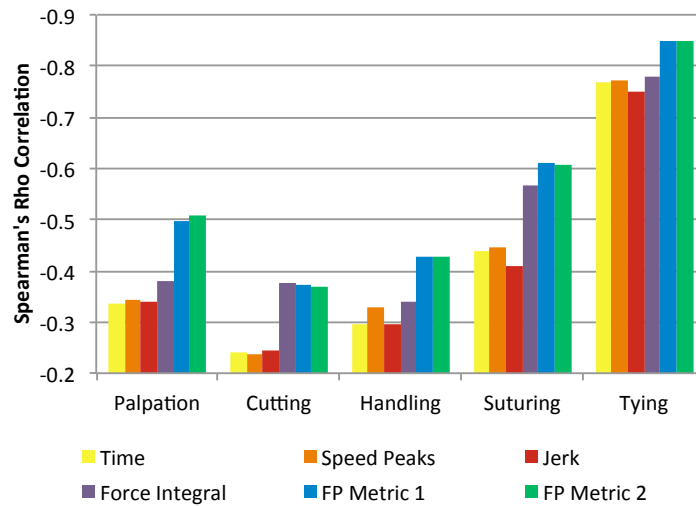


Figure 7.4: Comparison of the best possible Spearman's Rho correlations between the six levels of experience and several different metrics.

FP metric 2 was computed by normalizing the measures with respect to those of an expert. This figure shows that the force-based measures and the FP metrics show stronger correlations with experience level than task completion time and the position-based measures alone.

The results of the optimization for both of the measures show very different results for the resulting scaling factors, as shown in Tables 7.6 and 7.7. From these tables, it is interesting to see the metrics that dominated each FP metric. Most of the measures that dominate are force-based, with the exception of volume, which turned out to be important during the suturing task (Task 5).

7.5 Discussion

Computation of the derivatives of the force and position signals must be carefully performed to ensure that the resulting signal has an adequate signal-to-noise ratio. An appropriate design of the smoothing filter ensures that the signals corresponding to the first, second and third derivatives of the force and motion profiles are not dominated by noise; however, too much filtering (for example if successive filters are used) can eliminate the high frequency data that characterizes irregular movements.

To ensure that the selected filter was adequate, each time the metrics were calculated, the original signal and the three computed derivatives were plotted, as shown in Figure 7.5. Visual

Table 7.6: Scaling factors resulting from the optimization of FP Metric 1 (LH: left hand, RH: right hand).

Measure	Task 1: Palpation	Task 2: Cutting	Task 3: Handling	Task 4: Suturing	Task 5: Tying
Jerk RH	0.0744	0.0091	0.0271	0.021	0.2123
Jerk LH	0.0541	0	0.0243	0.0249	0.1928
ΔMAPR	0.0073	0	0.0273	0.0139	0.0177
Volume LH	0.0064	0.0004	0.0065	0.0117	0.316
Volume RH	0.008	0	0.0055	0.0253	0.1079
Speed Peaks LH	0.0367	0.0108	0.0295	0.0193	0.1988
Speed Peaks RH	0.0415	0	0.0216	0.0155	0.2363
Force Integral LH	0.1848	0.9769	0.0182	0.142	0.1138
Force Integral RH	0.0251	0	0.4493	0.7806	0.5922
Force Derivative LH	0.2861	0.001	0.0082	0.4157	0.0917
Force Derivative RH	0.3204	0	0.0364	0.0379	0.0679
Grasp Integral LH	0.3766	0.0026	0.0074	0.7401	0.3994
Grasp Integral RH	0.0078	0	0.657	0.1079	0.1477
Grasp Derivative LH	0.364	0.0004	0.0055	0.0247	0.4595
Grasp Derivative RH	0.5678	0	0.6738	0.9326	0.3773

inspection of these plots ensured that there were no significant jumps in any of the signals due to discontinuities or excessive noise in the data.

It is, however, important to recognize that the work presented herein seeks to find a metric that can distinguish the experience level of trainees, regardless of how accurately the speed, acceleration or jerk profiles are represented. If some noise is left in the resulting signal, the consequences for this work are not as significant as they might be for a different application, such as the control of a robotic system. In [150], the authors argue that not losing high-frequency characteristics when differentiating leads to increased sensitivity and robustness in the calculation of jerk-based performance metrics.

The results of the experiments presented above show that the SIMIS instruments provide an excellent tool for skills assessment during minimally invasive surgery. Not only were force-based measures able to provide stronger correlations with experience than those found with task completion time or position-based measures, but the relationships obtained with force are able to distinguish better between sub-levels within the expert category. In other words, when trainees are considered trained in basic skills, time- and position-based measures provide a measure of

Table 7.7: Scaling factors resulting from the optimization of FP Metric 2 (LH: left hand, RH: right hand).

Measure	Task 1: Palpation	Task 2: Cutting	Task 3: Handling	Task 4: Suturing	Task 5: Tying
Jerk RH	0.017	0.003	0.009	0.0086	0.0207
Jerk LH	0.0135	0	0.0105	0.0073	0.0123
Δ MAPR	0.0383	0	0.0273	0.177	0.2812
Volume LH	0.0773	0.0017	0.0162	0.0254	0.3555
Volume RH	0.0787	0	0.0033	0.0096	0.3143
Speed Peaks LH	0.0322	0.0064	0.0257	0.0341	0.0939
Speed Peaks RH	0.0338	0	0.0229	0.0332	0.1049
Force Integral LH	0.2238	0.7627	0.0291	0.0563	0.0284
Force Integral RH	0.0293	0	0.3966	0.732	0.4762
Force Derivative LH	0.3712	0.0063	0.0224	0.2059	0.1622
Force Derivative RH	0.3415	0	0.0134	0.0184	0.1289
Grasp Integral LH	0.6889	0.0093	0.0186	0.6132	0.4145
Grasp Integral RH	0.0145	0	0.7206	0.0612	0.2166
Grasp Derivative LH	0.2216	0.0025	0.0125	0.0172	0.4381
Grasp Derivative RH	0.5271	0	0.7669	0.1394	0.0938

proficiency similar to that achieved by expert surgeons who have been practicing for many years. However, some force-based metrics are able to distinguish between those different levels.

It is interesting to note that for experience Level 4 (subjects at the PGY 4–5 levels), task completion time for Tasks 2 to 4 was less than all other groups. Other studies have shown similar results, see e.g., [214, 228]. This can be explained by the fact that these trainees had recently completed their training in MIS, where time is the main measure of performance. In fact, [228] shows that there is a clear decline in performance after training (post-test evaluations) and even further in retention tests when assessing performance using the FLS metrics (which are mainly time-based).

Looking at task completion time as a measure of performance provides an easy way of establishing the difference between the levels, as time is the simplest metric to measure. It is clear that in any kind of activity that we perform, the more experience we have, the faster we are able to perform a task. However, care must be taken when using time as a measure of performance for several reasons:

1. Performing a task quickly means that the trainee has reached the automatous phase regard-

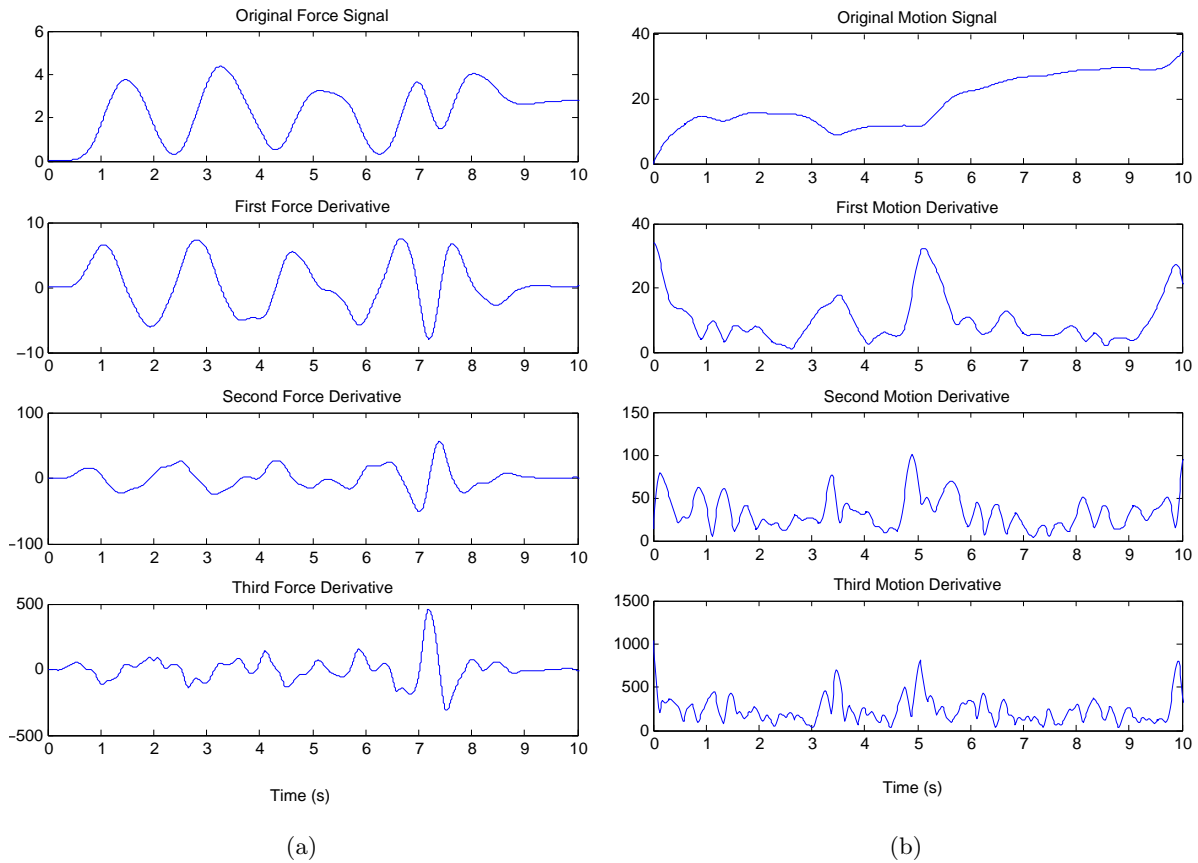


Figure 7.5: Sample graphs of force (*a*) and position (*b*) derivatives.

less of whether the task is performed properly [165]. When training novices, this stage has not been reached, so time is not a good measure to use.

2. There is a clear trade-off between speed and accuracy [214], hence performing a task faster is not necessarily better.
3. Everyone is different and what is fast for one person might not be fast for another person. Time is not a measure of ability [188] and it is important for surgeons to work at their own pace, especially when working near critical areas.
4. Depending on the specialty, doing things too fast could be a detriment to the overall outcome. This is especially true for thoracic surgeons who work close to critical anatomical features.
5. Training for time teaches trainees to focus on doing it fast, not necessarily correctly. Trainees may become aggressive in order to achieve the goals.

6. An overall time measure might be influenced by other aspects of the training scenario, for example, if there are distracting factors or other differences between the practice scenario and the assessment scenario.

Nevertheless, task completion time may be useful as a measure of trainee skill level when combined with other performance measures.

The results of the position- and force-based metrics show interesting trends for qualifying experience during a complex procedure composed of 5 tasks. Some of the position-based metrics and most of the force-based metrics proposed showed significant correlations with the 6 levels of experience proposed ($p < 0.05$), except for the cutting task (Task 2), where only a few measures correlated significantly with experience. As would be expected, the correlations found in the simpler tasks (1–3) are weak, while the ones found for the complex tasks (4–5) are the strongest.

The strongest correlations with the position-based measures were found with the peaks in speed and the jerk measure (Table 7.3). However, the correlations found with these measures and experience level were not that much stronger than those found with time, as shown in Figure 7.4, with the exception of the speed peaks during the tissue handling task (Task 3). Nevertheless, as the correlations found were significant, they can be used as a measure of movement smoothness, especially when looking at the normalized jerk measure (Fig 7.2), which is not coupled with task completion time.

The values presented in Table 7.4 show the typical values found for the different metrics, as well as the differences present between the novice and the expert groups. As the complexity of the task increases, more of these measures become significantly different between the two groups. A few of the force-based metrics showed greater correlations with experience level than those found with time and motion, as shown in Table 7.5. The strongest correlations are observed with the integral and the derivatives of the forces. A detailed task by task analysis of the results is presented below.

Palpation As Task 1 is very simple, task completion time for the novice and the expert groups was not significantly different. The forces applied by the left-handed instrument showed a significant difference between the novice and expert levels. The forces applied by both instruments were very similar, showing that subjects used both hands equivalently for palpation, and that the overall amount of applied force tended to decrease as experience level increased. The first derivative of the grasping forces and

the second and third derivatives of the grasping forces for the right hand showed stronger correlations, as well as the first derivative of the grasping forces and the maximum Cartesian forces on the right hand. The maximum grasping force also showed a consistently decreasing trend, as shown in Figure 7.3(a).

Cutting Task 2 is slightly more complicated than Task 1, requiring more dexterity and control of the instrument. It was observed that the time was significantly different between the two experience groups, with a decrease in the task completion time as the experience level increased. A limitation of this task was that the use of standard scissors did not allow forces to be measured on the dominant hand, hence the results for this task are limited. Nevertheless, the mean and the integral of the Cartesian forces showed greater correlations with experience level than task completion time.

Handling During Task 3, experience level showed a difference in time, with novices taking longer than experts. The mean, integral and the three derivatives of the grasping force and the integral of the Cartesian forces showed stronger correlations on the right hand only. The lack of more significant correlations is attributed to the overall simplicity of this task.

Suturing In Task 4, many of the position- and force-based measures showed a significant difference with experience level. All of the force metrics showed significant correlations with experience level during this task on the dominant hand. The integral of both the grasping force and the Cartesian forces showed stronger correlations with both hands, as well as many of the derivative measures. On the right hand, the Cartesian force integral and derivative as well as the grasping force derivative showed continually decreasing trends on the dominant hand, as shown in Figures 7.3(b), 7.3(d) and 7.3(e).

Tying During Task 5, the effect of experience was apparent in all measures and the correlations with experience are the strongest of all the tasks. Experts took less time and applied less force in all directions. However, the correlations are comparable to task completion time, only stronger in a few of the measures. Nevertheless, the force integral and the grasping force derivative showed decreasing trends as shown in Fig-

ures 7.3(c) and 7.3(f). As this is the most complex task, further differentiation may require breaking the task into smaller steps to observe the difference in the applied forces when handling the needle, as opposed to tightening the knot, for example.

Finally, an interesting analysis results from looking at the optimized scaling values presented in Tables 7.6 and 7.7. Larger scaling factors result from those measures that have the most influence on the final measure, so by looking at these parameters we can identify which measures are more affected by trainee experience level. The results show that the metrics that appear to be most important for the combined force–position measures include: Cartesian force integral (Tasks 2 to 5), grasping force integral and derivative (Tasks 1, 3–5), as well as the total volume (Task 5). These combined measures provided stronger correlations with experience than any of the other single metrics; however, their implementation is more difficult as they depend on systems that can measure instrument motion and applied forces in the different degrees of freedom (i.e., grasping and Cartesian directions).

7.6 Conclusions

This study evaluated the effect of experience level on performance when conducting a complex procedure composed of 5 tasks, with the goal of identifying new performance metrics. The results show that experience level correlates better with force-based metrics than those currently used in simulators. In particular, the integral and the derivative of the forces provide strong correlations that are much higher than those found with mean and average forces. The new metrics presented herein can be automatically computed, are completely objective (requiring no input from the evaluator), provide a measure throughout the task and measure aspects of performance that may actually have an effect on the outcome and the safety of the procedure.

Future work in this area includes an evaluation of the effect that training using force-based metrics may have on the trainees' development and learning curve, as well as identifying other possible combinations of metrics that include task completion time and the outcome of the procedure. Furthermore, it would be interesting to assess the value of implementing nonlinear performance metrics based on force and motion data.

Chapter 8

Conclusions and Future Work

The work presented in this thesis was aimed at addressing some of the current limitations present during MIS, in particular, the degraded haptic feedback that is caused by reduced access conditions. A thorough literature review was performed to clearly show the existing gaps in the state of the art. There are currently no commercially available multi-axis force sensors that could fit through standard endoscopic ports to allow tool–tissue interaction forces to be measured directly.

The SIMIS instruments presented herein provide a solution to the current inability to measure forces during MIS. The first prototype presented some good solutions to the problem of attaching sensors on a laparoscopic instrument in order to measure applied forces inside of the patient’s body. However, limitations in the design made it such that it was not possible to obtain a reliable measure of the axial or torsional forces. In spite of this, the first generation system was successfully used to show construct validity of the SIMIS system as a training tool, using both motion and applied force data.

The second-generation prototype of the SIMIS instruments solved many of the problems encountered with the first prototype and allowed several different evaluations to be performed, in order to assess the usefulness of force and position data during surgery and for skills assessment. A significant amount of work was also done towards the development of a sterilizable version of the instruments. After conducting extensive evaluations to select appropriate materials, a sterilizable version of the instruments is currently under construction.

The experiments performed with the SIMIS instruments have shown that force and position information recorded during minimally invasive procedures can be used to identify areas of different

stiffnesses to assist the surgeon in the localization of pathological abnormalities. Kinesthetic information can also be valuable for the development of haptic interfaces or better tissue models for physical or virtual reality simulators. Furthermore, force and/or position information is valuable for the development of objective and automated performance metrics, to be used during skills assessment and training, which truly reflect performance throughout the task.

8.1 Contributions

This work provides a justification for the development of instruments capable of measuring the applied forces during MIS, and outlines the applications in which the force information has been shown to be valuable. The specific contributions of this work are as follows:

- A set of instruments was developed that are capable of measuring forces and torques in all degrees of freedom present during MIS. The system was developed in a modular fashion, such that several different tasks can be performed by changing the tips and the handles of the instruments. A full instrument performance evaluation showed excellent accuracy, low hysteresis, noise and drift. The ability to measure instrument orientation allowed the force data to be corrected for the effect of gravity. An analysis of the effect of changing tips and the stability of the system over time was also presented. This is the first time that instruments have been developed specifically for laparoscopic surgery so as to measure tool–tissue interaction forces individually in different directions with minimal coupling.
- This work has advanced the knowledge of medical device design in that significant steps have been taken towards the development of sterilizable sensorized elements. Specifically, the experiments that were conducted show that, through the selection of appropriate materials and components, it is possible to construct devices sensorized with strain gauges that can be sterilized in an autoclave. This work can provide a solution for the measurement of applied forces during real surgical procedures.
- The effect of visual force feedback during MIS was also investigated. The results indicate that if visual force feedback is provided during a long and complex task composed of many steps, and is provided in a very general manner, such that it is up to the user to determine how to interpret the information, the effect on the forces applied by the user are minimal.

The experiments presented herein were properly designed and had sufficient power to allow these conclusions to be made. This is the first time that an experiment has been performed using an appropriate number of subjects, with the goal of establishing the effect of visual force feedback during a complex laparoscopic task.

- A feasibility study has been presented showing that force and position information recorded using the SIMIS instruments can be combined to provide a visual representation of the stiffness of the underlying tissue. The ability to measure tissue characteristics with the same instruments that are used for tissue manipulation is a significant advantage provided by the SIMIS system. This is the first time that a laparoscopic instrument has been presented that can be used for both tissue characterization and tissue manipulation.
- The *in vivo* trials performed provided an indication of the range of motion and forces that are required for the development of haptic interfaces specifically designed for surgical applications. The research shows that the SIMIS instruments can be used to inform the development of haptic interfaces for specific applications by recording the range of applied forces and the range of motion during surgical procedures.
- Further evaluations have presented evidence towards the effectiveness of applied forces as a basic performance metric to be used for skills assessment. The applied forces correspond to the true tool–tissue interactions, which represent safety and instrument control, as well as when and how the instrument comes in contact with the tissue or other elements in the surgical environment. Although these are important considerations when learning difficult tasks, surgical trainees are not currently being trained to apply adequate forces during laparoscopic surgery. The SIMIS system presents a solution to this problem, by providing feedback and performance metrics that allow trainees to know how much force they are applying and hence learn to control the applied forces.
- Finally, the force and position information was processed to develop new performance metrics that correlate better with experience than the metrics currently used in surgical simulators. These new metrics also allow smaller increments in performance level to be differentiated, including those that occur with years of practice in the operating room.

8.2 Future Work

Recognizing that the work presented herein is not complete, there are several research avenues that may be explored. The areas of future work that have been identified are presented below:

- The current calibration method is very time consuming and cumbersome. A more automated calibration method can be developed using a 6 DOF force/torque sensor as the basis for the calibration. The key to this solution is to develop an appropriate interface that ensures that as forces are applied in different directions, a corresponding measurement can be obtained from the force sensor. In this scenario, a SIMIS instrument would be inserted into a sleeve that contains the sensor and the instrument–sensor interface. The user would then run through a series of movements that would ensure that forces are applied in all directions. The data from the sensor and the instrument would be simultaneously recorded and an automatic relationship between the two could be computed to establish the calibration factors. Furthermore, a more automated calibration method could be implemented by having a mechanism that automatically moves the instrument according to a defined calibration sequence. This would ensure that an adequate range of forces would be applied in all directions and that the results would not be affected by the person performing the calibration. These solutions would also allow the calibration of an instrument that has been sterilized inside of a close-fitting wrapper. In this scenario, the instrument with the wrapper would be inserted into the calibration sleeve and automatically calibrated prior to use.
- Several improvements to the manufacturability of the instruments are possible. The current prototypes have been designed for manufacturing by using standard-sized components as much as possible. The machining of the parts is considered to be adequate for high volume production. The limitation in the instrument construction is related to the installation of the strain gauges. It currently takes about a week for a very skilled technician to apply all of the strain gauges, solder the cables and apply the coating to a single instrument. This process may be streamlined through the development of customized gauges that contain various gauges on one single foil, such that several of them can be installed at one time. These customized gauges could also have the lead wires already attached to simplify the wiring of the instrument. Custom cables with the exact number of strands and with each wire cut to the appropriate length would also help to reduce the assembly time.

- To fully develop a device that may be approved for use in humans there are several steps that are still required:
 - It is necessary to find a cable that does not have a braided shield that could cause debris to accumulate. This cable must still be flexible enough to be routed around the inner shaft of the device.
 - Solutions need to be found to properly clean crevices, hinges and joints present in the current device. If sealants are to be used to fill in some of these crevices, adequate materials need to be found that will not degrade with instrument sterilization.
 - It is necessary to find detergents and enzymatic cleaners that do not weaken the coating and adhesives that are proposed for the strain-gauge installation.
 - Finally, the process of approval for Health Canada needs to be followed, including the preparation of a large amount of documentation to prove the safety and usefulness of the devices.
- There is still no consensus as to whether the usability of an instrument improves with the availability of force information. An in-depth study that analyzes the need for force feedback through sensory substitution should be performed for each individual application. It is necessary to determine the number of degrees in which forces need to be sensed for different procedures, the required resolution and accuracy with which forces need to be measured, and which force directions are most valuable to provide for individual tasks. A significant amount of data is recorded using the instruments each time a task is performed. Establishing when it is important to consider the forces in each direction, and when certain forces may be ignored, would simplify the process of data analysis following an experiment.
- Future directions for the use of the SIMIS system for tissue characterization applications have been presented in Section 6.2.5. More elaborate algorithms can be developed to automatically determine when contact with the tissue begins and to determine the direction in which the forces are being applied with respect to the tissue surface. Research into the use of sliding instrument motion might provide a measure of tissue properties that better reflects the information perceived by a surgeon's hand during direct palpation. Tissue stiffness data can also be used to develop better tissue models for surgical simulators.

- Further research can be conducted towards the development of better performance metrics. Other position and force metrics could be computed, and other ways of combining the data should be evaluated. It would also be interesting to perform an analysis of the data by computing nonlinear measures. Furthermore, a validation of the metrics proposed should also be conducted. Current work is focusing on performing a concurrent validation of the system using the ICSAD system, as this information was also collected during the experiments presented in Chapters 6 and 7. Further experiments should also be performed to validate the metrics with a new set of subjects comprised of different experience levels and backgrounds.
- Implementing force-based metrics in training scenarios will have an impact on how trainees learn different skills. Evaluations that aim to assess the long-term effect of training with force feedback should be performed. This will require an assessment of how best to incorporate force-based metrics and the SIMIS system into a curriculum. Once incorporated, a randomized control trial can be performed, where trainees are exposed to either standard training methods or the new force-based curriculum.
- An experiment to validate the proposed metrics could be performed for use in robotic surgery. Other experiments have been performed at CSTAR using a haptics-enabled master–slave robotic system [26,229]. As this system allows for the measurement of tool–tissue interaction forces, experiments can be conducted to assess the validity of using the force-based performance metrics developed herein in robotics-assisted procedures. Force-based metrics could be used to guide the trainee when learning new tasks using haptic interfaces and through the implementation of virtual fixtures that ensure the development of proper techniques.
- The ideal outcome when developing sensors for MIS would be a 7-DOF force-torque-grip sensor that can enter the patient’s body through small incisions and that is biocompatible and sterilizable. The required sensing, materials and manufacturing technologies are almost there and the future appears promising. Researchers must continue to find novel designs for multi-axis sensing that can be miniaturized and still provide the required sensitivity. Studies to establish the levels of accuracy and resolution that are required for force sensors in MIS need to be performed [5].
- Possible areas of research within the human factors field include developing an understanding

of why force sensing is needed when performing surgical tasks [25] and how a loss of force information can be compensated for by other senses [5].

The ultimate goal of force sensing in MIS is to achieve a reduction in the levels of stress on the surgeon, which would benefit patients and the healthcare system in terms of increased safety, efficiency and cost [6]. To achieve this goal, the forces that are required for different tasks in conventional MIS or robotics-assisted procedures need to be determined. A significant amount of work is still required in this area, as discussed above.

Minimally invasive techniques have revolutionized surgical and therapeutic procedures. The lack of force feedback has not obstructed this major change in the delivery of patient care, but experts have recognized that its availability could significantly improve instrument control and overall safety. The future of MIS could be positively impacted by the development of smart surgical tools that can restore (or enhance) sensory capabilities [117], such as the SIMIS system presented in this thesis.

References

- [1] D. DelRizzo, W. Boyd, and R. Novick, “Safety and cost-effectiveness of MIDCABG in high-risk CABG patients,” *Annals of Thoracic Surgery*, vol. 66, pp. 1002–1007, 1998.
- [2] P. Dario, B. Hannaford, and A. Menciassi, “Smart surgical tools and augmenting devices,” *IEEE Transactions on Robotics and Automation*, vol. 19, no. 5, pp. 782–792, 2003.
- [3] B. Deml, T. Ortmaier, and U. Seibold, “The touch and feel in minimally invasive surgery,” in *IEEE International Workshop on Haptic Audio Visual Environments and Their Applications*, Ottawa, ON, Canada, 2005, pp. 33–38.
- [4] P. Puangmali, K. Altheofer, L. Seneviratne, D. Murphy, and P. Dasgupta, “State of the art in force and tactile sensing for minimally invasive surgery,” *IEEE Sensors Journal*, vol. 8, no. 4, pp. 371–381, 2008.
- [5] O. Van der Meijden and M. Schijven, “The value of haptic feedback in conventional and robot-assisted minimal invasive surgery and virtual reality training: a current review,” *Surgical Endoscopy*, vol. 23, pp. 1180–1190, 2009.
- [6] H. Xin, J. Zelek, and H. Carnahan, “Laparoscopic surgery, perceptual limitations and force: a review,” in *First Canadian Student Conference on Biomedical Computing*, Kingston, ON, Canada, March 17–19, 2006, pp. 44–46.
- [7] E. Scilingo, D. De Rossi, A. Bicchi, and P. Iacconi, “Sensors and devices to enhance the performances of a minimally invasive surgery tool for replicating surgeon’s haptic perception of the manipulated tissues,” in *International Conference of the IEEE Engineering in Medicine and Biology Society*, Chicago, IL, USA, October 30–November 2, 1997, pp. 961–964.
- [8] F. Tendick and L. Stark, “Analysis of the surgeon’s grasp for telerobotic surgical manipulation,” in *International Conference of the IEEE Engineering in Medicine and Biology Society*, Seattle, WA, USA, November 9–12, 1989, pp. 914–915.
- [9] A. L. Trejos, R. V. Patel, and M. D. Naish, “Force sensing and its application in minimally invasive surgery and therapy: a survey,” *Institution of Mechanical Engineers, Part C: Journal of Mechanical Engineering Science*, vol. 224, no. 7, pp. 1435–1453, 2010.
- [10] A. Okamura, L. N. Verner, T. Yamamoto, J. C. Gwilliam, and P. G. Griffiths, “Force feedback and sensory substitution for robot-assisted surgery,” in *Surgical Robotics: Systems Applications and Visions*, J. Rosen, B. Hannaford, and R. M. Satava, Eds. Springer, 2011, ch. 18, pp. 419–448.

- [11] E. Westebring-van der Putten, R. Goossens, J. Jakimowicz, and J. Dankelman, "Haptics in minimally invasive surgery – a review," *Minimally Invasive Therapy and Allied Technologies*, vol. 17, no. 1, pp. 3–16, 2008.
- [12] M. Ottermo, M. Ovstedal, T. Lango, O. Stavdahl, Y. Yavuz, T. Johansen, and R. Marvik, "The role of tactile feedback in laparoscopic surgery," *Surgical Laparoscopy, Endoscopy & Percutaneous Techniques*, vol. 16, no. 6, pp. 390–400, 2006.
- [13] K. Kuchenbecker, N. Gurari, and A. Okamura, "Effects of visual and proprioceptive motion feedback on human control of targeted movement," in *IEEE International Conference on Rehabilitation Robotics*, Noordwijk, The Netherlands, June 12–15, 2007, pp. 513–524.
- [14] A. Okamura, "Methods for haptic feedback in teleoperated robot-assisted surgery," *Industrial Robot: An International Journal*, vol. 31, no. 6, pp. 499–508, 2004.
- [15] A. L. Trejos, J. Jayender, M. T. Perri, M. D. Naish, R. V. Patel, and R. A. Malthaner, "Robot-assisted tactile sensing for minimally invasive tumour localization," *The International Journal of Robotics Research – Special Issue on Medical Robotics*, vol. 28, no. 9, pp. 1118–1133, 2009.
- [16] M. T. Perri, A. L. Trejos, M. D. Naish, R. V. Patel, and R. A. Malthaner, "New tactile sensing system for minimally invasive surgical tumour localization," *The International Journal of Medical Robotics and Computer Assisted Surgery*, 2010.
- [17] B. Bethea, A. Okamura, M. Kitagawa, T. Fitton, S. Cattaneo, V. Gott, W. Baumgartner, and D. Yuh, "Application of haptic feedback to robotic surgery," *Journal of Laparoendoscopic and Advanced Surgical Techniques A*, vol. 14, no. 13, pp. 191–195, 2004.
- [18] E. Braun, H. Mayer, A. Knoll, R. Lange, and R. Bauernschmitt, "The must-have in robotic heart surgery: haptic feedback," in *Medical Robotics*. Rijeka, Croatia: I-Tech Education and Publishing, 2008, pp. 9–20.
- [19] J. Gwilliam, M. Mahvash, B. Vagvolgyi, A. Vacharat, D. Yuh, and A. Okamura, "Effects of haptic and graphical force feedback on teleoperated palpation," in *IEEE International Conference on Robotics and Automation*, Kobe, Japan, May 12–17, 2009, pp. 667–682.
- [20] M. Kitagawa, A. Okamura, B. Bethea, V. Gott, and W. Baumgartner, "Analysis of suture manipulation forces for teleoperation with force feedback," in *Medical Image Computing and Computer Assisted Intervention*, ser. Lecture Notes in Computer Science, T. Dohi and R. Kikinis, Eds., vol. 2488. Tokyo, Japan: Springer, September 25–28, 2002, pp. 155–162.
- [21] M. MacFarlane, J. Rosen, B. Hannaford, C. Pellegrini, and M. Sinanan, "Force-feedback grasper helps restore sense of touch in minimally invasive surgery," *Journal of Gastrointestinal Surgery*, vol. 3, no. 3, pp. 278–85, 1999.
- [22] M. Tavakoli, R. V. Patel, and M. Moallem, "Robotic suturing forces in the presence of haptic feedback and sensory substitution," in *IEEE Conference on Control Applications*, vol. MA1.1, Toronto, Canada, August 28–31, 2005, pp. 1–6.

- [23] M. Tavakoli, A. Aziminejad, R. V. Patel, and M. Moallem, "Multi-sensory force/deformation cues for stiffness characterization in soft-tissue palpation," in *International Conference of the IEEE Engineering in Medicine and Biology Society*, New York City, USA, August 30–September 3, 2006, pp. 837–840.
- [24] G. Tholey, J. Desai, and A. Castellanos, "Force feedback plays a significant role in minimally invasive surgery," *Annals of Surgery*, vol. 241, no. 1, pp. 102–109, 2005.
- [25] C. Wagner, N. Stylopuolos, and R. Howe, "The role of force feedback in surgery: analysis of blunt dissection," in *International Symposium on Haptic Interfaces for Virtual Environment and Teleoperator Systems*, Orlando, FL, USA, March 24–25, 2002, pp. 68–74.
- [26] A. Talasaz, A. L. Trejos, and R. V. Patel, "Effect of force feedback on performance of robotics-assisted suturing," in *IEEE/RAS-EMBS International Conference on Biomedical Robotics and Biomechatronics*, Rome, Italy, June 24–27, 2012, pp. 823–828.
- [27] S. Salcudean and J. Yan, "Towards a force-reflecting motion-scaling system for microsurgery," in *IEEE International Conference on Robotics and Automation*, San Diego, CA, April 22–28, 1994, pp. 2296–2301.
- [28] D.-S. Kwon, K. Woo, S. Song, W. Kim, and H. Cho, "Microsurgical telerobot system," in *IEEE/RSJ International Conference on Intelligent Robots and Systems*, Victoria, B.C., Canada, October 13–17, 1998, pp. 945–950.
- [29] M. Kitagawa, D. Dokko, A. Okamura, and D. Yuh, "Effect of sensory substitution on suture-manipulation forces for robotic surgical systems," *Journal of Thoracic and Cardiovascular Surgery*, vol. 129, no. 1, pp. 151–158, 2005.
- [30] C. E. Reiley, T. Akinbiyi, D. Burschka, D. Chang, A. Okamura, and D. Yuh, "Effects of visual force feedback on robot-assisted surgical task performance," *Journal of Thoracic and Cardiovascular Surgery*, vol. 125, no. 1, pp. 196–202, 2008.
- [31] A. Bicchi, G. Canepa, D. De Rossi, P. Iaconi, and E. Scilingo, "A sensorized minimally invasive surgery tool for detecting tissutal elastic properties," in *IEEE International Conference on Robotics and Automation*, Minneapolis, Minnesota, April 22–28, 1996, pp. 884–888.
- [32] V. van Hemert tot Dingshof, M. Lazeroms, A. van der Ham, W. Jongkind, and G. Honderd, "Force reflection for a laparoscopic forceps," in *International Conference of the IEEE Engineering in Medicine and Biology Society*, Amsterdam, Netherlands, October 31–November 3, 1996, pp. 210–211.
- [33] N. Zemiti, T. Ortmainer, and G. Morel, "A new robot for force control in minimally invasive surgery," in *IEEE/RSJ International Conference on Intelligent Robots and Systems*, Sendai, Japan, September 28–October 2, 2004, pp. 3643–3648.
- [34] N. Abolhassani, R. V. Patel, and M. Moallem, "Needle insertion into soft tissue: a survey," *Medical Engineering & Physics*, vol. 29, no. 4, pp. 413–431, 2007.
- [35] A. Okamura, L. N. Verner, C. E. Reiley, and M. Mavash, "Haptics for robot-assisted minimally invasive surgery," in *13th International Symposium of Robotics Research*, vol. 19, Hiroshima, Japan, November 26–29, 2007, pp. 102–107.

- [36] G. Hanna, T. Drew, G. Arnold, M. Fakhry, and A. Cuschieri, "Development of force measure system for clinical use in minimal access surgery," *Surgical Endoscopy*, vol. 22, no. 2, pp. 467–471, 2007.
- [37] A. L. Trejos, S. Jayaraman, R. V. Patel, M. D. Naish, and C. M. Schlachta, "Force sensing in natural orifice transluminal endoscopic surgery," *Surgical Endoscopy*, vol. 25, no. 1, pp. 186–192, 2011.
- [38] S. De, J. Rosen, A. Dagan, B. Hannaford, P. Swanson, and M. Sinanan, "Assessment of tissue damage due to mechanical stress," *The International Journal of Robotics Research*, vol. 26, no. 11–12, pp. 1159–1171, 2007.
- [39] J. Rosen and B. Hannaford, "Force controlled and teleoperated endoscopic grasper for minimally invasive surgery – experimental performance evaluation," *IEEE Transactions on Biomedical Engineering*, vol. 46, no. 10, pp. 1212–1221, 1999.
- [40] J. Rosen, J. Brown, L. Chang, M. Barreca, M. Sinanan, and B. Hannaford, "The Blue-DRAGON – a system for measuring the kinematics and the dynamics of minimally invasive surgical tools in-vivo," in *IEEE International Conference on Robotics and Automation*, Washington, DC, USA, May 11–15, 2002, pp. 1876–1881.
- [41] J. Rosen, J. Brown, L. Chang, M. Sinanan, and B. Hannaford, "Generalized approach for modeling minimally invasive surgery as a stochastic process using a discrete Markov model," *IEEE Transactions on Biomedical Engineering*, vol. 53, no. 3, pp. 399–413, 2006.
- [42] W. Sjoerdsma, J. Herder, M. Horward, A. Jansen, J. Bannenberg, and C. Grimbergen, "Force transmission of laparoscopic grasping instruments," *Minimally Invasive Therapy and Allied Technologies*, vol. 6, no. 4, pp. 274–278, 1997.
- [43] S. Sukthankar and N. Reddy, "Towards force feedback in laparoscopic surgical tools," in *International Conference of the IEEE Engineering in Medicine and Biology Society*, Baltimore, MD, USA, November 3–6, 1994, pp. 1041–1042.
- [44] V. Gupta, N. Reddy, and P. Batur, "Force in surgical tools: comparison between laparoscopic and surgical forceps," in *International Conference of the IEEE Engineering in Medicine and Biology Society*, Amsterdam, The Netherlands, October 31–November 3, 1996, pp. 223–224.
- [45] G. Picod, A. Jambon, D. Vinatier, and P. Dubois, "What can the operator actually feel when performing a laparoscopy?" *Surgical Endoscopy*, vol. 19, no. 1, pp. 95–100, 2005.
- [46] J. Van den Dobbelen, A. Schooleman, and J. Dankelman, "Friction dynamics of trocars," *Surgical Endoscopy*, vol. 21, no. 8, pp. 1338–1343, 2006.
- [47] A. Krupa, G. Morel, and M. Mathelin, "Achieving high precision laparoscopic manipulation through adaptive force control," in *IEEE International Conference on Robotics and Automation*, Washington, DC, USA, May 11–15, 2002, pp. 1864–1869.
- [48] U. Seibold, B. Kubler, and G. Hirzinger, "Prototype of instrument for minimally invasive surgery with six-axis force sensing capability," in *IEEE International Conference on Robotics and Automation*, Barcelona, Spain, April 18–22, 2005, pp. 498–503.

- [49] M. Tavakoli, R. V. Patel, and M. Moallem, "Haptic interaction in robot-assisted endoscopic surgery: a sensorized end-effector," *The International Journal of Medical Robotics and Computer Assisted Surgery*, vol. 1, no. 2, pp. 53–63, 2005.
- [50] G. Tholey, A. Pillarisetti, W. Green, and J. Desai, "Design, development, and testing of an automated laparoscopic grasper with 3-D force measurement capability," in *International Symposium on Medical Simulation*, ser. Lecture Notes in Computer Science, S. Cotin and D. Metaxas, Eds., vol. 3078. Cambridge, MA, USA: Springer, June 17–18, 2004, pp. 38–48.
- [51] A. Madhani, G. Niemeyer, and J. J. Salisbury, "The Black Falcon: a teleoperated surgical instrument for minimally invasive surgery," in *IEEE/RSJ International Conference on Intelligent Robots and Systems*, Victoria, BC, Canada, October 13–17, 1998, pp. 936–944.
- [52] G. Tholey, T. Chanthasopeephan, T. Hu, J. Desai, and K. Lau, "Measuring grasping and cutting forces for reality-based haptic modeling," in *International Conference on Computer Assisted Radiology and Surgery*, ser. International Congress Series, vol. 1256. London, UK: Elsevier, June 25–28, 2003, pp. 794–800.
- [53] P. Dubois, "In vivo measurement of surgical gestures," *IEEE Transactions on Biomedical Engineering*, vol. 49, no. 1, pp. 49–54, 2002.
- [54] J. Jayender and R. V. Patel, "Wave variables based bilateral teleoperation of an active catheter," in *IEEE/RAS-EMBS International Conference on Biomedical Robotics and Biomechatronics*, Scottsdale, AZ, USA, October 19–22, 2008, pp. 27–32.
- [55] S. K. Prasad, M. Kitagawa, G. S. Fischer, J. Zand, M. A. Talamini, R. H. Taylor, and A. M. Okamura, "A molecular 2-DOF force-sensing instrument for laparoscopic surgery," in *Medical Image Computing and Computer Assisted Intervention*, ser. Lecture Notes in Computer Science, R. E. Ellis and T. M. Peters, Eds., vol. 2878. Montréal, Canada: Springer-Verlag, November 15–18, 2003, pp. 279–286.
- [56] N. Zemiti, G. Morel, and T. Ortmaier, "Mechatronic design of a new robot force control in minimally invasive surgery," *IEEE/ASME Transactions on Mechatronics*, vol. 12, no. 2, pp. 143–151, 2007.
- [57] J. Herder, M. Horward, and W. Sjoerdsma, "Laparoscopic grasper with force perception," *Minimally Invasive Therapy and Allied Technologies*, vol. 6, no. 4, pp. 279–286, 1997.
- [58] M. Mahvash and A. Okamura, "Friction compensation for enhancing transparency of a teleoperator with compliant transmission," *IEEE Transactions on Robotics and Automation*, vol. 23, no. 6, pp. 1240–1246, 2007.
- [59] B. Maurin, J. Gangloff, B. Bayle, M. de Mathelin, O. Piccin, P. Zanne, C. Doignon, L. Soler, and A. Gangi, "A parallel robotic system with force sensors for percutaneous procedures under CT-guidance," in *Medical Image Computing and Computer Assisted Intervention*, ser. Lecture Notes in Computer Science, C. Barillot, D. R. Haynor, and P. Hellier, Eds., vol. 3217. Saint-Malo, France: Springer, September 26–29, 2004, pp. 176–183.
- [60] H. Kataoka, T. Washio, K. Chinzei, K. Mizuhara, C. Simone, and A. Okamura, "Measurement of the tip and friction force acting on a needle during penetration," in *Medical Image*

- Computing and Computer Assisted Intervention*, ser. Lecture Notes in Computer Science, T. Dohi and R. Kikinis, Eds., vol. 2488. Tokyo, Japan: Springer, September 25–28 2002, pp. 216–223.
- [61] T. Washio and K. Chinzei, “Needle force sensor, robust and sensitive detection of the instant of needle puncture,” in *Medical Image Computing and Computer Assisted Intervention*, ser. Lecture Notes in Computer Science, C. Barillot, D. R. Haynor, and P. Hellier, Eds., vol. 3217. Saint-Malo, France: Springer, September 26–29, 2004, pp. 113–120.
- [62] L. N. Verner and A. M. Okamura, “Effects of translational and gripping force feedback are decoupled in a 4-degree-of-freedom telemanipulator,” in *Second Joint EuroHaptics and World Haptics Conference, Symposium on Haptic Interfaces for Virtual Environment and Teleoperator Systems*, Tsukuba, Japan, March 22–24, 2007, pp. 286–291.
- [63] W. Semere, M. Kitagawa, and A. Okamura, “Teleoperation with sensor/actuator asymmetry: task performance with partial force feedback,” in *International Symposium on Haptic Interfaces for Virtual Environment and Teleoperator Systems*, Chicago, IL, USA, March 27–28, 2004, pp. 121–127.
- [64] E. O. Doebelin, *Measurement Systems Application and Design*, 5th ed. New York, NY, USA: McGraw Hill, 2004.
- [65] G. Tholey and J.P. Desai, “A compact and modular laparoscopic grasper with tridirectional force measurement capability,” *Journal of Medical Devices*, vol. 2, no. 3, pp. 031001–1–031001–8, 2008.
- [66] P. Berkelman, L. Whitcomb, R. Taylor, and P. Jensen, “A miniature microsurgical instrument tip force sensor for enhanced force feedback during robot-assisted manipulation,” *IEEE Transactions on Robotics and Automation*, vol. 19, no. 5, pp. 917–922, 2003.
- [67] S. A. Liu and H. L. Tzo, “A novel six-component force sensor of good measurement isotropy and sensitivities,” *Sensors and Actuators A: Physical*, vol. 100, no. 2–3, pp. 223–230, 2002.
- [68] R. Ranganath, P. Nair, T. Mruthyunjaya, and A. Ghosal, “A force-torque sensor based on a stewart platform in a near-singular configuration,” *Mechanism and Machine Theory*, vol. 39, no. 9, pp. 971–998, 2004.
- [69] M. Uchiyama, E. Bayo, and E. Palma-Villalon, “A systematic design to minimize a performance index for robot force sensors,” *Journal of Dynamic Systems, Measurement and Control*, vol. 113, no. 3, pp. 388–395, 1991.
- [70] W. Huang, H. Jiang, and H. Zhou, “Mechanical analysis of a novel six-degree-of-freedom wrist force sensor,” *Sensors and Actuators A: Physical*, vol. 35, no. 3, pp. 203–208, 1993.
- [71] L.-P. Chao and K.-T. Chen, “Shape optimal design and force sensitivity evaluation of six-axis force sensors,” *Sensors and Actuators A: Physical*, vol. 63, no. 2, pp. 105–112, 1997.
- [72] H. Aviles, J. Gregory, H. Panissidi, and H. Wattenbarger, “Tri-axial force transducer for a manipulator gripper,” U.S. Patent 4,478,089, October 23, 1984.

- [73] A. Yee and H. Akeel, "Six-axis force sensor employing multiple shear strain gages," U.S. Patent 5,490,427, February 13, 1996.
- [74] T. Ohsato and Y. Hirabayashi, "Six-axis force sensor," U.S. Patent 6,823,744 B2, November 30, 2004.
- [75] S. Hirose and K. Yoneda, "Development of optical 6-axis force sensor and its signal calibration considering non-linear interference," in *IEEE International Conference on Robotics and Automation*, Tsukuba, Japan, May 13–18, 1990, pp. 46–53.
- [76] N. Takahashi, T. Mitsunori, J. Ueda, Y. Matsumoto, and T. Ogasawara, "An optical 6-axis force sensor for brain function analysis using fMRI," *IEEE Sensors Journal*, vol. 1, pp. 253–258, October 22–24, 2003.
- [77] S. Katsura, Y. Matsumoto, and K. Ohnishi, "Modeling of force sensing and validation of disturbance observer for force control," *IEEE Transactions on Industrial Electronics*, vol. 54, no. 1, pp. 530–538, 2007.
- [78] J. Jung, J. Lee, and K. Huh, "Robust contact force estimation for robot manipulators in three-dimensional space," *Proceedings of the Institution of Mechanical Engineers, Part C: Journal of Mechanical Engineering*, vol. 220, pp. 1317–1327, 2006.
- [79] M. Motamed and J. Yan, "A review of biological, biomimetic and miniature force sensing for microflight," in *IEEE/RSJ International Conference on Intelligent Robots and Systems*, Edmonton, AB, Canada, August 2–5, 2005, pp. 3939–3946.
- [80] A. L. Trejos, R. V. Patel, M. D. Naish, and C. M. Schlachta, "A sensorized instrument for skills assessment and training in minimally invasive surgery," *ASME Journal of Medical Devices*, vol. 3, no. 4, pp. 041 002–1 – 041 002–12, 2009.
- [81] M. Lazeroms, G. Villavicencio, W. Jongkind, and G. Honderd, "Optical fibre force sensor for minimal-invasive surgery grasping instruments," in *International Conference of the IEEE Engineering in Medicine and Biology Society*, Amsterdam, The Netherlands, October 31–November 3, 1996, pp. 234–235.
- [82] J. Peirs, J. Clijnen, D. Reynaerts, H. Van Brussel, P. Herijgers, B. Corteville, and S. Boone, "A micro optical force sensor for force feedback during minimally invasive robotic surgery," *Sensors and Actuators A: Physical*, vol. 115, no. 2, pp. 447–755, 2004.
- [83] K. Eom, I. Suh, W. Chung, and S.-R. Oh, "Disturbance observer based force control of robot manipulator without force sensor," in *IEEE International Conference on Robotics and Automation*, Leuven, Belgium, May 16–20, 1998, pp. 3012–3017.
- [84] K. Tadano and K. Kawashima, "Development of 4-DOFs forceps with force sensing using pneumatic servo system," in *IEEE International Conference on Robotics and Automation*, Orlando, FL, USA, May 15–19, 2006, pp. 2250–2255.
- [85] M. Tavakoli, R. V. Patel, and M. Moallem, "Bilateral control of a teleoperator for soft tissue palpation: design and experiments," in *IEEE International Conference on Robotics and Automation*, Orlando, FL, USA, May 15–19, 2006, pp. 3280–3285.

- [86] P. Dario and M. Bergamasco, "An advanced robot system for automated diagnostic tasks through palpation," *IEEE Transactions on Biomedical Engineering*, vol. 35, no. 2, pp. 118–126, 1988.
- [87] D. Kontarinis, J. Son, W. Peine, and R. Howe, "A tactile shape sensing and display system for teleoperated manipulation," in *IEEE International Conference on Robotics and Automation*, Nagoya, Aichi, Japan, May 21–27, 1995, pp. 641–646.
- [88] C. Y. K. Chee, L. Tong, and G. P. Steven, "A review on the modelling of piezoelectric sensors and actuators incorporated in intelligent structures," *Journal of Intelligent Material Systems and Structures*, vol. 9, no. 1, pp. 3–19, 1998.
- [89] S. Cetinkunt, *Mechatronics*. Hoboken, NJ, USA: John Wiley & Sons, Inc., 2007.
- [90] J. Henry and C. J. Ruoff, "Multi-axis load cell," U.S. Patent 4,092,854, June 6, 1978.
- [91] A. Grahn, "Triaxial normal and shear force sensor," U.S. Patent 5,553,500, September 10, 1996.
- [92] G. L. McCreery, A. L. Trejos, M. D. Naish, R. V. Patel, and R. A. Malthaner, "Feasibility of locating tumours in lung via kinaesthetic feedback," *The International Journal of Medical Robotics and Computer Assisted Surgery*, vol. 4, no. 1, pp. 58–68, 2008.
- [93] J. D. Brown, J. Rosen, M. Moreyra, M. Sinanan, and B. Hannaford, "Computer-controlled motorized endoscopic grasper for *in vivo* measurement of soft tissue biomechanical characteristics," in *Medicine Meets Virtual Reality*, ser. Studies in Health Technology and Informatics, J. D. Westwood, H. M. Hoffman, R. A. Robb, and D. Stredney, Eds., vol. 85, Newport Beach, CA, USA, January 23–26, 2002, pp. 71–73.
- [94] M. N. Helmus, D. F. Gibbons, and D. Cebon, "Biocompatibility: meeting a key functional requirement of next-generation medical devices," *Toxicologic Pathology*, vol. 36, no. 1, pp. 70–80, 2008.
- [95] J. Black, *Biological Performance of Materials: Fundamentals of Biocompatibility*, 4th ed. New York, NY, USA: CRC Press, 2005.
- [96] D. J. Dempsey and R. R. Thirucote, "Sterilization of medical devices: a review," *Journal of Biomaterials Applications*, vol. 3, no. 3, pp. 454–523, 1988.
- [97] G. C. C. Mendes, T. R. S. Brandão, and C. L. M. Silva, "Ethylene oxide sterilization of medical devices: a review," *American Journal of Infection Control*, vol. 35, no. 9, pp. 574–581, 2007.
- [98] J. Tegin and J. Wikander, "Tactile sensing in intelligent robotic manipulation – a review," *Industrial Robot: An International Journal*, vol. 32, no. 1, pp. 64–70, 2005.
- [99] P. Berkelman, L. Whitcomb, R. Taylor, and P. Jensen, "A miniature instrument tip force sensor for robot/human cooperative microsurgical manipulation with enhanced force feedback," in *Medical Image Computing and Computer Assisted Intervention*, ser. Lecture Notes in Computer Science, S. L. Delp, A. M. DiGoia, and B. Jaramaz, Eds., vol. 1935. Pittsburgh, PA, USA: Springer, October 11–14, 2000, pp. 897–906.

- [100] T. G. Beckwith, R. D. Marangoni, and J. H. Lienhard V, *Mechanical Measurements*, 5th ed. Addison-Wesley Publishing Company, 1993.
- [101] H. Mayer, I. Nagy, and A. Knoll, “Robotic system to evaluate force feedback in minimally invasive computer aided surgery,” in *ASME Design Engineering Technical Conferences*, Salt Lake City, Utah, USA, September 28–October 2, 2004, pp. 361–379.
- [102] F. Barbagli, K. Salisbury Jr., and R. Devengenzo, “Enabling multi-finger, multi-hand virtualized grasping,” in *IEEE International Conference on Robotics and Automation*, Taipei, Taiwan, September 14–19, 2003, pp. 809–815.
- [103] M. Tavakoli, R. V. Patel, and M. Moallem, “A haptic interface for computer-integrated endoscopic surgery and training,” *Virtual Reality*, vol. 9, no. 2, pp. 160–176, 2006.
- [104] E. Burdet, R. Gassert, F. Mani, F. Wang, C. Teo, and H. Bleuler, “Design of a haptic forceps for microsurgery training,” in *Proceedings of EuroHaptics*, Munich, Germany, June 5–7, 2004, pp. 74–81.
- [105] R. Feller, C. Lau, C. Wagner, D. Perrin, and R. Howe, “The effect of force feedback on remote palpation,” in *IEEE International Conference on Robotics and Automation*, New Orleans, LA, USA, April 26–May 1, 2004, pp. 782–788.
- [106] C. Wagner, D. Perrin, and R. Feller, “Integrating tactile and force feedback with finite element models,” in *IEEE International Conference on Robotics and Automation*, Barcelona, Spain, April 18–22, 2005, pp. 3942–3947.
- [107] T. Hoshino, H. Ishigaki, Y. Konishi, K. Kondo, T. Suzuki, T. Saito, K. Naoto, A. Wagatsuma, and K. Mabuchi, “A master-slave manipulation system with a force-feedback function for endoscopic surgery,” in *International Conference of the IEEE Engineering in Medicine and Biology Society*, vol. 4, Istanbul, Turkey, October 25–28, 2001, pp. 3446–3449.
- [108] B. Hannaford, J. Trujillo, M. Sinanan, M. Moreyra, J. Rosen, J. Brown, R. Leuschke, and MacFarlane, M, “Computerized endoscopic surgical grasper,” in *Medicine Meets Virtual Reality*, ser. Studies In Health Technology and Informatics, J. Westwood, Ed., vol. 50, San Diego, CA, USA, January 28–31, 1998, pp. 111–117.
- [109] M. Tavakoli, R. V. Patel, and M. Moallem, “A force reflective master-slave system for minimally invasive surgery,” in *IEEE/RSJ International Conference on Intelligent Robots and Systems*, Las Vegas, NV, USA, October 27–31, 2003, pp. 3077–3082.
- [110] E. U. Schirmbeck, H. Mayer, I. Nagy, A. Knoll, R. Lange, and R. Bauernschmitt, “Evaluation of force feedback in minimally invasive robotic surgery,” *Biomedical Technology*, vol. 49, no. 2, pp. 108–109, 2004.
- [111] H. Bassan, A. Talasaz, and R. V. Patel, “Design and characterization of a 7-DOF haptic interface for minimally invasive surgery test-bed,” in *IEEE/RSJ International Conference on Intelligent Robots and Systems*, St. Louis, MO, USA, October 11–15, 2009, pp. 4098–4103.
- [112] C. Wagner and R. Howe, “Mechanisms of performance enhancement with force finite element models,” in *IEEE International Conference on Robotics and Automation*, Barcelona, Spain, April 18–22, 2005, pp. 3942–3947.

- [113] G. S. Fischer, T. Akinbiyi, S. Saha, J. Zand, M. Talamini, M. Marohn, and R. Taylor, "Ischemia and force sensing surgical instruments for augmenting available surgeon information," in *EEE/RAS-EMBS International Conference on Biomedical Robotics and Biomechanics*, Pisa, Italy, February 20–23, 2006, pp. 1030–1035.
- [114] B. Kuebler, U. Seibold, and G. Hirzinger, "Development of actuated and sensor integrated forceps for minimally invasive robotic surgery," *The International Journal of Medical Robotics and Computer Assisted Surgery*, vol. 1, no. 3, pp. 96–107, 2005.
- [115] L. Beccai, S. Roccella, L. Ascari, P. Valdastri, A. Sieber, M. C. Carrozza, and P. Dario, "Development of experimental analysis of a soft compliant tactile microsensor for anthropomorphic artificial hand," *IEEE/ASME Transactions on Mechatronics*, vol. 13, no. 2, pp. 158–168, 2008.
- [116] A. Eisinberg, A. Menciassi, S. Micera, D. Campolo, M. C. Carrozza, and P. Dario, "PI force control of a microgripper for assembling biomedical microdevices," *IEE Proceedings on Circuits, Devices and Systems*, vol. 148, no. 6, pp. 348–352, 2001.
- [117] A. Menciassi, A. Eisinberg, G. Scalari, C. Anticolti, M. Carrozza, and P. Dario, "Force feedback-based microinstrument for measuring properties and pulse in microsurgery," in *IEEE International Conference on Robotics and Automation*, Seoul, Korea, May 21–26, 2001, pp. 10–17.
- [118] A. Mirbagheri and F. Farahmand, "A triple-jaw actuated and sensorized instrument for grasping large organs during minimally invasive robotic surgery," *The International Journal of Medical Robotics and Computer Assisted Surgery*, 2012, advanced online print.
- [119] Y. Kurita, F. Sugihara, J. Ueda, and T. Ogasawara, "Piezoelectric tweezer-type end effector with force- and displacement-sensing capability," *IEEE/ASME Transactions on Mechatronics*, 2011, advanced online print.
- [120] J. Rosen, M. MacFarlane, C. Richards, B. Hannaford, and M. Sinanan, "Surgeon-tool force/torque signatures—evaluation of surgical skills in minimally invasive surgery," in *Medicine Meets Virtual Reality*, ser. Studies In Health Technology and Informatics, J. Westwood, H. Hoffman, R. Robb, and D. Stredney, Eds., vol. 62, San Francisco, CA, January 17–20, 1999, pp. 290–296.
- [121] J. Rosen and B. Hannaford, "Markov modeling of minimally invasive surgery based on tool/tissue interaction and force/torque signatures for evaluating surgical skills," *IEEE Transactions on Biomedical Engineering*, vol. 48, no. 5, pp. 579–591, 2001.
- [122] J. Rosen, M. Solazzo, B. Hannaford, and M. Sinanan, "Task decomposition of laparoscopic surgery for objective evaluation of surgical residents' learning curve using hidden Markov model," *Computer Aided Surgery*, vol. 7, no. 1, pp. 49–61, 2002.
- [123] S. Shimachi, Y. Hakozaki, T. Tada, and Y. Fujiwara, "Measurement of force acting on surgical instrument for force-feedback to master robot console," in *International Conference on Computer Assisted Radiology and Surgery*, ser. International Congress Series, H. U. Lemke, M. W. Vannier, K. Inamura, A. G. Farman, K. Doi, and J. H. C. Reiber, Eds., vol. 1256. London, UK: Elsevier, June 25–28, 2003, pp. 538–546.

- [124] S. Shimachi, Y. Fujiwara, and Y. Hakozaiki, "New sensing method of force acting on instrument for laparoscopic robot surgery," in *International Conference on Computer Assisted Radiology and Surgery*, ser. International Congress Series, H. Lemke, K. Inamura, K. Doi, A. Farman, M. Vannier, and J. Reiber, Eds., vol. 1268. Chicago, IL, USA: Elsevier, June 23–26, 2004, pp. 775–780.
- [125] S. Shimachi, F. Kameyama, Y. Hakozaiki, and Y. Fujiwara, "Contact force measurement of instruments for force-feedback on a surgical robot: acceleration force cancellations based on acceleration sensor readings," in *Medical Image Computing and Computer Assisted Intervention*, ser. Lecture Notes in Computer Science, J. Duncan and G. Gerig, Eds., vol. 3750. Palm Springs, CA, USA: Springer-Verlag, October 26–30, 2005, pp. 97–104.
- [126] F. Van Meer, D. Esteve, A. Giraud, and A. Gué, "2D silicon macro-force sensor for a tele-operated surgical instrument," in *International Conference on MEMS, NANO and Smart Systems*, Banff, AB, Canada, August 25–27, 2004, pp. 468–472.
- [127] F. Van Meer, D. Esteve, A. Giraud, and A. Gué, "Si-micromachined 2D force sensor for a laparoscopic instrument," in *International Conference on Computer Assisted Radiology and Surgery*, ser. International Congress Series, H. U. Lemke, K. Inamura, K. Doi, M. W. Vannier, A. G. Farman, and J. H. C. Reiber, Eds., vol. 1268. Chicago, IL, USA: Elsevier, June 23–26, 2004, p. 1334.
- [128] D. Esteve, F. Van Meer, A. Giraud, and D. Villeroy, "Shear-stress microsensors and surgical instrument end tool," U.S. Patent US2006/0173383 A1, October 21, 2006.
- [129] P. Valdastri, K. Harada, A. Mencias, L. Beccai, C. Stefanini, M. Fujie, and P. Dario, "Integration of a miniaturised triaxial force sensor in a minimally invasive surgical tool," *IEEE Transactions on Biomedical Engineering*, vol. 53, no. 11, pp. 2397–2400, 2006.
- [130] H. Song, H. Kim, J. Jeong, and J. Lee, "Development of FBG sensor system for force-feedback in minimally invasive robotic surgery," in *International Conference on Sensing Technology (ICST)*, Palmerston North, New Zealand, November 28–December 1, 2011, pp. 16–20.
- [131] P. Puangmali, H. Liu, L. Seneviratne, P. Dasgupta, and K. Althoefer, "Miniature 3-axis distal force sensor for minimally invasive surgical palpation," *IEEE/ASME Transactions on Mechatronics*, vol. 17, no. 4, pp. 646–656, 2012.
- [132] P. Baki, G. Székely, and G. Kósa, "Miniature tri-axial force sensor for feedback in minimally invasive surgery," in *IEEE/RAS-EMBS International Conference on Biomedical Robotics and Biomechanics*, Rome, Italy, June 24–27, 2012, pp. 805–810.
- [133] G. Tholey, A. Pillarisetti, and J. Desai, "On-site three dimensional force sensing capability in a laparoscopic grasper," *Industrial Robot: An International Journal*, vol. 31, no. 6, pp. 509–518, 2004.
- [134] A. K. Morimoto, R. D. Foral, J. L. Kuhlman, K. A. Zucker, M. J. Curet, and T. Bocklage, "Force sensor for laparoscopic babcock," in *Medicine Meets Virtual Reality*, ser. Studies in Health Technology and Informatics, K. S. Morgan, S. J. Weghorst, and H. M. Hoffman, Eds., vol. 39, San Diego, CA, USA, January 22–25, 1997, pp. 354–361.

- [135] W. Rasband, “Imagej,” <http://imagej.nih.gov/ij/>, Bethesda, MD, USA, 2007–2011.
- [136] S. Jayaraman, “Validation of a sensorized laparoscopic surgery system,” Master’s thesis, Department of Electrical and Computer Engineering, The University of Western Ontario, 2008.
- [137] S. Jayaraman, A. L. Trejos, M. D. Naish, A. C. Lyle, R. V. Patel, and C. M. Schlachta, “Toward construct validity for a novel sensorized instrument-based minimally invasive surgery (SIMIS) simulation system,” *Surgical Endoscopy*, vol. 25, no. 5, pp. 1439–1445, 2011.
- [138] Provincial Infectious Diseases Advisory Committee, “Best practices for cleaning, disinfection and sterilization of medical equipment/devices,” Ministry of Health and Long-Term Care, Toronto, ON, Canada, Tech. Rep., 2010.
- [139] Cooner Wire, “Teflon multiconductor cable,” <http://www.coonerwire.com/teflon-multiconductor-cable/>, Chatsworth, CA, USA, 2012.
- [140] Fischer Connectors, “Core series catalogue,” <http://www.fischerconnectors.com/pdf/catalogue/en/Fischer-Core-Series-Catalog-EN.pdf>, Switzerland, 2012.
- [141] International Organization for Standardization, “Biological evaluation of medical devices,” <http://www.iso.org/iso/home.html>, Geneva, Switzerland, 2000–2010.
- [142] E. Samur, M. Sedej, C. Basdogan, L. Avtan, and O. Duzgun, “A robotic indenter for minimally invasive measurement and characterization of soft tissue response,” *Medical Image Analysis*, vol. 11, no. 4, pp. 361–373, 2007.
- [143] T. Yamamoto, B. Vagvolgyi, K. Balaji, L. Whitcomb, and A. Okamura, “Tissue property estimation and graphical display for teleoperated robot-assisted surgery,” in *IEEE International Conference on Robotics and Automation*, Kobe, Japan, May 12–17, 2009, pp. 4239–4245.
- [144] Center for Advance Life Cycle Engineering, “Material hardness,” http://www.calce.umd.edu/TSFA/Hardness_ad_.htm#8, University of Maryland, College Park, MD, USA, Tech. Rep., 2001.
- [145] R. A. Walsh, *Machinists’ and Metalworkers’ Pocket Reference*. New York, NY, USA: McGraw-Hill Professional, 2000.
- [146] The Chamberlain Group, “The suturable wound closure trainer insert,” <http://www.thecgroup.com/product/general-gastrointestinal/suturing/new-suturable-wound-closure>, Great Barrington, MA, USA, 2012.
- [147] J. Rosenberg, “Line, planes and MATLAB,” http://www2.math.umd.edu/~jmr/241/lines_planes.html, MD, USA, 2009.
- [148] J. Gwilliam, Z. Pezzementi, E. Jantho, A. Okamura, and S. Hsiao, “Human vs. robotic tactile sensing: detecting lumps in soft tissue,” in *IEEE Haptics Symposium*, Waltham, Massachusetts, USA, March 25–26, 2010, pp. 667–682.

- [149] F. Cavallo, G. Megali, S. Sinigaglia, O. Tonet, and P. Dario, "A biomedical analysis of a surgeon's gesture in a laparoscopic virtual scenario," in *Medicine Meets Virtual Reality*, ser. Studies In Health Technology and Informatics, J. D. Westwood, R. S. Haluck, H. M. Hoffman, G. T. Mogel, R. Phillips, R. A. Robb, and K. G. Vosburgh, Eds., vol. 119, Long Beach, CA, USA, January 24–26, 2006, pp. 79–84.
- [150] K. Takada, K. Yashiro, and M. Takagi, "Reliability and sensitivity of jerk-cost measurement for evaluating irregularity of chewing jaw movements," *Physiological Measurement*, vol. 27, pp. 609–622, 2006.
- [151] H.-L. Teulings, J. Contreras-Vidal, G. Stelmach, and C. Adler, "Parkinsonism reduces coordination of fingers, wrist, and arm in fine motor control," *Experimental Neurology*, vol. 146, pp. 159–170, 1997.
- [152] H. Hwang, J. Lim, C. Kinnaird, A. Nagy, O. Panton, A. Hodgson, and K. Qayumi, "Correlating motor performance with surgical error in laparoscopic cholecystectomy," *Surgical Endoscopy*, vol. 20, no. 4, pp. 651–655, 2006.
- [153] A. Talasaz, R. V. Patel, and M. D. Naish, "Haptics-enabled teleoperation for robot-assisted tumor localization," in *IEEE International Conference on Robotics and Automation*. Anchorage, Alaska, USA: IEEE, May 3–8, 2010, pp. 5340–5345.
- [154] A. Talasaz, "Haptics-enabled teleoperation for robotics-assisted minimally invasive surgery," Ph.D. dissertation, Department of Electrical and Computer Engineering, The University of Western Ontario, 2012.
- [155] J. Jayender, M. Azizian, and R. V. Patel, "Autonomous image-guided robot-assisted active catheter insertion," *IEEE Transactions on Robotics*, vol. 24, no. 4, pp. 858–871, 2008.
- [156] J. Jayender, R. V. Patel, and S. Nikumb, "Robot-assisted active catheter insertion: algorithms and experiments," *The International Journal of Robotics Research*, vol. 28, no. 9, pp. 1101–1117, 2009.
- [157] S. Saha, "Appropriate degrees of freedom of force sensing in robot-assisted minimally invasive surgery," Master's thesis, Department of Biomedical Engineering, Johns Hopkins University, 2005.
- [158] T. Chanthasopeephan, J. P. Desai, and A. C. W. Lau, "Measuring forces in liver cutting: New equipment and experimental results," *Annals of Biomedical Engineering*, vol. 31, no. 11, pp. 1372–1382, 2003.
- [159] T. Akinbiyi, C. Reiley, S. Saha, D. Burschka, C. Hasser, D. Yuh, and A. Okamura, "Dynamic augmented reality for sensory substitution in robot-assisted surgical systems," in *International Conference of the IEEE Engineering in Medicine and Biology Society*, New York City, USA, August 30 – September 3, 2006, pp. 567–570.
- [160] Y. Y. Yurko, M. W. Scerbo, A. S. Prabhu, C. E. Acker, and D. Stefanidis, "Higher mental workload is associated with poorer laparoscopic performance as measured by the NASA-TLX tool," *Simulation in Healthcare*, vol. 5, no. 5, pp. 267–71, 2010.

- [161] C. Reiley, H. Lin, D. Yuh, and G. Hager, "Review of methods for objective surgical skill evaluation," *Surgical Endoscopy*, vol. 25, no. 2, pp. 356–366, 2011.
- [162] Canadian Institute for Health Information, "Health care in Canada," <http://www.cihi.ca>, Ottawa, ON, Canada, 2004.
- [163] S. Regenbogen, C. Greenberg, D. Studdert, S. Lipsitz, M. Zinner, and A. Gawande, "Patterns of technical error among surgical malpractice claims: an analysis of strategies to prevent injury to surgical patients," *Annals of Surgery*, vol. 246, no. 5, pp. 705–711, 2007.
- [164] S. Arora, R. Aggarwal, N. Sevdalis, A. Moran, P. Sirimanna, R. Kneebone, and A. Darzi, "Development and validation of mental practice as a training strategy for laparoscopic surgery," *Surgical Endoscopy*, vol. 24, no. 1, pp. 179–187, 2010.
- [165] L. Beyer, J. D. Troyer, J. Mancini, F. Bladou, S. V. Berdah, and G. Karsenty, "Impact of laparoscopy simulator training on the technical skills of future surgeons in the operating room: a prospective study," *American Journal of Surgery*, vol. 202, no. 3, pp. 265–272, 2011.
- [166] A. R. Jensen, A. S. Wright, A. E. Levy, L. K. McIntyre, H. M. Foy, C. A. Pellegrini, K. D. Horvath, and D. J. Anastakis, "Acquiring basic surgical skills: is a faculty mentor really needed?" *The American Journal of Surgery*, vol. 197, no. 1, pp. 82–88, 2009.
- [167] H. W. R. Schreuder, G. Oei, M. Maas, J. C. C. Borleffs, and M. P. Schijven, "Implementation of simulation in surgical practice: minimally invasive surgery has taken the lead: the Dutch experience," *Medical Teacher*, vol. 33, no. 2, pp. 105–115, 2011.
- [168] R. K. Reznick and H. MacRae, "Teaching surgery skills – changes in the wind," *The New England Journal of Surgery*, vol. 355, no. 25, pp. 2664–2669, 2006.
- [169] L. S. Feldman, S. E. Hagarty, G. Ghitulescu, D. Stanbridge, and G. M. Fried, "Relationship between objective assessment of technical skills and subjective in-training evaluation in surgical residents," *Assessing Technical Skills*, vol. 198, no. 1, pp. 105–109, 2004.
- [170] A. B. Dayan, A. Ziv, H. Berkenstadt, and Y. Munz, "A simple, low-cost platform for basic laparoscopic skills training," *Surgical Innovation*, vol. 15, no. 2, pp. 136–142, 2008.
- [171] P. R. DeLucia, R. D. Mather, J. A. Griswold, and S. Mitra, "Toward the improvement of image-guided interventions for minimally invasive surgery: three factors that affect performance," *Human Factors*, vol. 48, no. 1, pp. 23–38, 2006.
- [172] P. M. Pierorazio and M. E. Allaf, "Minimally invasive surgical training: challenges and solutions," *Urologic Oncology*, vol. 27, no. 2, pp. 208–213, 2009.
- [173] N. Stylopoulos and K. G. Vosburgh, "Assessing technical skill in surgery and endoscopy: A set of metrics and an algorithm (C-PASS) to assess skills in surgical and endoscopic procedures," *Surgical Innovation*, vol. 14, no. 2, pp. 113–121, 2007.
- [174] M. Wentink, L. P. S. Stassen, I. Alwayn, R. J. A. W. Hosman, and H. G. Stassen, "Rasmussens model of human behavior in laparoscopy training," *Surgical Endoscopy*, vol. 17, no. 8, pp. 1241–1246, 2003.

- [175] M. S. Khan, S. D. Bann, A. Darzi, and P. E. M. Butler, "Assessing surgical skill," *Plastic and Reconstructive Surgery*, vol. 112, no. 7, pp. 1886–1889, 2003.
- [176] J. Sándor, B. Lengyel, T. Haidegger, G. Saftics, G. Papp, A. Nagy, and G. Wéber, "Minimally invasive surgical technologies: challenges in education and training," *Asian Journal of Endoscopic Surgery*, vol. 3, no. 3, pp. 101–108, 2010.
- [177] I. Balasundaram, R. Aggarwal, and A. Darzi, "Short-phase training on a virtual reality simulator improves technical performance in tele-robotic surgery," *The International Journal of Medical Robotics and Computer Assisted Surgery*, vol. 4, no. 2, pp. 139–145, 2008.
- [178] Y. Choi, F. Qi, J. Gordon, and N. Schweighofer, "Performance-based adaptive schedules enhance motor learning," *Journal of Motor Behavior*, vol. 40, no. 4, pp. 273–280, 2008.
- [179] E. Boyle, M. Al-Akash, A. G. Gallagher, O. Traynor, A. D. K. Hill, and P. C. Neary, "Optimising surgical training: use of feedback to reduce errors during a simulated surgical procedure," *Postgraduate Medical Journal*, vol. 87, no. 1030, pp. 524–528, 2011.
- [180] V. Datta, M. Mandalia, S. Mackay, A. Chang, N. Cheshire, and A. Darzi, "Relationship between skill and outcome in the laboratory-based model," *Surgery*, vol. 131, no. 3, pp. 318–323, 2002.
- [181] B. Tang, G. Hanna, and A. Cuschieri, "Analysis of errors enacted by surgical trainees during skills training courses," *Surgery*, vol. 138, no. 1, pp. 14–20, 2005.
- [182] T. N. Judkins, D. Oleynikov, and N. Stergiou, "Enhanced robotic surgical training using augmented visual feedback," *Surgical Innovation*, vol. 15, no. 1, pp. 59–68, 2008.
- [183] G. Wulf, C. Shea, and R. Lewthwaite, "Motor skill learning and performance: a review of influential factors," *Medical Education*, vol. 44, no. 1, pp. 75–84, 2010.
- [184] A. Dubrowski, R. Sidhu, J. Park, and H. Carnahan, "Quantification of motion characteristics and forces applied to tissues during suturing," *The American Journal of Surgery*, vol. 190, no. 1, pp. 131–136, 2005.
- [185] C. Cao, M. Zhou, D. Jones, and S. Schwaitzberg, "Can surgeons think and operate with haptics at the same time?" *Journal of Gastrointestinal Surgery*, vol. 11, no. 11, pp. 1564–1569, 2007.
- [186] B. Zheng, M. Cassera, D. Martinec, G. Spaun, and L. Swanström, "Measuring mental workload during the performance of advanced laparoscopic tasks," *Surgical Endoscopy*, vol. 24, no. 1, pp. 45–50, 2010.
- [187] M. Immenroth, T. Burger, J. Brenner, M. Nagelschmidt, H. Eberspacher, and H. Troidl, "Mental training in surgical education: a randomized controlled trial," *Annals of Surgery*, vol. 245, no. 3, 2007.
- [188] B. Goff, L. Mandel, G. Lentz, A. Vanblaricom, A.-M. A. Oelschlager, D. Lee, A. Galakatos, M. Davies, and P. Nielsen, "Assessment of resident surgical skills: is testing feasible?" *American Journal of Obstetrics and Gynecology*, vol. 192, no. 4, pp. 1331–8, 2005.

- [189] R. L. Lammers, M. Davenport, F. Korley, S. Griswold-Theodorson, M. T. Fitch, A. T. Narang, L. V. Evans, A. Gross, E. Rodriguez, K. L. Dodge, C. J. Hamann, and W. C. Robey, "Teaching and assessing procedural skills using simulation: metrics and methodology," *Academic Emergency Medicine*, vol. 15, no. 11, pp. 1079–87, 2008.
- [190] L. Moody, C. Baber, T. N. Arvanitis, and M. Elliott, "Objective metrics for the evaluation of simple surgical skills in real and virtual domains," *Presence: Teleoperators and Virtual Environments*, vol. 12, no. 2, pp. 207–221, 2003.
- [191] I. Oropesa, P. Lamata, P. Sanchez-Gonzalez, J. Pagador, M. Garcia, F. Sanchez-Margallo, and E. Gomez, "Virtual reality simulators for objective evaluation on laparoscopic surgery: current trends and benefits," in *Virtual Reality*, J. Kim, Ed. Rijeka, Croatia: Intech Open Access Publisher, 2011, ch. 16, pp. 349–374.
- [192] M. C. Vassiliou, L. S. Feldman, C. G. Andrew, S. Bergman, K. Leffondré, D. Stanbridge, and G. M. Fried, "A global assessment tool for evaluation of intraoperative laparoscopic skills," *The American Journal of Surgery*, vol. 190, no. 1, pp. 107–113, 2005.
- [193] A. M. Derossis, G. M. Fried, M. Abrahamowicz, H. H. Sigman, J. S. Barkun, and J. L. Meakins, "Development of a model for training and evaluations of laparoscopic skills," *The American Journal of Surgery*, vol. 175, no. 6, pp. 482–487, 1998.
- [194] L. L. Swanstrom, G. M. Fried, K. I. Hoffman, and N. J. Soper, "Beta test results of a new system assessing competence in laparoscopic surgery," *Journal of the American College of Surgeons*, vol. 202, no. 1, pp. 62–69, 2006.
- [195] M. Vassiliou, G. Ghitulescu, L. Feldman, D. Stanbridge, K. Leffondré, H. Sigman, and G. Fried, "The MISTELS program to measure technical skill in laparoscopic surgery," *Surgical Endoscopy*, vol. 20, no. 5, pp. 744–747, 2006.
- [196] G. Sroka, L. S. Feldman, M. C. Vassiliou, P. A. Kaneva, R. Fayez, and G. M. Fried, "Fundamentals of laparoscopic surgery simulator training to proficiency improves laparoscopic performance in the operating room – a randomized controlled trial," *American Journal of Surgery*, vol. 199, no. 1, pp. 115–20, 2010.
- [197] S. Bann, K.-F. Kwok, C.-Y. Lo, A. Darzi, and J. Wong, "Objective assessment of technical skills of surgical trainees in hong kong," *British Journal of Surgery*, vol. 90, no. 10, pp. 1294–1299, 2003.
- [198] R. Brydges, R. Sidhu, J. Park, and A. Dubrowski, "Construct validity of computer-assisted assessment: quantification of movement processes during a vascular anastomosis on a live porcine model," *American Journal of Surgery*, vol. 193, no. 4, pp. 523–529, 2007.
- [199] K. R. Wanzel, S. J. Hamstra, M. F. Caminiti, D. J. Anastakis, E. D. Grober, and R. K. Reznick, "Visual-spatial ability correlates with efficiency of hand motion and successful surgical performance," *Surgery*, vol. 134, no. 5, pp. 750–757, 2003.
- [200] H. C. Lin, I. Shafran, D. Yuh, and G. D. Hager, "Towards automatic skills evaluation: detection and segmentation of robot-assisted surgical motions," *Computer Aided Surgery*, vol. 11, no. 5, pp. 220–230, 2006.

- [201] B. Dunkin, G. L. Adrales, K. Apelgren, and J. D. Mellinger, "Surgical simulation: a current review," *Surgical Endoscopy*, vol. 21, no. 3, pp. 357–366, 2007.
- [202] Simulab Corporation, "LapTrainer with SimuVision," <http://www.simulab.com/product/surgery/laparoscopic/laptrainer-simuvision>, Seattle, WA, USA, 2012.
- [203] IEndosim, "LaproTrain," <http://www.laprotrain.com/>, Belfast, UK, 2012.
- [204] Gadelius Holding Ltd., "iSurgicals physical simulator 'i-Sim'," http://www.gadelius.com/products/clinical_training/_i-sim_e.html, Tokyo, Japan, 2012.
- [205] S. Cotin, N. Stylopoulos, M. Ottensmeyer, P. Neumann, R. Bardsley, and S. Dawson, "Surgical training system for laparoscopic procedures," U.S. Patent US2005/0 142 525 A1, June 30, 2005.
- [206] CAE Healthcare, "CAE PromIS simulator," <http://www.cae.com/en/healthcare/promis.simulator.asp>, Montreal, QC, Canada, 2012.
- [207] Mimic Technologies, "dV-Trainer," <http://www.mimicsimulation.com>, Seattle, WA, USA, 2012.
- [208] V. Chandra, D. Nehra, R. Parent, R. Woo, R. Reyes, T. Hernandez-Boussard, and S. Dutta, "A comparison of laparoscopic and robotic assisted suturing performance by experts and novices," *Surgery*, vol. 147, no. 6, pp. 830–839, 2010.
- [209] S. Cristancho, A. Hodgson, O. Pantou, A. Meneghetti, G. Warnock, and K. Qayumi, "Intraoperative monitoring of laparoscopic skill development based on quantitative measures," *Surgical Endoscopy*, vol. 23, no. 10, pp. 2181–2190, 2009.
- [210] A. M. Derossis, J. Bothwell, H. H. Sigman, and G. M. Fried, "The effect of practice on performance in a laparoscopic simulator," *Surgical Endoscopy*, vol. 12, no. 9, pp. 1117–1120, 1998.
- [211] V. Datta, S. Mackay, M. Mandalia, and A. Darzi, "The use of electromagnetic motion tracking analysis to objectively measure open surgical skill in the laboratory-based model," *Journal of the American College of Surgeons*, vol. 193, no. 5, pp. 479–485, 2001.
- [212] N. Hogan, "An organizing principle for a class of voluntary movements," *The Journal of Neuroscience*, vol. 4, no. 11, pp. 2745–2754, 1984.
- [213] C. Cao, C. MacKenzie, and S. Payandeh, "Task and motion analysis in endoscopic surgery," in *5th Annual Symposium on Haptic Interfaces for Virtual Environment and Teleoperator Systems*, Atlanta, GA, USA, November 17–22, 1996, pp. 583–590.
- [214] T. Judkins, D. Oleynikov, and N. Stergiou, "Objective evaluation of expert and novice performance during robotic surgical training tasks," *Surgical Endoscopy*, vol. 23, no. 3, pp. 590–597, 2009.
- [215] B. Rohrer, S. Fasoli, H. Krebs, R. Hughes, B. Volpe, W. Frontera, J. Stein, and N. Hogan, "Movement smoothness changes during stroke recovery," *The Journal of Neuroscience*, vol. 22, no. 18, 2002.

- [216] H. Beppu, M. Suda, and R. Tanaka, "Analysis of cerebellar motor disorders by visually guided elbow tracking movement," *Brain*, vol. 107, no. 3, pp. 787–809, 1984.
- [217] N. Hogan and D. Sternad, "Sensitivity of smoothness measures to movement duration, amplitude, and arrests," *Journal of Motor Behavior*, vol. 41, no. 6, pp. 529–534, 2009.
- [218] N. Sterigiou, Ed., *Innovative Analyses of Human Movement*. Champaign, IL, USA: Human Kinetics, 2004.
- [219] R. T. Harbourne and N. Sterigiou, "Movement variability and the use of nonlinear tools: principles to guide physical therapist practice," *Physical Therapy*, vol. 89, no. 3, pp. 267–82, 2009.
- [220] M. M. Awad, S. Cho, B. D. Matthews, I. Ohu, C. Gordon, and K. Hubbard, "A pilot study on real-time measures of surgical motions in minimally invasive surgery," in *4th Annual ACS AEI Consortium Meeting*, Chicago, IL, USA, March 29–30, 2011.
- [221] I. Ohu, S. Cho, M. Awad, and B. Matthews, "Motion analysis of simulated minimally invasive surgery," in *Annual Meeting of the American Society of Biomechanics*, Long Beach, CA, August 10–13, 2011.
- [222] I. H. Suh, K.-C. Siu, M. Mukherjee, E. Monk, D. Oleynikov, and N. Sterigiou, "Consistency of performance of robot-assisted surgical tasks in virtual reality," in *Medicine Meets Virtual Reality*, ser. Studies In Health Technology and Informatics, J. Westwood, S. Westwood, R. Haluck, H. Hoffman, G. Mogel, R. Phillips, R. Robb, and K. Vosburgh, Eds., vol. 142, Long Beach, CA, USA, January 19–22, 2009, pp. 369–373.
- [223] N. H. Kim, M. Wininger, and W. Craelius, "Training grip control with a Fitts' paradigm: a pilot study in chronic stroke," *Journal of Hand Therapy*, vol. 23, no. 1, pp. 63–72, 2010.
- [224] J. Gordon and C. Ghez, "EMG patterns in antagonist muscles during isometric contraction in man: relations to response dynamics," *Experimental Brain Research*, vol. 55, no. 1, pp. 167–171, 1984.
- [225] F. Cavallo, A. Pietrabissa, G. Megali, E. Troia, S. Sinigaglia, P. Dario, F. Mosca, and A. Cuschieri, "Proficiency assessment of gesture analysis in laparoscopy by means of the surgeon's musculo-skeleton model," *Annals of Surgery*, vol. 255, no. 2, pp. 394–398, 2012.
- [226] M. Zecca, F. Cavallo, M. Saito, N. Endo, Y. Mizoguchi, S. Sinigaglia, K. Itoh, H. Takanobu, G. Megali, O. Tonet, P. Dario, A. Pietrabissa, and A. Takanishi, "Using the Waseda Bioinstrumentation System WB-1R to analyze surgeon's performance during laparoscopy – towards the development of a global performance index," in *IEEE/RSJ International Conference on Intelligent Robots and Systems*, San Diego, CA, USA, October 29–November 2, 2007, pp. 1272–1277.
- [227] J. Berkley, "Automated support for da Vinci surgical system," Mimic Technologies, Inc., Tech. Rep., May 2011.
- [228] D. Stefanidis, W. W. Hope, J. R. Korndorffer, S. Markley, and D. J. Scott, "Initial laparoscopic basic skills training shortens the learning curve of laparoscopic suturing and is

- cost-effective,” *Journal of the American College of Surgeons*, vol. 210, no. 4, pp. 436–40, 2010.
- [229] S. Perreault, A. Talasaz, A. L. Trejos, C. D. W. Ward, R. V. Patel, and B. Kiaii, “7-DOF haptics-enabled teleoperated robotic system: kinematic modeling and experimental verification,” in *IEEE/RAS-EMBS International Conference on Biomedical Robotics and Biomechanics*, Tokyo, Japan, September 26–29, 2010, pp. 906–911.
- [230] A. L. Trejos, A. C. Lyle, A. Escoto, M. D. Naish, and R. V. Patel, “Force/position-based modular system for minimally invasive surgery,” in *IEEE International Conference on Robotics and Automation*, Anchorage, Alaska, USA, May 3–8, 2010, pp. 3660–3665.
- [231] National Instruments, “NI developer zone: strain gauge configuration types,” <http://www.ni.com/white-paper/4172/en>, Austin, TX, USA, 2008.

Appendix A

Software Development

A.1 Software Design

Customized software¹ was developed to capture, process, and record the information from the strain gauge amplifiers and from the EMTS, and to acquire video streams from a videoscope for the purpose of vision-based tracking of the instruments and for overlaying the visual force information. Details of the vision-based tracking method are considered outside the scope of this thesis, see [230] for more information.

The software interface was developed in C++ using the Qt GUI library over the course of 2 years with various changes and iterations. The final version of the software is presented below.

The SIMIS software was developed such that it is possible for the user to control the information that is being displayed and recorded. It takes the raw data from the strain gauges, filters it using a digital low-pass filter with a cutoff frequency of 10 Hz, and uses the equations presented in Section A.2 to compute the corresponding strain. A calibration interface allows the user to calibrate each direction and compute a calibration factor that is applied to the strain values in order to determine the applied forces. A screen capture of the complete GUI is shown in Figure A.1.

The force and position information are displayed in real time through two dynamically rescaling plots, as shown in Figures A.2 and A.3. The user can control which graphs are displayed by enabling or disabling different signals presented on a tree of checkboxes. The force graph can display the raw

¹The work presented in this appendix was performed by a software engineer working at CSTAR. My contribution to this work consisted of determining what the software needed to do, providing the equations that needed to be used to process the data, and evaluating its overall performance.

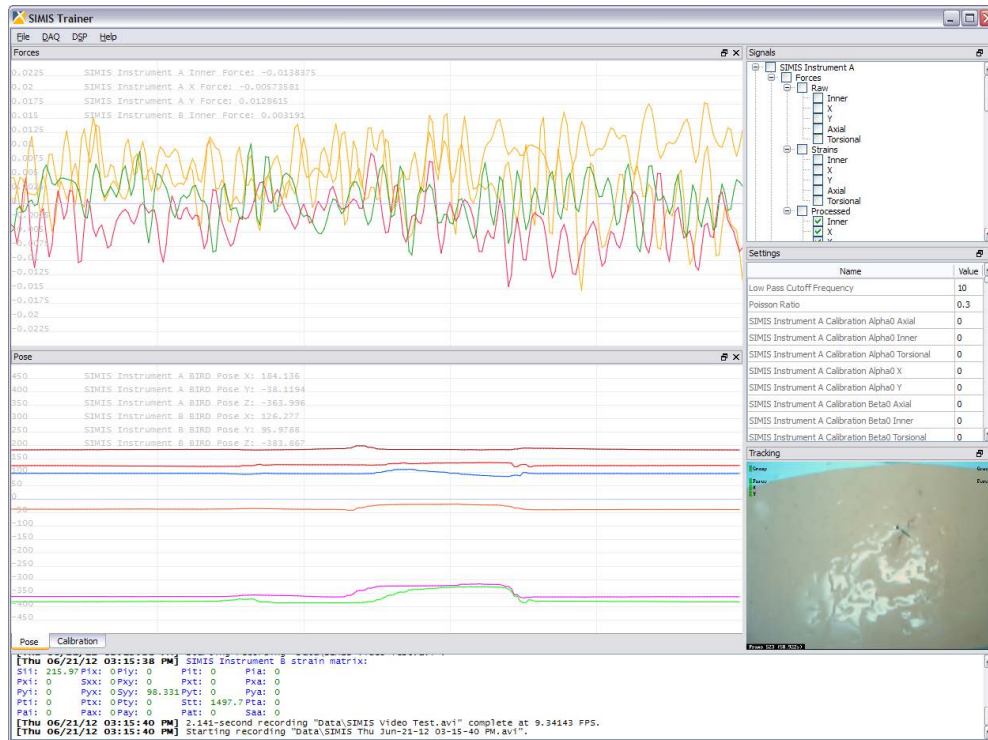


Figure A.1: Graphical user interface for the SIMIS software.

data of each signal, the computed strains, and/or the final force values. A simple command allows the offset of the signals to be removed (this eliminates the effect of drift). The position graph can display the calibrated position and/or orientation information for the different instruments based on the EMTS or the vision-based tracking system.

For increased control, several parameters related to each of the instruments can be entered or modified as needed by changing the values on a table, as shown in Figure A.4. These values include those parameters that influence the signal processing tasks carried out in the software, and include the following:

- Low-pass cutoff frequency of the filter
- Gravity compensation factors and offsets for each of the 5 signals: inner (grasping or actuation), torsional, x , y , or axial (z)
- Position calibration factors corresponding to the displacement values for the three Cartesian coordinates from the position of the sensor to the tip of the instruments
- Excitation voltage from the power supply connected to the amplifiers

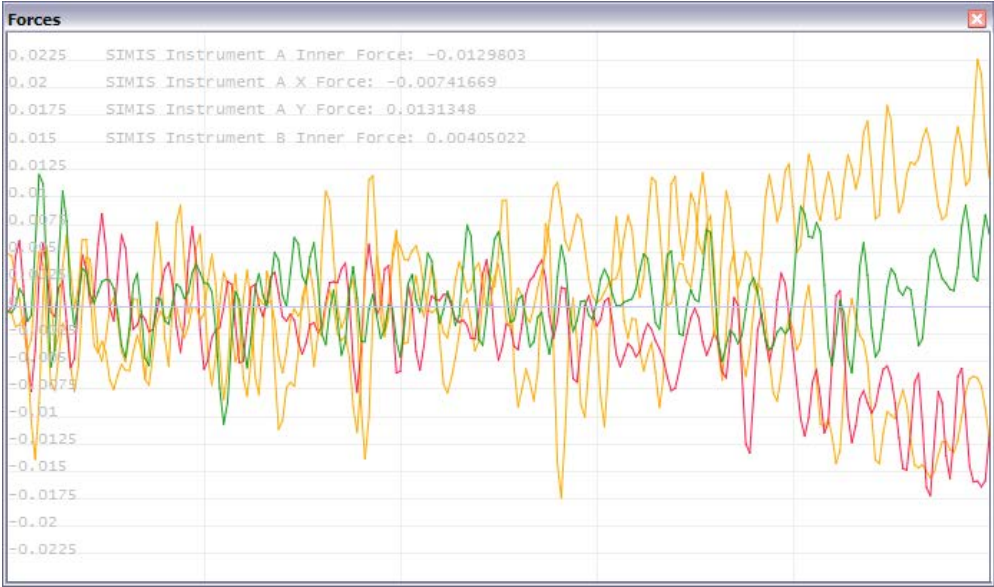


Figure A.2: Force graph included in the SIMIS GUI.

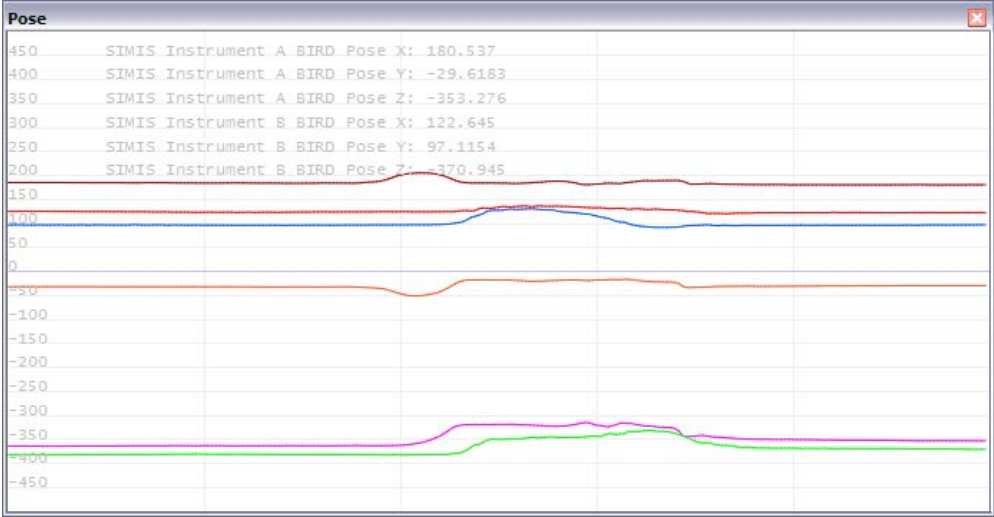


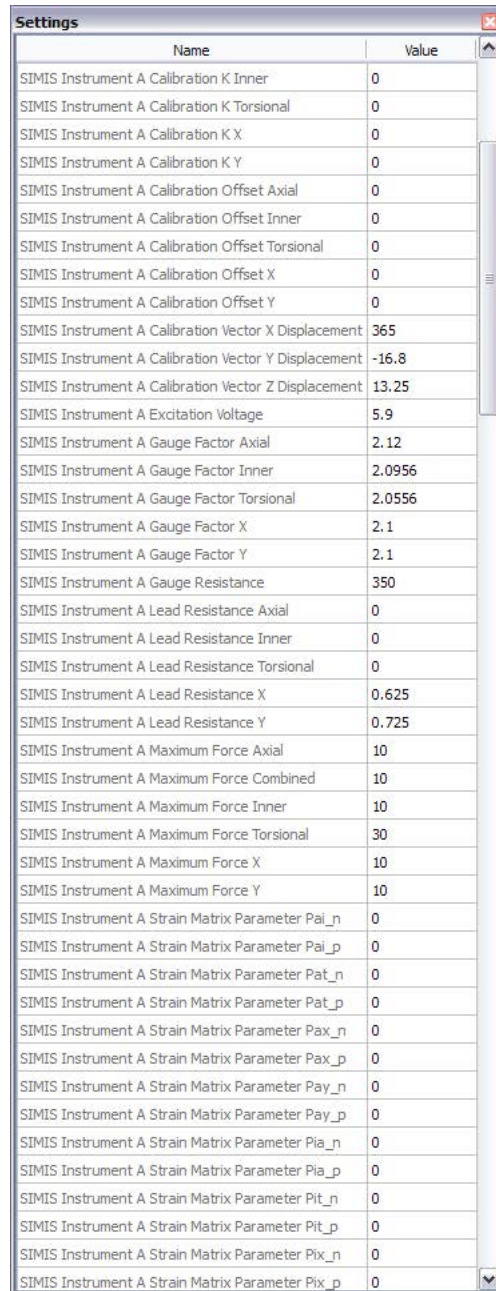
Figure A.3: Position graph included in the SIMIS GUI.

- Gauge factors for the gauges used in each of the 5 bridges
- Gauge resistance for all of the gauges (This assumes that all of the gauges have the same nominal resistance, but this is only used in the equations for the quarter and half-bridges, which do have the same nominal resistance, see Section A.2.)
- Lead resistances for each of the 5 bridges (These values are used in the equations for the quarter- and half-bridges.)
- Poisson ratio of the strain gauges
- Maximum force values for visual force feedback, corresponding to the individual directions, as well as the combined Cartesian forces (This corresponds to the point at which the displayed force bars turn to red.)
- Calibration and decoupling factors for each of the five signals (These values are acquired directly from the calibration process, but can be manually modified if needed.)

As mentioned above, a calibration interface allows the user to automatically record the measured signal and relate it to a particular load being applied on the instrument, see Figure A.5. This calibration interface provides the ability to control which signal is being calibrated, specify the instrument being calibrated, and input the weight increment used during calibration. The values are recorded and the slope and offset are automatically computed and displayed. Visualization of the data allows the user to determine if the relationship is linear, hence allowing the immediate detection of problems with the bridge or calibration process.

Finally, a video display is included in the GUI that corresponds to the video feed that is being recorded by the system, see Figure A.6. The same tree of checkboxes used to control the data displayed on the force graph can be used to control the visual feedback overlaid onto the video feed. The acquisition time and frame number are also overlaid directly on this image to facilitate synchronization of the video with the recorded force and position data.

Additional details on how the raw signals from the strain gauges are processed are presented in the following section.



The screenshot shows a window titled "Settings" with a table of parameters. The table has two columns: "Name" and "Value". The parameters listed are calibration constants and adjustment parameters for SIMIS Instrument A.

Name	Value
SIMIS Instrument A Calibration K Inner	0
SIMIS Instrument A Calibration K Torsional	0
SIMIS Instrument A Calibration K X	0
SIMIS Instrument A Calibration K Y	0
SIMIS Instrument A Calibration Offset Axial	0
SIMIS Instrument A Calibration Offset Inner	0
SIMIS Instrument A Calibration Offset Torsional	0
SIMIS Instrument A Calibration Offset X	0
SIMIS Instrument A Calibration Offset Y	0
SIMIS Instrument A Calibration Vector X Displacement	365
SIMIS Instrument A Calibration Vector Y Displacement	-16.8
SIMIS Instrument A Calibration Vector Z Displacement	13.25
SIMIS Instrument A Excitation Voltage	5.9
SIMIS Instrument A Gauge Factor Axial	2.12
SIMIS Instrument A Gauge Factor Inner	2.0956
SIMIS Instrument A Gauge Factor Torsional	2.0556
SIMIS Instrument A Gauge Factor X	2.1
SIMIS Instrument A Gauge Factor Y	2.1
SIMIS Instrument A Gauge Resistance	350
SIMIS Instrument A Lead Resistance Axial	0
SIMIS Instrument A Lead Resistance Inner	0
SIMIS Instrument A Lead Resistance Torsional	0
SIMIS Instrument A Lead Resistance X	0.625
SIMIS Instrument A Lead Resistance Y	0.725
SIMIS Instrument A Maximum Force Axial	10
SIMIS Instrument A Maximum Force Combined	10
SIMIS Instrument A Maximum Force Inner	10
SIMIS Instrument A Maximum Force Torsional	30
SIMIS Instrument A Maximum Force X	10
SIMIS Instrument A Maximum Force Y	10
SIMIS Instrument A Strain Matrix Parameter Pai_n	0
SIMIS Instrument A Strain Matrix Parameter Pai_p	0
SIMIS Instrument A Strain Matrix Parameter Pat_n	0
SIMIS Instrument A Strain Matrix Parameter Pat_p	0
SIMIS Instrument A Strain Matrix Parameter Pax_n	0
SIMIS Instrument A Strain Matrix Parameter Pax_p	0
SIMIS Instrument A Strain Matrix Parameter Pay_n	0
SIMIS Instrument A Strain Matrix Parameter Pay_p	0
SIMIS Instrument A Strain Matrix Parameter Pia_n	0
SIMIS Instrument A Strain Matrix Parameter Pia_p	0
SIMIS Instrument A Strain Matrix Parameter Pit_n	0
SIMIS Instrument A Strain Matrix Parameter Pit_p	0
SIMIS Instrument A Strain Matrix Parameter Pix_n	0
SIMIS Instrument A Strain Matrix Parameter Pix_p	0

Figure A.4: Window within the SIMIS GUI to input calibration constants and adjustment parameters.

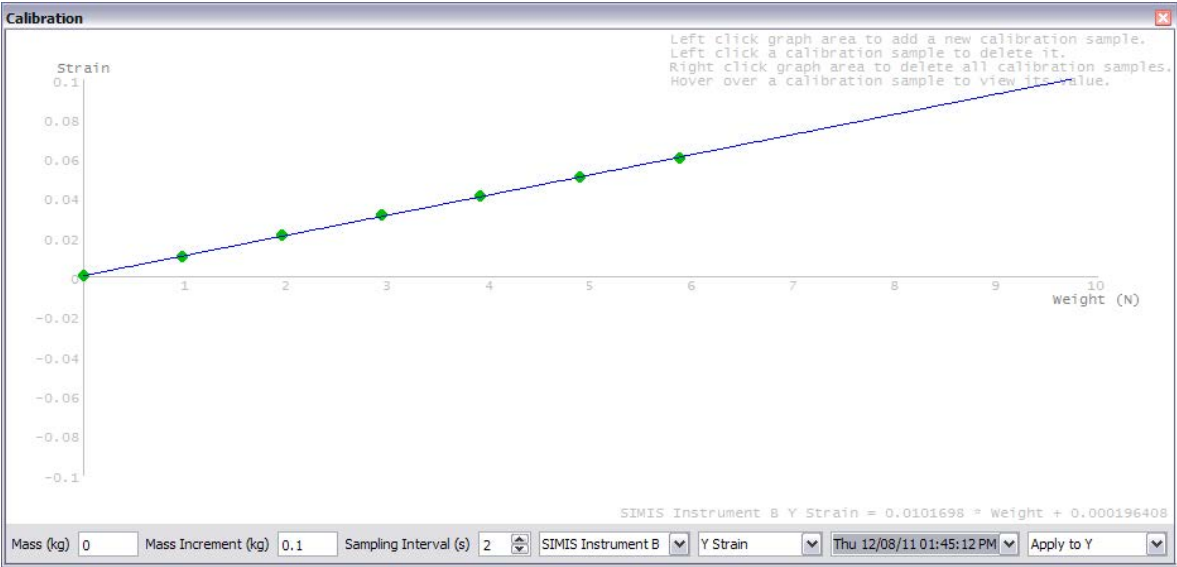


Figure A.5: Calibration interface included in the SIMIS GUI.



Figure A.6: Video with force overlay included in the SIMIS GUI.

A.2 Strain Gauge Processing

Strain gauge configurations are wired as a Wheatstone bridge [231] in order to maximize the signals and minimize noise. Depending on how the gauges are connected, it is possible to add or subtract their signals in order to measure strain acting in different directions. Details on the bridges used in the SIMIS instruments are presented below.

A.2.1 Type I Quarter Bridge

Type I quarter bridges are used in the first-generation prototype, see Figure 3.6. These bridges require only one strain gauge in order to measure axial or bending stress. The equation used to compute the strain is the following:

$$\varepsilon = \frac{-4V_r}{GF(1 + 2V_r)} \left(1 + \frac{R_L}{R_G} \right), \quad (\text{A.1})$$

where ε is the strain, GF is the gauge factor, R_L is the lead resistance, R_G is the nominal gauge resistance, and V_r is defined as follows:

$$V_r = \frac{\Delta V}{V_{\text{EX}}}, \quad (\text{A.2})$$

where ΔV is the change in voltage measured by the amplifier and V_{EX} is the excitation voltage used to power the amplifier.

A.2.2 Type II Half Bridge

Type II half-bridges are used in all of the prototypes to measure the bending moments related to the forces acting in the x and y directions, see Figure 3.5. The type II half bridge rejects axial measurements and measures bending. The equation used to compute the bending strain is the following:

$$\varepsilon = \frac{-2V_r}{GF} \left(1 + \frac{R_L}{R_G} \right). \quad (\text{A.3})$$

A.2.3 Type III Full Bridge

A type III full bridge is used for the actuation signals, as well as for the axial and torsional signals implemented in the second-generation prototype, see Figure 3.4. The equation used to compute the strain is the following:

$$\varepsilon = \frac{-2V_r}{\text{GF}[(\nu + 1) - V_r(\nu - 1)]}, \quad (\text{A.4})$$

where ν is the transverse sensitivity ratio (Poisson) of the strain gauges used in the bridge.

A.3 Generic Software Architecture

In addition to the SIMIS software, a generic software architecture was developed so that signals from different strain gauges could be acquired using any data acquisition card and displayed, calibrated and recorded based on any bridge configuration. The GUI of this generic interface is shown in Figure A.7. As with the SIMIS software, this interface allows the force measurements to be displayed according to what is selected in the tree of checkboxes. It also contains a calibration interface similar to the one available in the SIMIS software.

The main difference between this generic software interface and the SIMIS software lies in the ability to assign the channels that are being used and specify the type of bridge that is connected to each channel, as shown in Figure A.8. The generic software interface also allows the user to input the values for excitation voltage, gauge factor, Poisson ratio and gauge resistance for each of the channels.

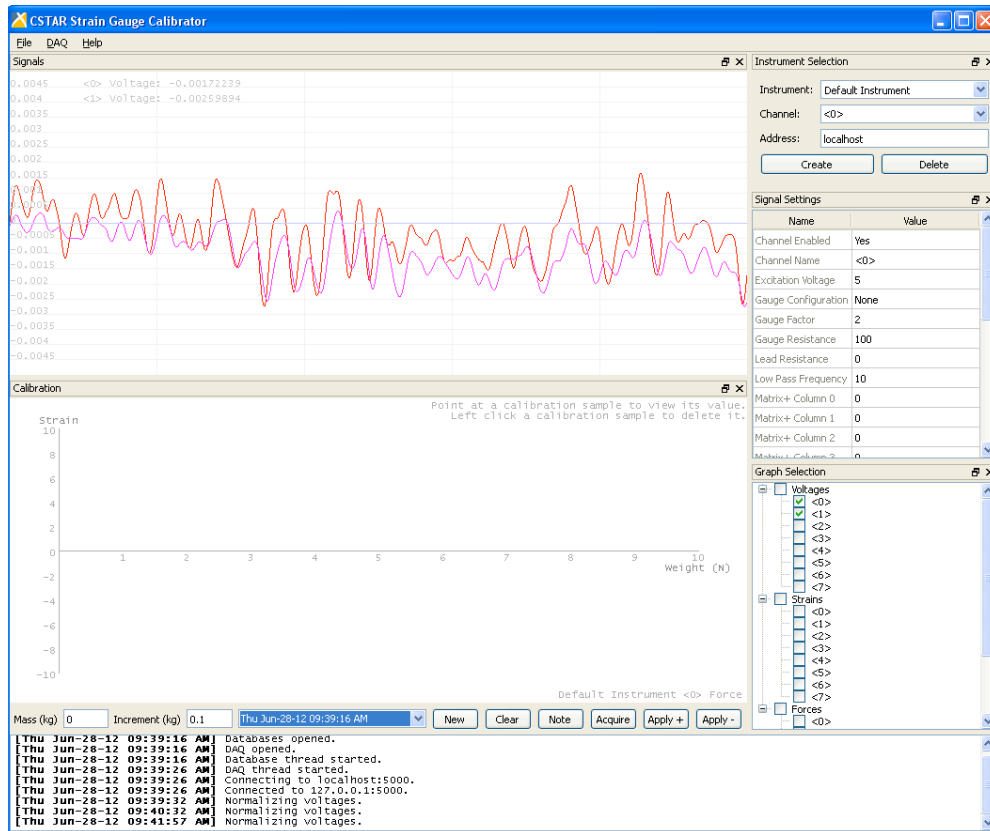


Figure A.7: Generic graphical user interface for displaying, recording and calibrating strain gauges.

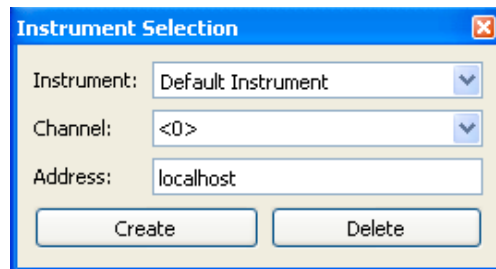


Figure A.8: Window within the generic GUI to select an input channel and assign a bridge type.

Appendix B

Permissions and Approvals

The following forms and permission statements are presented in this Appendix:

- Ethics approval for the experimental evaluation from the Research Ethics Board for Health Sciences Research Involving Human Subjects at the University of Western Ontario
- Ethics approval for the *in vivo* trials from the Animal Use Subcommittee of the University Council on Animal Care at the University of Western Ontario
- Permission statement from SAGE publications for the content of Chapter 2
- Written permission from ASME for the content of Chapter 3
- Permission statement from IEEE for some of the content included in Chapter 4



Office of Research Ethics

The University of Western Ontario
 Room 5150 Support Services Building, London, ON, Canada N6A 3K7
 Telephone: (519) 661-3036 Fax: (519) 850-2466 Email: ethics@uwo.ca
 Website: www.uwo.ca/research/ethics

Use of Human Subjects - Ethics Approval Notice

Principal Investigator: Dr. R.V. Patel

Review Number: 17525E

Review Date: October 25, 2010

Review Level: Expedited

Approved Local # of Participants: 200

Protocol Title: Systematic Evaluation of the Need for Force Feedback in Minimally Invasive Interventions

Department and Institution: Electrical & Computer Engineering, University of Western Ontario

Sponsor: NSERC-NATURAL SCIENCES ENGINEERING RESEARCH COUNCIL OF CANADA

Ethics Approval Date: December 23, 2010

Expiry Date: December 31, 2012

Documents Reviewed and Approved: UWO Protocol, Letter of Information and Consent (Version 1), Email.

Documents Received for Information:

This is to notify you that The University of Western Ontario Research Ethics Board for Health Sciences Research Involving Human Subjects (HSREB) which is organized and operates according to the Tri-Council Policy Statement: Ethical Conduct of Research Involving Humans and the Health Canada/ICH Good Clinical Practice Practices: Consolidated Guidelines; and the applicable laws and regulations of Ontario has reviewed and granted approval to the above referenced study on the approval date noted above. The membership of this REB also complies with the membership requirements for REB's as defined in Division 5 of the Food and Drug Regulations.

The ethics approval for this study shall remain valid until the expiry date noted above assuming timely and acceptable responses to the HSREB's periodic requests for surveillance and monitoring information. If you require an updated approval notice prior to that time you must request it using the UWO Updated Approval Request Form.

During the course of the research, no deviations from, or changes to, the protocol or consent form may be initiated without prior written approval from the HSREB except when necessary to eliminate immediate hazards to the subject or when the change(s) involve only logistical or administrative aspects of the study (e.g. change of monitor, telephone number). Expedited review of minor change(s) in ongoing studies will be considered. Subjects must receive a copy of the signed information/consent documentation.

Investigators must promptly also report to the HSREB:

- a) changes increasing the risk to the participant(s) and/or affecting significantly the conduct of the study;
- b) all adverse and unexpected experiences or events that are both serious and unexpected;
- c) new information that may adversely affect the safety of the subjects or the conduct of the study.

If these changes/adverse events require a change to the information/consent documentation, and/or recruitment advertisement, the newly revised information/consent documentation, and/or advertisement, must be submitted to this office for approval.

Members of the HSREB who are named as investigators in research studies, or declare a conflict of interest, do not participate in discussion related to, nor vote on, such studies when they are presented to the HSREB.

Fwd: FW: eSirius Notification - New Animal Use Protocol is APPROVED2008-011-02::5

12-08-23 1:38 PM

Fwd: FW: eSirius Notification - New Animal Use Protocol is APPROVED2008-011-02::5
From: Sheri VanLingen
To: Trejos, AnaLuisa
Date: Thursday - August 16, 2012 9:27 AM
Subject: Fwd: FW: eSirius Notification - New Animal Use Protocol is APPROVED2008-011-02::5

<<http://www.uwo.ca/animal/images/westernu.gif>>

AUP Number: 2008-011-02
PI Name: Schlachta, Chris
AUP Title: Society Of American Gastrointestinal Endoscopic Surgeons Resident
Course In Basic Laparoscopy And Endoscopy

Approval Date: 07/13/2012

Official Notice of Animal Use Subcommittee (AUS) Approval: Your new Animal Use Protocol (AUP) entitled "Society Of American Gastrointestinal Endoscopic Surgeons Resident Course In Basic Laparoscopy And Endoscopy

" has been APPROVED by the Animal Use Subcommittee of the University Council on Animal Care. This approval, although valid for four years, and is subject to annual Protocol Renewal.2008-011-02::5

1. This AUP number must be indicated when ordering animals for this project.
2. Animals for other projects may not be ordered under this AUP number.
3. Purchases of animals other than through this system must be cleared through the ACVS office. Health certificates will be required.

The holder of this Animal Use Protocol is responsible to ensure that all associated safety components (biosafety, radiation safety, general laboratory safety) comply with institutional safety standards and have received all necessary approvals. Please consult directly with your institutional safety officers.

Submitted by: Copeman, Laura
on behalf of the Animal Use Subcommittee
University Council on Animal Care
<<http://www.uwo.ca/animal/website/AUS/images/signature.png>>

<http://www.uwo.ca/animal/website/AUS/images/footer_auspc.png>

Journal Authors

Under the terms of your contributor agreement, without seeking permission, you may:

- At any time, distribute on a not-for-profit basis photocopies of the published article for your own teaching needs or to supply on an individual basis to research colleagues.
- At any time, circulate or post on any repository or website the version of the article that you submitted to the journal (i.e. the version before peer-review) or an abstract of the article.
- At least 12 months after publication, post on any non-commercial repository or website the version of your article that was accepted for publication.
- At least 12 months after publication, re-publish the whole or any part of the Contribution in a printed work written, edited or compiled by you provided reference is made to first publication by SAGE/SOCIETY.

When posting or re-using the article, please provide a link/URL from the article posted to the SAGE Journals Online where the article is published: <http://online.sagepub.com> and please make the following acknowledgment **'The final, definitive version of this paper has been published in <journal>, Vol/Issue, Month/Year by <<SAGE Publications Ltd.>>/<<SAGE Publications, Inc.>>, All rights reserved. © [as appropriate]**

The licenses granted above in this paragraph are expressly made subject to and limited by the following restrictions:

- The SAGE-created PDF of the published Contribution may not be posted at any time.
- In each instance of use of the Contribution, or any part of it, must include the copyright notice that appears on the issue of the Journal in which the Contribution is first published and a full bibliographic citation to the Journal as published by SAGE;
- Copies of the Contribution, or any part of it, shall not be sold, distributed, or reproduced for commercial purposes (i.e., for monetary gain on Contributor's own account or on that of a third party, or for indirect financial gain by a commercial entity);
- The Contribution, or any part of it, shall not be used for any systematic external distribution by a third party (e.g., a listserve or database connected to a public access server).

*All commercial requests and any other requests to re-use the article must be forwarded to SAGE.

UK Authors You may wish to register with the ALCS: <http://www.alcs.co.uk/> so that you will receive royalties due to you from any reprographic rights income.

For any use of your work not stated above, please request permission using the instructions on the Journals permissions webpage at www.sagepub.com/journalspermissions.nav.

Date: Friday - June 22, 2012 4:21 PM
Subject: FW: ASME PUBLICATIONS PERMISSION REQUEST FORM SUBMISSION
Attachments: Mime.822

Dear Ms. Trejos:

It is our pleasure to grant you permission to use the ASME paper "A Sensorized Instrument for Skills Assessment and Training in Minimally Invasive Surgery," by A.L. Trejos, R.V. Patel, M.D. Naish, A.C. Lyle, and C.M. Schlachta, Journal of Medical Devices, Volume 3, 2009, as cited in your letter for inclusion in a Doctoral Thesis entitled A Sensorized Instrument for Minimally Invasive Surgery for the Measurement of Forces during Training and Surgery: Development and Applications to be published by The University of Western Ontario.

Permission is granted for the specific use as stated herein and does not permit further use of the materials without proper authorization. Proper attribution must be made to the author(s) of the materials, and no alterations of the materials is permitted in any material manner.

As is customary, we request that you ensure full acknowledgment of this material, the author(s), source and ASME as original publisher. Acknowledgment must be retained on all pages printed and distributed.

Many thanks for your interest in ASME publications.

Sincerely,

Beth Darchi

Permissions & Copyrights



RightsLink®

[Home](#)
[Create Account](#)
[Help](#)


Title: Force/position-based modular system for minimally invasive surgery

Conference Proceedings: Robotics and Automation (ICRA), 2010 IEEE International Conference on

Author: Trejos, A.L.; Lyle, A.C.; Escoto, A.; Naish, M.D.; Patel, R.V.

Publisher: IEEE

Date: 3-7 May 2010

Copyright © 2010, IEEE

User ID
Password
<input type="checkbox"/> Enable Auto Login
<input type="button" value="LOGIN"/>
Forgot Password/User ID?
<p>If you're a copyright.com user, you can login to RightsLink using your copyright.com credentials.</p> <p>Already a RightsLink user or want to learn more?</p>

Thesis / Dissertation Reuse

The IEEE does not require individuals working on a thesis to obtain a formal reuse license, however, you may print out this statement to be used as a permission grant:

Requirements to be followed when using any portion (e.g., figure, graph, table, or textual material) of an IEEE copyrighted paper in a thesis:

- 1) In the case of textual material (e.g., using short quotes or referring to the work within these papers) users must give full credit to the original source (author, paper, publication) followed by the IEEE copyright line © 2011 IEEE.
- 2) In the case of illustrations or tabular material, we require that the copyright line © [Year of original publication] IEEE appear prominently with each reprinted figure and/or table.
- 3) If a substantial portion of the original paper is to be used, and if you are not the senior author, also obtain the senior author's approval.

Requirements to be followed when using an entire IEEE copyrighted paper in a thesis:

- 1) The following IEEE copyright/ credit notice should be placed prominently in the references: © [year of original publication] IEEE. Reprinted, with permission, from [author names, paper title, IEEE publication title, and month/year of publication]
- 2) Only the accepted version of an IEEE copyrighted paper can be used when posting the paper or your thesis on-line.
- 3) In placing the thesis on the author's university website, please display the following message in a prominent place on the website: In reference to IEEE copyrighted material which is used with permission in this thesis, the IEEE does not endorse any of [university/educational entity's name goes here]'s products or services. Internal or personal use of this material is permitted. If interested in reprinting/republishing IEEE copyrighted material for advertising or promotional purposes or for creating new collective works for resale or redistribution, please go to http://www.ieee.org/publications_standards/publications/rights/rights_link.html to learn how to obtain a License from RightsLink.

If applicable, University Microfilms and/or ProQuest Library, or the Archives of Canada may supply single copies of the dissertation.

[BACK](#)
[CLOSE WINDOW](#)

CURRICULUM VITAE

Name: Ana Luisa Trejos

Post-secondary Education and Degrees: Universidad de Costa Rica
San José, Costa Rica
1993–1996 B.Sc.
Mechanical Engineering

The University of British Columbia
Vancouver, British Columbia, Canada
1997–1999 M.A.Sc.
Mechanical Engineering

The University of Western Ontario
London, Ontario, Canada
2008–2012 Ph.D.
Electrical and Computer Engineering

Honours and Awards: ISCAS Best Poster Award, Barcelona, Spain, 2008
Alexander Graham Bell Canada Graduate Scholarship, NSERC, 2009–2012
Outstanding Presentation in ECE Graduate Symposium, Western, 2010
ISMICS Best Poster Finalist Award, Berlin, Germany, 2010
London Health Research Day, Second place, Platform Competition, 2012
Honourable Mention, CIHR National Competition, Winnipeg, MB, 2012

Related Work Experience: Teaching Assistant
The University of Western Ontario
2012

Research Associate
Canadian Surgical Technologies and Advanced Robotics
2004–2012

Relevant Publications:

T.P. Kurowski, A.L. Trejos, M.D. Naish, R.V. Patel and R.A. Malthaner, “Design of a minimally invasive lung tumor localization device,” Accepted for the *Dynamic Systems and Control Conference*, Fort Lauderdale, FL, USA, October 17–19, 2012.

A. Talasaz, A.L. Trejos, R.V. Patel, “Haptic feedback for a robot-assisted suture manipulation task,” *IEEE RAS/EMBS International Conference on Biomedical Robotics and Biomechanics*, Rome, Italy, June 24–27, 2012, pp. 3660–3665.

M. Currie, A.L. Trejos, R. Rayman, M.W.A. Chu, R.V. Patel, T.M. Peters, and B. Kiaii, “Is 3D better? Evaluating the effect of three dimensional visualization on force application and performance time during robotics-assisted mitral valve annuloplasty,” Submitted to *Innovations*, April 2012.

A. Escoto, A.L. Trejos, M.D. Naish, R.V. Patel and M.-E. LeBel, “Force sensing based simulator for arthroscopic skills testing in orthopaedic knee surgery,” *Medicine Meets Virtual Reality Conference*, Newport Beach, California, February 9–11, 2012, pp. 129–135.

M. Currie, A.L. Trejos, R. Rayman, M.W.A. Chu, R.V. Patel, T.M. Peters, and B. Kiaii, “The role of three-dimensional visualization in robotics-assisted cardiac surgery,” *SPIE Medical Imaging Conference*, San Diego, CA, USA, February 4–9, 2012, pp. 83160F-1–83160F-10

S. Jayaraman, A.L. Trejos, M.D. Naish, A. Lyle, R.V. Patel and C.M. Schlachta, “Toward construct validity for a novel sensorized instrument-based minimally invasive surgery (SIMIS) simulation system,” *Surgical Endoscopy*, vol. 25, no. 5, pp. 1439–1445, 2011.

M.T. Perri, A.L. Trejos, M.D. Naish, R.V. Patel and R.A. Malthaner, “Initial evaluation of a tactile/kinesthetic force feedback system for minimally invasive tumor localization,” *IEEE Transactions on Mechatronics*, vol. 15, no. 6, pp. 925–931, 2010.

M.D. Naish, M.T. Perri, D.A. Bottoni, A.L. Trejos, R.V. Patel and R.A. Malthaner, “Palpation system for minimally invasive localization of occult tumours,” *IEEE/RAS-EMBS International Conference on Biomedical Robotics and Biomechanics*, Tokyo, Japan, September 26–29, 2010, pp. 662–667.

S. Perreault, A. Talasaz, A.L. Trejos, C.D.W. Ward, R.V. Patel and B. Kiaii, “A 7-DOF haptics-enabled teleoperated robotic system: kinematic modeling and experimental verification,” *IEEE/RAS-EMBS International Conference on Biomedical Robotics and Biomechanics*, Tokyo, Japan, September 26–29, 2010, pp. 906–911.

A.L. Trejos, S. Jayaraman, R.V. Patel, M.D. Naish and C.M. Schlachta, “Force sensing in natural orifice transluminal endoscopic surgery,” *Surgical Endoscopy*, vol. 25, no. 1, pp. 186–192, 2010.

A.L. Trejos, A.C. Lyle, A. Escoto, M.D. Naish and R.V. Patel, “Force/position-based modular system for minimally invasive surgery,” *IEEE International Conference on Robotics and Automation*, Anchorage, Alaska, May 3–8, 2010, pp. 3660–3665.

A.L. Trejos, R.V. Patel and M.D. Naish, “Force sensing and its applications in minimally invasive surgery and therapy: a survey,” *Proceedings of the Institution of Mechanical Engineers, Part C: Journal of Mechanical Engineering Science on Robots and Devices in Surgery*, vol. 224, no. 7, pp. 1435–1453, 2010.

A.L. Trejos, R.V. Patel, M.D. Naish, A.C. Lyle and C.M. Schlachta, “A sensorized instrument for skills assessment and training in minimally invasive surgery,” *ASME Journal of Medical Devices*, vol. 3, no. 4, pp. 041002-1–041002-12, 2009.

A.L. Trejos, J. Jayender, M.T. Perri, M.D. Naish, R.V. Patel and R.A. Malthaner, “Robot-assisted tactile sensing for minimally invasive tumor localization,” *The International Journal of Robotics Research – Special Issue on Medical Robotics*, vol. 28, no. 9, pp. 1118–1133, 2009.

A.L. Trejos, J. Jayender, M.T. Perri, M.D. Naish, R.V. Patel and R.A. Malthaner, “Experimental evaluation of robot-assisted tactile sensing for minimally invasive surgery,” *IEEE RAS/EMBS International Conference on Biomedical Robotics and Biomechatronics*, Scottsdale, Arizona, October 19–22, 2008. pp. 971–976.

A.L. Trejos, R.V. Patel, M.D. Naish and C.M. Schlachta, “Design of a sensorized instrument for skills assessment and training in minimally invasive surgery,” *IEEE RAS/EMBS International Conference on Biomedical Robotics and Biomechatronics*, Scottsdale, Arizona, October 19–22, 2008, pp. 965–970.

G. McCreery, A.L. Trejos, M.D. Naish, R.V. Patel and R.A. Malthaner “Feasibility of locating tumours in lung via kinesthetic feedback,” *The International Journal of Medical Robotics and Computer Assisted Surgery*, vol. 4, no. 1, pp. 58–68, 2008.